A novel interaction of the myosin light chain phosphatase with the regulatory subunits of protein kinase A in platelets

Jawad Shah Khalil

PhD Medical Sciences

The University of Hull and The University of York

Hull York Medical School

May 2018

Abstract

Platelet activation initiates a series of events, such as shape change, degranulation and aggregation, which results in the formation of a haemostatic plug and arrest of blood loss at the sites of vascular damage. Shape change is accompanied by remodelling of the actin cytoskeleton and formation of an acto-myosin contractile ring. This process is regulated by phosphorylation of the myosin light chain (MLC), which in turn is controlled by the relative activities of myosin light chain kinase (MLCK) and phosphatase (MLCP). MLCP is a target of both inhibitory and activatory signalling molecules. Here we focussed on the control of MLCP activation by the cyclic adenosine 3', 5' monophosphate (cAMP) signalling pathway. cAMP signalling is a major inhibitory pathway that inhibits platelet function through its effector protein kinase A (PKA). One of the downstream targets of PKA is MLCP. In vascular smooth muscle cells cAMP activates MLCP to dephosphorylate MLC and regulate cytoskeletal rearrangement. However, the relationship between cAMP signalling, MLCP and platelet function is unclear. Here we investigated the molecular and biochemical regulation of MLCP by cAMP signalling.

We found that MYPT1, the targeting subunit of MLCP, is phosphorylated in platelets in response to cAMP elevating agents, suggesting that the phosphatase is a direct target for cAMP signalling. Our data suggests the possibility of at least two different splice variants of MYPT1 in platelets, but only one splice variant, possibly full length, was phosphorylated downstream of cAMP signalling. Using co-immunoprecipitation, cAMP pull-down assays and GST pull-down approaches we found that MYPT1 and PKA are part of the same complex and MYPT1 interacts with all four regulatory subunits of PKA (PKA-R) in platelets. Using a series of truncated proteins in HEK cells the interaction of MYPT1 and PKA-R was mapped to the central region of MYPT1 (aa501-706). Moreover, co-sedimentation assays with recombinant proteins confirmed the direct association of MYPT1 (aa501-706) with PKA-R. The conserved dimerisation and docking (D/D) domain of PKA-R, which facilitates interactions with A-kinase anchoring proteins (AKAP) was not required

for the interaction. Consistent with this observation, the AKAP disruptor peptide Ht31 did not disrupt the interaction, indicating that the interaction of MYPT1 with PKA-R does not occur in an AKAP modus.

These results were complemented with immunohistochemistry studies showing that MYPT1 co-localised with all four PKA regulatory subunits in both non-activated and spread platelets. In summary, our data identify MYPT1 as a novel PKA binding protein in platelets. The interaction of MYPT1 with PKA emerges as an important component of the signalling pathways that protect platelets from a hyperreactive state and may constitute a target towards preventing thrombogenic disorders.

Publications

- Joshi, P., Riley, D.R., **Khalil, J.S**., Xiong, H., Ji, W. and Rivero, F., 2018. The membrane-associated fraction of cyclase associate protein 1 translocates to the cytosol upon platelet stimulation. Scientific reports, 8(1), p.10804.
- **Khalil, J.S**., Wei, J., Naseem, K. & Rivero, F., 2018 "A novel interaction of myosin light chain phosphatase with protein kinase A in platelets" (manuscript in preparation).
- Berger, M., Riley, D., Lutz, J., **Khalil, J.S.**, Aburima, A.A., Naseem, K. & Rivero, F., 2018. "Impaired platelet function in RhoBTB3 knockout model" (submitted to Cells).

Oral presentations

- Khalil, J.S., Wei, J., Naseem, K. & Rivero, F., 2017. A novel interaction of the myosin light chain phosphatase with the regulatory subunits of protein kinase A in platelets. *6th HYMS Postgraduate Research Conference, Hull, UK.*

Poster presentations

- Khalil, J.S., Wei, J., Naseem, K.M. & Rivero, F., 2017. A novel interaction of the myosin light chain phosphatase with the regulatory subunits of protein kinase A. *1st Italian-UK Platelet Meeting, Bath, UK.*
- Khalil, J.S., Wei. J., Naseem, K.M. & Rivero, F., 2017. A novel interaction of the myosin light chain phosphatase with the regulatory subunits of protein kinase A in platelets. *6th HYMS Postgraduate Research Conference, Hull, UK.*
- Khalil, J.S., Wei, J., Naseem, K.M. & Rivero, F., 2016. Myosin phosphatase targeting subunit 1 (MYPT1) interacts with PKA in platelets. *North of England Cell Biology Meeting, Bradford, UK.*
- Khalil, J.S., Naseem, K.M. & Rivero, F., 2015. Coronin 1A, a regulator of actin cytoskeleton rearrangement and a signalling modulator in platelets. *North of England Cell Biology Meeting, York, UK.*

Table of contents

List of tables

1. General introduction

2. Materials and methods

List of figures

1. General introduction

2. Materials and methods

3. Phosphorylation of myosin light chain phosphatase in platelets

5. Cellular distribution of MYPT1 and PKA

6. General discussion

Abbreviations

5-HT	5-hydroxytryptamine (serotonin)
αIIbβ3	Integrin alpha IIb beta 3
α2β1	Integrin alpha 2 beta 1
AA	Amino acid(s)
AC	Adenylyl cyclase
ACD	Acid citrate dextrose
ADAMTS13	A disintegrin and metalloproteinase with a thrombospondin type 1 motif, member 13
ADP	Adenosine 5'-diphosphate
AKAP	A-kinase anchoring protein
ANOVA	Analysis of variance
APS	Ammonium persulfate
Arp2/3	Actin-related protein 2/3
ATP	Adenosine triphosphate
BCA	Bicinchoninic acid
Bis	N,N-methylene bis-acrylamide
Bp	Base pairs
BSA	Bovine serum albumin
cAMP	Cyclic adenosine 3',5'-monophosphate
Cdc42	Cell division control protein 42
cGMP	Cyclic guanosine 3',5'-monophosphate
cDNA	complementary DNA
COX	Cyclooxygenase
c-Src	Cellular sarcoma
dH_2O	distilled water
DAG	Diacylglycerol
DMEM	Dulbecco's Modified Eagle's Medium
DMSO	Dimethyl Sulfoxide

DNA	Deoxyribonucleic acid
dNTP	Deoxyribonucleotide triphosphate
DTS	Dense tubular system
DTT	Dithiothreitol
E.coli	*Escherichia coli*
ECL	Enhanced chemiluminescence
ECM	Extracellular matrix
EDTA	Ethylenediaminetetraacetic acid
EGTA	Ethyleneglycoltetraacetic acid
eNOS	Endothelial nitric oxide synthase
E-NTPDase-1	Ecto-nucleoside triphosphate diphosphohydrolase-1
ER	Endoplasmic reticulum
ERK	Extracellular stimuli response kinase
FBS	Fetal bovine serum
FcR γ-chain	Fc receptor gamma chain
FCS	Fetal calf serum
FITC	Fluorescein isothiocyanate
GAPDH	Glyceraldehyde-3-phosphate dehydrogenase
GFP	Green fluorescent protein of *Aequorea victoria*
GKAP	Guanylate kinase-associated protein
GP	Glycoprotein
GPIb-V-IX	Glycoprotein Ib-V-IX receptor complex
GPCR	G protein-coupled receptor
GPVI	Glycoprotein VI
GSNO	S-nitrosoglutathione
GTP	Guanosine 5'-triphosphate
HEK	Human embryonic kidney 293 cell line
HeLa	Carcinoma cell line
HEPES	4-(2-Hyrdoxyethyl)-1-piperazineethanesulfonic acid

HRP	Horseradish peroxidase
Ht31	Human thyroid clone 31 (AKAP disruptor peptide)
HUVECs	Human umbilical vein endothelial cells
Ig	Immunoglobulin
IL-8	Interleukin 8
iNOS	Inducible nitric oxide synthase
IP_3	Inositol 1, 5, 4-triphosphate
IPTG	Isopropyl β-D-1-thiogalactopyranoside
ITAM	Immunoreceptor tyrosine-based activatory motif
ITIM	Immunoreceptor tyrosine-based inhibitory motif
kDa	Kilo Dalton
LAT	Linker for activation of T cells
MAPK	Mitogen activated protein kinases
MCP-1	Monocyte chemoattractant protein 1
MDCK	Madin-Darby Canine Kidney epithelial cells
MIP1α	Macrophage inflammatory protein 1α
MLC	Myosin light chain
MLCK	Myosin light chain kinase
MLCP	Myosin light chain phosphatase
MOPS	3-(N-Morpholino) propanesulfonic acid
mRNA	Messenger ribonucleic acid
MYPT1	Myosin light chain phosphatase
NP-40	Nonidet P-40
OCS	Open canalicular system
OD	Optical density
PAGE	Polyacrylamide gel electrophoresis
PAR1	Protease-activated receptor-1
PAR4	Protease-activated receptor-4
PBG	PBS-BSA-gelatin mix

PBS	Phosphate buffered saline
PC	Phosphatidylcholine
PCR	Polymerase chain reaction
PDE	Phosphodiesterase
Pen/Strep	Penicillin/Streptomycin
PF4	Platelet factor 4
PFA	Paraformaldehyde
PGE_1	Prostaglandin E1
PGF2α	Prostaglandin F2α
PGH_2	Prostaglandin H2
PGI_2	Prostacyclin
PI3K	Phosphatidylinositol 3-kinase
PIP2	Phosphatidylinositol 4, 5-bisphosphate
PKA	Protein kinase A
PKAc	Protein Kinase A catalytic subunit
PKC	Protein kinase C
PKG	Protein kinase G
PLA_2	Phospholipase A_2
PLCβ	Phospholipase C beta
PLCγ2	Phospholipase C gamma 2
PMSF	Phenylmethanesulfonylfluoride
Ponceau S	3-Hydroxy-4-[2-sulfo-4-(s1`ulfo-phenylazo)phenylazo]-2,7-naphthalindisulfon acid
PPP	Platelet poor plasma
PRP	Platelet rich plasma
PS	Phosphatidylserine
PTvWD	Platelet-type von Willebrand disease
PVDF	Polyvinylidene fluoride
RANTES	Regulated on activation, normal T cell expressed and secreted

ROCK	Rho kinase
RhoGEF	Rho guanine nucleotide exchange factor
SAP	Shrimp alkaline phosphatase
SCCS	Surface connected open canalicular system
SDS	Sodium dodecyl sulphate
SEM	Standard error of the mean
SFK	Src family kinase
sGC	Soluble guanylyl cyclase
SH2	Src homology 2
SH3	Src homology 3
SLP-76	Src homology 2 domain-containing leukocyte protein of 76 kDa
SMCs	Smooth muscle cells
SNARE	Soluble N-ethylmaleimide-sensitive fusion protein attachment protein receptor
Syk	Spleen tyrosine kinase
TAE	Tris-Acetate-EDTA
TAFI	Thrombin activated fibrinolysis inhibitor 1
Taq	*Thermus aquaticus*
TBE	Tris-Borate-EDTA
TBS-T	Tris buffered saline with Tween 20
TE	Tris-EDTA
TEMED	N,N,N',N'-tetramethylethylenediamine
Tris	Trishydroxyaminomethane
TRITC	Tetramethylrhodamine
TXA_2	Thromboxane A_2
VASP	Vasodilator-stimulated phosphoprotein
vWF	von Willebrand factor
WASP	Wiskott-Aldrich syndrome protein
X-Gal	5-bromo-4-chloro-3-indolyl-β-D-galactopyranoside

Amino acid abbreviations

A	Ala	Alanine
C	Cys	Cysteine
D	Asp	Aspartic Acid
E	Glu	Glutamic Acid
F	Phe	Phenylalanine
G	Gly	Glycine
H	His	Histidine
I	Ile	Isoleucine
K	Lys	Lysine
L	Leu	Leucine
M	Met	Methionine
N	Asn	Asparagine
P	Pro	Proline
Q	Gln	Glutamine
R	Arg	Arginine
S	Ser	Serine
T	Thr	Threonine
V	Val	Valine
W	Trp	Tryptophan
Y	Tyr	Tyrosine

Acknowledgements

First, I would like to thank Allah Almighty for giving me strength and stamina to finish this long and demanding journey. Without the support and help of a number of people, this PhD would not have been possible. I am hugely indebted to my supervisors, Dr Francisco Rivero and Professor Khalid Naseem. They have been incredibly helpful and supportive, and their achievements have been an inspiration to me. I would also like to extend my gratitude to the University of Hull for funding my PhD.

I would like to express my deepest thanks to my colleagues for their support. Dr Ahmed Aburima's advice and assistance with the practical and academic sides of my research have been invaluable. Thanks for being patient with me and answering all my questions. Dr Ji Wei and Dr Pooja Joshi have been very generous, supportive and incredibly helpful friends. Their knowledge and assistance in cellular and molecular biology have helped me greatly. Pooja, I owe you a big debt of gratitude. Thank you so much for your encouragements along the way.

Members of the entire platelet group, past and present, thanks for the many enjoyable chats and good memories for the last 3 years. Anisha, Yusra, Kochar, Branden, Matt, Andrew, David S, Sandrine, Peggy, Mihray, Zaher, Yusuf, David R, Lloyd, Martin, Costantine, Arti, Robert, Cassey and Katie, I will always treasure your friendships and enduring personalities.

Million thanks to every single blood donor, without their help this work would not be possible. I am also very thankful to my friends, Dr Shakoor, Waqas, Hassan and Naveed for their unconditional friendship. Thank you all.

I would also like to thank my mother, brothers and sister for all their prayers and my wife and daughter for their ongoing and unending support. Life would not have been nearly as much wonderful as it is now without you all. I am so grateful to have you all in my life. Rayann, you have been such an amazing daughter. I love you lots.

Finally, I would like to thank my late father, Waqif Shah Khalil, for all the sacrifices he has made to build our future. I miss you a lot, abbu. I dedicate this thesis to you.

Author's declaration

I confirm that this work is original and that if any passage(s) or diagram(s) have been copied from academic papers, books, the Internet or any other sources these are clearly identified by the use of quotation marks and the reference(s) is fully cited. I certify that, other than where indicated, this is my own work and does not breach the regulations of HYMS, the University of Hull or the University of York regarding plagiarism or academic conduct in examinations. I have read the HYMS Code of Practice on Academic Misconduct, and state that this piece of work is my own and does not contain any unacknowledged work from any other sources.

Chapter 1: General introduction

Platelets are specialised blood cells that play pivotal roles in haemostasis, thrombosis, immune cells recruitment, inflammation, wound healing and angiogenesis (Boilard *et al*., 2010; Leslie, 2010). Out of these functions, the primary physiological role of platelets is the formation of a haemostatic plug that arrests blood loss at the site of vascular injury. However, this function must be tightly regulated as excessive activation leads to thrombosis and results in pathological conditions such as myocardial infarction, ischemic heart failure, stroke, deep venous thrombosis and pulmonary embolism (Davi and Patrono, 2007). On the other hand, defective activation of platelet leads to life threatening bleeding disorders including Bernard-Soulier syndrome, Glanzmann's thrombasthenia, platelet storage pool diseases and platelet-type von Willebrand disease (PTvWD) (Kirchmaier & Pillitteri, 2010).

Under normal physiological conditions platelets are in a quiescent “non-adherent” state due to the presence of endothelial derived anti-thrombogenic factors such as nitric oxide (NO) and prostacyclin (PGI_2). Both NO and PGI_2 trigger a series of intracellular events via cyclic nucleotide-mediated protein kinase G (PKG) and protein kinase A (PKA) that keeps platelets in a non-activatory state (Smolenski, 2012). However, the exact molecular mechanism of PKA and PKG mediated platelet inhibition is not clearly defined. In platelets, there is a wide range of substrate proteins of PKA, such as glycoproteins, G-protein coupled receptors (GPCRs), cytoskeleton proteins, phosphatases and kinases, indicating that the PKA signalling pathway is involved in almost every aspect of platelet function. This chapter will review in detail the literature regarding platelet biology with particular focus on PKA-mediated regulation of myosin light chain phosphatase (MLCP).

1.1 Platelets

Blood platelets were first described by Max Schutze in 1865 as small "spherules" of the circulatory system. They were later characterised in detail by G. Bizzozero in 1882, who described them as *piastrine*, "little plates" that play an important role in blood coagulation and thrombosis (Bizzozero, 1882). Mammalian platelets are microscopic (0.5 to 3 µm in diameter), anucleated disc shaped fragments of the megakaryocytes with a life span of 5-9 days in circulation. The normal platelet count in healthy individual is 150-400 x 10^3/µl of blood. A healthy person can produce up to 10^{11} platelets per day (Italiano & Hartwig, 2007).

1.1.1 Platelet formation

Platelets are produced from the cytoplasm of their progenitor cells, the megakaryocytes in a process called thrombopoiesis (Ogawa, 1993). Megakaryocytes are the largest (50-100 µm) bone marrow cells that account for less than 1% of the total nucleated bone marrow cells (Patel *et al*., 2005). Like other blood cells, they are also derived from pluripotent haematopoietic stem cells in the bone marrow through a process called megakaryopoiesis. However, recent studies have revealed that stem cell-like megakaryocyte progenitors share many features with the pluripotent haematopoietic stem cells and are directly involved in megakaryopoiesis during acute inflammation (Haas *et al*., 2015). To assemble and release platelets, megakaryocytes undergo a series of endomitosis (DNA replication without cell division), differentiation and maturation stages in which their cytoplasm is arranged into long pseudopodial projections called proplatelets and the nucleus is extruded. These proplatelets are then released into circulation through a mechanism requiring thrombopoietin, a cytokine required for megakaryocytes to synthesis platelets (Patel *et al*., 2005). Thrombopoietin is a primary megakaryocyte growth and development factor responsible for proliferation, maturation and differentiation of megakaryocytes (Kaushansky, 2006). Although megakaryocytes develop in the bone marrow, they can migrate into the blood circulation and as a result platelet biogenesis may occur at non-

marrow sites (Machlus & Italiano, 2013). Recent literature suggests the presence of a large number of megakaryocytes in intravascular sites within the lung, where they actively release platelets. The contribution of the lungs to platelet formation accounts for almost 50% of the total circulating platelets (Lefrançais *et al*., 2017).

A single megakaryocyte can produce up to 2000-5000 new discoid shaped platelets. The total time required for megakaryocyte from endomitosis to platelets release is approximately 5 days in human and 2-3 days in mice (Machlus & Italiano, 2013). Mouse platelets are similar to human platelets; however, they are smaller in size (mean volume ~4.7 vs. ~7.5-10 fl) and more abundant in circulation (~1.1x 10^6/µl of blood) (Schmitt *et al*., 2001). Once aged, platelets are removed from circulation via phagocytosis by reticuloendothelial cells primarily in the spleen and liver.

1.1.2 Platelet ultrastructure

Studies investigating the ultrastructural features of platelets distinguish three different zones, peripheral zone, sol-gel zone and organelle zone. The peripheral zone comprises the thicker external coat called glycocalyx. This dynamic structure is randomly embedded with numbers of glycoprotein receptors, such as GPIb-IX-V, $\alpha_2\beta_1$ and $\alpha_{IIb}\beta_3$ that are involved in platelet aggregation and adhesion to the exposed subendothelial matrix (White & Gerrard, 1976). Underneath the glycocalyx is the lipid bilayer that is composed of phosphatidylcholine and sphingomyelin in the outer leaflet and phosphatidylserine and phospatidylethanolamine in the inner leaflet. During platelet activation these inner leaflet anionic phospholipids play an important role in blood coagulation (Zwaal *et al*., 1998). Underneath the lipid bilayer is a submembrane area that takes part in signal transduction due to the presence of signalling and cytoskeleton molecules as well as the cytoplasmic domains of transmembrane receptors. The surface connected open canalicular system (SCCS) is not only part of the plasma

membrane but also weaves through the platelet cytoplasm and functions in granule release (White, 2007).

The sol-gel zone is composed of a marginal band of microtubules, a spectrin-based membrane skeleton and a filamin-based cytosolic actin network. This zone is primarily responsible for the shape, stability and contours of plasma membrane in non-activated platelets and rapid changes in shape in the activated platelets.

The organelle zone is majorly comprised of alpha granules, dense granules, lysosomal granules, mitochondria, dense tubular system (DTS), free glycogen particles and energy storing glycosomes. Alpha granules are the most abundant of all platelet organelles, 40 to 80 per platelet, are approximately 200-500 nm in diameter and comprise 10% of total platelet volume. Alpha granules are rich in von Willebrand Factor (vWF), P-selectin, thrombospondin, coagulation factor V, fibrinogen and chemokines, which plays an important role in haemostasis, immunity, inflammation and wound healing (Blair & Flaumenhaft, 2009). Dense granules are less abundant, 3 to 8 per platelet, approximately 150 nm in diameter and contain nucleotides (ADP, ATP, GTP, GDP), membrane proteins (CD63/LAMP3, LAMP2), neurotransmitters (serotonin) and ions (pyrophosphate, calcium and magnesium) that take part in platelet activation (Flaumenhaft & Koseoglu, 2016). Platelet lysosomal granules are few in number, 0-3 per platelet, are approximately 200-250 nm in diameter and are rich in lysosomal membrane proteins (LAMP1, LAMP2, CD63), cathepsins, and acid hydrolases that are involved in the degradation of carbohydrates, proteins and lipids (Fukami *et al*., 2001). Platelet mitochondria and glycosomes are fewer in numbers and are significantly involved in the energy metabolism of platelets (Flaumenhaft & Koseoglu, 2016). The platelet DTS is believed to be the residual of smooth endoplasmic reticulum from the bone marrow megakaryocyte that mainly store calcium and magnesium and is also involved in the thromboxane synthesis (Blair & Flaumenhaft, 2009). The ultrastructural features of platelet are shown in Figure 1.1.

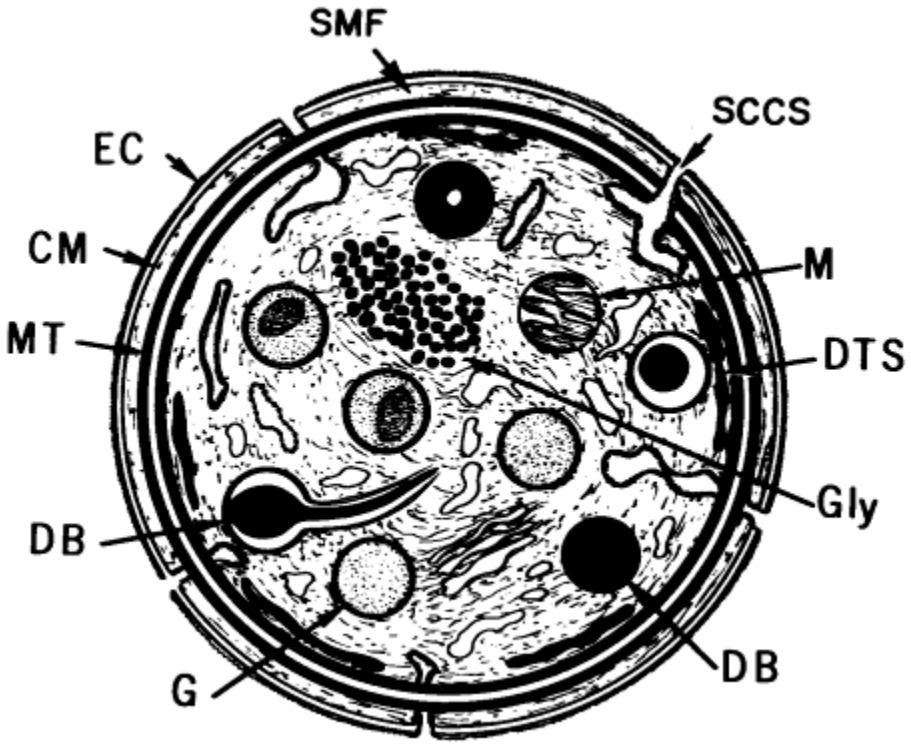

Figure 1.1: Schematic representation of ultrastructural components of blood platelets. The peripheral zone is composed of exterior coat (EC) also called glycocalyx, trilaminar unit membrane (CM), submembrane area (SMF) and channels of surface connected canalicular systems (SCCS). The sol-gel zone comprises a circumferential microtubules band (MT), submembrane actin filaments (SMF) and cytosolic actin network that is embedded with mitochondria (M), alpha granules (G), dense granules (DB), glycogen (Gly) and channels of dense tubular system (DTS). Taken from White & Gerrard, 1976.

1.2 Role of platelets in haemostasis

Haemostasis is an essential physiological process that stops bleeding at sites of vascular injury. This process is primarily divided into two waves, primary haemostasis and secondary haemostasis. Blood platelets are considered as chief mediators of both primary and secondary haemostasis. Under normal physiological conditions platelets are in an inactive state, however, upon vascular damage platelets react quickly, undergo a series of sequential events such as adhesion, activation, granule secretion and aggregation (primary haemostasis events); and, moreover, take part in cell based thrombin synthesis (secondary haemostatic response), which markedly increases haemostatic events and arrest of blood loss at the site of vascular damage.

1.2.1 Platelet adhesion

Under physiological conditions the majority of blood platelets never interact with the endothelial surface during their entire life. However, following vascular injury to the blood vessel wall, the endothelial barrier is compromised and the prothrombotic extracellular matrix (ECM) proteins such as vWF, collagen, laminin, fibronectin and thrombospondin are exposed to flowing blood (Ruggeri & Mendolicchio, 2007). Circulating platelets promptly adhere to these exposed thrombogenic proteins via an array of surface adhesion receptors that result in platelet adhesion and subsequent activation.

This initial interaction is a coordinated process that varies among different types and sizes of blood vessels (Varga-Szabo *et al*., 2008). In venous circulation and large arteries, where platelets are in low shear rate (20-200/s), platelets interact mainly with collagen, fibronectin and laminin, whereas in arterioles (300-800/s) and stenotic blood vessels (800-10,000/s) platelets are in high shear rate environment and interact primarily with immobilised vWF via their surface glycoprotein Ib alpha (GPIbα) (Dopheide *et al*., 2002; Goto *et al*., 1995). These initial interactions of platelets with ECM proteins are very important to decelerate

circulating platelets, establish stable adhesion and subsequent activation responses that are prerequisite for normal haemostasis. The model of platelet adhesion and activation is illustrated in figure 1.2.

1.2.1.1 Initial interaction of platelets with vWF

vWF, a multimeric adhesive glycoprotein is mainly generated by endothelial cells and bone marrow megakaryocytes. Endothelial vWF is either stored in Weibel-Palade bodies or secreted in the blood stream, whereas megakaryocytic vWF is primarily stored in the α-granules of blood platelets (De Meyer *et al*., 2009). Upon vessel damage, circulating vWF interacts with exposed collagen via its A1 and A3 domains (Hoylaerts *et al*., 1997; Lankhof *et al*., 1996). This immobilised vWF then sequesters circulating platelets by interacting with the GPIbα subunit of the GPIb-V-IX complex via its A1 domain (Lopez & Dong, 1997).

Under normal conditions, circulating vWF is unable to associate with platelet GPIbα as the binding domain A1 stays encrypted (Martin *et al*., 2007). This initial tethering of vWF and GPIbα is responsible for platelets to slow down and a rolling effect is seen in the direction of blood flow where platelets stay in close contact with the exposed ECM until stable adhesion takes place via several high affinity β1 and β3 integrins. The importance of GPIbα-vWF interaction is evident in both von Willebrand disease and Bernard-Soulier syndrome where patients have severe bleeding disorders due to deficiencies of either vWF or GPIbα (De Meyer *et al*., 2009; Salles *et al*., 2008).

1.2.1.2 Initial interaction of platelets with collagen

Collagen is considered as one of the most potent prothrombotic factors of the ECM that trigger platelet activation, aggregation and coagulation activity through both direct and indirect (via vWF) pathways (Varga-Szabo *et al*., 2008; Broos *et al*., 2011; Clemetson, 2012). Over 20 different types of collagen have been reported so far of which 9 are mainly present in the vessel wall. Collagen type I and III are

considered as the two major components of the ECM of blood vessel (Nieswandt & Watson, 2003). In platelets there are at least two different types of collagen receptors, GPVI and integrin $\alpha_2\beta_1$ (Farndale *et al*., 2004). Despite extensive studies, the differential contribution of these receptors in platelet function remains a subject of intense debate (Nieswandt & Watson, 2003). However, it is now generally accepted that GPVI is important for platelet activation and aggregation and integrin $\alpha_2\beta_1$ for stable adhesion (Varga-Szabo *et al*., 2008).

GPVI is a member of the immunoglobulin superfamily consisting of two immunoglobulin-like extracellular domains (D1 & D2), a mucin-like serine/threonine stalk, a transmembrane region and a short cytoplasmic tail. It interacts with Fc receptor (FcR) γ-chain via a salt bridge that acts as a signalling transduction subunit of the receptor (Moroi & Jung, 2004). Despite its major role in platelet activation, GPVI is unable to initiate stable platelet adhesion. This is majorly due to its low affinity for collagen with rapid association and dissociation rates (Pugh *et al*., 2010). Like other tyrosine kinase receptors, GPVI activation requires dimerisation in the membrane. In resting platelets, GPVI is predominantly expressed as a monomer; however, once activated, GPVI dimerises for collagen binding and triggers intracellular signalling events (Jung *et al*., 2012). The role of GPVI dimerisation for ligand binding and signalling is debateable. Onselaer et al.'s (2017) work, for instance, has shown that novel GPVI ligand, fibrin, binds to monomeric GPVI and induces GPVI signalling. The same reserachers have also reported that fibrin mediated platelet aggregation is attenuated in GPVI KO platelets and the D-dimer of fibrinogen inhibits both fibrin and collagen mediated platelet aggregation.

The importance of GPVI for platelet-collagen interaction has been well illustrated through the use of antibodies against the receptor and GPVI knockout mice. Platelets of these respective models failed to establish stable adhesion to a collagen matrix (Sachs & Nieswandt, 2007). On the other hand, collagen interaction with integrin $\alpha_2\beta_1$ not only triggers the integrin conformation change

from low affinity to high affinity state but also promotes cellular activation by augmenting GPVI-collagen interaction. Furthermore, collagen interaction with $\alpha_2\beta_1$ also initiates outside-in signalling that ultimately leads to the activation of $\alpha_{IIb}\beta_3$, an integrin responsible for stable platelet adhesion and aggregation (Bernardi *et al*., 2006).

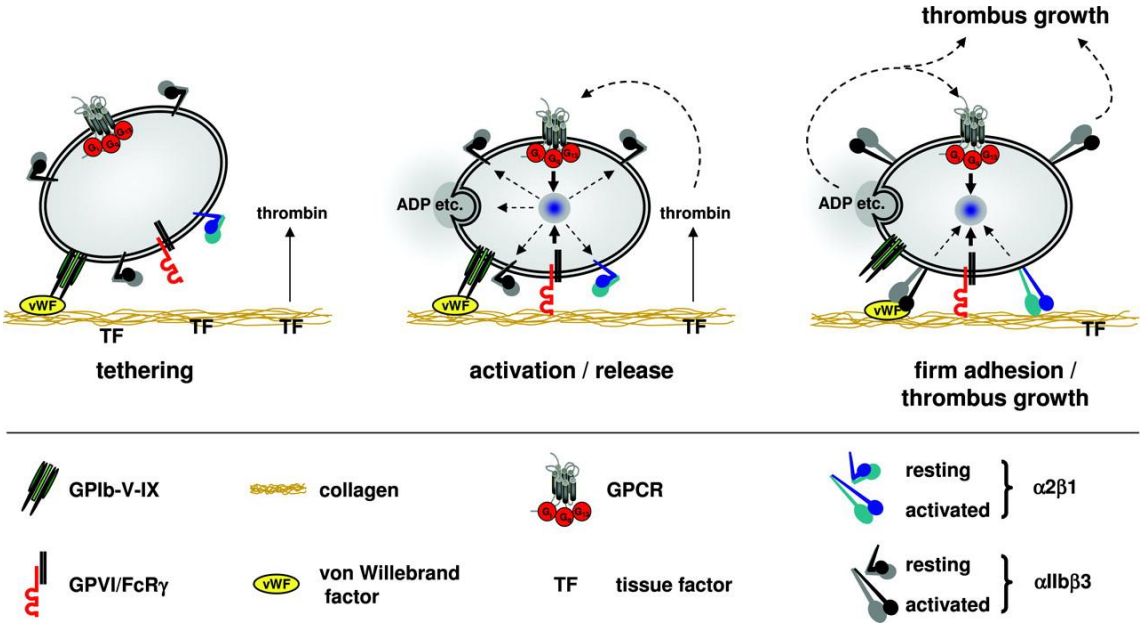

Figure 1.2: Platelet adhesion and activation at sites of vascular injury. Platelet adhesion to the ECM is triggered by GPIbα-vWF interaction followed by GPVI-collagen interaction that shifts integrins $\alpha_2\beta_1$ and $\alpha_{IIb}\beta_3$ to high-affinity state and releases ADP, TXA_2. At the same time exposed tissue factor (TF) triggers formation of thrombin that also contributes in platelet activation. Taken from Sachs & Nieswandt, 2007.

1.2.2 Platelet activation

Following adhesion to the exposed subendothelial matrix protein collagen, the platelet triggers the activation process via several intracellular signalling pathways that ultimately lead to platelet shape change, degranulation, integrins activation, aggregation and formation of a haemostatic plug. These pathways are summarised as follows.

1.2.2.1 Tyrosine kinase-mediated platelet activation

The initial interaction of collagen via GPVI or vWF via GPIbα triggers clustering of their respective receptors and initiates phosphorylation of FcRγ chain at the immunoreceptor tyrosine-based activation motif (ITAM) by Src-family kinases (SFK), Lyn and Fyn. The activation of Lyn and Fyn remains in question; however, both either stay in close proximity or bound to the proline rich region of the cytoplasmic tail of GPVI via their Src homology 3 (SH3) domain (Senis *et al*., 2013). The phosphorylation of ITAM then results in docking of spleen tyrosine kinase (Syk) via its SH2 domain, which is subsequently activated by SFK. Activation of Syk results in the phosphorylation of downstream adaptor proteins like LAT, SLP-76, Btk and Gads that causes the formation of a signalling hub called signalosome. The signalosome then finally causes the activation of phospholipase Cγ2 (PLCγ2) via tyrosine phosphorylation of its SH2 domains (Watson *et al*., 2010) (Figure 1.3). Activated PLCγ2 hydrolyses phosphatidylinositol 4, 5 bisphosphate into inositol 1, 4, 5 trisphosphate (IP_3) and membrane bound diacylglycerol (DAG) (Watson *et al*., 2005). IP_3 diffuses through the cytosol, interacts with IP_3 receptors located on the DTS and triggers an efflux of calcium ions from DTS into the cytoplasm. This increased cytosolic concentration of calcium also triggers the activation of membrane bound calcium release-activated calcium channel protein (Orai1) allowing further calcium to enter into the cell (Ahmad *et al*., 2011). Furthermore, increased levels of cytosolic calcium trigger the surface exposure of phosphatidylserine that recruits prothrombinase complex to the cell membrane and causes the formation of thrombin from prothrombin, an important player of

the coagulation cascade (Kodigepalli *et al.,* 2015). On the other hand, membrane bound DAG together with calcium activates serine/threonine protein kinase C (PKC). Both increased intracellular calcium level and activation of PKC play a major role in platelet shape change, granule secretion and integrin activation (Bye *et al*., 2016).

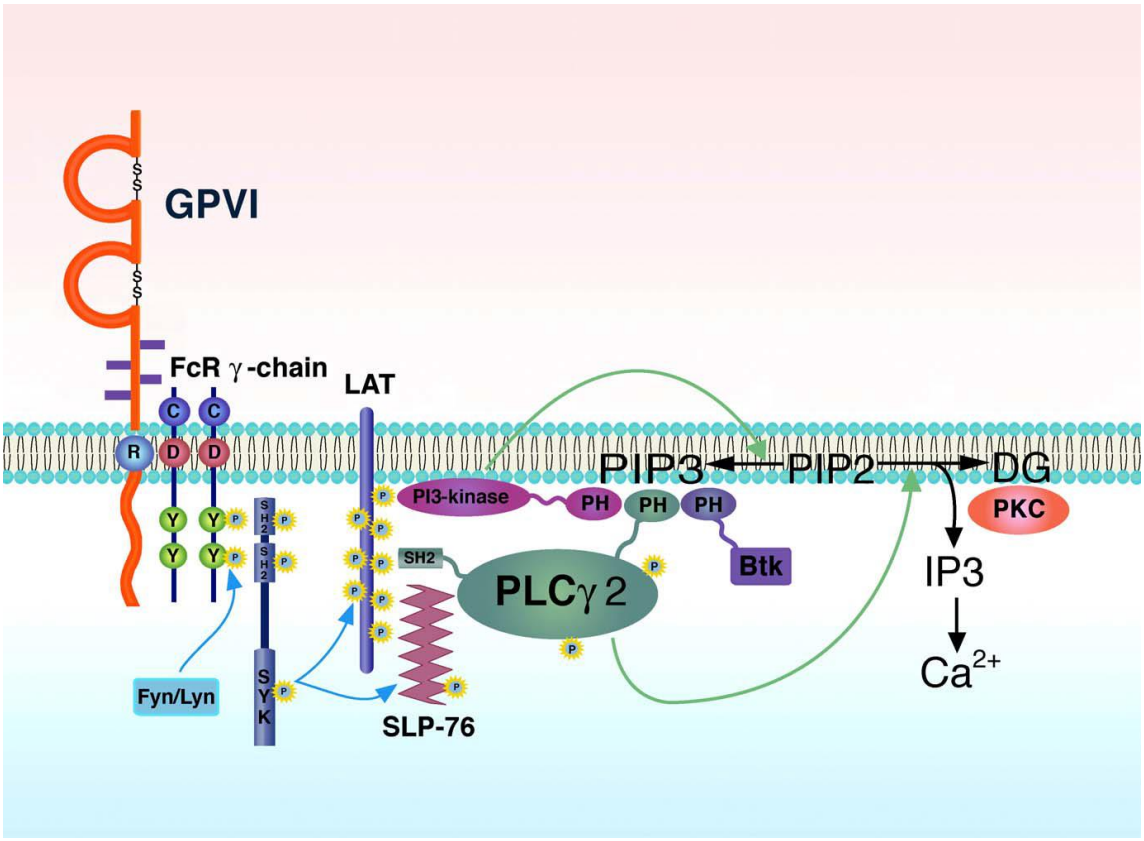

Figure 1.3: Diagram of the tyrosine kinase signalling pathway in blood platelets. Collagen mediated cross-linking of GPVI induces phosphorylation of tyrosine residues in the FcR *γ*-chain ITAM via SFK (Fyn and Lyn). This provides docking sites for Syk. SFK activates Syk and initiates phosphorylation of downstream effectors, LAT, SLP-76, Btk (signalosome) that results in PLC*γ*2 activation. PLC*γ*2 then propagates signals via PIP2 into DAG and IP_3. IP_3 activates calcium release from the DTS and DAG activates PKC that leads to platelet shape change, degranulation and subsequent platelet aggregation. Abbreviations: PH, pleckstrin-homology domain; SH2, Src-homology 2 domain; C; Cysteine, R; Arginine, D; Aspartic acid Y; Tyrosine. Taken from Moroi & Jung, 2004.

1.2.2.2 GPCR-mediated platelet activation

Platelet expresses a variety of seven transmembrane G-protein coupled receptors (GPCR) that initiate both activatory and inhibitory signalling events through heterotrimeric G-proteins. The G-proteins are composed of α, β and γ subunits (Offermanns, 2006). In an inactive state the GDP bound Gα remains tightly associated with β and γ subunits. Upon activation by agonists the GDP is substituted by GTP, the α subunit dissociates from the βγ subunits and interacts with the downstream target proteins to transmit GPCR signals. βγ subunits have also been reported to interact with the downstream effectors such as phosphatidylinositol 3-kinase (PI3K) and PLCβ during GPCR signalling, however very little is known about their function (Gurbel *et al*., 2015). G-proteins are generally divided into four families based on the identity and function of α subunits, such as $G\alpha_i$, $G\alpha_q$, $G\alpha_{12/13}$ and $G\alpha_s$ (Offermanns, 2006). All of these G-proteins are coupled to a variety of GPCRs that are activated by numbers of locally produced platelet agonists, including ADP, thromboxane A_2 (TXA_2), thrombin, ATP and PGI_2.

The ADP receptor $P2Y_1$, TXA_2 receptors TPα and TPβ, thrombin receptors PAR1 and PAR4 (PAR3 and PAR4, respectively, in mice) are all coupled with $G\alpha_q$ that stimulates the activity of phospholipase Cβ (PLCβ), which in turn hydrolyses PIP_2 into IP_3 and DAG. Both IP_3 and DAG then activate PKC and trigger the release of calcium from the intracellular DTS depot (Brass *et al*., 1997) (Figure 1.4). TP and PAR receptors are also linked with $G\alpha_{12/13}$ that activates the small GTPase RhoA (Klages *et al*., 1999). RhoA activates Rho kinase (ROCK), which phosphorylates and inhibits MLCP; this promotes the phosphorylation of myosin light chain (MLC) and MLC-mediated platelet contractile events. These contractile events are associated with platelet shape change and granule secretion (Getz *et al*., 2010). Recent studies have shown that $G\alpha_{13}$ also directly interacts with the cytoplasmic domain of β_3 integrin and plays an important role in the integrin outside-in signalling (Gong *et al*., 2010). One of the ADP receptors, $P2Y_{12}$ is coupled with $G\alpha_i$, which not only

prevents the formation of cAMP by inhibiting adenylyl cyclase activity but also stimulates PI3K. This kinase in turn activates Akt/protein kinase B (PKB), which results in calcium mobilisation and granule secretion (Garcia *et al*., 2010).

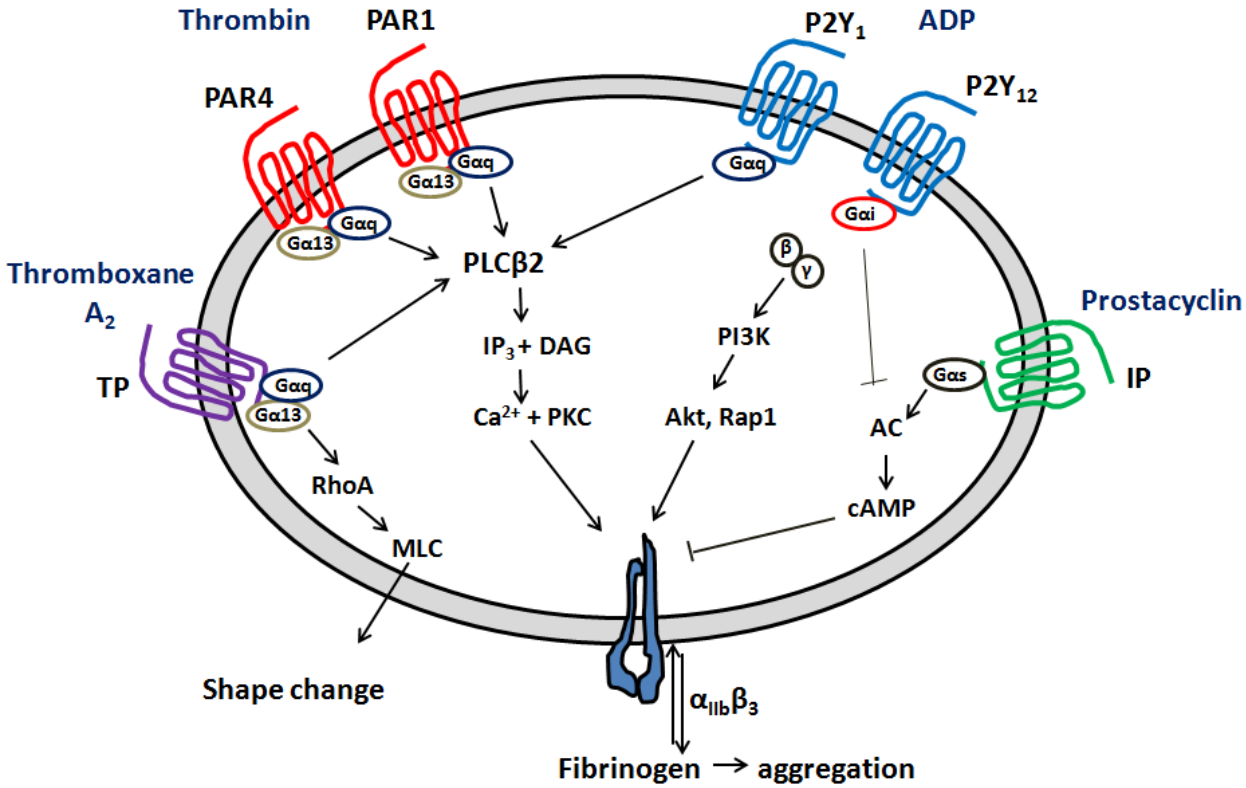

Figure 1.4: GPCR signalling in blood platelets. Schematic diagram of platelet agonists, GPCRs and their respective G-protein-mediated platelet signalling cascades that result in platelet activation.

1.2.2.3 Integrin $\alpha_{IIb}\beta_3$ mediated platelet activation

The final target of the above signalling pathways initiated via GPIb, GPVI and GPCRs is the activation and cross-linking of integrin $\alpha_{IIb}\beta_3$, the primary integrin for stable platelet adhesion and aggregation (Ma *et al*., 2007). Under resting conditions integrin $\alpha_{IIb}\beta_3$ stays in a low affinity conformation for its ligands fibrinogen and vWF. This low affinity state that keeps the extracellular domains of integrin $\alpha_{IIb}\beta_3$ bent is mainly due to the association of the cytoplasmic tail regions of α and β subunits (Vinogradova *et al*., 2002). The Increased cytosolic calcium concentration that ensues upon platelet activation activates guanine nucleotide exchange factor I (CalDAG-GEFI) (Crittenden *et al*., 2004). CalDAG-GEFI then activates the Ras family small GTPase Rap1b, which interacts with Rap1 GTP-interaction adaptor molecule (RIAM) and activates cytoskeleton protein talin that leads to interact with the cytoplasmic tail of the integrin $\alpha_{IIb}\beta_3$ (Li *et al*., 2010). Consequently, the interaction between the integrin α and β subunits is disrupted, stimulating a conformational change that propagates from the cytoplasmic tail through transmembrane regions to the extracellular domains. This is referred to as inside-out signalling, which results in low affinity conformation "bent" transforming into the high affinity state "stretch", exposes integrin sites for ligand binding and mediates stable platelet adhesion, aggregation and thrombus formation (Broos *et al*., 2011).

Recently it has been shown that the interaction of kindlin-3 with the cytoplasmic domain of integrin β_3 also plays an important role in the activation process as mice lacking this protein have defective integrin activity (Malinin *et al*., 2009; Moser *et al*., 2008). However, the precise molecular mechanism how kindlin-3 activates integrin remains unclear. The importance of integrin $\alpha_{IIb}\beta_3$ is evident in a severe bleeding disorder, Glanzmann's thrombasthenia, where $\alpha_{IIb}\beta_3$ is either missing or non-functional (Bellucci & Caen, 2002).

After integrin $\alpha_{IIb}\beta_3$ becomes activated fibrinogen interacts with it and triggers a series of intracellular signalling events referred to as outside-in signalling. These

signalling events result in the interaction of $G\alpha_{13}$ with the cytoplasmic domain of β_3 and trigger the activation of SFK. SFK activates Syk and facilitates the formation of a signalosome as seen in GPVI mediated ITAM signalling (see section 1.2.2.1 and figure 1.3), which is required for PLCγ activity and subsequent platelet activation (Li *et al*., 2010). Furthermore, interaction of fibrinogen with $\alpha_{IIb}\beta_3$ also initiates aggregation responses via formation of molecular bridges between platelets.

1.2.3 Platelet shape change

Once a platelet becomes activated, the intracellular signalling events induce rapid remodelling of the platelet cytoskeleton that is responsible for shape change from biconcave disc shaped to fully spread cells at the sites of vascular injury. During this process activated platelets form various actin based molecular structures such as filopodia, lamellipodia, actin nodules and stress fibres that help platelets to increase its surface area at the site of injury (Calaminus *et al*., 2008).

In circulation, blood platelets have a discoid shape. This discoid shape is maintained by the cytoskeleton, which is composed of a marginal band of microtubules and two sets of actin networks, the spectrin-based membrane skeleton and the filamin-based cytosolic actin network (Hartwig, 2013). In resting platelets, nearly 50% of the total tubulin content is in polymerised state forming numbers of acetylated and tyrosinated microtubules organised in a circumferential marginal band (Sadoul, 2015). The antagonistic microtubule motor proteins, such as dynein and kinesin keep the marginal band in resting state, which is responsible for discoid shape of quiescent platelets. During platelet activation, the kinesin actions are inhibited and the dynein slides microtubules apart, which leads to marginal band extension. This then induces the disc-to-sphere shape transition of activating platelets (Diagouraga *et al*., 2014). This process is similar to dynein-mediated microtubules extension, which drives proplatelet production and elongation in megakaryocytes (Bender *et al*., 2015; Patel *et al*., 2005). Furthermore, upon activation the intracellular signalling events trigger the marginal band to compress at the cell centre and the microtubules become

deacetylated by histone deacetylase 6 (HDAC6), which also contributes in platelet shape change from discoid to spheroid (Aslan *et al*., 2013; Sadoul *et al*., 2012). Concurrent intracellular signalling events activate small Rho family GTPases, Cdc42, RhoA and Rac1, which are considered as chief regulators of the platelet cytoskeleton. These proteins trigger rapid polymerisation and branching of actin filaments leading to the formation of different cytoskeleton structures. In platelets, RhoA activation causes stress fibre formation via the RhoA-ROCK pathway (Yusuf *et al*., 2017), whereas Cdc42 and Rac1 have been reported in the formation of molecular structures such as filopodia and lamellipodia via activation of the Arp2/3 complex mediated by Wiskott-Aldrich Syndrome protein (WASp) and Scar/Wave proteins, respectively (Pula & Poole, 2008; McCarty *et al*., 2005; Jaffe & Hall, 2005) (Figure 1.5).

Previous reports have also suggested that a strong correlation exists between the phosphorylation of regulatory light chain of myosin IIa and the initiation of platelet shape change (Daniel *et al*., 1984). Agonist mediated platelet activation results in the phosphorylation of MLC at Ser19 via two independent pathways, calcium/calmodulin and RhoA-ROCK (Paul *et al*., 1999). This allows myosin IIa, a motor protein, to push two long actin filaments to one another by hydrolysing ATP to generate a contractile force that is responsible for platelet shape change, granule secretion and wound closure (Klages *et al*., 1999).

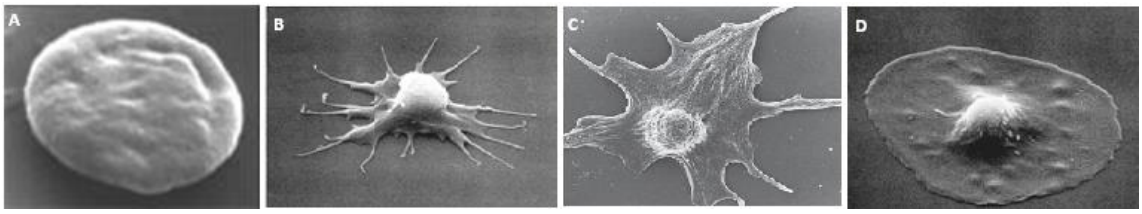

Figure 1.5: Scanning electron micrographs of various stages of platelet shape change. A) Resting platelet of discoid shape, **B)** filopodia, finger like projections formed after platelet activation, **C)** lamellipodia (sheet-like structures) formation and early spreading **D)** fully spread platelet. Taken from White, 2007.

1.2.4 Platelet secretion

Following platelet activation and cytoskeleton rearrangement, the centralisation and secretion responses of platelet granules take place. In resting state platelet granules are randomly distributed throughout the cytoplasm. Upon activation granules accumulate in the centre of the cell and fuse with one another and with the OCS before emptying their contents in the local extracellular environment (Flaumenhaft, 2003). Degranulation via interaction with the plasma membrane has also been reported in blood platelets (Offermanns, 2006). The molecular mechanism behind this involves a group of proteins present both on platelet granules and plasma membrane called soluble NEM-sensitive attachment protein receptors (SNARE) proteins that regulate degranulation responses (Flaumenhaft, 2003). Following secretion, the granular contents not only recruit nearby platelets at the site of injury but also promote platelet activation in both autocrine and paracrine fashion (Broos *et al*., 2011) that significantly contribute in thrombus growth.

As mentioned earlier (section 1.1.2), in platelets there are three different types of granules, alpha, dense and lysosomal that play a critical role in normal platelet activity. Alpha granules release a number of adhesive (fibrinogen, vWF, fibronectin, thrombospondin, vitronectin), coagulative (factor V, XI, XIII), angiogenic (VEGF, IGF-1), anti-angiogenic (endostatin) and fibrinolytic (PAI-1, TAFI) proteins that are responsible for platelet-platelet interaction, angiogenesis, clot formation and clot dissolution (Italiano *et al*., 2008; Ren *et al*., 2008). Studies suggest that platelets contain a heterogeneous population of alpha granules that are differentially packaged with certain angiogenesis regulatory proteins. Immunofluorescence and immunoelectron microscopy showed that pro-angiogenic protein, VEFG, is housed in one set of alpha granules, while anti-angiogenic protein, endostatin, in second set of alpha granules (Italiano *et al*., 2008). Similar heterogeneous populations of alpha granules were also reported in mouse megakaryocytes. Consistently, other studies have also reported similar

heterogeneous populations of alpha granules that are separately housed with vWF and fibrinogen (Sehgal & Storrie, 2007). Furthermore, stimulating platelets with different agonists cause differential release of certain granular cargo (Chaterjee *et al*., 2011). This leads to the idea that platelet releases specific sets of cargo in response to specific agonist. Furthermore, alpha granules also release various proinflammatory chemokines and cytokines, such as CXCL4 (PF4), CXCL7 (β-thromboglobulin), CCL5 (RANTES), CXCL8 (IL-8), CCL2 (MCP-1), CCL3 (MIP1α) that promote the activation and the chemotaxis of leukocytes and take part in the inflammatory and immune responses (Blair & Flaumenhaft, 2009).

Dense granules, on the other hand, contain fewer proteins but are equally important in the direct amplification of platelets activation. They release large amounts of small molecules including ADP, ATP, serotonin and calcium that amplify activation responses, aggregation and thrombus formation (Ren *et al*., 2008).

ADP strongly activates platelets via interaction with two purinergic GPCRs on the platelet surface, $P2Y_1$ and $P2Y_{12}$ (Murugappa & Kunapuli, 2006). Binding of ADP with $G\alpha_q$ coupled $P2Y_1$ increases intracellular calcium level that triggers platelet shape change and aggregation responses via activation of PLCβ2 (Kahner *et al*., 2006). Studies have also shown that ADP induced platelet shape change does not necessarily require calcium mobilisation because it also triggers the RhoA-ROCK pathway that directly induces shape change via MLC phosphorylation (Suzuki*et al*., 1999). Binding of ADP with $G\alpha_i$ coupled $P2Y_{12}$ is essential for increased platelet aggregatory responses by inhibiting adenylyl cyclase activity. Thus, the activation of both ADP receptors is important for maximum calcium mobilisation and full platelet aggregatory responses. Foster and co-workers (2001) have reported that the deficiency of ADP receptors markedly affects platelet aggregation.

The increased intracellular calcium also triggers the activation of cytoplasmic phospholipase A_2 (PLA_2), which cleaves membrane bound phosphatidylcholine (PC)

into arachidonic acid. The arachidonic acid is then converted by cyclooxygenase-1 (COX-1) and thromboxane synthase into TXA_2, a potent but short-lived prostanoid (Offermanns, 2006). Following production, TXA_2 diffuses through the plasma membrane into the microenvironment where it acts on its receptors in autocrine and paracrine manner. TXA_2 binds to two thromboxane receptors, TPα and TPβ, which are both associated with $G\alpha_q$ and $G\alpha_{12/13}$, activate calcium mobilisation, and platelet aggregation, thus drastically amplifying platelets activation responses (Bye *et al*., 2016). Deficiency of TP receptors significantly prolonged bleeding time and impaired platelet aggregatory responses (Thomas *et al*., 1998).

1.2.5 Platelet aggregation

Platelet aggregation is a dynamic and a complex process that is initiated by platelet adhesion, activation and subsequent platelet-platelet interaction facilitated by numerous soluble adhesive proteins (fibrinogen, vWF, fibronectin) and membrane receptors (GPIb, $\alpha_{IIb}\beta_3$) at the site of vascular injury (Jackson, 2007). This complex process has long been recognized as an important physiological event that is responsible for haemostatic plug formation and thrombosis (Bizzozero, 1882). Recent technical advances in platelet aggregation processes confirmed that this dynamic mechanism chiefly relies on the rate of blood flow at the sites of vascular injury (Goto *et al*., 1998). Three distinct mechanisms of platelet aggregation have been proposed *in vivo*.

Under low shear rates (<1000 s^{-1}) usually found in venules and large veins, this process is primarily initiated by $\alpha_{IIb}\beta_3$ and fibrinogen interactions. *In vitro* studies have shown that this process is independent of vWF-GPIbα interactions, as inhibition of vWF did not abolish platelet aggregation on collagen-coated surfaces (Savage *et al*., 1998). However, *in vivo* studies in deep vein thrombosis mouse models have revealed that vWF is also a requirement for platelet aggregation under low shear rate (Brill *et al*., 2011).

At shear rates between 1000-10000 s^{-1}, which are typically found in small arteries, platelet aggregation is proposed to occur in two stages. The first stage relies on the adhesive properties of GPIbα of flowing platelets with the immobilised vWF. This interaction initiates dynamic thin membrane protrusions termed membrane tethers. The rate and extent of elongation of these membrane tethers are under the influence of high shear rate and are responsible for slowing down circulating platelets for sustained platelet-platelet interactions and subsequent platelet aggregation. Dopheide and co-workers (2002) have reported the importance of vWF and GPIbα in the formation of membrane tether by using antibodies targeting the vWF-GPIbα interaction under flow. They have reported that an antibody against the A1 domain of vWF markedly reduced membrane tether formation and significantly affected the slowing down of circulating platelets. The second stage depends on the irreversible activation of integrin $\alpha_{IIb}\beta_3$ that is significantly mediated by soluble agonist released in the micro environment by stable platelet adhesion and activation responses and is also responsible for the formation of stable platelet aggregates (Kulkarni *et al*., 2000). The functional importance of integrin $\alpha_{IIb}\beta_3$ is evident in many mouse models of thrombosis where mice lacking β_3 integrin exhibit no thrombi.

Finally, at shear rate greater than 10,000 s^{-1} mostly seen in stenotic vessels, platelet aggregation is entirely dependent on vWF and GPIbα interactions and independent of platelet or integrin $\alpha_{IIb}\beta_3$ activation; however, the physiological relevance of this interaction is not clear (Ruggeri, 2007; Reininger, 2008).

1.2.6 Thrombus consolidation

The irreversible activation of $\alpha_{IIb}\beta_3$ and the fibrinogen mediated platelet aggregation lead to the formation of initial haemostatic plug. This initial plug provides a procoagulant surface area, expressing phosphatidylserine (PS), which facilitates the conversation of prothrombin into thrombin by forming prothrombinase complex (activated factor X, activated factor V and calcium). Once

active, thrombin, a key serine protease of the blood coagulation cascade, further encapsulates and strengthens the haemostatic plug by hydrolysing $\alpha_{IIb}\beta_3$ bound fibrinogen into fibrin mesh (Brass *et al*., 2005). Recent studies have reported that the centre of the growing thrombus (called the core), where the concentration of thrombin is at peak, is composed of fully activated platelets. By contrast, the periphery of the thrombus (called the shell) contains less activated platelets and is mainly under the influence of ADP (Welsh*et al*., 2014; Stalker *et al*., 2013; Brass *et al*., 2006). In this core/shell model the core is proposed to arrest blood loss at the site of injury, whereas the shell restricts the growth of thrombus by reducing platelet accumulation (Golebiewska & Poole, 2015). Several other participants have also been reported to take role in the thrombus stability, such as junctional adhesion molecules (JAM-A and JAM-C), ephrine family kinases (EphA4, EphB1 and ephrin B),gap junction proteins (connexin 37 & connexin 40) and soluble CD40 ligand; however, $\alpha_{IIb}\beta_3$ is regarded as the key player (Vaiyapuri *et al*., 2013 & 2012; Naik *et al*., 2012; Prevost *et al*., 2002; Andre *et al*., 2002).

1.3 Regulation of platelet function

Upon vascular injury, platelets adhere to immobilised vWF or exposed collagen of the injured vessel wall, which triggers a series of intracellular activatory events including calcium mobilisation, degranulation, integrins activation and subsequent platelet thrombus formation required for haemostasis (Ozaki *et al*., 2005). Under physiological conditions, these intracellular events are tightly regulated due to the presence of various negative regulatory mechanisms. For example, platelet activatory signals trigger phosphorylation of platelet endothelial cell adhesion molecules like PECAM-1 or CD31. PECAM-1 is a member of the Ig superfamily that is composed of immunoreceptor tyrosine-based inhibitory motif (ITIM) that inhibits platelet activation. PECAM-1 attenuates thrombin and $\alpha_{IIb}\beta_3$ mediated platelet activation as well as GPVI and GPIbα mediated thrombus formation (Wee & Jackson, 2005; Rathore *et al*., 2003; Cicmil *et al*., 2002). The ITIM-containing receptor G6b-B has emerged as a critical regulator of platelet production and

activation recently (Geer *et al*., 2018). However, the molecular mechanism by which G6b-B inhibits platelet function is not fully understood. It is thought that G6b-B mediates its inhibitory functions by interacting with SH2 domain-containing protein-tyrosine phosphatases, Shp1 and Shp2, which then dephosphorylate and inactivate signalling proteins of the ITAM-containing receptor pathway (Coxon *et al*., 2017). Mice lacking G6b-B showed severe macrothrombocytopenia and aberrant proplatelet formation (Mazharian *et al*., 2012). Proteomic and transcriptomic studies revealed several other ITIM-containing receptors that regulate various platelet activatory signals. Some of these are TREM-like transcript-1, carcinoembryonic antigen-related cell adhesion molecule 1 (CEACAM1), CEACAM2 and Leukocyte immunoglobulin-like receptor subfamily B member 2 (LILRB2) (Coxon *et al*., 2017). ADAMTS13, a metalloprotease, has also been reported to down regulate platelet adhesion and thrombus formation in the injured vessel wall via cleaving large vWF multimers that are formed on the surface of growing thrombus (Chauhan *et al*., 2006). Furthermore, CD39, an ecto-nucleoside triphosphate diphosphohydrolase-1 (E-NTPDase-1) present on the membrane of endothelial cells and platelets continuously degrade platelet activators ADP and ATP into platelet inhibitor adenosine. Adenosine binds to the platelet adenosine receptor (A_2), triggers cAMP production via adenylyl cyclase and thus restricts the activation of platelets and growth of thrombus at the injury site (Marcus *et al*., 1997).

Several studies have indicated that the endothelial-derived nitric oxide (NO) and prostacyclin (PGI_2) are the chief among all platelet negative regulators as they suppress various nodes of platelets haemostatic events including adhesion, activation, calcium mobilisation, cytoskeletal rearrangement, degranulation and aggregation (Smolenski, 2012). Both NO and PGI_2 initiate intracellular cyclic nucleotides (cAMP and cGMP) signals that interfere with platelet activity via two known serine/threonine kinases, PKA and PKG (Schwarz *et al*., 2001).

1.3.1 Platelet regulation by nitric oxide

1.3.1.1 Nitric oxide

NO is a free radical gaseous messenger that functions as platelet negative regulator, inhibits platelet adhesion, secretion and aggregation responses (Naseem & Riba, 2008). NO is synthesised from the amino acid L-arginine by the enzyme nitric oxide synthase (NOS) in either a constitutive or inducible manner (Palmer *et al*., 1988). To date three distinct isoforms of NOS have been identified, nNOS mainly expressed in neuronal cells, iNOS primarily found in immune cells and small amount in platelets and eNOS expressed in endothelial cells, red blood cells, cardiomyocytes, megakaryocytes and platelets (Gkaliagkousi *et al*., 2007; Naseem & Riba, 2008).

It is generally accepted that endothelial-derived NO regulates platelet function. However, in 1990, Radomski *et al* (1990) were the first to report the role of platelet-derived NO in the regulation of platelet activity. They have shown that platelet-derived NO is calcium/calmodulin dependent and inhibits platelet aggregation and adhesion to the growing thrombus in a negative feedback mechanism. Malinski and co-workers (1993) and later Freedman and colleagues (1997, 1999) have shown that platelet derived NO significantly inhibits platelet aggregation. Although the role of platelet derived NO is controversial, the chief regulatory of platelet functions is the endothelial cell derived NO (Naseem & Riba, 2008; Gambaryan *et al*., 2008; Lafrati *et al*., 2005; Özüyaman *et al*., 2005).

Once released by endothelial cells into the lumen of blood vessels, NO diffuses into the platelet and stimulates soluble guanylyl cyclase (sGC), which converts GTP into the cyclic guanosine 3', 5'monophosphate (cGMP) (Schmidt *et al*., 1993).

1.3.1.2 Guanylyl cyclase and cyclic GMP synthesis

Guanylyl cyclases (GCs) are a family of enzymes that catalyzes the conversion of GTP into cGMP. The family is composed of two types of GCs, soluble guanylyl

cyclases (sGC) located in the cytoplasm and particulate guanylyl cyclases (pGC) located in the membrane. In platelets only sGC has been reported so far. GCs are heterodimeric proteins composed of α and β subunits; each of the subunit comprises an N-terminal heme binding domain, a central dimerisation domain and a C-terminal catalytic domain responsible for the conversion of GTP into cGMP (Friebe & Koesling, 2003) (Figure 1.6). In platelets only α_1 and β_1 subunits are well characterised (Zabel *et al*., 1998). Once NO diffuses across the plasma membrane into the platelet cytoplasm it binds to the prosthetic heme group of the sGC and causes increase in the catalytic activity of the enzyme that result in an approximately 10-fold elevation of the cGMP level (Smolenski, 2012). Increased cGMP level activates the foremost effector, PKG that regulates various platelet activatory signalling pathways including calcium mobilisation, cytoskeleton remodelling, integrin activation and degranulation (Schwarz *et al*., 2001).

It is generally accepted that most inhibitory effects of NO in platelets are mainly regulated by sGC and cGMP. However, recent studies using platelet-specific sGC knock-out mice have also reported the stimulatory role of sGC in platelet activation. Zhang *et al* (2011) reported that sGC deficient platelets have significant defects in aggregation and ATP secretion responses to low doses of thrombin and collagen. More importantly, these mice had prolonged bleeding times and impaired thrombus formation *in vivo*. Similarly, Dangel and colleagues (2010) have also noticed prolonged bleeding time in whole body sGC deficient mice. However, Gambaryan and co-workers (2012) used similar platelet-specific and whole body sGC knock-out mouse models and found no stimulatory role of sGC in platelets activation. They suggested that NO/sGC/cGMP pathway exclusively play an inhibitory role in platelets. Hence, a possible role of sGC in platelet activation requires further investigations. Functional role of platelet sGC has also been reported in various diseases conditions, such as ischemic heart disease, diabetes and heart failure (Chirkov & Horowitz, 2007). Furthermore, NO mediated

activation of sGC and elevation of cGMP protect platelets from apoptosis (Rukoyatkina *et al*., 2011).

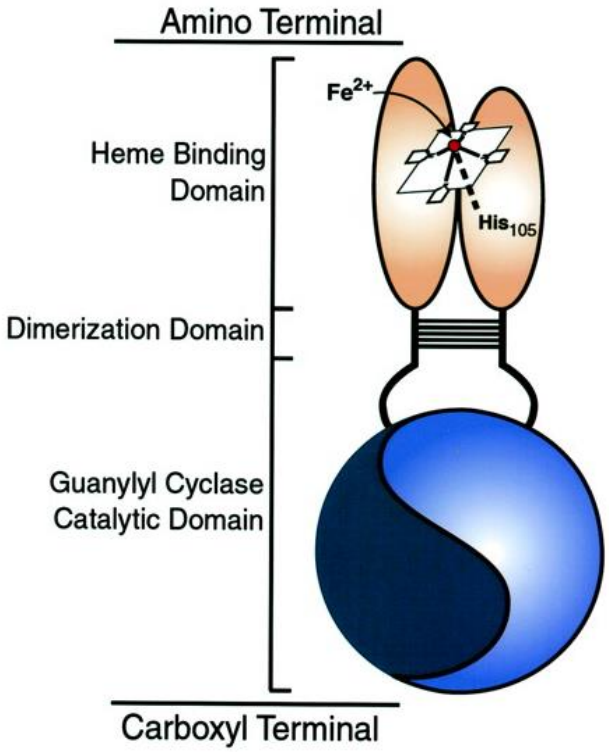

Figure 1.6: Schematic diagram of soluble guanylyl cyclase. The N-terminal heme-binding domain with a ferrous (Fe^{+2}) core that is ligated with His105 of the β subunit, followed by a central domain mediating dimerisation of α and β monomers required for catalytic activity. The C-terminal catalytic domain converts GTP into cGMP. Taken from Lucas *et al*., 2000.

1.3.1.3 Protein kinase G

Protein kinase G (PKG) is a homodimeric serine/threonine kinase that is widely distributed in many cell types including blood platelets (Hofmann *et al*., 2009). In mammals there are two homologous forms of PKG. PKG type I is usually found in the cytoplasm and is encoded by the *PRKG1* gene, whereas PKG type II is generally associated with the membrane and is encoded by *PRKG2* gene (Francis *et al*., 2010). PKG type I is further divided into two closely related isoforms generated by alternative splicing of the *PRKG1* gene, *PKGIα* and *PKGIβ*. Structurally, PKG is composed of three functional domains, N-terminal domain, regulatory domain and C-terminal catalytiFc domain on a single polypeptide chain. The N-terminal domain carries a leucine zipper motif required for homodimerisation and inhibitory residues involved in autoinhibition; the regulatory domain contains two non-identical cGMP binding sites arranged in tandem and the catalytic domain includes a Mg^{2+}/ATP subdomain and a protein substrate binding subdomain (Feil *et al*., 2003). The binding of two cGMP molecules to each regulatory domain of a homodimer triggers a conformational change that leads to the release of the catalytic domain from the N-terminal inhibitory residues and allows the phosphorylation of downstream substrate proteins (Wall *et al*., 2003). In platelets, PKGIβ is reported to be the predominant cGMP effector and is mainly membrane associated (Eigenthaler *et al*., 1992). Once activated, PKGIβ regulates various platelet activatory pathways and intracellular molecules including MLC-kinase (Nishikawa *et al*., 1984), vasodilator-stimulated phosphoprotein (VASP) (Halbrügge *et al*., 1990), PKC (Gopalakrishna *et al*., 1993), PI3-Kinase (Pigazzi *et al*., 1999), extracellular stimuli-response kinase (ERK) pathway (Li *et al*., 2001), and thromboxane A2 receptor (Reid & Kinsella, 2003) (See section 1.3.3 and Table 1.3 for more detail).

The importance of cGMP-mediated PKG in the inhibition of platelet functions has been well studied in the PKGI-knock-out models. PKGI knock-out mice have shown a strong prothrombotic phenotype. Platelets from these knock-out mice exhibited

rapid accumulation at the site of vascular injury and were unresponsive to both cGMP analogues and NO donors (Massberg *et al*., 1999; Haslam *et al*., 1999). As cGMP analogues and NO donors increase intracellular cGMP level, physiological agonists, such as thrombin, collagen, ADP, are also observed to increase cGMP level in platelets (Haslam *et al*., 1999), indicating that cGMP may possibly be taking part in the activation of platelets. Later, Li *et al* (2003) have demonstrated the activatory role of PKGI in platelet functions. They reported that PKGI knock-out mice showed prolonged bleeding time and platelets from these mice exhibited impaired responses to vWF. Furthermore, studies by Stojanovic and colleagues (2006) revealed the biphasic role of membrane permeable cGMP analogues; low doses trigger PKGI mediated platelet activation, whereas high doses initiated platelet inhibition. However, this biphasic concept has been questioned by other researchers (Marshall *et al*., 2003; Gambaryan *et al*., 2004). They have shown that platelet activation at low doses is an unspecific effect of cGMP analogues.

1.3.2 Platelet regulation by prostacyclin

1.3.2.1 Prostacyclin

Prostacyclin (PGI_2), an endogenous prostanoid, has strong vasodilatory and antithrombotic effects. It was first discovered by John Vane in 1976 and is produced from arachidonic acid in a multistep process involving the enzymes COX and prostacyclin synthase. COX exists in two main isoforms, COX-1, a constitutive isoform and COX-2, an inducible isoform synthesised by inflammatory responses (Mitchell & Warner, 2006). The first step in the production of PGI_2 involves liberation of arachidonic acid from membrane phospholipids by phospholipase A_2 (PLA_2) (Mitchell & Warner, 1999). PLA_2 exists in multiple forms; however, the cytosolic PLA_2 activated by intracellular calcium and in some cases the calcium independent PLA_2 are thought to be involved in the release of arachidonic acid in many cell types including endothelial cells. Studies have also shown that arachidonic acid can also be liberated after PLC hydrolyses inositol triphosphate

group into DAG, which then later hydrolysed by lipases to generate monoacylglycerol and free arachidonic acid (Rindlisbacher *et al*., 1990). Once liberated in the cytoplasm, the arachidonic acid is metabolised by COX enzyme in two stages. In the first stage the arachidonic acid is converted via an oxygenase reaction into prostaglandin G_2 (PGG_2). In the second stage, PGG_2 is then converted via peroxidase reaction into the unstable prostaglandin endoperoxide H (PGH_2). The third and final stage is the conversion of PGH_2 into PGI_2 by the enzymatic activity of prostacyclin synthase, which is one of a number of synthases downstream of COX (Weksler *et al*., 1977).

These downstream synthases are of critical importance as their relative expression decides the profile of prostanoids released by the specific cell type under certain conditions. For example, endothelial cells are rich in COX and prostacyclin synthase enzymes and activation of PLA_2 leads to the production of PGI_2 as their main prostanoid, which inhibits platelet activation. Platelets are also rich in COX enzymes but they have little or no prostacyclin synthase and therefore the activation of PLA_2 leads to the production of TXA_2, a strong platelet activator and vasoconstrictor. This is because platelets primarily express thromboxane synthase (Needleman *et al*., 1976). As a result, although both endothelial cells and platelets highly express COX enzyme, their downstream prostanoid products have opposed functions in the cardiovascular system and therefore the balance between them helps maintaining the vascular homeostasis. Drugs such as aspirin that selectively lower TXA_2 synthesis tip the balance in favour of PGI_2 and establish an anti-thrombogenic environment, which protects people from cardiovascular diseases. Similar to COX, the expression of prostacyclin synthase in the endothelial cells is regulated by physiological shear stress and growth factors (Frangos *et al*., 1985).

In the blood vessel the PGI_2 released by the intact endothelium not only inhibits platelet adhesion to the vascular wall, activation and aggregation, but also regulates the functional activity of neighbouring vascular smooth muscle cells (Armstrong, 1996).

1.3.2.2 Prostacyclin receptor

The human PGI_2 receptor (IP) belongs to the prostanoid family of seven transmembrane GPCRs that performs critical roles in the regulation of platelet functions and vascular smooth muscle reactivity (Narumiya *et al*., 1999). IP receptor is distributed throughout body tissues with most abundant expression on blood platelets and vascular smooth muscle cells. The human IP receptor is classified as a Class A, rhodopsin type. The extracellular domain includes a short N-terminal region and three extracellular loops. The transmembrane region comprises seven transmembrane-spanning α-helices that carry the ligand binding site. The intracellular domain is made up of three intracellular loops, a putative intracellular eight helix and a C-terminal tail region (Reid *et al*., 2010; Narumiya *et al*., 1999). Within each of these regions, several post-translational modifications are required for normal function of the IP receptor. These modifications are glycosylation, disulfide bond formation, phosphorylation, isoprenylation and palmitoylation. Glycosylation (Zhang *et al*., 2001) and disulfide bond formation between cysteine residues (Stitham *et al*., 2006) in the N-terminal are reported to be important for ligand binding, receptor activation, agonist-induced sequestration, cell-surface expression and trafficking. Phosphorylation of serine residues (Ser328 and Ser374) in the C-terminal is mediated by GPCR kinases or PKC that causes receptor desensitisation and subsequent internalisation, followed by either recycling to the plasma membrane or later degradation by lysosomes (Donnellan & Kinsella, 2009; Miggin & Kinsella, 2002). Isoprenylation of the C-terminus is required for G-protein coupling (Hayes *et al*., 1999; Miggin *et al*., 2003) and palmitoylation of the C-terminus at Cys311 for agonist-induced intracellular trafficking, respectively (Reid *et al*., 2010). Studies have also reported the homodimerisation of the IP receptor, which may possibly be required for receptor trafficking (Giguère *et al*., 2004); however, this homodimerisation concept requires further studies to understand the mechanism behind it.

Upon ligand binding, the IP receptor undergoes a conformational change that directly activates intracellular receptor-associated stimulatory G-protein ($G\alpha_s$) subunit, which is mainly involved in signal transduction. Numerous studies have shown the importance of the IP receptor in the regulation of the cardiovascular system by using IP knock-out mouse models. Murata *et al.* (1997) have reported that mice lacking IP receptor exhibited increased propensities toward thrombosis. Similarly, Xiao and co-workers (2001) have noticed reperfusion injuries in these mice. Egan and colleagues (2004) have shown that the IP knock-out mice, particularly female ones, lost the atheroprotective role of the IP receptor. Patients lacking IP receptor have also shown increased severity of coronary artery disease (Arehart *et al*., 2008). Thus, the expression of IP receptor both on platelets and vascular smooth muscle cells is pivotal for normal haemodynamic activity and protection against thrombogenic disorders.

1.3.2.3 Adenylyl cyclase and cAMP synthesis

Adenylyl cyclases are a family of ubiquitously expressed transmembrane glycoproteins that catalyze the synthesis of cAMP from ATP. To date, 9 membrane-associated isoforms of AC and two splice variants of AC8 have been cloned and characterised in mammalian tissues. Proteomics and transcriptomics data suggests that platelet expresses three different isoforms of AC, AC3, AC5 and AC6 (Burkhart *et al*, 2012, Rowley *et al*., 2011). However, their biochemical confirmation in platelets is still missing, mainly due to low expression of ACs and poor isoform-specific antibodies. Membrane-bound ACs are activated by G-protein-associated receptor signalling. Ligation of PGI_2 to its IP receptor on the surface of platelets initiates the activation of intracellular receptor-coupled $G\alpha_s$. Once activated, $G\alpha_s$ then binds to the cytoplasmic domain of ACs and triggers the hydrolysis of ATP into cAMP.

All nine AC share a primary structure consisting a highly variable intracellular N-terminus, two hydrophobic domains (TM1 and TM2), each containing 6 transmembrane-spanning helices and two cytoplasmic domains (C1 and C2)

(Figure 1.7). The physiological role of the transmembrane region is not clearly understood aside from membrane localisation. The cytoplasmic domains, C1 and C2 are further divided into C1a and C1b; and C2a and C2b, respectively (Hurley, 1999). The homo or heterodimerisation of C1a and C2a regions initially initiated by $G\alpha_S$ or forskolin (FSK) forms the catalytic core that harbours a single ATP binding site, regions for FSK and G-proteins sites (Zhang *et al*., 1997). $G\alpha_i$ has been reported to inhibit the heterologous association of C1a and C2a, which subsequently prevents the formation of catalytic core and thus inhibits enzymatic activity of AC (Dessauer *et al*., 2002). Both *In vitro* and *in vivo* studies have shown that PKA act as a feedback inhibitor, reducing AC activity by phosphorylating Ser674 residue in the C1b domain (Beazely *et al*., 2005; Chen *et al*., 1997). There are also extracellular *N*-glycosylation sites (Asn850 and Asn890) on the 5^{th} and 6^{th} extracellular loop of TM2 helices. Wu *et al.* (2001) have reported that mutation and deglycosylation of these extracellular *N*- glycosylation sites not only impaired catalytic activity of the AC in response to forskolin, but also altered its regulation by $G\alpha_i$ and PKC. Several studies have also reported PKC-mediated phosphorylation of the N-terminus that impairs the enzymatic activity of ACs (Lin *et al*., 2004; Lai *et al*., 1999; Lai *et al*., 1997). Once activated, the catalytic core hydrolyses ATP into cAMP, which inhibits numbers of platelet functions via its foremost downstream effector PKA (Smolenski, 2012).

In mammalian tissues there is also a soluble isoform of AC (sAC). Unlike membrane-bound ACs, it is not regulated by G-proteins but directly activated by bicarbonate and calcium. sAC also works as a sensor for calcium, ATP, bicarbonate at different intracellular locations including nucleolus, organelles, vesicles (Steegborn, 2014). This particular AC mainly expresses in testes and to some extent in kidney and bones, plays an important role in sperm activation, glucose metabolism and in many cancerous conditions (Pierre *et al*., 2009).

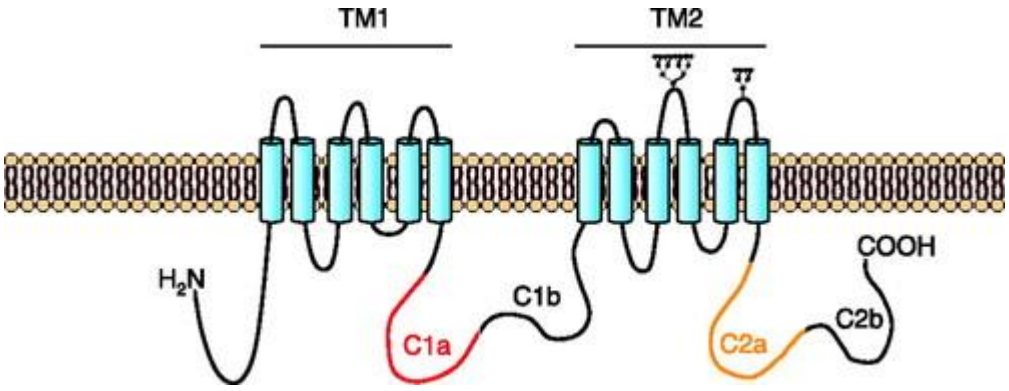

Figure 1.7: Structure of membrane-associated adenylyl cyclase (AC). Five structural domains of ACs: The N-terminus, the first transmembrane helices (TM1, blue cylinders), the first cytoplasmic loop comprised of C1a (red) and C1b (black), the second transmembrane helices (TM2, blue cylinders) with extracellular *N*-glycosylation regions, and the second cytoplasmic loop comprising C2a (orange) and C2b (black). Heterologous binding of C1a and C2a forms a catalytic core with ATP-binding region. Taken from Willoughby & Cooper, 2007.

1.3.2.4 Protein Kinase A

Protein kinases are a large family of enzymes that regulate various cellular responses by addition of inorganic phosphate group to target substrate proteins. A member of protein kinase family, PKA is a broad specificity heterotetrameric serine/threonine kinase that is ubiquitously expressed in all eukaryotic cells. The PKA holoenzyme is composed of two regulatory subunits and two catalytic subunits (Corbin *et al*., 1973; Potter & Taylor, 1979). Proteomic and biochemical studies have confirmed four functionally non-redundant regulatory (RIα, RIβ, RIIα, RIIβ) and four catalytic (Cα, Cβ, Cγ, PrKX) subunits that are differentially expressed, giving rise to four different PKA isoforms with varying structural and biochemical properties and cellular distribution (Pidoux & Taskén, 2010). The PKA isoforms are categorised into two main classes, type I and type II on the basis of their regulatory subunit (Corbin *et al*., 1975). The type I comprises either homo or heterodimers of RIα and RIβ, whereas type II comprises only homodimers of RIIα and RIIβ (Pidoux & Taskén, 2010).

The binding of cAMP molecules to four nucleotide-binding sites on the regulatory subunit dimer leads to a conformational change that reversibly unleashes the catalytic subunits from the complex (Johnson *et al*., 2001) (Figure 1.8). The free catalytic subunits then phosphorylate numbers of nearby substrate proteins on serine and threonine residues at a conserved consensus sequence (Arg-Arg-X-Ser/Thr, Arg-Lys-X-Ser/Thr, Lys-Arg-X-Ser/Thr, or Lys-Lys-XSer/Thr) (Taylor *et al*., 2008).

Proteomic and transcriptomic data suggest that both human and mouse platelet expresses all four PKA regulatory subunits and two catalytic subunits (Cα & Cβ) (Zeiler *et al*., 2014; Burkhart *et al*., 2012; Rowley *et al*., 2011) (Table 1.1 & 1.2). However, the relative roles of individual PKA isoforms in platelet function are not clearly understood (Smolenski, 2012). Recent studies have shown that platelets lacking PKA RIIβ have reduced activatory responses, indicating unregulated inhibitory activity of the catalytic subunits (Nagalla *et al*., 2011). Research studies have also reported a cAMP-independent mechanism of PKA activation in platelets

involving the release of PKA catalytic subunit from a nuclear factor-NFκB-IκB complex (Gambaryan *et al*., 2010). Both thrombin and collagen elicit the release of the PKA catalytic subunit from IκB that subsequently phosphorylates VASP and Rap1GAP2 proteins, suggesting a negative feedback mechanism for thrombin and collagen-induced platelet activation (Gambaryan *et al*., 2010).

In vivo, the PKA regulatory subunits exhibit different binding affinities to cAMP, giving rise to PKA with different thresholds for activation, with PKA type I activating at 2-4 fold lower levels of cAMP than PKA type II (Jarnæss *et al*., 2008). PKA isoforms also exhibit different subcellular distributions in different cell types. In lymphoid cells and cardiomyocytes PKA type I is mainly found in the cytosol, whereas type II is chiefly recovered in particulate fractions (Di Benedetto *et al*., 2008; Skalhegg & Taskén, 2000). However, in platelets PKA type I is mainly found in the membrane fraction, whereas type II is found in the soluble fraction (Raslan *et al*., 2015). These differences in subcellular distribution and cAMP binding affinities between PKA isoforms are suggested to contribute to the specificity in the cAMP-mediated PKA-signalling.

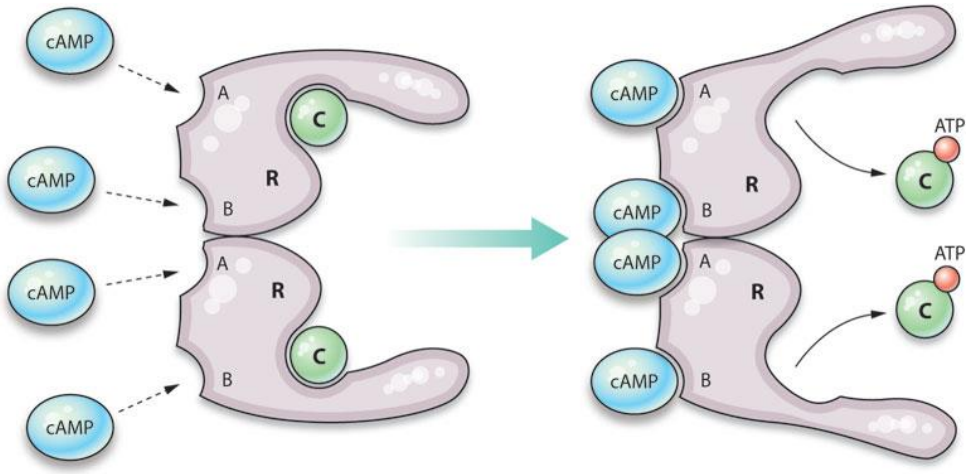

Figure 1.8: cAMP-mediated activation of PKA. PKA holoenzyme is composed of two regulatory (R) and two catalytic subunits (C). Each regulatory subunit has two cAMP binding sites (A and B). When four cAMP molecules bind to regulatory subunits, unleash the catalytic subunits and result in PKA activation. Taken from Murray, 2008.

Table 1.1: PKA regulatory and catalytic subunits protein and RNA expression levels in human platelets.

Accession no (UniProt)	Gene name	Protein name	Human platelet	
			Protein expression	Gene expression
P10644	*PRKAR1A*	PKA RIα	7900	96.65
P31321	*PRKAR1B*	PKA RIβ	2600	50.38
P13861	*PRKAR2A*	PKA RIIα	3500	0.69
P31323	*PRKAR2B*	PKA RIIβ	7600	647.41
P17612	*PRKACA*	PKA Catα	3400	8.06
P22694	*PRKACB*	PKA Catβ	3400	7.71

Table 1.2: PKA regulatory and catalytic subunits protein and RNA expression levels in mouse platelets.

Accession no (UniProt)	Gene name	Protein name	Mouse platelet	
			Protein expression	Gene expression
Q9DBC7	*Prkar1a*	PKA RIα	10,674	215.66
P12849	*Prkar1b*	PKA RIβ	Not detected	0.015
P12367	*Prkar2a*	PKA RIIα	Not detected	0.08
P31324	*Prkar2b*	PKA RIIβ	18,614	526.20
P05132	*Prkaca*	PKA Catα	6825	42.04
P68181	*Prkacb*	PKA Catβ	1604	5.67

Protein expression, estimated number of copies per platelet in human and mouse quantitative proteomic studies (Zeiler *et al*., 2014; Burkhart *et al*., 2012); gene expression, mean reads per kilobase of exon model per million mapped reads values in human and mouse platelet quantitative transcriptomic studies (Rowley *et al*., 2011).

1.3.2.5 Protein kinase A structure: regulatory subunits

PKA regulatory subunits are the primary intracellular receptors for cAMP in many cell types including platelets. The domain organisation of all PKA regulatory subunit isoforms is highly conserved and comprises stable and well-folded an N-terminal dimerisation and docking domain (D/D domain) followed by a highly variable linker region that harbours an inhibitor site, and two highly homologous cAMP binding domains (CNB) in tandem at the C-terminus, designated as A and B (Figure 1.9). The D/D domain, which is highly conserved in all regulatory subunits, provides a docking site for A kinase anchoring proteins (AKAPs) (see section 1.4). The inhibitor site within the linker region contains an autoinhibitory sequence that resembles a peptide substrate and docks to the active cleft of the catalytic subunits and thus either autophosphorylate or pseudophosphorylate the holoenzyme. The RI regulatory subunits posses alanine or glycine residues in the inhibitor site, which acts as pseudosubstrate for catalytic subunits that is, they mimic the substrate. On the other hand, RII regulatory subunits carry serine residue in the inhibitor site that act as substrate for catalytic subunit and thus maintain the holoenzyme complex. This is a fundamental difference between PKA RI and RII types. Structural studies have also revealed that each CNB domain carries a phosphate-binding cassette (PBC) that act as universal docking sites for cAMP molecules (Taylor *et al*., 2012 & 2008).

A)

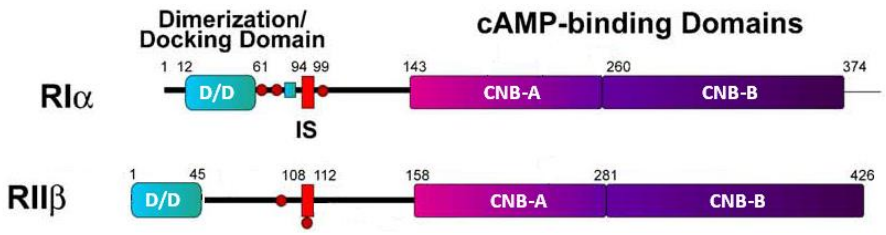

B)

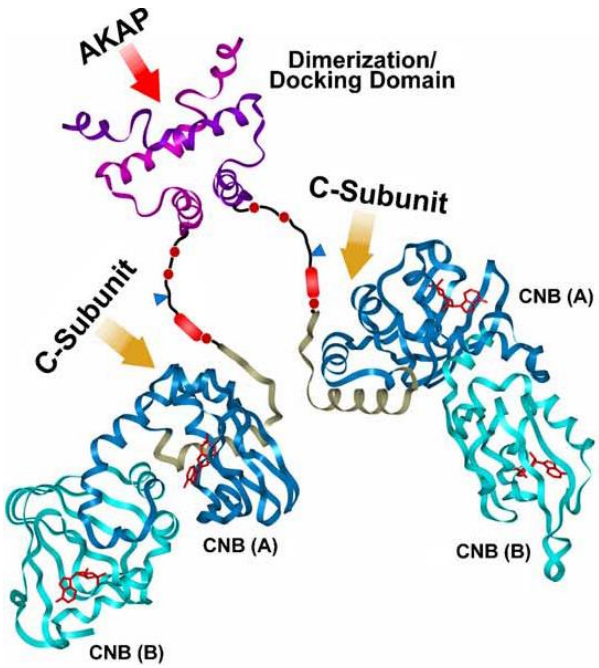

Figure 1.9: Schematic representation of PKA regulatory subunit. A) Domain organisation of PKA regulatory subunits RIα and RIIβ: N-terminal dimerisation and docking domain (D/D), followed by a linker region housing phosphorylation residue, serine (red circles), a proline box (green square looks cyan, not green), inhibitor site (IS) (red rectangle) and two C-terminal cyclic nucleotide binding domains (CNB-A and CNB-B). **B)** Ribbon illustration of the NMR structure of PKA RIα dimmer including AKAP binding site D/D domain, inhibitor sites (red rectangular box), serine residues (red circles) in the linker region followed by four cyclic nucleotide binding domains designated as CNB-A and CNB-B. Modified from Taylor *et al.*, 2005.

1.3.2.6 Protein kinase A structure: catalytic subunit

The PKA catalytic subunit is a bilobal enzyme with two major domains, N-terminal and C-terminal lobes that are highly conserved throughout the protein kinase family (Knighton & Zheng, 1991). The N-terminal lobe (N-lobe) constitutes the nucleotide binding domain is short and highly dynamic, composed of five anti-parallel strands of beta sheets, a short linker strand followed by a large α-helical C-terminal lobe (C-lobe) that carries substrate docking sites and many conserved residues that are important for the catalytic machinery (Figure 1.10). In addition, the C-lobe is flanked by an N-terminal tail (N-tail) and a C-terminal tail (C-tail). The C-tail, which is highly conserved and a vital part of the enzyme, can be further divided into three parts. The part tethered to the N-terminal lobe, called N-lobe Tether (NLT), and the part tethered to the C-terminal lobe, known as C-lobe Tether (CTL). Both these two parts are quite stable and have allosteric role in organising the active conformation of the enzyme for catalysis. The middle part of the C-tail is called Active Site Tether (AST). AST is highly dynamic and is responsible for ATP binding. The N-tail on the other hand, is not structurally conserved among members of the protein kinase family and is reported to play a major role in the subcellular localisation of PKA via interaction with membranes (Taylor *et al*., 2012 & 2008).

In the inactive holoenzyme, only the CNB-B site is exposed and available for cAMP interaction. Once occupied by a cAMP molecule the CNB-B undergoes a conformational change and exposes the CNB-A for cAMP interaction (Skalhegg & Taskén, 2000; Taylor *et al*., 1990). Binding of a cAMP molecule to a CNB-A site then triggers a global conformational change in the regulatory subunits that reduces their affinity towards catalytic subunits and subsequently releases catalytic subunits, which then are able to act on their nearby substrate proteins (Taylor *et al*., 2008).

Although extensive structural and biochemical studies have provided insight into the mechanism of cAMP-mediated PKA activation, very little is known about how

catalytic subunits reassociate with the regulatory subunits in mammalian cells. Moorthy *et al.* (2011) have suggested that cAMP-associated RI first binds to PDE, which in turn hydrolyses RI-bound cAMPs. The free catalytic subunits then displace PDE and reassociate with cAMP-free RI to regenerate the inactive PKA holoenzyme. On the other hand, Oliveria *et al.* (2007) have proposed that a calcineurin-mediated dephosphorylation of RII is involved in the reassociation cycle of PKA regulatory and catalytic subunits after activation.

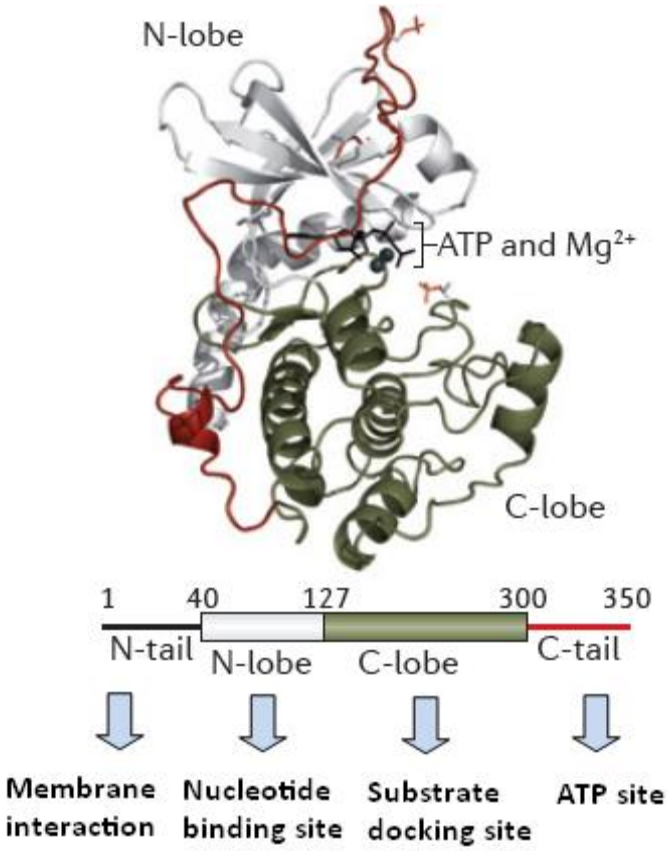

Figure 1.10: Schematic representation of PKA catalytic subunit. Ribbon diagram of the catalytic subunit of PKA: contains an N-lobe and a C-lobe flanked by N-tail and C-tail respectively. Adapted from Taylor *et al*., 2012.

1.3.3 Protein kinase A and G targets in blood platelets

cAMP-mediated PKA and cGMP-mediated PKG inhibit various platelet functions both *in vitro* and *in vivo* settings, such as platelet adhesion, activation, shape change, calcium mobilisation, degranulation, aggregation, apoptosis, thrombosis (Zhao *et al*., 2017; Aburima *et al*., 2017; 2013; Smolenski, 2012; Schwarz *et al*., 2001). However, the precise molecular mechanism by which both PKA and PKG inhibit these platelet functions is not clearly explained. PKA and PKG phosphorylate numbers of downstream substrate proteins in platelets including $G\alpha_{13}$, inositol triphosphate receptor (IP_3), VASP, actin binding proteins (ABP) and many more as listed in Table 1.1 (Smolenski, 2012). Nevertheless, the physiological importance of the phosphorylation of these substrate proteins is unclear, as most of the knowledge has been gained from *in vitro* studies by using cAMP/cGMP mimetics that act as global cAMP/cGMP modulators or evade adenylyl/guanylyl cyclases. An interesting point about these substrate proteins is that the majority of them are phosphorylated by both PKA and PKG; however, some are differentially regulated in a kinase specific manner (Schwarz *et al*., 2001). Unlike other mammalian cell types, blood platelets contain micromolar concentrations of both PKA and PKG proteins, pointing to the functional importance of protein phosphorylation in regulating platelet activity (Eigenthaler *et al*., 1992). To date only small numbers of PKA and PKG substrates have been characterised in detail, total numbers and identities of substrate proteins still needs to be investigated. Some PKA and PKG substrates are briefly summarised in the following subsections.

1.3.3.1 Receptor mediated signalling events

As mentioned earlier, platelet adhesion and activation at the site of vascular injury are two critical events for both haemostasis and thrombosis. These events are triggered by numbers of surface glycoproteins and GPCRs. Most of these receptors are under the influence of both PKA and PKG signalling in blood platelets. GPIbβ, a subunit of the GPIb-V-IX complex, is involved in initial platelet adhesion to immobilised vWF at the sites of vascular injury. PKA-mediated phosphorylation of

GPIbβ on Ser166 not only negatively regulates GPIbβ interaction with vWF but also impairs vWF mediated platelet aggregation (Bodnar *et al*., 2002; Raslan *et al*., 2015b). Furthermore, platelet interacts with collagen via $\alpha_2\beta_1$ and GPVI receptors. Both *in vivo* and *in vitro* studies have reported that PKA and PKG inhibit initial platelet interaction with collagen via down regulating integrin $\alpha_2\beta_1$ activity (Sim *et al*., 2004; Polanowska-Grabowska & Gear, 1994).

In addition to surface adhesion molecules, Rap1b, a most abundant small GTPase of the Ras family in platelets, is also regulated by PKA and PKG signalling. Agonist-induced platelet activation rapidly activates Rap1b, which strongly regulates integrin $\alpha_{IIb}\beta_3$ activation and platelet aggregation (Franke *et al*., 1997). Rap1b knock-out mice exhibited increased bleeding time due to defective platelet function. Furthermore, platelets from RapIb-deficient mice have impaired agonist-induced platelet aggregation and defective integrin $\alpha_{IIb}\beta_3$ activation (Chrzanowska-Wodnicka *et al*., 2005). Both PKA and PKG phosphorylate Rap1b at Ser179; however, very little is known about the functional relevance of this phosphorylation in platelets (Siess *et al*., 1990; Danielewski *et al*., 2005) apart from its impact on the subcellular distribution of RapIb (Hata *et al.,* 1991). Schultess *et al.* (2005) have identified Rap1GAP2, a GTPase-activating protein that is required to terminate signalling by Rap1. However, platelet activation by thrombin and ADP significantly increases Rap1GAP2 association with 14-3-3 protein. This interaction may possibly dampen Rap1GAP2 activity. Both PKA and PKG phosphorylate Rap1GAP2 at Ser7, inhibit its interaction with 14-3-3 and result in marked reduction in Rap1b activity in blood platelets (Hoffmeister *et al*., 2008). Recent studies have also shown that CalDAG-GEFI, a Rap1b GEF, is directly phosphorylated by PKA at Ser587, which prevents Rap1b activation (Subramanian *et al*., 2013).

In platelets, TXA_2 receptors are also reported under the influence of cyclic nucleotides signalling. These receptors have seven transmembrane domains that are coupled to $G\alpha_q$ and $G\alpha_{13}$. In platelets activation of $G\alpha_{13}$ is responsible for stress fibre formation through RhoA-ROCK pathway. PKA directly phosphorylates $G\alpha_{13}$ at

Thr203 and thus inhibits RhoA activation, which is required for activation of RhoA-ROCK pathway that is responsible for platelet shape change (Manganello *et al*., 2003). Investigations in human embryonic kidney 293 (HEK293) cells have suggested that the TXA_2 receptor (TPα) is desensitized by both PKA-mediated phosphorylation at Ser329 and PKG-mediated phosphorylation at Ser331 (Reid & Kinsella, 2003; Walsh *et al*., 2000). However, in platelets, PKA and PKG-mediated TPα phosphorylation has not been confirmed yet.

1.3.3.2 Intracellular calcium mobilisation

Agonist-induced platelet activation is responsible for increased intracellular calcium concentration. This increased intracellular calcium facilitates the regulation of many calcium-dependent enzymes including protein kinase C, MLCK, PLA_2 and Rap1b (Smolenski, 2012). Stimulation of various platelet surface receptors activates PLCβ and PLCγ isoforms that trigger the synthesis of IP_3 by hydrolysing PIP_2. IP_3 then binds to IP_3R receptors and triggers the release of calcium from cytoplasmic depots. The increased cytoplasmic calcium also triggers entry of the extracellular calcium via Orai1 store-operated calcium entry (SOCE) channels (Varga-Szabo *et al*., 2009). Both cyclic nucleotide-mediated PKA and PKG strongly inhibit calcium release by targeting various stages of platelet activatory pathways. Studies have suggested that PKA and PKG inhibit PLC mediated synthesis of IP_3 possibly by inhibiting PIP2 resynthesis (Ryningen *et al*., 1998). PKA and PKG have also been reported to target IP_3 receptors downstream of PLC. Platelet expresses all three isoforms of IP_3R and all are inhibited via phosphorylation by PKA and PKG at yet unknown sites (Tertyshnikova *et al*., 1998; El-Daher *et al*., 2000). However, the exact molecular mechanism in the inhibition of IP_3Rs via phosphorylation is not clearly defined.

Like in smooth muscle cells, PKG has also been shown to inhibit calcium release via IP_3R from DTS in platelets mainly by phosphorylating IP_3R-associated PKG substrate protein (IRAG) at Ser664 and Ser667 residues (Schinner & Schlossmann, 2011; Antl

et al., 2007). The importance of PKG-mediated phosphorylation of IRAG has been investigated in both IRAG knock-out and mutant mouse platelets, where intracellular calcium release was significantly impaired (Antl *et al*., 2007).

As of SOCE, PKA indirectly decrease extracellular calcium entry possibly via down-regulating IP_3 receptors (Nakamura *et al*., 1995). *In vitro* studies have shown that high concentration of NO donors significantly reduced extracellular calcium entry in thrombin activated platelets (Blackmore, 2011).

Besides SOCE, other calcium entry mechanisms also exist in platelets. For example, TRPC6 has been demonstrated to form a non-store operated calcium (non-SOC) channels (Hassock *et al*., 2002). These channels are activated downstream of PLC and are independent of intracellular calcium release from DTS. Hassock *et al.* (2002) have demonstrated that TRPC6 is phosphorylated both by PKA and PKG signalling; however, functional importance of this phosphorylation is not clearly explained and requires further investigations.

1.3.3.3 Cytoskeletal remodelling

One of the initial platelet activation events is shape change, which is essential for stable adhesion, degranulation, aggregation and spreading, and requires the reorganisation of the actin cytoskeleton. This initial event is driven by both signalling events and cytoskeleton binding proteins that rearrange the platelet cytoskeleton, causing nucleation and polymerisation of actin filaments and deacetylation of microtubules; this leads to disintegration of the marginal band and centralisation of platelet granules. PKA and PKG have been shown to inhibit cytoskeleton remodelling by phosphorylating numerous cytoskeleton-binding proteins.

One of the major substrates of PKA and PKG is VASP (Halbrügge & Walter, 1989). In platelets VASP is present in high concentration and carries three functionally important phosphorylation sites, Ser157, Ser239 and Thr278 (Butt *et al*., 1994;

Eigenthaler *et al*., 1992; Smolenski *et al*., 1998). All three sites are phosphorylated by PKA and PKG, however, with varying affinities in intact platelets (Butt *et al*., 1994). Analysis of phosphorylation kinetics both *in vivo* and *in vitro* has indicated that PKA prefers the Ser157 residue. On the other hand, PKG shows different *in vivo* and *in vitro* kinetics, with preference for Ser239 *in vitro* and similar kinetics for both Ser157 and Ser239 *in vivo* (Smolenski *et al*., 1998). In mammalian cells VASP has been shown to affect and regulate both actin polymerisation and F-actin bundling via binding of profilin that recruit monomeric G-actin to the barbed ends of F-actin (Fox, 2001). *In vitro* studies have shown that PKA-mediated phosphorylation of VASP down-regulates its actin polymerisation-promoting activity and F-actin bundling (Harbeck *et al*., 2000). VASP phosphorylation has also been reported to regulate focal adhesion dynamics (Smolenski *et al*., 2000) and actin cytoskeleton rigidity (Galler *et al*., 2006). In platelets, VASP phosphorylation is associated with integrin $\alpha_{IIb}\beta_3$ regulation (Horstrup *et al*., 1994). VASP knock-out mice have shown enhanced collagen and thrombin-mediated fibrinogen binding ability with integrin $\alpha_{IIb}\beta_3$ (Aszódi *et al*., 1999; Hauser *et al*., 1999); hence suggesting a possible role of VASP in integrin activation. Both cAMP and cGMP-mediated inhibition of thrombin and collagen-induced platelets aggregation was also impaired in VASP knock-out mice. Furthermore, platelets from VASP knock-out mice revealed increased thrombin-mediated $\alpha_{IIb}\beta_3$ activation, increased rate of degranulation, increased P-selectin expression and reduced aggregation time (Aszódi *et al*., 1999; Hauser *et al*., 1999). Together these studies suggest that VASP phosphorylation is required by PKA and PKG-mediated inhibition of integrin $\alpha_{IIb}\beta_3$ activation. VASP phosphorylation at Ser157 is also known to be triggered by PKC and Rho kinase in platelets stimulated with thrombin (Wentworth *et al*., 2006), thus questioning the reliability of VASP phosphorylation as a marker for platelet inhibition. However, in platelets the molecular consequences of VASP phosphorylation on cytoskeletal remodelling and integrin activation still needs to be characterised in detail.

Other important proteins that regulate the platelet cytoskeleton via phosphorylation by PKA and PKG are Lim and SH3 domain protein (LASP), heat shock protein 27 (HSP27), filamin-A, caldesmon and MLCK. *In vitro* PKA and PKG mediate phosphorylation of LASP at Ser146 and inhibit its F-actin and focal adhesion interactions (Butt *et al*., 2003). HSP27 play important roles in actin polymerisation during platelet activation. Both PKA and PKG significantly reduced its actin polymerisation activity especially via phosphorylation at Thr143 (Butt *et al*., 2001).

Another actin binding protein involved in the regulation of the platelet cytoskeleton is filamin-A. Filamin A was initially described as actin-myosin binding protein (ABP) (Wang *et al*., 1975). In platelets, filamin A is responsible for the organisation of the cytosolic network of actin filaments. Filamin-A cross-links cytosolic actin filaments into a three-dimensional gel. It also anchors the platelet cytoskeleton to the plasma membrane primarily via interacting with the cytoplasmic tail of glycoprotein GPIbβ (Fox, 2001). During platelet activation calcium-sensitive calpain proteolyses filamin-A, resulting in irreversible loss of its actin cross-linking properties that may contribute to cytoskeleton rearrangement (Truglia & Stracher, 1981). The phosphorylation of filamin-A by PKA at Ser2152 increases its resistance to calpain cleavage and thus blocks cytoskeleton rearrangement (Chen & Stracher, 1989; Jay *et al*., 2004).

Caldesmon is an actin and myosin binding protein that facilitates the translocation of myosin to the actin cytoskeleton during platelet activation (Hemric *et al*., 1994). *In vitro* studies have shown that purified platelet caldesmon can be phosphorylated by PKA, however the functional relevance of this phosphorylation in respect to platelet cytoskeleton rearrangement has not been explained (Hettasch & Sellers, 1991).

Another important effect of PKA and PKG on blood platelets is the inhibition of MLC phosphorylation at Ser19, which plays critical roles in cytoskeletal

remodelling during shape change and granule secretion. In platelets MLC phosphorylation is induced by two pathways, the calcium/calmodulin-dependent MLC kinase (MLCK) pathway and the calcium/calmodulin-independent RhoA-ROCK pathway (Klages *et al*., 1999; Paul *et al*., 1999). *In-vitro* studies have shown that MLCK is directly phosphorylated by both PKA and PKG, resulting in reduced activity of this enzyme and subsequent inhibition of MLC phosphorylation at Ser19 (Nishikawa *et al*., 1984). Recent studies have also revealed that cyclic nucleotides signalling specifically targets RhoA-ROCK pathway during platelet activation. PKA and PKG phosphorylate RhoA at Ser188 and prevent the RhoA association with the ROCK kinase, which is required for the inhibition of myosin light chain phosphatase (MLCP) and increased phosphorylation of MLC (Aburima *et al.*, 2013, 2017). There is also a possibility that both PKA and PKG may directly phosphorylate MLCP at its activatory residue, Ser695 in platelets. This direct effect may possibly enhance the activity of MLCP, which inhibits both RhoA-ROCK and MLCK-mediated phosphorylation of MLC. However, this direct effect needs to be confirmed in platelets. The PKA-mediated phosphorylation of MLCP is the focus of this study and is discussed more in detail in section 1.5.

Table 1.3: List of known PKA and PKA substrates

Substrate	MW (kDa)	PKA	PKG	Role in platelets	Reference
LASP	40	Platelets	?	Inhibits of F-actin interaction	Butt *et al.*, 2003
HSP27	27	?	Platelets	Inhibits actin polymerisation	Butt *et al.*, 2001
Filamin-A	250	Platelets	?	Protects against degradation	Chen & Stracher, 1989
Caldesmon	82	Platelets	?	Possibly stabilizing platelet cytoskeleton	Hettash & Sellers, 1991
MLCK	105	*In vitro*	*In vitro*	Reduces MLC phosphorylation	Nishikawa *et al.*, 1984
VASP	46/50	Platelets	Platelets	Down-regulates integrin $\alpha_{IIb}\beta_3$ activity	Hauser *et al.*, 1999
RhoA	22	Platelets	Platelets	Down-regulates MLC phosphorylation	Aburima *et al.*, 2013, 2017
Gα_{13}	44	Platelets	?	Inhibits RhoA-ROCK pathways	Manganello *et al.*, 2003
GPIbβ	24	Platelets	?	Inhibits actin polymerisation	Bodnar *et al.*, 2002
IP_3 receptor	230	Platelets	Platelets	Down-regulates calcium mobilisation	Tertyshnikova *et al.*, 1998
IRAG	98	?	Platelet	Down-regulates calcium mobilisation	Antl *et al.*, 2007
TXA_2 receptor	50	HEK cells	HEK cells	Desensitisation of TXA_2 receptor	Reid & Kinsella, 2003
Rap1b	22	Platelets	Platelets	Inhibits RapIb activity	Danielewski *et al.*, 2005
Rap1GAP2	80	Platelets	Platelets	Inhibits Rap1b activity	Hoffmeister *et al.*, 2008
CalDAG-GEFI	69.2	Platelets	?	Inhibits Rap1b activity	Subramanian *et al.*, 2013
PDE3	110	Platelets	?	Increases cAMP hydrolysis	Hunter *et al.*, 2009
PDE5	92	?	Platelets	Increases cGMP hydrolysis	Mullershausen *et al.*, 2003
TRPC6	100	Platelets	Platelets	Unknown	Hassock *et al.*, 2002
MYPT1	130	*In vitro*	Smooth muscle cells	Disinhibits MLCP and reduces MLC phosphorylation	Wooldridge *et al.*, 2004

1.3.4 Cyclic nucleotides degradation and phosphodiesterases

Cyclic nucleotides (cAMP and cGMP) are considered important inhibitory intracellular second messengers that regulate numbers of platelet activatory signalling events (Haslam *et al*., 1999; Gresele *et al*., 2011). In many cell types including platelets, the intracellular levels of cyclic nucleotides are not only regulated by their synthesis but also by their hydrolysis. The later is achieved primarily by a group of enzymes called phosphodiesterases (PDEs).

PDEs are a superfamily of metalophosphohydrolases that selectively catalyse hydrolysis of cAMP and cGMP into biologically inactive 5'-AMP and 5'-GMP metabolites. These enzymes limit the intracellular level of cyclic nucleotides and consequently regulate amplitude, duration and localisation of cyclic nucleotide signalling within subcellular compartments. To date over 60 isoforms and splice variants of PDEs have been identified that are encoded by 21 different genes in mammalian tissues (Francis *et al*., 2011). These isoforms are grouped into 11 different familiesf (PDE1-PDE11) based on their amino acid sequence, regulatory properties, intracellular localisation, cellular expression and sensitivity to endogenous regulators and chemical inhibitors. Structurally, PDEs comprise an N-terminal domain specifically involved in cyclic nucleotide binding and subcellular localisation and a C-terminal domain involved in enzymatic activity (Omori & Kotera, 2007). Platelet expresses three different types of PDEs: the cGMP-stimulated PDE2, the cGMP-inhibited PDE3 and the cGMP-specific PDE5 (Hidaka & Asano, 1976). Together these three isoforms account for at least 90% of platelet PDE activity.

PDE2 is a dual substrate enzyme that hydrolyses both cAMP and cGMP at similar rates. It has two GAF domains (GAF-A and GAF-B) in the N-terminus. The GAF domain is named after the proteins it was initially found in c**G**MP-specific phosphodiesterases, **a**denylyl cyclases and **F**hIA. GAF-A is involved in homodimerisation, whereas GAF-B is identified as a specific cGMP-binding site. Once cGMP interacts with GAF-B the protein undergoes a conformational change

that results in increased enzyme activity (Haslam *et al*., 1999; Bender & Beavo, 2006). Hence increased level of cGMP is responsible for the enzymatic activity of PDE2 (Bender & Beavo, 2006).

PDE3 hydrolyses both cAMP and cGMP, although it has higher affinity towards cAMP. Unlike PDE2, PDE3 is inhibited by the binding of cGMP and is therefore called the cGMP-inhibited PDE. In fact, there is substantial evidence suggesting that cGMP exerts most of its inhibitory effects on platelet function by acting as a competitive inhibitor of PDE3 (Maurice & Haslam, 1990). Studies by Manns *et al.* (2002) have demonstrated the physiological role of PDE3 in platelet function. They reported that the selective inhibition of PDE3 with cilostazol results an increased level of cAMP that compromised thrombin-induced platelet aggregation and calcium mobilisation responses. Several groups working on PDE3 in platelets have shown that the hydrolytic activity of this enzyme is upregulated by PKA mediated phosphorylation, suggesting a negative feedback loop, which rapidly decreases not only cAMP level but also imposes a reduced cAMP-regulated threshold for platelet activation (Grant *et al*., 1988; Macphee *et al*., 1988). Recent studies have also shown that the PDE3 activity is upregulated via phosphorylation by PKC and possibly by Akt, indicating an increased cAMP hydrolysis mechanism required for agonist-induced platelet activation (Zhang & Colman, 2007; Hunter *et al*., 2009).

PDE5 was first identified in platelets and is described as cGMP-binding, cGMP-specific PDE. It is activated by binding of cGMP at the GAF-A domain, which significantly increases enzymatic activity. Unlike the other two PDEs, it selectively hydrolyses cGMP. Biochemical studies have also reported the phosphorylation-dependent activation of PDE5 by PKA and PKG that may possibly provide negative feedback on cGMP levels (Corbin *et al*., 2000).

1.3.5 Compartmentalisation of cyclic nucleotides signalling

It is now generally accepted that the precision of cellular function mainly relies upon how an extracellular signal triggers correct intracellular second messengers

and effector proteins both spatially and temporally. This is known as compartmentalisation of the cellular signalling. This concept was first proposed by Buxton and Brunton in the early 1980s while studying cAMP signalling in cardiomyocytes. They observed that different $G\alpha_s$-coupled GPCRs triggered common an intracellular second messenger, cAMP, that differentially activated foremost effectors PKA type I and type II isoforms (Buxton & Brunton, 1983). This led to the idea of different PKA compartments that are selectively regulated by cAMP within the cell. The discovery of A-kinase anchoring proteins (AKAPs) and PDEs consolidated this concept further. AKAPs are scaffold proteins that not only tether different PKA isoforms close to their substrate proteins in distinct subcellular locations but also scaffold various signalling molecules, including PDEs. Thus, AKAPs dictate PKA isoforms distribution in distinct cellular compartments, whereas PDEs provides an enzymatic barrier to that particular compartment and restrict not only intracellular diffusion of cAMP from that particular compartment but also limit cAMP level and cAMP mediated PKA activation (Figure 1.11). This spatio-temporal regulation of cAMP gradients and PKA isoforms distribution contributes to the formation of distinct subcellular cAMP signalling hubs (Wong & Scott, 2004; Mongillo *et al*., 2004). Furthermore, the development of various fluorescent probes has allowed us to visualise cAMP concentrated microdomains inside the cells, contributing enormously to this PKA tethering hypothesis and the role of PDEs in compartmentalised cAMP signalling (Zaccolo & Pozzan, 2002). The advantages of this compartmentalised signalling would enable faster activation of target proteins that generate specific responses with limited pools of second messenger molecules.

In platelets the idea of compartmentalisation of cyclic nucleotides signalling was first proposed by El-Daher *et al.* (1996, 2000). They suggested differential localisation of both PKA and PKG and their substrate proteins in the distinct subcellular compartments of blood platelets. Later, the compartmentalisation and compartment-specific regulation of cAMP and cGMP signalling in platelet function

was proposed by Wilson *et al.* (2008) and Bilodeau *et al.* (2007). They have demonstrated that both cAMP and cGMP signalling in particular subcellular compartments are spatio-temporally regulated by sets of AKAPs, GKAP (guanylate kinase-associated protein) and PDEs. However, none of these studies has investigated the selective distribution of different PKA isoforms in these intracellular compartments. Recently, Raslan *et al.* (2015) have suggested differential distribution of PKA isoforms in human platelets. PKA type I is mainly found in the membrane fraction, whereas PKA type II in supernatant fraction. They have also noticed that in the membrane fraction, especially in the lipid rafts, a pool of PKA type I is localised, possibly tethered there via association with a novel AKAP, moesin. This anchored-PKA then potentially phosphorylates lipid raft resident glycoprotein GPIbβ and results in restriction of vWF interaction with raft GPIbβ. This is the first line of evidence of membrane compartmentalisation of PKA signalling in blood platelets. However, in platelets this concept of compartmentalisation is still in early stages and requires further investigation to understand the mechanism facilitating the formation of signalling hubs that contain kinases, target substrates, AKAPs, GKAPs and PDEs in particular compartments.

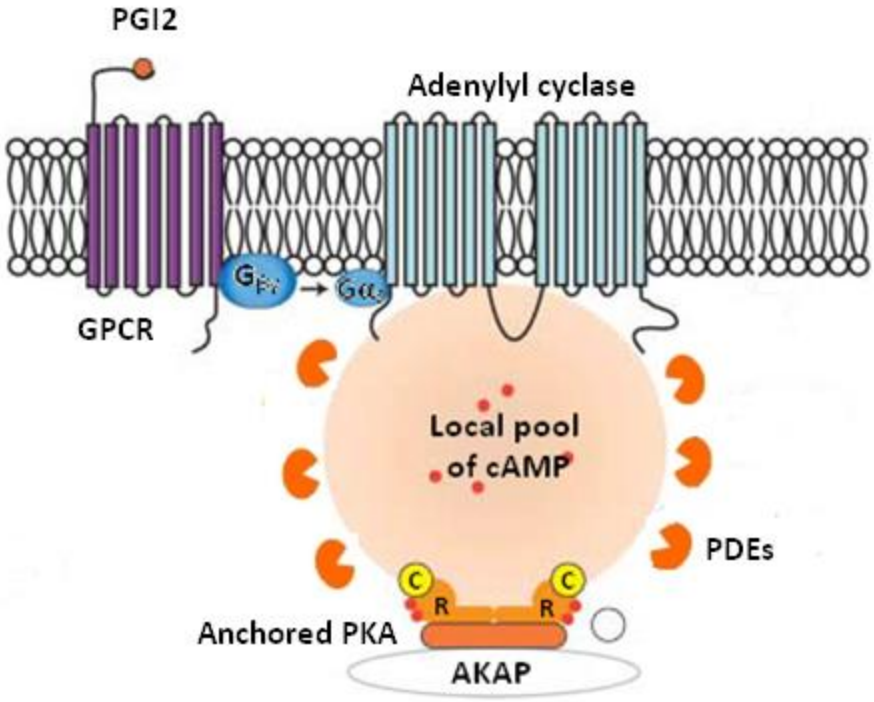

Figure 1.11: Compartmentalisation of cAMP signalling by AKAPs and PDEs. Stimulation of various GPCRs activates membrane-bound adenylyl cyclases that form localised pools of cAMP. The increased cAMP level activates the downstream effector PKA. AKAPs tether different PKA isoforms close to their substrate in these cAMP rich areas. AKAPs may also scaffold PDEs, which control concentration and distribution of cAMP in these pools, thus providing spatio-temporal specificity of the cAMP signalling. Adapted and modified from Pidoux & Taskén, 2010.

1.4 A-Kinase anchoring proteins

A-kinase anchoring proteins, AKAPs, are a family of structurally diverse but functionally similar proteins that share the capacity to interact with PKA (Pidoux & Taskén, 2010). To date more than 70 different AKAPs including splice variants have been identified in mammalian cells that are encoded by 43 different genes (Rababa'h *et al*., 2014). The majority of these AKAPs associate only with the type II PKA isoform; however, some AKAPs have dual specificity and interact with type I PKA too (Means *et al*., 2011; Alto *et al*., 2003). The characteristic feature of all AKAPs, even though they do not share any sequence homology, is an anchoring domain that comprises a conserved 14-18 amino acids long amphipathic helix that associates with the N-terminal dimerisation and docking (D/D) domain of the PKA regulatory subunit dimer (Carr *et al*., 1991) (Figure 1.12). The distinctive feature of an amphipathic helix is the arrangement of hydrophobic residues on one side and hydrophilic residues on alternate sides forming hydrophobic and hydrophilic faces.

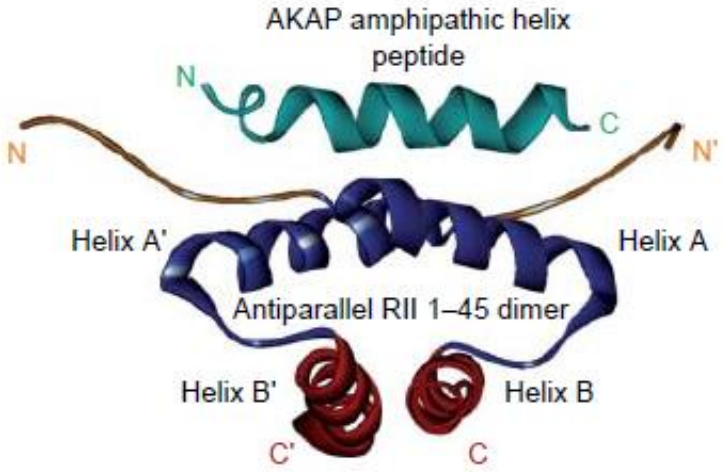

Figure 1.12: The structural complex of AKAP-PKA interaction. The NMR-solved illustration of an AKAP amphipathic helix (green) associated with the D/D domain of PKA dimer (red and blue). Taken from Pidoux & Taskén, 2010.

The functional importance of AKAPs has been well documented in many cell types by disrupting the PKA-AKAP interaction (Carr *et al*., 1992). This is mostly achieved

by using a disruptor peptide, Ht31 (aa493-515), a fragment of an endogenous AKAP cloned from human thyroid that forms a PKA binding domain (Carr *et al*., 1992). In cardiac and skeletal muscles Ht31 has been shown to disrupt PKA-AKAP79 interaction, which is involved in the regulation of L-type calcium channels (Gao *et al*., 1997). In the pancreatic β-cell line RINm5F, Ht31 disruptor peptide has been reported to block cAMP mediated insulin secretion and intracellular calcium elevation (Lester *et al*., 1997). Similarly, in mammalian sperm cells Ht31 prevented cAMP-dependent motility both in a dose and a time dependent manner (Vijayaraghavan *et al*., 1997). Additionally, in cardiomyocytes Ht31 mediated disruption markedly reduced phosphorylation of PKA substrates and cardiac contractile forces after stimulation with isoproterenol (McConnell *et al*., 2009). Together, these studies clearly suggest the importance of PKA anchoring for the regulation of various cellular responses.

Besides targeting PKA to different subcellular loci, many AKAPs also function as a scaffold for several other proteins that are involved in signal transduction, such as PDEs, protein phosphatases and other kinases, and thus provide precise spatiotemporal regulation of cAMP-PKA signalling (Taskén *et al*., 2001). The ability of AKAPs to scaffold enzymes other than PKA was first reported by Coghlan *et al.* (1995) for AKAP79, which also interacts with phosphatase 2B (PP2B). As the numbers of regulatory enzymes found to interact with AKAPs has increased, the notion of cAMP-PKA signal compartmentalisation has developed accordingly.

Proteomic and transcriptomic studies suggest that platelets potentially express 15 different types of AKAPs including AKAP1, AKAP2, AKAP5, AKAP7, AKAP8, AKAP8L, AKAP9, AKPA10, AKAP11, AKAP13, microtubule-associated protein 2 (Map2), ezrin, moesin, Ras-related protein 32 (Rab32), small membrane AKAP (smAKAP) and WAS protein family member 1 (WAVE-1) (Burkhart *et al*., 2012; Margarucci *et al*., 2011; Rowley *et al*., 2011). However, the functional role of only one AKAP, moesin, has been verified so far. It is believed that in platelets moesin targets PKA type I to lipid rafts, where it facilitates the phosphorylation of raft-residing GPIbβ

receptor that results in inhibition of platelet-vWF interactions and interferes with thrombus formation (Raslan *et al*., 2015b).

1.5 Myosin light chain phosphatase

Platelet shape change is one of the earliest events during platelet activation and is accompanied by a dramatic reorganisation of the actin cytoskeleton (Fox, 1993). The major factor in this rearrangement is thought to be phosphorylation of non-muscle myosin IIa and its increased association with the actin cytoskeleton (Fox, 1993). However, the precise details of these changes are not clear. Myosin IIa is a hexameric ATPase motor protein composed of two heavy chains and four light chains. The 220 kDa heavy chains form two globular motor head domains containing ATP and actin binding sites, a neck region, a long α-helical coiled-coil forming a rod-shaped domain, which dimerises the myosin and enables it to form shorter filaments of 20-30 molecules and a short non-helical domain (Billington *et al*., 2013). Two regulatory light chains of 20 kDa interact with the neck region of the heavy chains and regulate myosin activity via phosphorylation at Ser19. Two essential light chains of 17 kDa stabilise the myosin heads along with the regulatory light chains (Clark *et al*., 2007) (Figure 1.13). In its inactive form non-muscle myosin IIa forms a compact molecule in which the coiled-coil tail wraps around the motor heads and unables the motor heads to interact with actin filaments and generate force. When the regulatory light chains are phosphorylated at Ser19, their interaction with the tail domain of the heavy chains is disrupted and the myosin then adopts an extended conformation and forms filaments. The extended myosin head domains are then able to interact with actin filaments and generate contractile force that causes cytoskeletal rearrangement and subsequent platelet shape change. Dephosphorylation of MLC at Ser19 reverses the myosin extended conformation back to inactive compact conformation (Vicente-Manzanares *et al*., 2009). However, the mechanism behind these conformational changes is not clearly understood.

Previously, it was thought that only the non-muscle myosin heavy chain IIa was expressed in platelets but recent proteomic studies have reported other class II isoforms, such as myosin IIB, myosin IIc as well as several unconventional myosins, myosin V, myosin VI, myosin VII, in platelets (Burkhart *et al*., 2012; Qureshi *et al*., 2009). Genetic mutations of the non-muscle myosin heavy chain gene (*MYH9*) are associated with *MYH9*-related disorders, which comprise four different autosomal-dominant diseases previously known as May-Hegglin anomly, Fechtner syndrome, Sebastian syndrome and Epstein syndrome. All affected individuals display macrothrombocytopenia, characteristic leukocyte inclusions and abnormal myosin aggregates (Léon *et al*., 2007). Similarly, Léon *et al*. (2007) showed that genetic deletion of the non-muscle myosin IIa in megakaryocytes caused severe defects in platelet myosin expression levels with a phenotype, which was similar to that of *MYH9*-related disorders. Furthermore, platelet shape change, outside-in signalling, thrombus growth, bleeding time and clot retraction were markedly impaired in MYH9 KO platelets, however; platelet aggregation and granular secretion responses were only moderately attenuated (Léon *et al*., 2007).

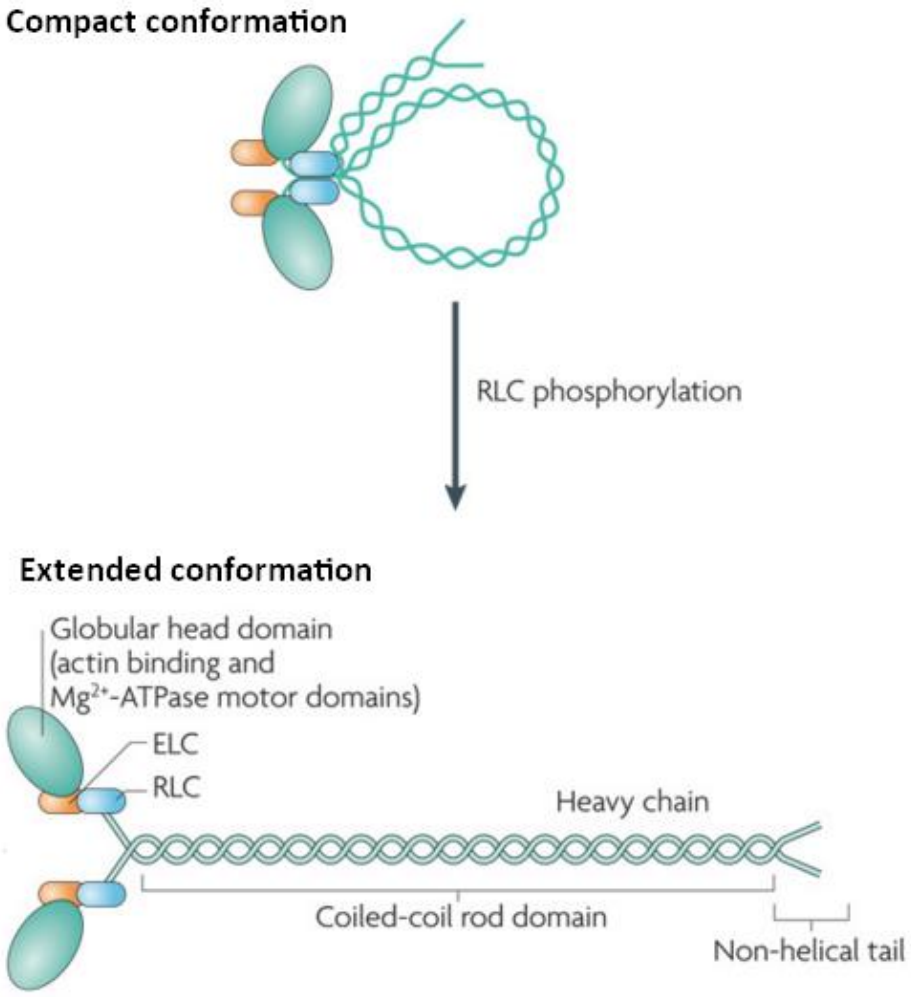

Figure 1.13: Domain architecture of non-muscle myosin IIa. Myosin IIa is composed of two regulatory light chains (RLC), two essential light chains (ELC) and two heavy chains including two motor heads containing actin and ATP binding regions, neck, coiled-coil rod and non-helical tail domains. The RLCs and ELCs interact with the head domains at neck region and link head and coiled-coil rod domains. In the absence of RLC phosphorylation, myosin IIa organised in a compact conformation, once phosphorylated at RLC, myosin adopts an extended conformation. Adapted from Vicente-Manzanares *et al*., 2009.

Numerous platelet agonists trigger phosphorylation-dependent activation of myosin IIa. The level of myosin phosphorylation is basically dependent on the activities of two regulatory enzymes, MLCK and MLCP. MLCK triggers phosphorylation of MLC at Ser19 that facilitates the generation of acto-myosin contractile forces responsible for platelet shape change and granule secretion (Johnson *et al*., 2007). MLCP dephosphorylates MLC at the same residue, which prevents the initiation of acto-myosin contractile forces and thus inhibits platelet shape change (Muranyi *et al*., 1998). In smooth muscle cells MLCP acts as a focal point for both activatory and inhibitory signalling, which controls the acto-myosin contractile machinery of the cells required for smooth muscle tone. In platelets, soluble agonists, such as thrombin and TXA_2 stimulate simultaneously a Ca^{2+}/calmodulin-dependent MLCK activation and Ca^{2+}-independent RhoA-ROCK-mediated MLCP inhibition that promotes net phosphorylation of MLC required for platelet shape change, and granule secretion (Aburima & Naseem, 2014). By contrast, platelet inhibitory agonists such as PGI_2 and NO stimulate cyclic nucleotide-mediated PKA and PKG that activate MLCP required dephosphorylating MLC and inhibit acto-myosin contractile forces (Figure 1.14). Both platelets and vascular smooth muscle cells contains similar isoforms of MLCP (Nakai *et al*., 1997; Muranyi *et al*., 1998); however, the molecular and biochemical mechanisms of MLCP activity are poorly defined in blood platelets.

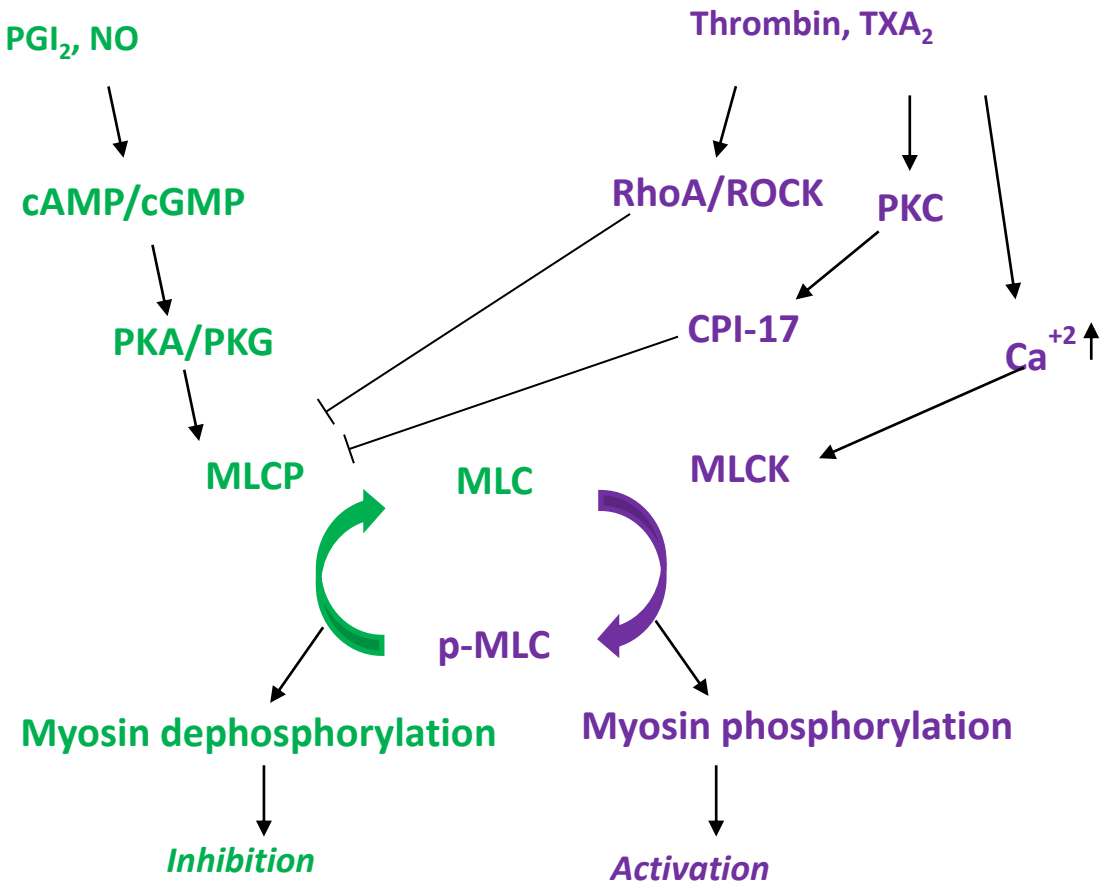

Figure 1.14: Putative mechanisms of MLCP regulation in blood platelets. PGI_2 and NO induce MLCP activation via cAMP/cGMP-mediated PKA/PKG that leads to dephosphorylation of myosin IIa, which is required for inhibition of acto-myosin contractile forces. Whereas thrombin and TXA_2 induce inhibition of MLCP activity either via RhoA-ROCK pathway or via PKC-mediated CPI-17 and thus increases net calcium sensitivity that leads to MLCK activation and results in acto-myosin contractile events responsible for platelet activation.

MLCP is a primary serine/threonine phosphatase that is composed of a 38 kDa catalytic subunit of the protein phosphatase type 1 (PP1cδ), a 130 kDa regulatory myosin phosphatase targeting subunit 1 (MYPT1) and a 20 kDa small subunit (M20) of yet not known function (Figure 1.12) (Alessi *et al*., 1992). The regulatory subunit MYPT1 interacts with PP1cδ via its N-terminus and with M20 via its C-terminus, thus forming the holoenzyme of MLCP. The majority of the characteristics of MLCP are determined by MYPT1, which acts as targeting protein and drives the catalytic subunit of the holoenzyme complex to particular cellular locations where it is in close proximity to its substrate proteins (Ito *et al*., 2004). Terrak *et al.* (2004) has reported that PP1c in complex with MYPT1 has increased phosphatase activity (~15 fold) and ~10 fold higher affinities towards phosphorylated myosin than the isolated catalytic subunit. Phosphorylation of MYPT1 via RhoA-ROCK pathway markedly reduced phosphatase activity, while phosphorylation of MYPT1 via cAMP/PKA signalling moderately increased phosphatase activity (Ahmed *et al*., 2013). These findings suggest that MLCP activity is primarily modulated by phosphorylation of MYPT1.

1.5.1 MYPT1

1.5.1.1 Structure of MYPT1

A characteristic feature of MYPT1 (1030aa) is the presence of 8 ankyrin repeats at the N-terminus (aa39-296) that are divided into two groups separated by a hinge at Glu172. Each ankyrin repeat is ~33 aa long and consists of two antiparallel α-helices connected by β-hairpin loops (Sedgwick & Smerdon, 1999). Based on structural studies it is generally accepted that ankyrin repeats are involved in protein-protein interactions. In MYPT1 ankyrin repeats play an important role in modulating the catalytic activity of PP1c (Terrak *et al*., 2004). Biochemical studies also suggested that ankyrin repeats provide increased MYPT1 specificity towards binding with the substrate protein myosin IIa (Hirano *et al*., 1997; Gailly *et al*., 1996). Structural domains of MYPT1 are represented in figure 1.15.

At the beginning of the first ankyrin repeat sits the PP1c-binding motif commonly known as the RVXF motif (aa35-38). This motif interacts with the hydrophobic grove of PP1c without influencing the catalytic activity of the enzyme. In MYPT1 RVXF act as a primary interaction site for PP1c; however, there are two more regions that are involved in the interaction. First, the N-terminal 34 basic and C-terminal 22 acidic residues flanking the RVXF motif are required for MYPT1 interaction with PP1c (Terrak *et al*., 2004). Second, ankyrin repeats 5-8 interact with the C-terminus of PP1c, involving Tyr305 and Tyr307 residues (Terrak *et al*., 2004). There are also two nuclear localization sequences (NLS) present in the N-terminus (aa27-33) and C-terminus (aa845-854). These sequences are involved in subcellular distribution of MYPT1 (Wu *et al*., 2005).

At the centre of MYPT1 is a highly variable central insert (aa552-608) region that generates different isoforms of MYPT1 in different species once alternatively spliced. There are four heptad repeats of leucine zipper motif (aa1003-1030) at the end of the C-terminus that play an important role in PKG-mediated MYPT phosphorylation. There is also a binding site for the small subunit M20 of MLCP holoenzyme at the C-terminal end between amino acids 934 and 1006 (Butler *et al*., 2013).

Additionally, MYPT1 also contains many serine and threonine phosphorylation sites mostly at the C-terminal half including Ser692, Ser695, Thr696, Ser852, Thr853, however, only three of them are well studied, namely Ser695 and Thr696 and Thr853, which directly influence the activity of MLCP. Phosphorylation of Thr696 and Thr853 causes inhibition of MLCP activity. Numbers of protein kinases phosphorylate MYPT1 at Thr696, such as zipper-interacting protein kinase (ZIPK), ROCK, PKC, integrin-linked kinase (ILK) and p21-activated protein kinase (PAK) (Ito *et al*., 2004; Hirano *et al*., 2003). Phosphorylation of MYPT1 at Thr853 is thought to be specifically ROCK mediated (Matsumura & Hartshorne, 2008). On the other hand, phosphorylation of Ser695 was demonstrated to cause activation of MLCP activity possibly via impeding the phosphorylation of neighbouring Thr696 by

ROCK (Wooldridge *et al*., 2004; Nakamura *et al*., 2007). The Thr853 is also preceded by a serine residue; however, the effect of phosphorylation of Ser852 on the neighbouring Thr853 has not been investigated yet due to lack of phospho-specific antibodies of Ser852.

The C-terminal half of MYPT1 also acts as a scaffold for many signalling and cytoskeletal molecules, such as PKA, PKG, GTP-RhoA, ROCK, myosin and moesin (Aburima & Naseem, 2014; Buttler *et al*., 2013; Grassie *et al*., 2011). These molecules either inhibit or activate MLCP activity via targeting serine and threonine residues of MYPT1 protein.

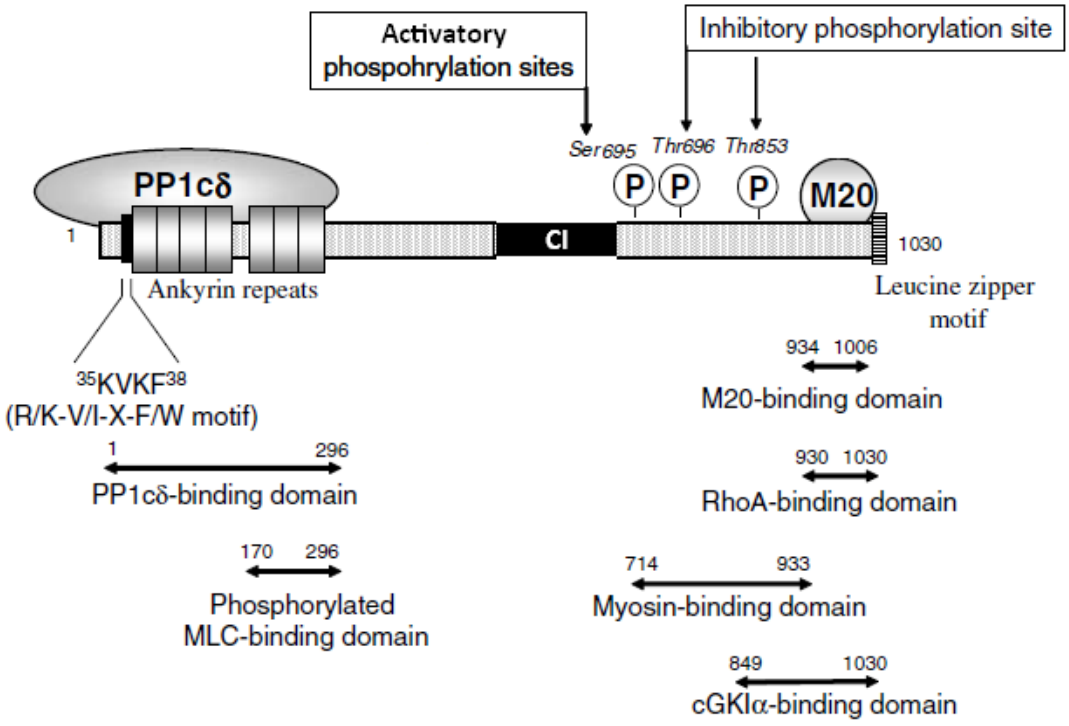

Figure 1.15: Structural domains of MYPT1 and its association with the catalytic PP1cδ and small subunit M20 of MLCP holoenzyme. N-terminal domain with PP1c binding site (RVXF, aa35-38), followed by 7-8 ankyrin repeats (aa39-296) serves as stage for protein-protein interaction, a highly variable central insert that produces different splice variants in different species and a coiled-coil C- terminal domain with four repeats of leucine zipper motifs (aa1003-130) and binding sites for cGKIα (PKG), RhoA, myosin, and M20 binding domain are indicated. The C-terminus also carries three well-characterised phosphorylating residues, Ser695, Thr696 and Thr853. Adapted from Ito *et al*., 2004.

1.5.1.2 Isoforms of MYPT1

The human MYPT1 protein expression is encoded by a single gene, Protein Phosphatase 1 Regulatory Subunit 12A (*PPP1R12A*), which is located on chromosome 12. Numerous MYPT1 splice variants are also reported in various species and tissues. These splice variants are product of cassette-type alternative splicing of MYPT1 gene at two regions, the central part and the 3'-end of the transcript near the leucine zipper domain.

In rats and mice, alternative splicing of 123 bp exon 13 or 14 in the central part generate five different splice variants of MYPT1 that vary in size from 50 to 100 amino acids at the central insert (CI) region (Dirksen *et al*., 2000; Ito *et al*., 2004). In human alternative splicing of exon 15, corresponding to rats exon 13 or avian exon 12, also occurs that generates MYPT1 central insert positive or negative variants. These central insert splice variants are not evolutionarily conserved; however, their expression is tissue specific in birds and to some extent in mammals. The functional relevance of MYPT1-CI variants is not very well explained. Recent *In vitro* studies have reported differences in the rate of phosphorylation of MYPT1-CI positive vs MYPT1-CI negative variants at Ser695 by PKG suggesting that CI may possibly regulate MYPT1 phosphorylation (Yuen *et al*., 2011).

Similarly, the cassette-type alternative splicing of a 31 bp alternative exon at the 3'-end generates distinct C-terminal leucine zipper positive (LZ+) or negative (LZ-) splice variants of MYPT1 (Khatri *et al*., 2001). The isoform lacking leucine zipper domain contains an additional 31 bp exon (in mice exon 23 and in human exon 25, in birds exon 24) that shifts the reading frame resulting in a premature termination codon, which produces a completely different C-terminal amino acid sequence (Fu *et al*., 2012). This C-terminal splicing is evolutionarily conserved, highly tissue-specific, developmentally regulated, and modulated by disease states (Fisher, 2010). The MYPT1-LZ negative splice variant is predominantly expressed in the phasic smooth muscle cells of the gut, bladder, intestine, portal vein and small

mesenteric arteries, whereas the MYPT1-LZ positive splice variant is primarily expressed in the tonic smooth muscle cells of the large arteries and veins (Payne *et al*., 2006). In chicken gizzard the expression of these LZ variants is developmentally regulated with switching of LZ positive to LZ negative variant at about the time of hatching (Khatri *et al*., 2001). Many researchers have reported a functional importance of these LZ splice variants of MYPT1 in various mammalian tissues (Karim *et al*., 2004; Payne *et al*., 2006; Zhang & Fisher, 2007). For example, tissues that express MYPT1-LZ negative variant, such as chicken gizzard, rat portal vein and intestine, failed to exhibit calcium desensitisation in response to cGMP-mediated PKG, whereas tissues including aorta with LZ positive variant demonstrated cGMP-dependent PKG dimerisation and activation of MLCP (Dippold & Fisher, 2014).

1.5.1.3 Subcellular distribution of MYPT1

Several immunofluorescence and cell fractionation studies have reported distinct subcellular distribution of MYPT1 in different cell types including vascular smooth muscle cells, fibroblasts, epithelial cells, endothelial cells and platelets (table 1.2). In permeabilised fibroblasts and smooth muscle cells MYPT1 was localised on stress fibers in the cytoplasm along with myosin IIa. However, in non-permeabilised fibroblasts and smooth muscle cells MYPT1 was primarily localised in the cytoplasm and nucleus, whereas myosin was mainly observed in the cell periphery (Murata *et al*., 1997). In the rat embryo fibroblast cell line REF-52 and non-confluent monolayer of Madin-Darby Canine Kidney (MDCK) epithelial cells, MYPT1 was observed in the cytoplasm along with myosin on stress fibers. However, in confluent MDCK cells MYPT1 was mostly seen in cell-cell adhesion sites, whereas myosin was mainly in cell cytoplasm (Inagaki *et al*., 1997). Additionally, in MDCK cells, MYPT1 was also reported in the tetradecanoylphorbol-13-acetate (TPA)-induced membrane ruffling area along with the ERM family member moesin (Fukata *et al*., 1998). Similarly, in confluent endothelial cells and

intestinal epithelial cells MYPT1 is only observed in cell-cell contact sites and not in the cytoplasm (Zha *et al*., 2016; Hirano *et al*., 1999).

In ferret portal vein cells, MYPT1 was distributed throughout the cytoplasm along with PP1c. However, upon stimulation with prostaglandin F2α (PGF2α) the MYPT1-PP1c complex translocated from the cytoplasm to the cell periphery, where PP1c dissociated and returned to the cytosol, whereas MYPT1 remained in the cell periphery for at least 15min. This agonist-mediated translocation of MYPT1 was accompanied by phosphorylation of MYPT1 at Thr696, which was significantly blocked by ROCK inhibitor, Y27632 (Shin *et al*., 2002).

Similarly, Lontay *et al.* (2005) have showed that in non-stimulated human hepatocarcinoma (HepG2) cells, MYPT1 is distributed throughout the cytoplasm including the nucleus. Once stimulated by the cell permeable phosphatase inhibitor okadaic acid, MYPT1 translocated from the cytoplasm to the plasma membrane in association with an increased phosphorylation of Thr696, which was not affected by the ROCK inhibitor Y27632. MYPT1-Thr853 phosphorylation induced by okadaic acid triggered perinuclear and nucleus distribution of MYPT1, which was significantly blocked by Y27632, indicating that phosphorylation of MYPT1 at Thr853 is mostly ROCK dependent. In colonic smooth muscle cells acetylcholine-mediated phosphorylation of Thr696 triggered MYPT1 translocation along with HSP27 to the insoluble membrane fraction (Patil & Bitar, 2006). This phosphorylation-mediated translocation of MYPT1 has been challenged by Neppl *et al.* (2009). They have reported that phosphorylation of MYPT1 at Thr696 or Thr853 is not a prerequisite for membrane translocation. They demonstrated that in intact cerebral vasculature, pre-treatment with 8-Br-cGMP (a cGMP analogue) completely inhibited U-46619 (TXA_2 analogue)-mediated membrane association without inhibiting U-46619-mediated phosphorylation of MYPT1 at Thr696 and Thr853. In platelets MYPT1 is majorly reported in the actin cytoskeleton and membrane fractions (Muranyi *et al*., 1998; Kiss *et al*., 2002). However, there is no

immunofluorescence based data that can verify the presence of platelet MYPT1 in these fractions.

Together these studies clearly suggest that MYPT1 is distributed in various subcellular locations in different cell types. Whether the translocation of MYPT1 is under the influence of phosphorylation at activatory serine and inhibitory threonine residues requires further investigations.

Table 1.4: Summary of cellular distribution of MYPT1.

Cell type	Cell line	Subcellular localisation of MYPT1	Effects of various substances on phosphorylation and localisation	Reference
Fibroblast		Cytoplasm, nucleus		Murata *et al*., 1997
Smooth muscle cells (SMCs)		Cytoplasm, nucleus		Murata *et al*., 1997
Intestinal epithelial cells	**Caco-2 Cells**	Cell-cell contacts		Zha *et al*., 2016
Endothelial cells		Cell-cell contacts		Hirano *et al*., 1999
Ferret portal vein cells		Cytoplasm	PGF2α: Thr696- cell periphery	Shin *et al*., 2002
Colonic SMCs		Cytosol	Acetylcholine- membrane fraction	Patil & Bitar, 2006
Intact cerebral vasculature		Cytoplasm	U-46619: membrane association.	Neppl *et al*., 2009
Platelet		Cytoskeleton, membrane fractions		Muranyi *et al*., 1998; Kiss *et al*., 2002
	REF-52 Cells	Cytoplasm		Inagaki *et al*., 1997
	MDCK Cells	Cytoplasm, cell-cell contacts, membrane ruffling area		Inagaki *et al*., 1997; Fukata *et al*., 1998
	HepG2 cells	Cytoplasm, nucleus	Okadaic acid: Thr696- plasma membrane and Thr853- perinuclear, nucleus.	Lontay *et al*., 2005

1.5.1.4 Members of the MYPT family

The mammalian MYPT family comprises four other isoforms that are encoded by separate genes with varying degrees of similarity to MYPT1, namely MYPT2, MYPT3, protein phosphatase 1 myosin binding subunit of 85kDa (MBS85) and TGF-β-inhibited membrane associated protein (TIMAP) (Grassie *et al*., 2011) (Figure 1.15). An RNA-sequence analysis of both human and mouse platelet transcriptomes suggested the presence of all family members of MYPT protein; however, only two of them were confirmed by proteomics (see table 1.5 & 1.6).

MYPT2 is encoded by *PPP1R12B* gene containing 982 residues with a molecular weight of 110 kDa and having 61% sequence similarity to MYPT1. As with MYPT1, the N-terminus of MYPT2 contains a PP1c binding motif (RVRF) followed by 7 ankyrin repeats and a C-terminal leucine zipper domain (Fujioka *et al*., 1998). There is also the inhibitory ROCK phosphorylation site (Thr646) at the central sequence and ROCK-mediated phosphorylation of Thr646 inhibits phosphatase activity (Okamoto *et al*., 2006). MYPT2 specifically interacts with PP1cδ and increases its activity toward phosphorylated striated muscle myosin. Similar to MYPT1, it also associates with RhoA via its C-terminus (Okamoto *et al*., 2006). Two splice variants of MYPT2 (MYPT2A and MYPT2B) have been reported with marked difference at the C-terminus, although both contain leucine zipper domain. These splice variants are the products of alternatively spliced exon 24 and are preferentially expressed in heart, skeletal muscle and brain (Arimura *et al*., 2001).
MBS85 was first identified as a substrate protein for myotonic dystrophy kinase-related Cdc42 binding kinase (MRCK) that mediates Cdc42-induced actin rearrangement (Tan *et al*., 2001). This protein is encoded by *PPP1R12C* gene comprising 782aa with a molecular weight of 85 kDa. MBS85 has 39% sequence similarities with MYPT1 containing N-terminal PP1c binding motif (RTVRF) and 7 ankyrin repeats followed by conserved central sequence inhibitory phosphorylation site (Thr560) and C-terminal leucine zipper motif resembling

those of MYPT1 and MYPT2. MBS85 is ubiquitously expressed; however, with higher concentration in cardiac muscle (Tan *et al*., 2001).

MYPT3 is encoded by the *PPP1R16A* gene. It displays 30 to 40% similarity to other members of the MYPT family (MYPT1/2) and contains 524 residues with a molecular weight of 58 kDa. It has an N-terminal PP1c binding motif (KHVLF), 5 central ankyrin repeats and a C-terminal prenylation motif (CAAX box; where "A" represents an aliphatic amino acid) possibly involved in membrane interaction. It also has an ATP/GTP binding-motif (Walker A type) and two SH3 sites. Contrary to other MYPT family members, the inhibitory phosphorylation site is absent in MYPT3. In the mouse it is predominantly expressed in heart, brain and kidney at higher concentrations. Interestingly, MYPT3 has also been reported to inhibit PP1cδ activity towards phosphorylated myosin, whereas MYPT1/2-PP1cδ activates phosphatase activity towards phosphorylated myosin (Skinner & Saltiel, 2001).

TIMAP is encoded by *PPP1R16B* gene, comprises 567 residues and has a molecular weight of 64 kDa. It has 44% sequence similarity to MYPT3, contains an N-terminal nuclear localisation consensus sequence, 5 ankyrin repeats, a PP1c binding motif (KVSF) and a C-terminal CAAX box. TIMAP is highly reported in endothelial, haematopoietic cells, central nervous system, lung and spleen (Cao *et al*., 2002).

The physiological roles of the above described four members of MYPT family are not well established. The MYPT2-PP1c complex is thought to be involved in the dephosphorylation of skeletal and cardiac muscle myosin (Okamoto *et al*., 2006). MBS85 appears to be involved in interaction with phosphorylated myosin and targeting PP1c to dephosphorylate MLC (Tan *et al*., 2001). MYPT3 is possibly involved in targeting myosin phosphatase to the plasma membrane where it regulates cytoskeletal protein (Skinner & Saltiel, 2001). Similarly, TIMAP appears involved in restoring endothelial barrier activity by directing PP1c to the plasma membrane of endothelial cells, where it dephosphorylate proteins involved in the regulation of the actin cytoskeleton (Cao *et al*., 2002).

Table 1.5: MYPT family protein and RNA expression levels in human platelets.

Accession no (UniProt)	Gene name	Protein name	Human platelet	
			Protein expression	Gene expression
O14974	*PPP1R12A*	MYPT1	2700	1.58
O60237	*PPP1R12B*	MYPT2	Not detected	0.086
Q96I34	*PPP1R16A*	MYPT3	Not detected	1.24
Q9BZL4	*PPP1R12C*	MBS85	1400	10.99
Q96T49	*PPP1R16B*	TIMAP	Not dectected	0.52

Table 1.6: MYPT family protein and RNA expression levels in mouse platelets.

Accession no (UniProt)	Gene name	Protein name	Mouse platelet	
			Protein expression	Gene expression
Q9DBR7	*Ppp1r12a*	MYPT1	10,620	2.11
Q8BG95	*Ppp1r12b*	MYPT2	Not detected	1.98
Q923M0	*Ppp1r16a*	MYPT3	Not detected	1.62
Q3UMT1	*Ppp1r12c*	MBS85	4020	40.39
Q8VHQ3	*Ppp1r16b*	TIMAP	Not detected	1.01

Protein expression, estimated number of copies per platelet in human and mouse quantitative proteomic studies (Zeiler *et al*., 2014; Burkhart *et al*., 2012); gene expression, mean reads per kilobase of exon model per million mapped reads values in human and mouse platelet quantitative transcriptomic studies (Rowley *et al*., 2011).

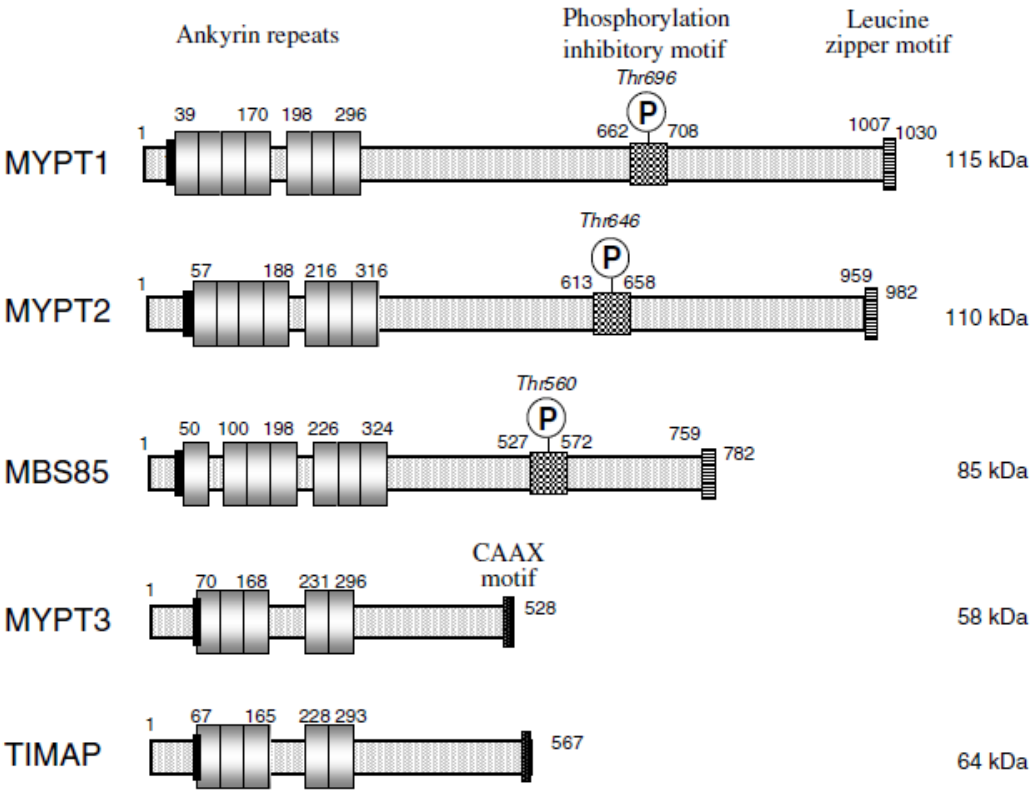

Figure 1.16: Domain structure of mammalian MYPT family members. PP1c binding motif indicated as bold black line near the N-terminus followed by ankyrin repeats indicated as rectangular boxes and a central sequence containing inhibitory phosphorylation residue conserved in MYPT1, MYPT2 and MBS85. The leucine zipper domain of MYPT1, MYPT2 and MBS85 is located at the C-terminus are indicated. A CAAX box (prenylation motif) at the C-terminus of MYPT3 and TIMAP is shown as bold black line. Taken from Ito *et al*., 2004.

1.5.2 Protein phosphatase type 1

PP1c is a member of the large phosphoprotein phosphatases (PPP) family, which in humans comprises seven different members: PP1, PP2A, PP2B (calcineurin), PP4, PP5, PP6 and PP7 (Shi, 2009). In mammalian tissues PP1c is encoded by three different genes that generate three isoforms of PP1c, α, γ and δ (also known as β). Both α and γ isoforms generate two splice variants each (Cohen, 2002). The main differences between PP1c isoforms reside in the N-terminal and C-terminal extremities. PP1c is a primary serine/threonine phosphatase that regulates a variety of cellular functions via interaction with the regulatory subunit. To date over hundred different regulatory subunits have been identified that associate with PP1c in various cell types including platelets (Butler *et al*., 2013). These regulatory subunits direct PP1c to specific subcellular locations; modulate substrate specificity possibly by an allosteric mechanism or sometimes act as substrates themselves. Thus, the association of PP1c with the regulatory subunit is central to phosphatase activity (Cohen, 2002). MYPT1 specifically interacts with PP1cδ and this interaction significantly enhances the activity and specificity of the catalytic subunit towards a substrate protein, such as MLC in smooth muscle cells (Ito *et al*., 2004).

1.5.3 Small subunit M20

M20 is a non-catalytic subunit of MLCP that interacts with the C-terminal end of MYPT1 (Hartshorne *et al*., 1998). M20 was first cloned from chicken gizzard and has two splice variants, M18 (161aa) and M21 (186aa). The structural difference between these two splice variants is the presence of a leucine zipper motif at the C-terminal part in M21 that is absent in M18 variant. Similar to MYPT1 isoforms, the expression of these splice variants is also tissue specific, M18 is mainly expressed in gizzard, whereas M21 is mainly expressed in aorta (Mabuchi *et al*., 1999). Moorhead and co-workers (1998) have revealed that M20 may possibly be encoded by *PPP1R12B*, the gene encoding MYPT2, as the last 120 residues of M20

are identical to the last residues of MYPT2. However, M20 has not been observed in tissues expressing MYPT2, i.e. brain and striated muscle.

The functional relevance of M20 has not been reported. It is thought that M20 may increase calcium sensitivity in renal artery and cardiac myocytes (Arimura *et al*., 2001). Additionally, it is suggested that M20 may bind to microtubules and regulate microtubule dynamic by enhancing the rate of tubulin polymerisation (Takizawa *et al*., 2003). Furthermore, the interaction of M20 with MYPT1 does not influence the activity of the phosphatase (Hartshorne *et al*., 1998).

1.5.4 Role of MLCP in platelets

In platelets MLCP is chiefly responsible for regulating the acto-myosin contractile machinery that is required for platelet shape change, spreading, granule secretion and aggregation. When platelets become activated by an agonist such as thrombin or TXA_2, the stimulatory signalling events activate Rho-specific guanine nucleotide exchange factor (p115RhoGEF), which converts GDP bound RhoA to active GTP-RhoA. GTP-RhoA once translocated to the plasma membrane binds and activates the downstream effector ROCK that leads to the phosphorylation of MYPT1 at Thr696 and Thr853 and results in the formation of a complex molecule RhoA/ROCK/MYPT1 (Aburima *et al*., 2013; Watanabe *et al*., 2001). As in smooth muscle cells, phosphorylation of MYPT1 at threonine residues inhibits MLCP activity in platelets and elicits increased phosphorylation of MLC at Ser19, which is required for platelet shape change (Aburima *et al*., 2013; Watanabe *et al*., 2001). Previous studies have reported that platelet shape change and MLC phosphorylation also requires calcium/calmodulin-dependent activation of MLCK (Bauer *et al*., 1999). Thereby, indicating that both RhoA-ROCK and MLCK simultaneously contribute in the MLC-mediated platelet shape change. Overexpression studies have shown the increased association of ubiquitously expressed 14-3-3 adaptor protein with RhoA-ROCK phosphorylated MYPT1. This interaction reduces MLCP activity by dissociating MLCP from myosin IIa (Koga *et al*., 2008). In platelets, ROCK-mediated phosphorylation of MYPT1 results in

translocation and dissociation of MYPT1 from PP1cδ (Aburima *et al*., 2013). Once free, PP1cδ showed low affinity and catalytic activity towards substrate proteins (Terrak *et al*., 2004). It has also been reported that the substrate site of PP1cδ is only approachable when the inhibitory residues of MYPT1 are not phosphorylated. After phosphorylation these inhibitory residues interact physically with the PP1cδ active site and result in autoinhibition of MLCP activity (Khromov *et al*., 2009). In platelets PKC-mediated phosphorylation of inhibitory phosphoprotein of myosin phosphatase (CPI-17) at Thr38 inhibits MLCP activity independent of MLCK and RhoA-ROCK pathways (Watanabe *et al*., 2001); however, the detailed picture of this inhibitory pathway is not clear. Aburima & Naseem (2014) have suggested that RhoA-ROCK mediated phosphorylation of MYPT1 results in dissociation of PP1cδ from MLCP holoenzyme and may potentially bind to PKC-mediated CPI-17 in a pseudosubstrate manner.

1.5.5 Regulation of MLCP activity in platelets

Initially it was assumed that the activity of MLCP is not regulated; however, later agonist-dependent inhibition and activation of MLCP activity in many cell types including platelets was discovered (Aburima & Naseem, 2014; Hartshorne & Ito, 2004). Inhibition of MLCP is more extensively studied and several mechanisms have been proposed as mentioned above in section 1.5.1.4; however, activation of MLCP is less defined. In general, this is thought to be associated with an increase in cAMP and cGMP levels that promote MLC dephosphorylation through targeting calcium-dependent MLCK and calcium-independent RhoA-ROCK pathways. In platelets, cyclic nucleotides-mediated PKA and PKG inhibit the activation of G-protein ($G\alpha_{13}$) that is responsible for the activation of RhoA-ROCK pathway required for MLCP inhibition (Manganello *et al*., 2003). Biochemical studies have also suggested that $G\alpha_{13}$-coupled TXA_2 receptor (TPα) is desensitised by both PKA and PKG-mediated phosphorylation (Reid & Kinsella, 2003; Walsh *et al*., 2000). In platelets cyclic nucleotide-mediated TPα receptor desensitisation have not been confirmed yet but would clearly reduce signalling events that lead to MLCP

inhibition. Moreover, in platelets, cAMP-mediated PKA and cGMP-mediated PKG directly block the activation of RhoA via phosphorylation at Ser188 and subsequent ROCK mediated inhibitory phosphorylation of MYPT1 at threonine residues that leads to reactivation of MLCP activity and inhibition of acto-myosin contractile responses (Aburima *et al*., 2013; Aburima *et al*., 2017); however, the molecular mechanism that lead to MLCP disinhibition is not very clear.

In smooth muscle cells, cGMP-mediated PKG controls MLCP activity via directly phosphorylating MYPT1 at Ser695 that is required for MLC dephosphorylation and smooth muscle relaxation (Nakamura *et al*., 2007; Wooldridge *et al*., 2004). Cyclic nucleotides-mediated phosphorylation of MYPT1 at Ser695 does not, in fact, activate MLCP, but rather disinhibits MLCP by inhibiting RhoA-ROCK mediated inhibitory phosphorylation of Thr696 and Thr853 (Nakamura *et al*., 2007; Wooldridge *et al*., 2004). Similar to smooth muscle cells, in platelets cyclic nucleotides prevent thrombin-mediated dissociation of PP1c from MYPT1, which is a prerequisite for holoenzyme complex formation and MLCP activity (Aburima & Naseem, 2014).

In platelets PKC-dependent phosphorylation of CPI-17 has been shown to inhibit MLCP activity during agonist-induced platelet activation (Watanabe *et al*., 2001). However, the role of cyclic nucleotides in the regulation of CPI-17 dependent inhibition of MLCP in platelets has not been investigated yet. Only in endothelial cells, cAMP/PKA restores endothelial barrier function via inhibiting thrombin-mediated CPI-17 phosphorylation that inhibits MLCP activity (Aslam *et al*., 2010).

Collectively these studies clearly suggest the possible role of cyclic nucleotides in the regulation of MLCP activity in platelets.

1.6 Aims of the study

Under normal conditions platelet functions are chiefly regulated by endothelial derived PGI_2 and NO (Palmer *et al*., 1987, Weksler *et al*., 1977). Both exert their effect via membrane bound adenylyl and soluble guanylyl cyclases which synthesize cAMP and cGMP, respectively. cAMP activates downstream effector PKA, whereas cGMP stimulates PKG to phosphorylate a number of substrate proteins that inhibit multiple aspects of platelet function, such as adhesion, granule secretion and aggregation *in vitro* and thrombosis *in vivo* (Smolenski, 2012). A recent study has shown the effects of cAMP/PKA signalling on the activity of MLCP, which modulates platelet shape change (Aburima *et al*., 2013); however, the molecular and biochemical regulation of MLCP activity by cAMP/PKA signalling is poorly clarified. Therefore, the overall aim of this study is to identify in detail how cAMP/PKA signalling regulates MLCP at the molecular level. To achieve this, we propose:

1. To characterise in detail the phosphorylation of the targeting subunit of MLCP (MYPT1) by PGI_2 and thrombin signalling in platelets.

2. To determine the presence of different splice variants of MYPT1 and their differential regulation by cAMP and PKC signalling in platelets.

3. To study a possible association of MYPT1 with the different PKA regulatory subunits.

4. To investigate whether MYPT1 is an AKAP.

5. To examine the subcellular distribution of MYPT1 and PKA regulatory subunits in platelets.

Chapter 2: Materials and Methods

2.1. Materials

2.1.1. Primary antibodies used in this study

No	Antibody	Host	Dilution		2% (w/v) Blocking	Source
			WB	IF		
1	MYPT1	Rabbit poly*	1:500	1:50	BSA	Santa Cruz
2	MYPT1	Mouse mono*	1:500	1:50	BSA	Santa Cruz
3	pMYPT1^{Ser695}	Rabbit poly	1:100	1:50	Milk	Santa Cruz
4	pMYPT1^{Thr696}	Rabbit poly	1:1000	1:50	Milk	Cell Signalling
5	pMYPT1^{Thr853}	Rabbit poly	1:1000	1:50	Milk	Cell Signalling
6	PKA cat sub	Mouse mono	1:1000	1:50	BSA	BD Sciences
7	PKA RI	Mouse mono	1:1000	1:50	BSA	BD Sciences
9	PKA RIα	Rabbit poly	1:1000	1:50	BSA	Cell Signalling
10	PKA RIα	Mouse mono	1:1000	1:50	BSA	BD Sciences
11	PKA RIβ	Mouse mono	1:1000	1:50	BSA	Santa Cruz
12	PKA RIIα	Mouse mono	1:1000	1:50	BSA	BD Sciences
13	PKA RIIβ	Mouse mono	1:1000	1:50	BSA	BD Sciences
14	PP1c	Rabbit poly	1:500	-	BSA	Millipore
15	Myc	Mouse mono	-	-	-	Angelika A. Noegel (U. of Cologne)
16	GST	Rabbit poly	1:5000	-	-	Angelika A. Noegel (U. of Cologne)
17	GAPDH	Mouse mono	1:6000	-	Milk	Calbiochem
18	pVSAP^{Ser157}	Rabbit poly	1:1000	-	BSA	Cell Signalling
19	pMLC^{Ser19}	Mouse mono	1:1000	-	BSA	Cell Signalling
20	CD36	Rabbit poly	1:1000	-	BSA	Cell Signalling
21	Syk	Mouse mono	1:1000	-	BSA	Santa Cruz
22	RhoA	Mouse mono	1:500	-	BSA	Santa Cruz
23	Beta3 integrin	Rabbit poly	1:1000	-	BSA	Millipore
24	Myosin IIa	Rabbit poly	-	1:300	-	Novus Biological
25	HRP-β-Actin	Mouse mono	1:5000	-	BSA	Abcam

*****Polyclonal antibody has multivalent affinity that recognises different epitopes of a particular antigen, whereas monoclonal has monovalent affinity that reacts with a single epitope of a particular antigen.

2.1.2. Secondary antibodies used in this study

No	Antibody	Host	WB	IF	Source
1	Anti-rabbit IgG, HRP conjugated	Goat	1:10,000	-	Sigma-Aldrich
2	Anti-mouse IgG, HRP conjugated	Goat	1:10,000	-	Sigma-Aldrich
3	IR Dye 800CW Anti-rabbit IgG, fluorescently labelled	Goat	1:20,000	-	Li-Cor
4	IR Dye 680CW anti-rabbit IgG, fluorescently labelled	Goat	1:20,000	-	Li-Cor
5	IR Dye 800CW Anti-mouse IgG, fluorescently labelled	Goat	1:20,000	-	Li-Cor
6	IR Dye 680CW anti-mouse IgG, fluorescently labelled	Goat	1:20,000	-	Li-Cor
7	IR Dye 800CW Anti-mouse IgG, fluorescently labelled	Donkey	1:20,000	-	Li-Cor
8	IR Dye 680CW anti-mouse IgG, fluorescently labelled	Donkey	1:20,000	-	Li-Cor
9	Anti-mouse IgG, Alexa 488 conjugated	Goat	-	1:1000	Invitrogen
10	Anti-mouse IgG, Alexa 568 conjugated	Goat	-	1:1000	Invitrogen
11	Anti-rabbit IgG, Alexa 488 conjugated	Goat	-	1:1000	Invitrogen
12	Anti-rabbit IgG, Alexa 568 conjugated	Goat	-	1:1000	Invitrogen

2.1.3. Primers used for cloning purposes

PCR amplicon	Forward primer (5' to 3')	Reverse primer (5' to 3')
HsMYPT1-FL	CCG GA ATT CGG **ATG** AAG ATG GCG GAC GCG	CGG GGT ACC**TTA** TTT GGA AAG TTT GC
HsMYPT1-NT	A GGA TCC**ATG** CAG ATG GCG GAC GCG	AAG CTT**TCA** ATT TTT CTC TGG TTC
HsMYPT1-CT	GA ATT CAACCA GAG AAA AAT GC	GCGGCCGC**TTA** TTT GGA AAG TTT GC
HsMYPT1-C1f	CCG GA ATT CCA GAG AAA AAT GCA TCC	CGG GGT ACC**TCA** TCT CCT TGT ATA TGA ACT AC
HsMYPT1-C2	CCG GA ATT CCA AGA CGA CTA GCC AGT AC	CGG GGT ACC**TCA** TTC TTG AAG ATC AGT TAA TG
HsMYPT1-C3	CCG GA ATT CAA GAG TCT GAA TCC CAA AG	CGG GGT ACC**TCA** TTC TTT CTT ATT GGA TCC C
HsMYPT1-C4	CCG GA ATT CAA GAA GGA GAA GAT AAA TCA C	CGG GGT ACC**TTA** TTT GGA AAG TTT GCT TAT AAC

HsPKARIα	GGA TCC**ATG** GAG TCT GGC AGT ACC	CTC GAG**TCA** GAC AGA CAG TGA CAC
HsPKARIβ	AAGA TCTGGA TGG CCT CCC CG	A GAA TTC**TCA** GAC GGT GAG
HsPKARIIα	GGA TCC**ATG** AGC CAC ATC CCG CCG	CTC GAG**CTA** CTG CCC GAG GTT GCC
HsPKARIIβ	AAGA TCTGGA TGA GCA TCG AGA TCC CG	A GAA TTC **TCA** TGC AGT GGG TTC AAC
HsMYPT1-CI	CCG GA ATT CAA AGT TGC TCC TTT GGT AG	CGG GGT ACC**TCA** ACT GCT TTG TGT GCC TGC
HsMYPT1-C2NCI	CCG GA ATT CCA AGA CGA CTA GCC AGT AC	CGG GGT ACC**TCA** TTT ATG ATA CGT TGA TCC
HsMYPT1-C2CCI	CGG GA ATT CGT ACC TCA AAT CGT TTG TGG	CGG GGT ACC**TCA** TTC TTG AAG ATC AGT TAA TG
HsMYPT1-LZ	CCG GA ATT CGG **ATG** AAG ATG GCG GAC GCG	CGG GGT ACC**TCA** AGA TAT TCT TCT TTC TAG
HsPKARIβ-D/D	CCG GG ATC CCA AAC TCA CAG TCG GAC TCC	CGG GGT ACC**TCA** GAC GGT GAG GGA GAT GAA G
HsPKARIIβ-D/D	CCG GG ATC CTC TGC CAT GAG GGC AGG ACC TG	CGG GGT ACC**TCA** TGC AGT GGG TTC AAC AAT ATC

Built-in restriction enzyme sites are underlined, start or stop codons are bold. Bases are grouped by codons according to the reading frame in both forward and reverse primers. All primers were custom made by Eurofins Genomics.

2.1.4. Primers used for sequencing

Vector	Forward primer
pCMV- myc	GATCCGGTACTAGAGGAACTGAAAAAC
pRK5-myc	GAAATTTGTGATGCTATTGC
pGEX	GGGCTGGCAAGCCACGTTTGGTG
pQE	CCCGAAAAGTGCCACCTG
pEGFP	CATGGTCCTGCTGGAGTTCGTGAC

2.1.5. List of vectors used

Vector	Features	Source
pCMV-Myc	3.8 kb; Myc-N-terminal, ampicillin resistance, for transient expression in mammalian cells	Clontech
pRK5-Myc	5.4 kb; Myc-N-terminal, ampicillin resistance, for transient expression in mammalian cells	Clontech
pGEM-Teasy	3.15kb, ampicillin resistance, for transient expression of proteins in bacteria.	Promega
pGEX-3X, pGEX-4T-2	4.9 kb, GST-N-terminal, ampicillin resistance, for expression of GST fusions in *E. coli.*	GE Healthcare
pEGFP-C2	4.7 kb, GFP-N-terminal, kanamycin resistance, for expression of GFP fusions in mammalian cells.	Clontech
pQE32	3.46 kb, 6X His-N-terminal, ampicillin resistance, for transient expression in bacteria.	Qiagen

2.1.6. Mammalian cell lines and bacterial strain

	Name	Origin	Description
Mammalian cell lines	293T HEK cells	*Homo sapiens*	Human embryonic kidney cells transformed with large T antigen of SV40, used for mammalian protein expression
	HeLa cells	*Homo sapiens*	Cervix carcinoma, used for mammalian protein expression
Bacterial strains	XL1-Blue	*E.coli*	For routine cloning
	M15 (pREP4)	*E.coli*	Expression host for pQE vectors
	Rosetta-gami	*E.coli*	Enhanced expression of eukaryotic proteins
	Rosetta 2	*E.coli*	Enhanced expression of eukaryotic proteins
	BL21	*E.coli*	For general protein expression

2.1.7. cDNA clones used as template

cDNA	Backbone	Source
HsMYPT1	pCR-BluntII-TOPO	Purchased from cDNA repository
HsPKA RIα	pRSETB	Gift from Prof Kjetil Taskén
HsPKA RIβ	pCMV-SPORT6	Purchased from cDNA repository
HsPKA RIIα	pDEST	Gift from Prof Kjetil Taskén
HsPKA RIIβ	pCR-BluntII-TOPO	Purchased from cDNA repository

2.1.8. Expression constructs used in HEK cells

Insert	Residues	Backbone
Myc-HsMYPT1-FL	1-1030	pCMV-Myc
Myc-HsMYPT1-NT	1-330	pRK5-Myc
Myc-HsMYPT1-CT	327-1030	pCMV-Myc
Myc-HsMYPT1-C1	327-531	pCMV-Myc
Myc-HsMYPT1-C2	501-706	pCMV-Myc
Myc-HsMYPT1-C3	676-881	pCMV-Myc
Myc-HsMYPT1-C4	825-1030	pCMV-Myc
HsPKARIβ	1-381	pEGFP-C2
HsPKARIIβ	1-418	pEGFP-C2

All of these plasmids were specifically constructed for this study.

2.1.9. Expression constructs used in *E.coli*

Insert	Residues	Backbone
HsPKARIα	1-381	pGEX-4T-2
HsPKARIβ	1-381	pGEX-3X
HsPKARIIα	1-404	pGEX-4T-2
HsPKARIIβ	1-418	pGEX-3X
HsMYPT1-C2	501-706	pGEX-4T-2
HsMYPT1-CI	552-608	pGEX-4T-2
HsMYPT1-C2NCI	501-551	pGEX-4T-2
HsMYPT1-C2CCI	609-706	pGEX-4T-2
HsMYPT1-C2fwdCIrev	501-608	pGEX-4T-2
HsMYPT1-CIfwdC2rev	552-706	pGEX-4T-2
HsMYPT1-lack LZ	1-995	pGEX-4T-2
HsPKARIβ lack DD	71-381	pQE32
HsPKARIIβ lack DD	51-418	pQE32

All of these plasmids were specifically constructed for this study.

2.1.10. Molecular biology enzymes used in this study

Name	Source
Q5 High fidelity DNA polymerase	New England BioLabs
Pfu DNA polymerase	New England BioLabs
Taq DNA polymerase	ThermoScientific, Promega
Ribonuclease A (RNAse A)	Macherey-Nagel
Restriction endonucleases	Fermentas, ThermoScientific, Jena Biosciences, New England Biolabs
Shrimp alkaline phosphatase (SAP)	Roche
T4 DNA ligase	Fermentas, Promega
Klenow fragment (DNA polymerase I)	Roche
Mung bean nuclease	New England BioLabs

2.1.11. Fluorescent dyes

Name	Source
4´, 6´- diamidino – 2 phenylindol (DAPI)	Sigma
TRITC-Phalloidin	Sigma
FITC-Phalloidin	Sigma

2.1.12. Inhibitors

Name	Source
Phenylmethylsulfonyl fluoride (PMSF)	Sigma
Protease Inhibitor Cocktail	Sigma
Calyculin A	Sigma
Latrunculin A &B	Calbiochem
Indomethacin	Sigma-Aldrich
Apyrase	Sigma-Aldrich
Sodium orthovanadate (Na_3VO_4)	Sigma-Aldrich
AKAP St-Ht31 inhibitor peptide (St-Ht31)	Promega

2.1.13. Transfection reagent

Name	Source
Lipofectamine® Transfection Reagent (Cat no: 18324012)	Invitrogen

2.1.14. Antibiotics

Name	Source
Ampicillin	Sigma
Kanamycin	Melford Laboratories
Penicillin/Streptomycin	Thermo Fisher Scientific

2.1.15. Molecular weight markers

Name	kDa	Source
EZ-Run™ Prestained Rec protein ladder	170/130/95/72/55/43/34/26/17/10	Fisher Scientific
Precision Plus protein standards (Dual Color)	250/150/100/75/50/37/25/20/15/10	Bio-Rad
Low molecular weight marker	97/66/45/30/20/14.4	Amersham Biosciences
1 kb Full scale DNA Ladder	10000, 8000, 6000, 4000, 3000, 2000, 1550, 1400, 1000, 750, 500, 400, 300, 200, 100, 50 bp	Fisher Scientific
100 bp scale DNA Ladder	2000, 1550, 1400, 1000, 750, 500, 400, 300, 200, 100, 50 bp	Fisher Scientific

2.1.16. Kits

Name	Source
pGEM-T easy cloning kit	Promega
High Pure plasmid purification kit (for mini prep)	Roche
Nucleobond AX 100 (for midi prep)	Macherey Nagel
NucleoSpin gel and PCR cleanup Kit	Macherey Nagel
Pierce® BCA protein assay kit	Pierce (ThermoScientific)
Precision Red advanced protein assay	Cytoskeleton Inc.

2.1.17. Laboratory materials

Name	Source
6-well plates	Nunc
24-well plates	Nunc
Petri dishes: 60x15 mm, 100x20 mm, 140x20 mm	Nunc
Serological pipettes: 5 ml, 10 ml, 25 ml	Sarstedt
Cell scraper 25 cm	Sarstedt
Coverslips: 12 mm in diameter	Fisher Scientific
Microscope slides 76x26 mm	Fisher Scientific
Neubauer improved chamber depth: 0.100 mm; 0.0025 mm^2	Labor Optik
PCR reaction tubes: 0.2 ml	VWR
Filters: 0.20 µm, 0.45 µm	Millipore
Falcon tubes: 15 ml, 50 ml	Star Labs
Eppendorf tubes: 0.5 ml, 1.5 ml, 2 ml	Eppendorf
Pipette tips (10, 200, 1000 µl)	Star Labs
Parafilm	Pechiney
Cryotubes 1 ml	Nunc
Nitrocellulose transfer membrane	Pall
PVDF transfer membrane	Pall, Bio-Rad, GE Healthcare Life Sciences
Hyperfilm ECL 18x24 cm	GE Healthcare Life Sciences
Syringes	BD Plastipak
Needles	BD Plastipak
Pipettes: 1-10 µl, 1-20 µl, 20-200 µl und 200-1000 µl	Gilson

2.1.18. Chemicals

Laboratory reagents and materials were obtained from following suppliers: Amersham, Biomol, Fluka, Invitrogen, Melford Laboratories, Merck, National Diagnostic, Pharmacia, Promega, Sigma-Aldrich, Serva, Roche and Roth.

2.2. Sterilisation

Media, buffers, glassware and agar were sterilised by autoclaving at 120°C and 15 psi. If sterilisation by autoclaving was not possible, 0.2 µm or 0.45 µm filter units were used.

2.3. Molecular biology methods

Below are the molecular biology techniques used to analyse and manipulate DNA, RNA or protein applied in this study.

2.3.1. Polymerase chain reaction (PCR)

This is one of the most important techniques used in molecular biology to copy a single DNA sequence into millions of DNA molecules in a very short period of time. It can also be used to introduce a mutation in a particular base of DNA or add restriction enzyme sites to the ends of DNA.

In this study standard PCRs were performed in a Bio-Rad Thermo Cycler C1000 to amplify particular cDNA templates of our proteins of interest. Amplification reactions were as follows.

10 µl of 5x Q5 Reaction Buffer
1 µl of 10 mM deoxynucleotide triphosphates (dNTPs)
2.5 µl of 10 pmol/µl forward primer
2.5 µl of 10 pmol/µl reverse primer
0.5 µl Q5 High-Fidelity DNA polymerase
1 µl of cDNA as template

32.5 µl of ultrapure water

50 µl of PCR reaction was gently mixed in PCR tubes, tubes spun to collect all the liquid at the bottom of the tube and then transferred to the thermocycler for amplification.

Thermocycling conditions for PCR using high-fidelity DNA polymerase are as follows:

Step	Temperature	Time
Initial Denaturation	98℃	30 sec
32 Cycles	98℃ 53℃ 72℃	5-10 sec 30 sec 30 sec/kb
Final Extension	72℃	2 min
Hold	4-10 ℃	Indefinite

2.3.2. DNA agarose gel electrophoresis

Agarose gel electrophoresis was performed to resolve and purify DNA fragments after PCR or restriction endonuclease digestions. Gel was prepared by boiling 1% (w/v) agarose in 1x TAE buffer. After agarose had cooled down, ethidium bromide or midori green was added (final concentration 0.1 µg/ml) and the gel was poured in a casting chamber containing appropriate size of combs. After gelation the gel was submerged in a horizontal electrophoresis tank containing 1x TAE buffer. All DNA samples were mixed with DNA loading buffer. DNA size marker (100 bp or 1 kb) and DNA samples were loaded before electric current was applied. The gel was run until the bromophenol blue dye present in the DNA-loading buffer had migrated the appropriate distance through the gel. The gel was examined under UV light and a picture was taken using either a phone camera or a Bio-Rad VersaDoc 1000 imaging system (Bio-Rad laboratories, Hertfordshire, UK).

TAE buffer, pH 8.3	DNA loading buffer	TE buffer, pH 8.0
40 mM Tris base	6% (v/v) Glycerol	10 mM Tris base
20 mM Acetic acid	0.05% (w/v) Bromophenol blue	1 mM EDTA
2 mM EDTA	Dissolve in TE buffer	

2.3.3. Recovery and purification of PCR amplified products from agarose gels

A commercial NucleoSpin Extraction Kit was used to clean the PCR product from the agarose gel after electrophoresis. The desired DNA fragment was quickly and carefully cut out from the agarose gel with a clean scalpel on a UV transilluminator. The excised piece of gel was dissolved in a clean labelled eppendorf tube containing NT1 buffer (200 µl NT1 buffer/100 mg of gel) for 10 min at 50°C and 300 rpm. The mix was loaded into a PCR cleanup column with collection tube before spinning at 11,000xg for 30 sec. The flow through was discarded and the DNA bound column was washed twice with NT3 buffer. Next the column was dried prior to elution with elution buffer. The concentration and quality of the eluted DNA was tested on by spectrophotometry (see 2.4.10) and by running an aliquot on an agarose gel.

2.3.4. Restriction endonuclease reaction and DNA precipitation

DNA was cut with chosen restriction enzymes in a reaction mixture containing suitable enzyme buffers as per manufacturers' instructions for 2 hrs at 37°C. Subsequently the cut DNA was precipitated using 2.5 volumes of absolute ethanol and 1/10th of 3 M sodium acetate followed by centrifugation at 15,000xg for 10 min at 4°C. Precipitated DNA was washed once with 70% ethanol and dried before redissolved in 10 mM Tris EDTA, pH 8.0. The quality of the cut PCR product was tested on agarose gel.

2.3.5. Blunt end generation of linearised plasmids

In some cases it was necessary to convert the 5' or 3' sticky ends generated by restriction enzymes into blunt ends. Filling of 5' overhangs was performed by polymerase activity of the Klenow fragment. First DNA was dissolved in 1x NEB buffer supplemented with 1mM dNTP. 2U of Klenow fragment was added to the mix and incubated for 15 min at 37°C, another 2U were added and the mix incubated for further 15 min at 37°C. The activity of the Klenow fragment was stopped by either heat inactivation at 65°C for 10 min or by ethanol precipitation.

Mung bean nuclease was used to generate blunt ends by removing 3' overhangs. DNA (0.1 µg/µL) was dissolved in 1x mung bean nuclease buffer and 1U of mung bean nuclease per µg DNA was added before incubation at 37℃ for 30 min. The enzyme was inactivated by addition of 0.01 % SDS and DNA was recovered by ethanol precipitation.

2.3.6. Dephosphorylation of plasmid DNA 5´- ends

5´- ends of linearised plasmid DNA were dephosphorylated to prevent self-ligation and facilitate ligation the insert. 1U of shrimp alkaline phosphatase (SAP), 10x SAP buffer and ultrapure water where added to the linearised plasmid to the final reaction volume of 10 µl. The reaction was mixed gently and incubated for 10 min at 37℃. The reaction was stopped by heat inactivating the enzyme at 65℃ for 15 min.

<u>10x SAP buffer</u>
0.5 M Tris-HCl, pH 8.5
10 mM $MgCl_2$

2.3.7. Ligation of vector and insert

Dephosphorylated plasmid DNA and purified insert DNA fragment were mixed with T4 DNA ligase, T4 DNA ligase buffer and ATP as shown below and the ligation reaction was mixed gently and left for 15 min at room temperature. The reaction was stopped by heat inactivating the enzyme at 65℃ for 10 min.

<u>Ligation Reaction</u>

Linearised plasmid DNA (vector):	1 µl
Purified DNA fragment (insert):	14 µl
T4 DNA ligase:	2 µl
10x T4 DNA ligase buffer:	2 µl
ATP (100 mM):	1 µl
and ultrapure water to make up to	20 µl

10x Ligase buffer

660 mM Tris-HCl, pH 7.5
50 mM $MgCl_2$
50 mM DTT
10 mM ATP

2.4. Bacterial culture methods

2.4.1. Preparation of media for *E.coli* culture

The Luria Bertani (LB) broth, a nutritionally rich medium for bacterial growth was prepared with deionised water and autoclaved at 120℃. Ampicillin (0.1 mg/ml) or kanamycin (0.05 mg/ml) were added to the autoclaved medium after cooling it down to approximately 55℃.

For LB agar plates, 1.5% of agar was added to the LB medium and then autoclaved at 120℃ in a benchtop autoclave (Prestige medical ltd, Blackburn, UK). The autoclaved medium was cooled down to about 55℃ and an appropriate antibiotic was added. For blue-white selection of *E. coli* transformants, 10 µl of 1M IPTG solution (isopropyl β-D-1-thiogalactopyranoside) and 40 µl of X-gal solution (20 mg/ml solution of 5-bromo-4-chloro-3-indolyl-β-D-galactopyranoside dissolved in N,N´- dimethyl-formamide) were spread on the agar plate and let dry for 30 min at 37℃ before using.

LB medium (pH 7.0 at 37˚C) (Sambrook *et al*., 1989)

1% (w/v) Bacto-Trypton
0.5 % (w/v) Yeast Extract
0.5 % (w/v) NaCl
Add dH_2O to make 1 litre

LB agar plates (pH 7.0 at 37˚C)

1 % (w/v) Bacto-Trypton
0.5 % (w/v) Yeast Extract
0.5 % (w/v) NaCl
1.5 % (w/v) Agar-Agar

2.4.2. Preparation of competent cells (*E.coli* XL-1 blue)

For routine cloning, XL-1 blue bacterial strain was streaked out onto an LB agar plate and grew overnight at 37°C. Next day a single colony was picked up from the LB agar plate, used to inoculated 20 ml of LB medium and grew overnight at 37°C with shaking at 200 rpm. 250 ml of LB medium were inoculated with this overnight culture and allowed to grow with shaking to an optical density of OD_{600}=0.4-0.5. The culture was then left on ice for 20 min and spun at 2500xg for 10 min at 4°C. The supernatant was discarded and the pellet was resuspended in 80 ml of ice cold TB buffer, rested on ice for 10 min and centrifuged again at 2500xg for 10 min at 4℃. After centrifugation the pellet was resuspended in 20 ml of TB buffer and mixed with 1.6 ml of DMSO. The cell suspension was aliquoted in fresh labelled eppendorf tubes, flash-frozen in liquid nitrogen and stored at -80℃.

Transformation buffer (TB buffer) (pH 6.7)
10 mM PIPES
15 mM $CaCl_2$
250 mM KCl
Set pH 6.7 with KOH and then
$MnCl_2$ was added to the final concentration of 55 mM.

2.4.3. Preparation of $CaCl_2$ competent *E.coli* cells (Quick method)

An overnight grown culture of *E.coli* (20 µl) was inoculated into a flask containing 20 ml of LB medium and incubated at 37°C, with shaking at 200 rpm for 4 hrs. After 4 hrs, 1 ml of culture (per transformation) was transferred to a 1.5 ml sterile eppendorf tube and incubated on ice for 10 min before being harvested by centrifugation at 10,000xg for 2 min at 4°C. Bacterial pellet was resuspended in 1 ml of ice cold $CaCl_2$ (50 mM) before harvesting again by centrifugation at 10,000xg for 2 min at 4°C. The cells were resuspended this time in 100 µl of ice cold $CaCl_2$ (50 mM) and incubated on ice for 30 min before transformation.

2.4.4. Transformation of *E.coli*

100 µl of XL-1 blue competent cell suspension was thawed on ice for 30 min. Ligation reaction mix was added to the cell suspension, mixed gently and incubated on ice for 1 hr. A heat shock of 42°C was applied to the cells for 90 sec and they were immediately placed on ice for 2 min. 1 ml of filtered SOC (super optimal broth) medium (without antibiotic) was added to cells and incubated for 1 hr at 37°C with shaking at 180 rpm before spinning at 6000xg for 2 min. Most of the supernatant was discarded and pellet resuspended in 50-100 µl residual medium or fresh LB medium. The suspension was plated out on a LB agar plate in a laminar flow cabinet and incubated overnight at 37℃.

SOC medium (pH 7 at 37˚C) (autoclaved at 121℃ and filtered through 0.2 µm filter unit) (Sambrook *et al*., 1989)

2 % (w/v) Bacto-trypton
0.5 % (w/v) Yeast Extract
10 mM NaCl
2.5 mM KCl
20 mM Mg^{2+} (1:1 $MgCl_2 \cdot 6H_2O$ and $MgSO_4 \cdot 7H_2O$)
20 M glucose

2.4.5. Colony PCR

Colony PCR was performed to test bacterial colonies from agar plates for the presence or absence of insert DNA in a plasmid construct after transformation.

A single bacterial colony was picked with a micropipette tip and transferred to a microcentrifuge tube containing 50 µl of LB medium with the appropriate antibiotic. The microcentrifuge tube was placed in a heating block for 1 hr at 37℃. Next a PCR reaction was setup for each colony as described below. For convenience, a master mix was prepared and 24 µl was added to each PCR tube. For positive control 10 ng pure plasmid and a negative control (no template) were used.

10x PCR buffer	2.5 µl
25 mM $MgCl_2$	1 µl
10 mM dNTPs	0.5 µl
10 mM (=10 pmol/µl) Forward primer	0.5 µl
10 mM (=10 pmol/µl) Reverse primer	0.5 µl
Taq polymerase 5U/µl	0.5 µl
Milli Q water	18.5 µl

25 µl of PCR reaction was gently mixed in PCR tubes spun all the liquid to the bottom of the tube and then transfer to a thermocycler.

Thermocycling conditions for colony PCR using Taq DNA polymerase are as follows:

95°C 2 min	1 cycle
95°C 15 sec 55°C 15 sec 72°C 1 min per kb	30 cycles
72°C 5 min	1 cycle
4 °C	Hold

After PCR, the reaction was mixed with 6 µl of DNA loading buffer and loaded on an agarose gel. Next the gel was inspected under UV transilluminator and positive colonies were propagated by inoculation in a large amount of LB medium with appropriate antibiotic for either further analysis or subsequent applications.

2.4.6. Preparation of glycerol stock

Glycerol stock of all bacterial strains/transformants was prepared by mixing 345 µl of 87% sterile glycerol with 655 µl of an overnight bacterial culture in 1.5 ml sterile eppendorf tube. The tube was then clearly labelled with date, stock number, plasmid name and number before storing at -80°C for future use.

2.4.7. Purification of plasmid DNA by the alkaline lysis method

This lysis method of Birnboim & Doly (1979) was used for screening a large number of clones simultaneously for desired recombinant plasmid. Briefly, 1.5 ml LB media containing single bacterial colony and an appropriate antibiotic were grown overnight at 37°C and 200 rpm. Next day overnight culture was spun at 6000xg for

2 min at room temperature. The pellet was first resuspended in 150 µl suspension buffer containing RNase A then 150 µl of lysis buffer was added and the lysate was incubated for 5 min on the bench. Next 150 µl ice cold binding buffer were added and the mix was incubated for 5 min on ice before being spun at ≥ 15000xg for 10 min at room temperature. The supernatant was transferred into a clean eppendorf tube and the plasmid DNA was precipitated as described in section 2.3.4.

Suspension buffer, pH 8.0
50 mM Tris-HCl,
10 mM EDTA
100 µg/ml RNase A

Lysis buffer
0.2 M NaOH
1% SDS

Binding buffer, pH 4.2
4 M guanidine hydrochloride
0.5 M potassium acetate

TE buffer, pH 8.0
10 mM Tris base
1 mM EDTA

2.4.8. Purification of plasmid DNA (mini prep)

A commercial High Pure Plasmid Isolation Kit was used to extract high quality plasmid DNA for sequencing, PCR and transformation. First 5 ml of LB medium containing ampicillin (0.1 mg/ml) and a single colony of *E. coli* from a glycerol stock were inoculated in a 5 ml glass tube overnight at 37°C and 200 rpm. Next day the overnight culture was spun at 6000xg for 2 min at 4°C. The bacterial pellet was resuspended in 250 µl of suspension buffer containing RNase. 250 µl of lysis buffer were added prior to incubation for 5 min at room temperature. The lysate was neutralised with 350 µl of ice cold binding buffer on ice for 5 min and was spun at >15,000xg for 10 min at 4°C. The plasmid DNA present in the supernatant was passed through a filter tube containing silica matrix, washed with buffer I and buffer II containing ethanol and then eluted with 50 µl of elution buffer.

Suspension buffer, pH 8.0
50 mM Tris-HCl,
10 mM EDTA
100 µg/ml RNase A

Wash buffer I, pH 6.6
5 M guanidine hydrochloride
20 mM Tris-HCl
20 ml absolute ethanol

Lysis buffer
0.2 M NaOH
1% SDS

Binding buffer, pH 4.2
4 M guanidine hydrochloride
0.5 M potassium acetate

Wash buffer II, pH 7.5
5 M guanidine hydrochloride
2 mM Tris-HCl
20 mM NaCl
Add 40 ml absolute ethanol

Elution buffer, pH 8.5
10 mM Tris-HCl

2.4.9. Purification of plasmid DNA for mammalian cell transfection

High quality plasmid for transfection of mammalian cells was isolated using a commercial kit Nucleobond AX 100. 50 ml of LB medium were inoculated overnight with a single colony of *E.coli* picked from a plate at 37°C with shaking at 200 rpm. The overnight culture was then centrifuged at 6000xg for 30 min at 4°C. The bacterial pellet was resuspended in 4 ml of buffer S1 containing RNase A. Cells were lysed with 4 ml of buffer S2 for 3 min before being neutralised with 4 ml of buffer S3 on ice for 5 min. The lysate was clarified by filtration and then passed through a column pre-equilibrated with buffer N2. Plasmid DNA remained bound to the silica-base anion-exchange resin while proteins, polysaccharides and tRNA flew through the column. mRNA and rRNA were washed out with buffer N3 and plasmid DNA was subsequently eluted with 5 ml of elution buffer N5. After elution plasmid DNA was precipitated by incubating at -80°C for 2 hrs in 0.1 volume of 3 M sodium acetate and 2.5 volumes of absolute ethanol. The precipitated DNA was pelleted by centrifugation at ≥ 15,000xg for 10 min at 4°C, washed with 70% ethanol, dried at 37°C and redissolved in TE buffer. Quality and quantity of the isolated plasmid were determined by spectrophotometry (see section 2.4.10).

Buffer S1, pH 8.0
50 mM Tris-HCl
10 mM EDTA
100 µg/ml RNase A

Buffer S2
200 mM NaOH
1% SDS

Buffer N3
100 mM Tris
15% ethanol
1.15 M KCl

Buffer N5
100 mM Tris
15% ethanol
1 M KCl

Buffer S3, pH 5.1
2.8 M Potassium acetate

Buffer N2
100 mM Tris
15% ethanol
900 mM KCl
0.15% Triton X-100

TE buffer, pH 8.0
10 mM Tris base
1 mM EDTA

2.4.10. Determination of plasmid DNA concentration

Plasmid DNA concentration was measured by spectrophotometry using a Thermofisher Nanodrop 1000 at wavelength λ = 260 nm. The purity of the DNA was assessed by the absorbance ratio at 260 nm and 280 nm. A ratio close to 1.8 is generally means pure DNA, whereas if the ratio is considerably lower than 1.8 means contamination with protein or other contaminants that absorb strongly at or near 280 nm.

2.4.11. DNA sequencing

Most of the PCR amplified products were verified by sequencing with specific primers. DNA sequencing was performed by Eurofin Genomics.

2.4.12. Computer analysis

DNA sequence analysis was performed by ExPASY translate tool (https://web.expasy.org/translate/), protein structure analysis was performed by using Heliquest software (http://heliquest.ipmc.cnrs.fr/cgi-bin/ComputParams.py), restriction enzyme mapping was performed by using NEB cutter website (http://nc2.neb.com/NEBcutter2/) and the BLAST tool of NCBI (https://blast.ncbi.nlm.nih.gov/Blast.cgi?PROGRAM=blastn&PAGE_TYPE=BlastSearch&LINK_LOC=blasthome) was used for multiple sequence alignments.

2.5. Cell biology methods

2.5.1. Mammalian cell culture

Mammalian cells (239T HEK and HeLa cells) were grown at 37˚C in a humidified incubator supplied with 5% CO_2. The cells were grown in Dulbecco's Modified Eagle (DME) medium supplemented as below.

Mammalian cell culture medium

DME medium “high glucose” (4.5 g/l)
10% heat inactivated fetal bovine serum (FBS)
2 mM glutamine
100 U/ml penicillin and 100 µg/ml streptomycin
1 mM sodium pyruvate

2.5.2. Thawing of mammalian cell stocks

A cryovial containing frozen mammalian cells was removed from liquid nitrogen storage and immediately thawed in a 37°C water bath. 10 ml of pre-warmed DME medium was added to the thawed cells to remove DMSO (dimethylsulfoxide). The cell suspension was centrifuged at 200xg for 5 min at 4°C. Supernatant was removed and the cells were resuspended in fresh prewarmed DME medium and transferred to 25 to 75 cm flasks. Next day the cells were ready for splitting.

2.5.3. Subculturing of mammalian cells

After discarding spent cell culture media, the cells were washed with sterile PBS in culture hood. 1 ml of prewarmed trypsin (0.05%) and EDTA (0.53 mM) mix was added to the wash cells and incubated at 37˚C for 90 sec to detach the cells. 500 µl of FBS were immediately added to inactivate the trypsin. The cells were then transferred to a 15 ml conical tube and spun at 200xg for 5 min at 4˚C. The supernatant was discarded and the pellet was gently resuspended in prewarmed fresh growth medium before removing a sample for counting. Cells were counted using a haemocytometer under an inverted microscope. Subsequently, the

required number of cells were transferred to a fresh labelled flask containing pre-warmed growth medium and incubated at 37˚C.

2.5.4. Transient transfection of mammalian cells

Transient transfection of 239T HEK cells with Lipofectamine was performed 24 hrs after splitting cells. 2 µg of DNA and 15 µl of Lipofectamine (for 5 cm plate) were mixed separately in 200 µl of prewarmed DME medium without FBS. After 5 min both DNA and Lipofectamine mix were added together and incubated for 30 min at room temperature. 400 µl of prewarmed medium without FBS were then added to the Lipofectamine-DNA complexes before adding the mix to the HEK cells containing 800 µl of freshly changed prewarmed medium without FBS and incubated at 37°C for 4 hrs. After 4 hrs 1600 µl of prewarmed medium containing 20% FBS were added to the transfected cells and incubated overnight at 37°C. If larger amounts of transfected cells were required, cells were split to bigger plates and the amount DNA and Lipofectamine were scaled up according to the surface area of the plates as shown in table 2.2.

Table 2.2: List of suggested amounts of reagents used for transfection

Culture dish/plate	Surface area (cm^2)	Volume of platting medium	Cells per dish/well (cell/ml)	Volume of dilution medium	DNA	Lipofectamine® Transfection Reagent
100 mm	55	10 ml	$13.7x10^6$	2x500 µl	4 µg	30 µl
60 mm	21	5 ml	$5x10^6$	2x200 µl	2 µg	15 µl
6 well plate	9	2 ml	$1x10^6$	2x100 µl	1 µg	10 µl
24 well plate	2	1 ml	$5x10^4$	2x40 µl	0.4 µg	6 ul

2.5.5. Lysis of mammalian cells

239T HEK cells were scraped off the culture plate (5 cm) in ice cooled lysis buffer containing protease inhibitor cocktail. The lysate was transferred to a clean labelled eppendorf tube and incubated on ice for 30 min. The cell lysate was centrifuged at 10,000xg for 10 min at 4˚C to remove unbroken cells and debris. The supernatant was transferred to a fresh 1.5 ml eppendorf tube.

Lysis buffer
150 mM NaCl
1% Triton X-100
50 mM Tris-HCl, pH 8.0

2.5.6. Cryopreservation of mammalian cells

To prepare mammalian cells for cryopreservation in liquid nitrogen, a confluent monolayer from a 10 cm culture plate was trypsinised and resuspended in cold DME medium without FBS and incubated for 30 min on ice. The cells were then centrifuged for 10 min at 200xg and at 4°C. The pellet was resuspended in 1 ml of freezing medium and transferred to clean and labeled cryotubes. The tubes were then placed into a pre-cooled cryorack (Nalgene Mr Frosty^{TM} Cryo) with special filling soaked in isopropanol and left at -80°C overnight. Following day the cryotubes were transferred to liquid nitrogen until further use.

Freezing medium

70% DMEM
20% FBS
10% DMSO

2.6. Platelet biology methods

2.6.1. Isolation of human platelets

Whole blood was collected from healthy consented male and female volunteers, who confirmed that they were not under any medication that affects platelet

activity such as NSAID, anti-histaminics etc. for at least two weeks before blood donation. Ethical approval for the use of human blood in the study described herein was granted by the Hull York Medical School. The blood was drawn by a puncture of the median-cubital vein via a 21-gauge butterfly needle mounted on plastic tubing (20 cm in length) directly into a 20 ml plastic syringe containing an anticoagulant, acid citrate dextrose (ACD) at a ratio of 1:5 (1 volume of ACD and 4 volumes of blood). ACD functions as calcium chelator and therefore prevents the coagulation events. The first 2-4 ml of blood were discarded to avoid contamination of tissue factor and traces of thrombin that would result in platelet activation.

Immediately after collection the citrated blood was gently transferred into a 50 ml conical tube and centrifuged at 200×g for 15 min at room temperature (RT) in a swing-out rotor centrifuge. Centrifugation separated the whole blood into three layers; the bottom layer consists of erythrocytes, an intermediate layer contains leukocytes (thin buffy coat) and the top layer contains platelet-rich plasma (PRP). The PRP was carefully collected into a 15 ml conical tube without contaminating it with the intermediate layer by using a Pasteur pipette. Platelets were isolated from the PRP by centrifugation at 800×g for 12 min at RT in the presence of 0.3 M citric acid (20 µl/ml of PRP), which is used to prevent platelet activation during isolation process (Mustard *et al*., 1989). Platelet poor plasma (PPP) was discarded and the platelet pellet was gently suspended in 1ml of wash buffer before adding a further 4 ml of wash buffer. Platelets were centrifuged again at 1000×g for 10 min in a swing-out rotor centrifuge in order to ensure that no plasma proteins would be present in pelleted platelets. The pellet was resuspended at the desired concentration in modified Tyrode's buffer (an iso-osmotic phosphate buffer). In some cases, Tyrode's buffer contained 1 mM ethylene glycol-bis ((3-aminoethyl ether)-N,N,N',N'-tetraacetic acid (EGTA) to prevent integrin activation (Gogstad *et al*., 1982), as well as apyrase (2 U/ml) and indomethacin (10 µM) to neutralise the effect of ADP and TXA_2, respectively (Mustard *et al.*, 1972; Smith, 1971).

Platelet count was carried out in a Beckman Coulter Z1 Particle Counter by adding 5 µl of platelet suspension to 10 ml of isotonic buffer within a Beckman Coulter Accuvette. In brief the machine counts cells per millilitre by measuring the electrical resistance of cells as they are passed through a micro-aperture. Platelets were then allowed to rest at 37°C for 30 min before experimentation.

Acid citrate dextrose (ACD), pH 6.5

29.9 mM Tri-sodium citrate
2.9 mM citric acid
72.6 mM NaCl
113.8 mM D-glucose

Modified Tyrode's buffer, pH 7.4

150 mM NaCl
5 mM HEPES
0.55 mM NaH_2PO_4
7 mM $NaHCO_3$
2.7 mM KCl
0.5 mM $MgCl_2$
5.6 mM D-glucose

Wash buffer, pH 6.5

0.036 mM citric acid
0.01 mM EDTA
0.005 mM D-glucose
0.005 mM KCl
0.09 mM NaCl

All solutions used here were filtered through 0.22 µm filter units and stored at 4°C.

2.6.2. Measurement of platelet functional responses

2.6.2.1 Light transmission aggregometry

Functional sensitivity of platelets was always checked prior to experimentation using light transmission aggregometry. This technique was first introduced by Born in 1962 and is based on changes in the transmission of light through a stirred

suspension of platelets, which is detected by a photometer (Born, 1962). A tube containing platelet suspension is placed between a light source and a photocell. When light passes through the suspension containing platelets it scatters, therefore less transmission of unobstructed light is detected by the photocell. However, on addition of platelet agonists, such as thrombin, platelet aggregates are formed that scatter less light, therefore more transmission of unobstructed light is detected by the photocell. Thus, the amount of light transmission is directly proportional to the degree of platelet aggregation, which is in turn dependent on the level of platelet activation (Figure 2.1).

Platelet aggregation was measured using a Chrono-log dual-channel light aggregometer. Aggregation tubes containing 250 µl of human washed platelets (2.5×10^8 platelets/ml) were incubated at 37°C for 1 min under stirring condition (1000 rpm) to allow temperature to equilibrate. Platelet suspensions were then stimulated with desired agonist and aggregation traces were recorded for 5 min using Aggro/link software from Chrono-log. The platelet aggregometer was calibrated for each sample using non-stimulated human washed platelets as 0% aggregation and modified Tyrode's buffer as 100%.

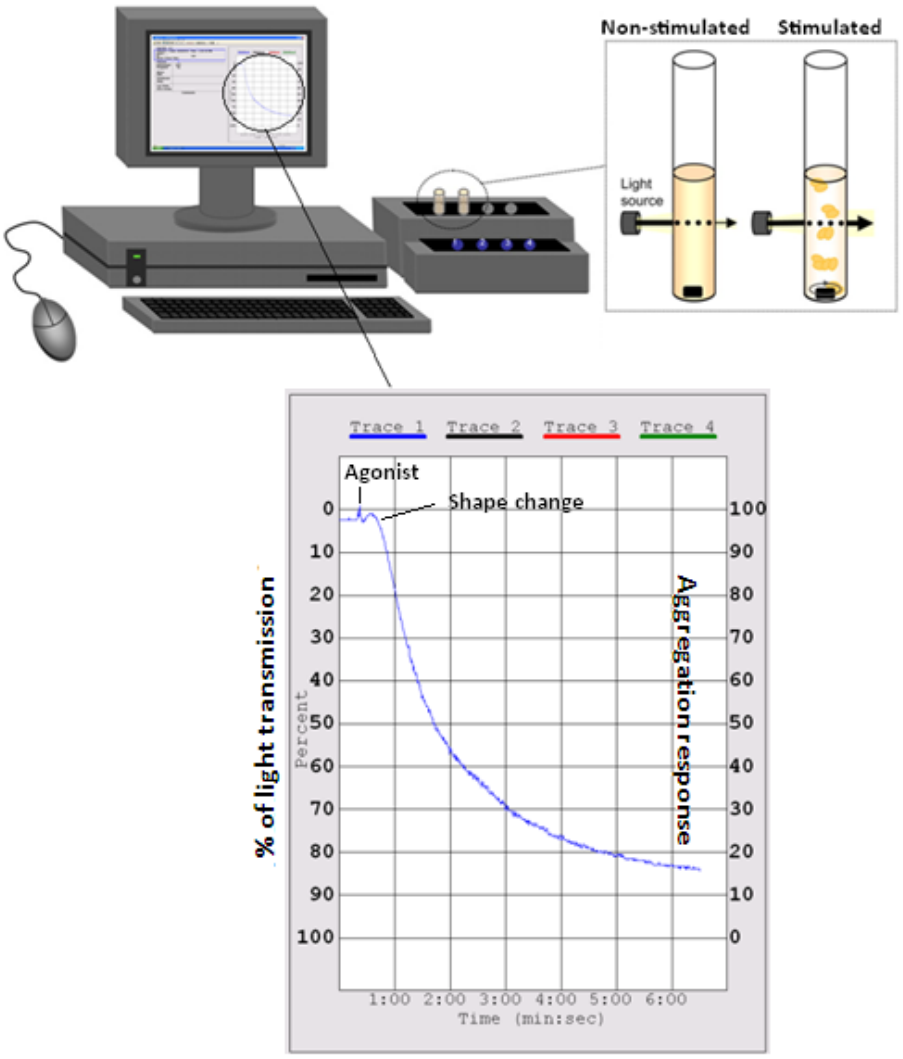

Figure 2.1: The principle of platelet aggregometry. Experimental setup and principle of platelet aggregation adapted from Jackson (2007) (top) and a representative trace when platelets are stimulated with 0.1 U/ml thrombin (bottom).

2.6.3. Fixation of platelets spread on fibrinogen

Glass coverslips (12 mm) were placed on parafilm coated glass plate resting in a humid chamber and coated with 100 µg/ml human fibrinogen (Enzyme Research, Swansea, UK) overnight at 4°C. Next day to remove residual unbound proteins coverslips were washed twice with PBS and to prevent non-specific binding of platelets to exposed glass, coverslips were blocked with 0.5% BSA for 1 hr at room temperature. After blocking, coverslips were washed twice with PBS and incubated with washed platelets ($2x10^7$/ml) for 45 min at 37°C. Unbound platelets were washed away with PBS and adhered platelets were fixed with 4% paraformaldehyde in PBS for 10 min at room temperature. After washing twice with PBS, fixed platelets were permeabilised with 0.3% Triton X-100 in PBS for 5 min before immunolabelling (see section 2.6.5).

2.6.4. Fixation of platelets in suspension

Glass coverslips (12 mm) were placed in a 24-well plate and coated with 0.01% poly-L-lysine for 30 min at 37°C. After incubation glass coverslips were washed twice with PBS and air-dried.

Washed platelets ($5x10^6$/ml) were first fixed in suspension with 4% paraformaldehyde for 10 min at room temperature then centrifuged at 4000 rpm for 3 min to pellet fixed platelets and washed once with PBS to remove any residual paraformaldehyde and resuspended in PBS. Platelet suspension was dispensed in the wells of the 24-well plate containing poly-L-lysine coated coverslips. The plate was then spun for 10 min at 250xg and 37°C. After centrifugation, coverslips were washed twice with PBS before being transferred on a parafilm coated glass plate resting in a humid chamber. Platelets were then permeabilised with 0.3% Triton X-100 for 5 min followed by blocking with 0.5% BSA in PBS for 30 min at room temperature before immunolabelling (see section 2.6.5).

2.6.5. Immunodetection of proteins in fixed platelets

To prevent unspecific antibody binding, coverslips with fixed platelets were blocked with 5% FBS in PBG for 30 min at room temperature. Cells were then incubated with primary antibody at the desired dilution in PBG for 1 hr at room temperature. After incubation, the coverslips were washed 3 times with PBG before incubation with secondary antibody for 45 min at room temperature. If actin staining was required, FITC or TRITC-labelled phalloidin (final concentration 2 μg) were added to the diluted secondary antibody. Thereafter, the cover slips were washed again 3 times with PBG and once with distilled water before being mounted on glass slides as described in section 2.6.6.

PBG pH 7.4
0.5% (w/v) bovine serum albumin (BSA)
0.05 % (w/v) fish gelatin
Dissolve in 1x PBS

2.6.6. Mounting of coverslips

After immunostaining of the fixed cells, the coverslips were once immersed in deionised water and the extra water soaked off on a tissue paper. Then a drop of gelvatol was placed on a clean glass slide and the coverslip was mounted with the cell surface facing downward on the top of gelvatol. Care was taken not to trap any air bubble between the coverslip and the glass slide. Mounted slides were then rest in dark overnight and imaged under fluorescence microscope.

Gelvatol
14.3% (v/v) Gelvatol (Polyvinylalcohol)
28.6% (v/v) Glycerine
2.5% (w/v) DABCO (1,4- diazabicyclo[2.2.2] octane) in PBS

2.6.7. Microscopy and image processing

Images were acquired with a fluorescence microscope Zeiss Axio Observer (Zeiss, Cambridge, UK) equipped with AxioCam506 camera and a 100x oil immersion objective lens (1.4 oil DIC). Images were deconvolved using Zen Pro software (Carl Zeiss, Cambridge, UK). All images were single planes overlaid and processed in CorelDRAW X6 (Corel).

2.7. Protein biochemistry

2.7.1. Expression and purification of GST and His tagged proteins

E. coli strains (XL1 blue, BL21, Rosetta-gami, Rosetta 2, M15 (pREP4)) were transformed with pGEX-4T-2 and pQE32 vectors for the expression of glutathione S-transferase (GST) and his-tagged fusion proteins respectively.

2.7.1.1. Small scale protein expression

Small-scale expression of fusion proteins was performed to check and standardise not only the efficiency of expression but also the conditions before proceeding for the large-scale expression and purification as well. Single colonies (3-6) of transformed bacteria were picked with the help of a pipette tip in a sterile culture hood and grown overnight in 5 ml of LB medium containing ampicillin (100 µg/ml) at 37℃ and shaking at 200 rpm. 1 ml of the overnight culture was inoculated into 15 ml of fresh LB medium containing ampicillin (100 µg/ml) to an optical density at 600 nm (OD_{600}) of 0.1. The culture was then allowed to grow at 37℃ till an OD_{600} of 0.7 was achieved. At this point 1 ml aliquot as a non-induced sample was collected in an eppendorf tube and processed as in section 2.7.1.2. The culture was now induced by adding 0.5 mM IPTG. In order to optimise the conditions for maximum protein expression, induction was carried out with varying concentrations of IPTG (0.1 mM, 0.2 mM, 0.5 mM and 1 mM final concentration) at three different temperature conditions (20℃, 30℃ and 37℃) for 2 to 16 hrs. After incubation 1 ml aliquot as an induced sample was collected and processed as in section 2.7.1.2.

The culture was then centrifuged to pellet cells at 6000xg for 30 min at 4℃. Pelleted cells were resuspended in 2 ml of lysis buffer containing PIC and PMSF and incubated on ice for 30 min before disrupted with sonication. After sonication, pellet and supernatant (soluble) fractions were obtained by centrifugation at 15000xg for 30 min at 4℃. Both pellet and supernatant were dissolved in an equal volume of 2x Laemmli buffer and heated at 95℃ for 5 min. 20 µl of each sample (non-induced, induced, pellet, supernatant) were resolved on a SDS-polyacrylamide gel electrophoresis (see section 2.7.9) and analysed by Coomassie blue staining (see section 2.7.10).

2.7.1.2. Preparation of lysate from bacterial pellet

1 ml aliquot of both non-induced and induced bacterial suspension was spun in a microcentrifuge at >15,000xg for 1 min. Supernatant was discarded and pellet was resuspended in Laemmli buffer at following proportion.

1 absorbance unit – add 50 µl of Laemmli buffer to pellet

For example if the OD_{600} = 0.7, pelleted cells were resuspended in 35 µl of Laemmli buffer, boiled for 5 min at 95°C and stored at -20°C until further use.

2.7.1.3. Large scale protein expression and purification of GST fusion protein

After optimisation of the expression conditions to get a maximum of soluble protein in the lysate, large-scale protein expression was performed. A single colony of recombinant *E. coli* XL-1 blue strain was picked from an LB agar plate, inoculated with 50 ml of LB medium containing ampicillin (0.1 mg/ml) and grew overnight at 37℃ and 200 rpm. The overnight culture was added to 950 ml of fresh LB medium containing ampicillin (0.1 mg/ml) to an OD_{600} = 0.1 and allowed to grow *at* 37°C to an optical density of OD_{600} = 0.7. The culture was then induced by adding 0.5 mM IPTG for 12-16 hrs at 20°C. After induction the culture was spun at 6000xg for 30 min at 4°C. The supernatant was discarded and the pellet was resuspended in 30 ml of bacterial lysis buffer and incubated on ice for 30 min. An ice-cold French

press was used to lyse bacterial cells. The French press cycle was repeated 2 to 4 times to ensure efficient bacterial lysis. After French press the lysate was spun at 17,000xg for 30 min at 4℃ to remove insoluble proteins from soluble ones.

Both pellet and supernatant were saved for monitoring of the process. The supernatant was incubated with pre-equilibrated glutathione-sepharose bead slurry for 1 hr at 4℃ to purify GST fusion proteins. After 1 hr, the glutathione-sepharose beads with bound protein were washed twice with washing buffer and twice with wash buffer without Triton X-100. Elution buffer or boiling at 95℃ with 2x Laemmli buffer was used to elute purified proteins from glutathione sepharose beads.

Lysis buffer
20 mM HEPES
300 mM NaCl
10 mM DTT (add fresh)
0.5% Triton X-100
1 mM PMSF (add fresh)
PIC (added fresh)

Elution buffer
1 M Tris-HCl, pH 8.0
100 mM NaCl
20 mM reduced glutathione

Washing buffer
Same as lysis buffer

2.7.1.4. Large scale protein expression and purification of His-tagged proteins

After optimisation of the expression conditions to get more soluble protein in the lysate, large scale protein expression was performed in 1 litre LB medium essentially as described in section 7.2.1.2. Bacterial pellet was resuspended in 30 ml of lysis buffer containing 10 mM imidazole (to minimize unspecific binding) and incubated on ice for 30 min. The cell suspension was lysed using a French press and the lysate centrifuged as described in section 7.2.1.2. The supernatant was incubated with 50% pre-equilibrated Ni-NTA bead slurry for 1 hr at 4℃ with gentle agitation. The beads were then washed three times with wash buffer and the bound proteins were either eluted with elution buffer or by boiling at 95℃ with 2x Laemmli buffer.

Lysis buffer, pH 8.0	Wash buffer, pH 8.0	Elution buffer, pH 8.0
50 mM NaH_2PO_4	50 mM NaH_2PO_4	50 mM NaH_2PO_4
300 mM NaCl	300 mM NaCl	300 mM NaCl
10 mM imidazole	20 mM imidazole	250 mM imidazole

2.7.2. GST pull-down assay

GST pull-down assay is a common *in vitro* assay to detect protein-protein interactions and map the interaction sites. This method relies on the immobilisation of bait protein (GST fusion protein) on glutathione sepharose beads, which provide a solid phase. The GST protein-beads complex is then incubated with either whole cell lysate or a purified protein. Non-bound proteins are washed off and the binding complex is eluted, resolved by SDS-PAGE and analysed by Coomassie staining or western blotting (Figure 2.2).

First, supernatants of bacteria expressing GST fusion protein or GST only were prepared as in section 2.7.2.2. Next, 50% (v/v) glutathione sepharose bead slurry was pre-equilibrated by washing once with PBS and twice with lysis buffer to remove storage ethanol. Beads slurry was incubated with the supernatant of GST fusion or GST only proteins for 1 hr at 4°C with gentle agitation.

Beads were collected by centrifugation at 500xg for 3 min at 4°C, the supernatant was discarded and the beads were washed 3 times with bacterial lysis buffer. The beads with bound GST and GST fusion protein were then incubated with either platelet lysate, supernatant of bacteria expressing His-tagged proteins or lysates of mammalian cells expressing Myc-tagged proteins and further incubated for 1 hr at 4°C with gentle rolling. After incubation beads were collected by centrifugation at 500xg for 3 min at 4°C, the supernatant was discarded and the beads were washed 3 times with bacterial lysis buffer before being boiled in Laemmli buffer for 5 min at 95°C. The released proteins were resolved on SDS-PAGE and analysed by Coomassie staining and western blotting.

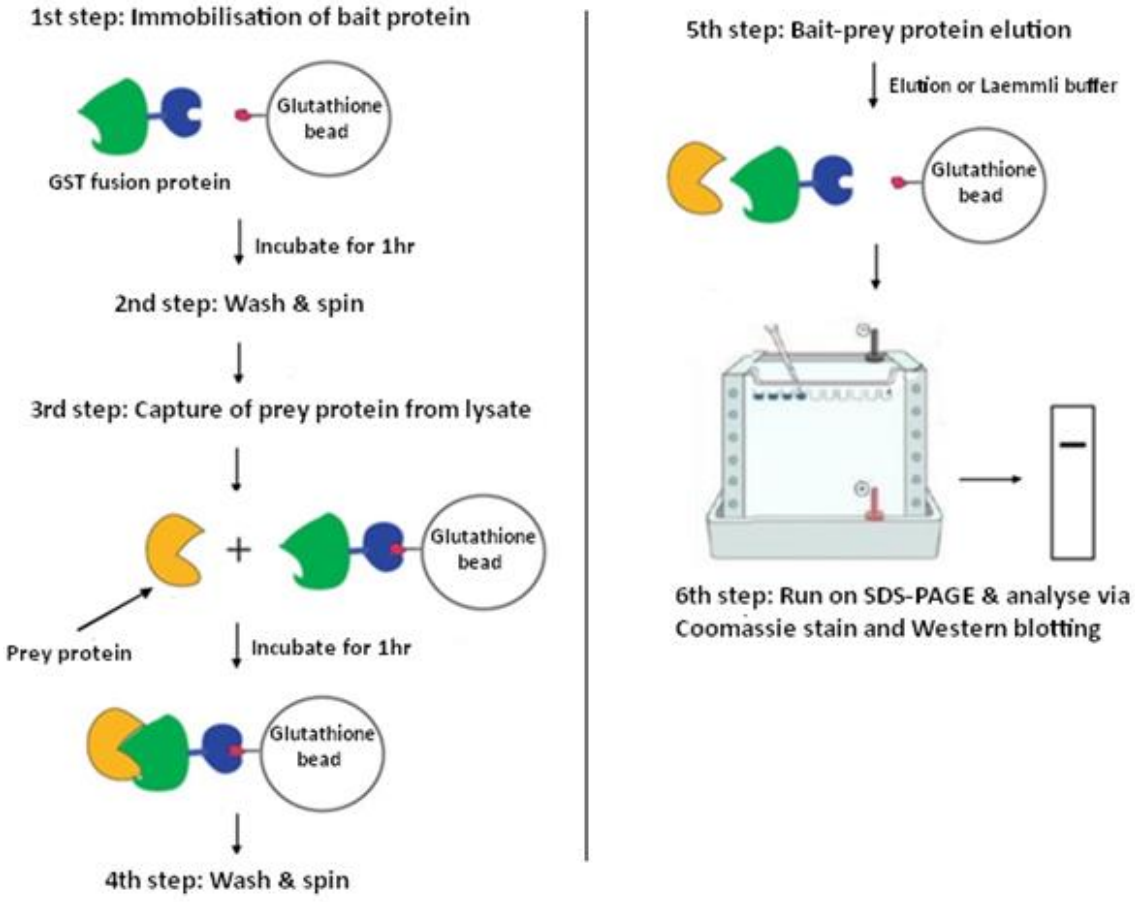

Figure 2.2: Principle of GST pull-down assay. Schematic showing various steps involved in the GST pull-down method.

2.7.3. Preparation of washed platelet samples for SDS-PAGE

To examine individual intracellular protein, isolated washed human platelets (1×10^9 platelets/ml) were incubated in the presence of 10 µM indomethacin, 2 U/ml apyrase and 1 mM EGTA for 30 min at 37°C in all cases.

Platelets were then treated with or without an agonist under stirring conditions (1000 rpm). The reaction was stopped by the addition of 5× Laemmli buffer which results in cell lysis, heated at 95°C for 5 min to ensure denaturation of the proteins and stored at -20°C until required.

2.7.4. Measurement of protein concentrations

For equal loading, protein concentrations of samples were determined using a detergent-compatible Pierce BCA protein assay kit that is based on the Lowry method (Lowry *et al*, 1951). This colorimetric assay is divided into two steps. The first step is called Biuret reaction in which protein reduces cupric ion (Cu^{+2}) to cuprous ion (Cu^{+1}) in an alkaline medium to form a light blue complex. In the second step bicinchoninic acid (BCA) reacts with the cuprous ion, resulting in an intense purple colour that is water-soluble and gives maximum light absorbance at 562 nm. The change in light absorption can be detected spectrophotometrically.

Different concentrations (0, 25, 125, 250, 500, 750, 1000, 1500, 2000 µg/ml) of bovine serum albumin (BSA) were prepared in lysis buffer as protein standards. Next an aliquot of sample suspension was lysed in lysis buffer at a ratio of 1:1 (v/v) before preparing dilutions in PBS (1:25, 2:25 and 5:25). Then 25 µL of each protein standard (in duplicate) and diluted lysate were added in duplicate into the corresponding wells of the 96 well Nunclon microplate. This was followed by addition of 200 µL of the BCA reagent mix to each well. The microplate was mixed thoroughly on a plate shaker for 30 sec before incubating at 37°C for 30 min.

The plate was then cooled at room temperature and light absorbance was measured at 562 nm using a Tecan plate reader. A standard curve was plotted by

using absorption values from the protein standards and protein concentrations were calculated from the curve.

2.7.5. Immunoprecipitation

Immunoprecipitation (IP) is a routinely used biochemical technique that involves isolation of a protein of interest from cell lysate by using a specific antibody. A primary antibody selective to a protein of interest is added to the cell lysate to form antibody-antigen complexes. Antibody-antigen complexes are then precipitated via incubation with sepharose or agarose beads, which are conjugated to protein A or G. Both protein A and G derive from the bacterial cell wall of *Staphylococcus aureus* and *Streptococcal* strains preferentially binds to the Fc fragment of a wide range of IgG antibodies. By using centrifugation, antibody-antigen complexes attached to beads are pelleted. After several washes, target proteins are removed from the beads by boiling in Laemmli buffer for 5 min at 95°C and studied further by SDS-PAGE (see section 2.7.9) and Coomassie staining (section 2.7.10) or western blotting (section 2.7.11).

2.7.5.1. Immunoprecipitation of platelet proteins

Washed platelets (1 x 10^9/ml) were lysed in ice-cold IP lysis. The lysates were then incubated on ice for at least 30 min and protein concentration of each sample was determined (see section 2.7.4.). 300-600 µg of platelet lysate were incubated with 1-5 µg of primary antibody overnight at 4°C with gently rolling.

Next day either protein A or G sepharose or agarose beads (50%, v/v) slurry was prepared by washing once with PBS and twice with TBS-T to remove storage ethanol. 25 µl of bead slurry was added to each sample and incubated for 2 hrs with gentle rolling. Beads were collected by centrifugation at 1000xg and washed once with IP lysis buffer and twice with TBS-T. After these washes the beads were boiled in Laemmli buffer at 95°C for 5 min and released proteins were run on SDS-PAGE and analysed by western blotting.

IP lysis buffer

10 mM Tris base
150 mM NaCl
1 mM EDTA
1 mM EGTA
2% Trition-X 100
1 mM PMSF (add fresh)
1:100 dilution of protease inhibitor cocktail (v/v) (add fresh)

TBS-T

150 mM NaCl
10 mM Tris-HCl, pH 8.0
0.1% Tween 20

2.7.6. Co-immunoprecipitation

Co-immunoprecipitation (Co-IP) is an extension of conventional IP technique which helps determine whether two proteins are part of the same complex *in vivo.* Both co-IP and IP share the same basic principle of specific antibody-antigen reaction; however, co-IP is focused on additional proteins that are associated with the target protein by native interactions in the same mixture as shown in figure 2.3.

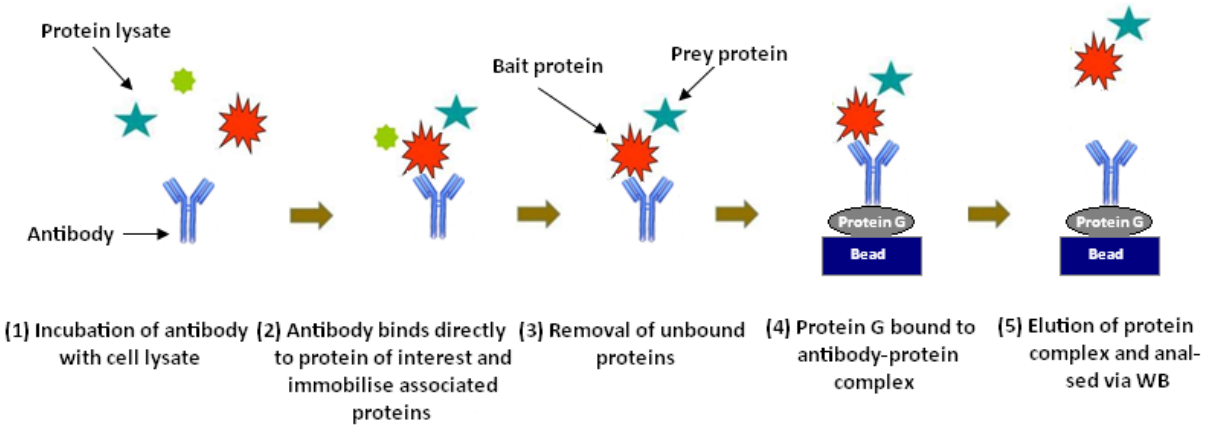

Figure 2.3: Principle of co-immunoprecipitation. Schematic representation of co-immunoprecipitation method involved in the isolation of proteins from protein lysate.

2.7.7. cAMP pull-down assay

The cAMP pull-down assay is a common biochemical technique used to enrich cAMP binding proteins from tissue and cell lysates (Aye *et al*., 2009). This assay involves incubation of lysates with cAMP bound agarose beads, followed by affinity purification and separation by SDS-PAGE of enriched proteins.

Washed platelets (1 x 10^9/ml) were lysed in ice-cold lysis buffer supplemented with PIC (1:100) and PMSF (1:100). The lysates were immediately incubated on ice for at least 30 min and protein concentration of each sample was determined (see section 2.7.4). Next, pre-equilibrated cAMP agarose and control beads (ethanolamine blocked) slurries were incubated with 400-600 µg of platelet lysate at 4°C overnight with rotary shaking. Beads were collected by centrifugation at 1000xg, washed twice with TBS-T and boiled in Laemmli buffer at 95°C for 5 min. The eluted proteins were run on SDS-PAGE and analysed by western blotting (see section 2.7.11).

Lysis buffer

Platelet IP lysis buffer was used and the composition is mentioned in section 2.7.5.1.

2.7.8. Sodium dodecyl sulphate-polyacrylamide gel electrophoresis

Sodium dodecyl sulphate-polyacrylamide gel electrophoresis (SDS-PAGE) is a common technique that uses a combination of an ionic detergent SDS and chemically inert polyacrylamide gels to separate proteins according to their molecular masses under the influence of electric current. Polyacrylamide gels are formed from monomers of acrylamide and bis-acrylamide. The polymerisation of acrylamide and bis-acrylamide is due to the presence of free radicals generated by the addition of ammonium persulphate (APS). N,N,N',N'-tetramethylethylenediamine (TEMED) is added to catalyse free radical formation from APS (Shi & Jackowski, 1998). The free radicals transfer electrons to acrylamide/bis-acrylamide monomers and cause them to react with each other to form a porous gel. The percentage of acrylamide used in these solutions determines the pore size and therefore the relative separation of the proteins within the mixture.

The movement of any charged proteins through an electric field is influence by its shape, charge density and molecular weight. So as to separate proteins solely in an electrical field based on their molecular weight, SDS is added to the protein mixture (Shapiro *et al*., 1967). SDS is a detergent that masks the intrinsic net charge of the protein and gives a uniform negative charge. Furthermore, a reducing agent such as 2-mercaptoethanol breaks disulfide bridges changes the folded protein into its linear form. Thus, proteins treated this way will have electrophoretic mobility based on their molecular weight only.

2.7.8.1. Procedure for SDS-PAGE

In this study all the samples were run in a discontinuous buffer system using a Mini Protean III gel kit (Bio-Rad). The discontinuous buffer system was first described by

Laemmli (1970) and requires different buffers in the gel and electrophoresis tank. Proteins were separated using 1.5 mm thick polyacrylamide gels that comprise 10-18% separating gel (pH 8.8) and 4% stacking gel (pH 6.8) (Tables 2.3 and 2.4). Gels were placed in the electrophoresis tank containing running buffer in both upper and lower chambers. Pre-stained protein ladder and protein sample (20-60 µg) were loaded in wells and gels were run at 70 volts for the first 30 min followed by 120 volts for the next 1.5 to 2.5 hrs depending on the size of the protein of interest. After electrophoresis resolved proteins were analysed either by Coomassie staining or western blotting.

Table 2.3: Concentrations of each reagent for four resolving gels

Resolving Gel	**18%**	**15%**	**10%**
30% Acrylamide/Bis-acrylamide (ml)	18	15	10
1.5 M Tris HCl (pH 8.8) (ml)	7.5	7.5	7.5
10% SDS (µl)	300	300	300
Distilledwater (ml)	3.6	6.9	11.9
10 % ammonium persulfate (APS) (µl)	300	300	300
TEMED (µl)	30	30	30

Table 2.4: Concentration of each reagent for two stacking gels

Stacking Gel	**4%**
30% Acrylamide/Bis-acrylamide (ml)	0.83
0.5 M Tris-HCl pH 6.8 (ml)	0.63
10% SDS (µl)	50
Distilled water (ml)	3.4
10% ammonium persulfate (APS) (µl)	50
TEMED (µl)	10

<u>Running buffer</u>

25 mM Tris base
192 mM glycine
0.1% SDS (w/v)

2.7.9. Coomassie blue staining of polyacrylamide gels

After SDS-PAGE, the separated proteins were visualised by staining the gel with Coomassie-Brilliant-Blue R250 solution overnight at room temperature with gentle shaking. Next day the gel was either destained with destaining solution at room temperature with shaking or boiled in distilled water 3x in a microwave until the protein bands were clearly visible. Then the destained gel was imaged either using Odyssey CLx imaging machine (Li-Cor, Germany) or scanned via a scanner.

Coomassie blue staining solution
0.1% (w/v) Coomassie-Brilliant-Blue R 250
50% (v/v) Methanol
10% (v/v) Acetic acid

Destaining solution
10% (v/v)Ethanol
7% (v/v)Acetic acid

2.7.10. Western blotting

Western (immuno) blotting is a routine method used to identify specific proteins from a complex mixture of proteins extracted from cells (Towbin *et al*., 1979). This method involves transferring and immobilizing proteins from an SDS-PAGE gel to an adhesive support matrix such as nitrocellulose or polyvinylidene fluoride (PVDF) membranes under an electric field. The membranes are then probed with specific primary antibodies that bind to target proteins via specific epitopes. A secondary antibody raised against the primary antibody species is then added to the membrane. Secondary antibodies are commonly conjugated to a detection molecule, either HRP (horseradish peroxidase) enzyme or to fluorescence emitting dyes, which allows the detection of their position on the membrane. In case of HRP, the addition of luminol, coumaric acid and H_2O_2 to the HRP linked secondary antibodies results in the emission of light (425 nm), which can be captured and visualised on X-ray films. In case of fluorescence emitting dyes, the signal can be detected via an imaging machine.

2.7.10.1. Methodology used for western blotting

After separation of proteins by SDS-PAGE were transferred to a PVDF membrane using a Bio-Rad Trans-blot Turbo transfer system (Bio-Rad laboratories, Hertfordshire, UK) for 12 min at constant voltage (25 volts). In this method, blotting papers, polyacrylamide gel and methanol-activated PVDF membrane were first soaked in Bio-Rad transfer buffer before arranged in the correct order in the Bio-Rad transfer system, such as bottom cassette electrode, filter paper, PVDF membrane, gel, filter paper and top cassette electrode. Care was taken not to trap any air bubbles between PVDF membrane and gel. Under these conditions, proteins migrating towards the anode were captured by the PVDF membrane. Following transfer, membranes were blocked with 5% (w/v) BSA/TBS-T or 5% (w/v) semi-skimmed milk/TBS-T depending on the primary antibody to be used, for 1 hr at room temperature in order to prevent non-specific antibody binding. After blocking membranes were incubated with the appropriately diluted (1:100 - 1:1000) primary antibody in TBS-T containing 2% BSA or 2% milk (w/v) overnight at 4°C with gentle agitation. After collecting primary antibody for future use, membranes were rinsed twice with TBS-T for 10 min with gentle agitation and incubated either with HRP-conjugated or fluorescent dye-linked secondary antibodies.

In case of HRP detection, membranes were probed with the HRP-conjugated secondary antibodies, anti-mouse or anti-rabbit in TBS-T (1:10000 (v/v)) for 1 hr at room temperature under gentle agitation. Membranes were washed 3 times with TBS-T 10 min each wash with gentle agitation and incubated with peroxide containing enhanced chemiluminescence (ECL) buffer 1 and luminol containing ECL buffer 2 for 90 sec in the dark for detection of horseradish peroxidase coupled antibodies. Membranes were placed in an X-ray film cassette and exposed to autoradiography film in a specific dark room. The film was then developed using Kodak developer solution (diluted 1:5 in distilled water (v/v)),

followed by washing with water and finally fixation in Kodak fixer solution (diluted 1:5 in distal water (v/v)).

In case of fluorescent dye detection, membranes were probed with fluorescent dye linked secondary antibodies, anti-mouse or anti-rabbit in TBS-T (1:20000 (v/v)) for 1hr at room temperature under gentle agitation followed by 5 washes with TBS-T, 10 min each wash. Care was taken to ensure membranes were protected from light, as fluorescent dyes are light sensitive. Blots were imaged using an Odyssey CLx imaging machine (Li-Cor, Germany).

Table 2.5: Composition of enhanced chemiluminescence buffer

Chemical	**ECL1**	**ECL2**
100 mM Tris base, pH 8.5	10 ml	10 ml
Distilled water	88.6 ml	90 ml
Hydrogen peroxide (Sigma)	---	65 µl
Luminol (250 mM) (Sigma)	0.996 ml	
p-Coumaric acid (90 mM) (Sigma)	0.465 ml	

2.7.11. Ponceau S staining of PVDF membranes

Sometimes proteins transferred to PVDF membranes were visualised with Ponceau S staining. This served as a control of protein transfer after the blotting. The staining was removed by washing with TBS-T buffer 3 times. TBS-T composition was mentioned in section 2.7.5.1.

<u>Ponceau S</u>
0.1% Ponceau S
1% Acetic acid

2.7.12. Stripping and reprobing of PVDF membranes

In some cases, PVDF membranes were stripped to remove primary and secondary antibodies by using a stripping buffer. This technique enabled us to investigate more than one protein on the same membrane and thus saves time, samples and materials.

This method involved washing PVDF membranes twice with stripping buffer for 10 min, followed by two 10 min washes with PBS and two 10 min washes with TBS-T. All incubation and washes were performed with gentle shaking. Membranes were then blocked with 5% (w/v) BSA/TBS-T or 5% (w/v) milk/TBS-T for 1 hr at room temperature and reprobed overnight at 4°Cwith new primary antibody.

Stripping buffer, pH 2.2

15 g glycine
1 g SDS
10 ml Tween20 (v/v)
bring volume up to 1L with ultrapure water

2.8. Statistical Analysis

Data expressed as mean ±standard error of the mean (SEM) were analysed by using the Student *t*-test or one-way analysis of variance (ANOVA) followed by Bonferroni post-hoc test for statistical significance. Statistical tests were carried out using Microsoft excel 2007 and IBM SPSS version 22. The results were considered significant when *P* values were less than 0.05.

Chapter 3: Phosphorylation of MLCP by cAMP/PKA and RhoA-ROCK signalling pathways in platelets

3.1. Introduction

MLCP is a primary serine/threonine phosphatase that plays a critical role in the myosin contractile machinery of cells of different origins including platelets. As in smooth muscle cells, the contractile responses of activated platelets are mainly regulated by two enzymes, MLCK and MLCP. MLCK triggers myosin regulatory light chain (MLC) phosphorylation at Ser19 to facilitate the formation of the acto-myosin contractile unit that is required for platelet activation (Klages *et al*., 1999); on the other hand, MLCP dephosphorylates MLC at the same residue and diminishes acto-myosin contractile forces, which results in platelet inhibition (Muranyi *et al*., 1998). Additionally, MLCK has been reported to be activated by intracellular calcium signalling, whereas MLCP is negatively regulated by two mechanisms, either via RhoA-ROCK pathway (Suzuki *et al*., 1999), or by phosphorylation of CPI-17 (Watanabe *et al*., 2001) (see Figure 1.14). The RhoA-ROCK signalling inhibits MLCP activity via phosphorylation of MYPT1 (the regulatory subunit of MLCP) at Thr696 and Thr853 (Khromov *et al*., 2009; Watanabe *et al*., 2001). These phosphorylated threonine residues bind to the active site of myosin phosphatase, causing autoinhibition of MLCP activity (Khromov *et al*., 2009). Phosphorylation of MYPT1 at threonine residues also triggers the dissociation of MLCP holoenzyme from MLC to reduce MLC dephosphorylation (Velasco *et al*., 2002) and subsequently translocate MYPT1 to the plasma membrane (Neppl *et al*., 2009; Aburima *et al*., 2013). *In vitro* studies have shown that PKAc triggers phosphorylation of MYPT1 at Ser695 and restores MLCP activity in ileal smooth muscle by blocking the RhoA-ROCK mediated phosphorylation of Thr696 (Wooldridge *et al*., 2004). Furthermore, Aburima and co-workers (2013, 2017) have demonstrated that PKA/PKG signalling in platelets restored MLCP activity via inhibiting RhoA-ROCK mediated phosphorylation of

MYPT1 at Thr853. All these studies suggest that the activity of MLCP is regulated by phosphorylation of MYPT1; however, the molecular mechanism of MLCP activity via phosphorylation is poorly defined in platelets.

Several splice variants of MYPT1 have been reported to date in various cells types (Kim *et al*., 2012; Xia *et al*., 2005). These splice variants are products of cassette-type alternative splicing of the gene encoding MYPT1, *PPP1R12A* (Protein Phosphatase 1 Regulatory Subunit 12A), at central and a 3' exons (Hartshorne *et al*., 1998; Grassie *et al*., 2012) regions. These splice variants are highly conserved across mammals, birds and worms and are expressed in a tissue specific and developmentally regulated manner (Lin & Brozovich, 2016). In smooth muscle cells alternative splicing produces four known MYPT1 variants, with C-terminal leucine zipper domain, without leucine zipper domain, with central insert and without central insert (Figure 3.8). However, the expression of MYPT1 splice variants has not been reported in blood platelets previously.

In this chapter we explore in detail the phosphorylation of MYPT1 at Ser695, Thr696 and Thr853 in response to various ligands and the expression of different splice variants of MYPT1 in human blood platelets.

The aims of this chapter are:

- To determine the specificity and optimise the working conditions of commercially available phospho-specific MYPT1 antibodies.
- To investigate the maximum phosphorylation level of Ser695, Thr696 and Thr853 of MYPT1 in platelets.
- To examine dose and time dependent changes in the phosphorylation of MYPT1 in platelets.
- To explore the expression of different splice variants of MYPT1 in platelets.

3.2. Optimisation of conditions for anti-phospho-MYPT1-Ser695 antibody

Phosphorylation of MYPT1 at Ser695 was first identified by Wooldridge and colleagues (2004). They reported that cAMP/PKA signalling-mediated phosphorylation of MYPT1 at Ser695 is responsible for the smooth muscle relaxation. However, phosphorylation of MYPT1 at Ser695 has not been studied in platelets before. In the next set of experiments we characterised the phosphorylation of MYPT1 by using phospho-specific antibodies. However, before experimentation the optimal conditions for commercially available phospho-specific MYPT1 antibodies were determined. In these and following experiments we used washed human platelets isolated as in section 2.6.1. Their functional sensitivity was tested with thrombin via light transmission aggregometry.

Platelets ($1x10^9$/ml) were stimulated with PGI_2 (100 nM) for 60 sec and whole cell lysates were prepared and run on SDS-PAGE. Two different blocking reagents (5% milk powder and 5% BSA) were used with three different dilutions of site-specific p-MYTP1-Ser695 antibody (1:400, 1:200 and 1:100). At lower dilutions the antibody detected a band of the expected molecular weight (approximately 140 kDa) upon blocking the PVDF membrane with 5% milk powder (Figure 3.1 upper panel). However, an additional band could be seen at around 120 kDa that may suggest either some of the MYPT1 protein has been degraded during preparation, which is detected by phospho-MYPT1-Ser695 antibody, or the phospho specific antibody is non-specifically recognising other proteins. However, this particular band was not detected in subsequent experiments.

In case of PVDF membrane blocked with 5% BSA a very faint or no bands were detected at the expected molecular weight (Figure 3.1, lower panel). Consequently 5% milk powder was used for blocking in subsequent experiments. Conditions for phospho-MYPT1-Thr696 and phospho-MYPT1-Thr853 antibodies were established previously with washed platelets in Professor Naseem's lab. Their recommended guidelines suggested using 5% milk powder as blocking agent.

phospho-VASP-Ser157 antibody, which detects a band of expected molecular weight of 50 kDa, was used as a positive control to validate PGI_2 activity in these experiments. GAPDH was used as a control for equal loading.

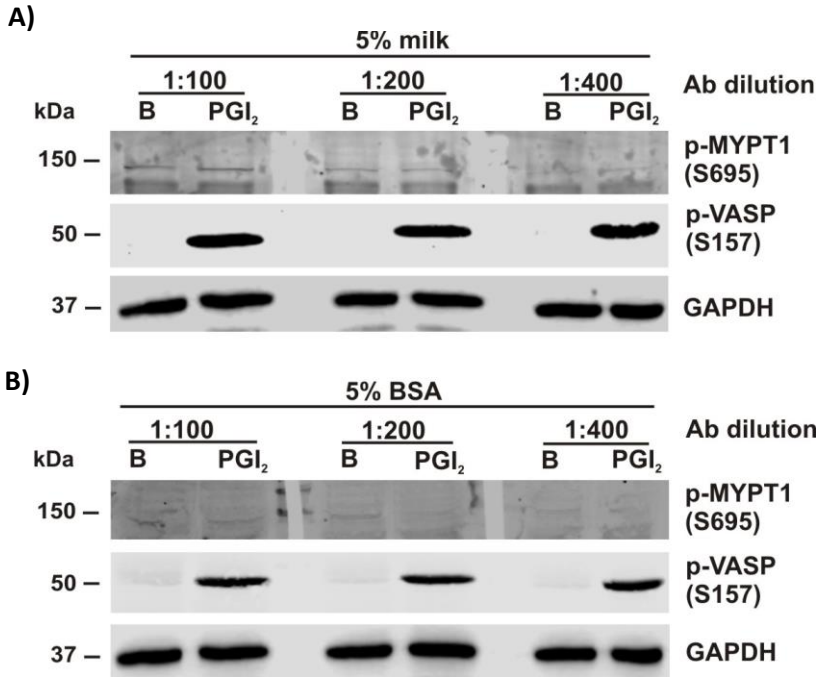

Figure 3.1: Optimisation of conditions for phospho-MYPT1-Ser695 antibody in platelets. Human washed platelets (1×10^9/ml) were left unstimulated (B) or stimulated with PGI_2 (100 nM) for 60 sec at 37°C before lysing in Laemmli buffer. The proteins (70 µg) were resolved by 10% SDS-PAGE and transferred to PVDF. Membranes were blocked with either 5% skim milk powder (**A**) or 5% BSA (**B**) before probing with the indicated dilutions of anti-phospho-MYPT-Ser695 antibody overnight at 4°C. Next day the fluorescently labelled secondary antibody was used to visualise proteins with an Odyssey™ CLx electronic imaging system (Li-Cor). Blots were reprobed with anti-phospho-VASP-Ser157 antibody as a positive control and anti-GAPDH antibody as a loading control. The shown blot is representative of one independent experiment.

3.3. Specificity of phospho-MYPT1 antibodies

Throughout this study we have used commercially available site-specific phospho-MYPT1 antibodies, which were raised against Ser695, Thr696 and Thr853 residues. As two of the phosphorylation sites, Ser695 and Thr696 are adjacent to each other; it was necessary to investigate the site specificity of these phospho-MYPT1 antibodies under our conditions. Cross-reactivity of commercially available phospho-MYPT1 antibodies is well documented in the literature (Grassie *et al*., 2012). Furthermore, Wooldridge *et al.* (2004) have reported that phosphorylation of MYPT1 at Ser695 or Thr696 triggers inhibition of the adjacent residue. Hence it was important to determine whether this is the case or whether the phosphorylation of these sites is mutually exclusive in platelets. In addition, we also aimed at investigating the maximum phosphorylation level of Ser695, Thr696 and Thr853 of MYPT1 in platelets. To answer these questions, calyculin A, a protein phosphatase type 1 and type 2A inhibitor, was used. It has been reported that calyculin A increases the phosphorylation of MYPT1 at Ser695, Thr696 and Thr853 by blocking myosin phosphatase activity (Kitazawa *et al*., 2003; Kaneko-Kawano *et al*., 2012).

Washed human platelets ($1x10^9$/ml) were prepared in the presence of indomethacin, apyrase and EGTA to block secondary signalling events. Platelets were then stimulated with PGI_2, PGE_1, GSNO (a nitric oxide donor) or thrombin in the presence or absence of calyculin A and lysates were prepared, run on SDS-PAGE and immunoblotted with phospho-MYPT1-Ser695, Thr696 and Thr853 antibodies (Figure 3.2). PGI_2, PGE_1 and GSNO are negative regulators of platelet activity, causing phosphorylation of MYPT1 at Ser695, whereas thrombin causes phosphorylation of MYPT1 at Thr696 and Thr853.

A relatively high basal phosphorylation of MYPT1 at Ser695 was observed in human platelets; treatments with PGI_2, PGE_1 and GSNO, used as positive controls, moderately enhanced the phosphorylation levels at Ser695, whereas calyculin A markedly increased this. PGI_2, PGE_1 and GSNO had no apparent additional effect on

the phosphorylation of Ser695 in calyculin A treated platelets. Similarly, thrombin had no effect on the phosphorylation of MYPT1 at Ser695 as it was equivalent to the basal level phosphorylation. This is consistent with the time course experiments described in section. 3.4. Calyculin A treatment also resulted in the detection of an additional, possibly non-specific, band by the phospho-MYPT1-Ser695 antibody.

A very faint band of the expected molecular weight (140 kDa) was observed in basal and PGI_2, PGE_1, GSNO treated platelets with phospho-MYPT1-Thr696 and Thr853 antibodies. In the presence of calyculin A both phospho-MYPT1-Thr696 and Thr853 antibodies revealed a band at expected molecular weight with higher intensity. Thrombin alone, used as a positive control, markedly increased the phosphorylation of both Thr696 and Thr853.

This calyculin A results strongly indicate that all three phospho-antibodies are site-specific and the phosphorylation of Thr696 is not physically blocking the phosphorylation of adjacent Ser695 and vice versa.

Next, maximal level of MYPT1 phosphorylation at serine and threonine residues was analysed via western blotting. Blot 3.2 suggests that MYPT1 at Ser695 is highly phosphorylated at basal level which increased with PGI_2, PGE_1 and GSNO fairly close to maximum level and treatment with calyculin A moderately enhanced this. On the other hand, there is almost no phosphorylation of Thr696 and Thr853 in basal platelets. Thrombin increased the phosphorylation of these residues although far from the maximal level achieved by treatment with calyculin A. This suggests that platelet agonists do not induce maximum level of phosphorylation of MYPT1 possibly due to the presence of active phosphatases. Furthermore, the effect of calyculin A on the phosphorylation of Ser695 is less dramatic suggesting that there is a high basal kinase activity, whereas the kinases that phosphorylate Thr696 and Thr853 are only activated upon agonist stimulation.

phospho-VASP-Ser157 was used to confirm the activity of PGI_2, PGE_1, GSNO. GAPDH was used for equal loading of samples.

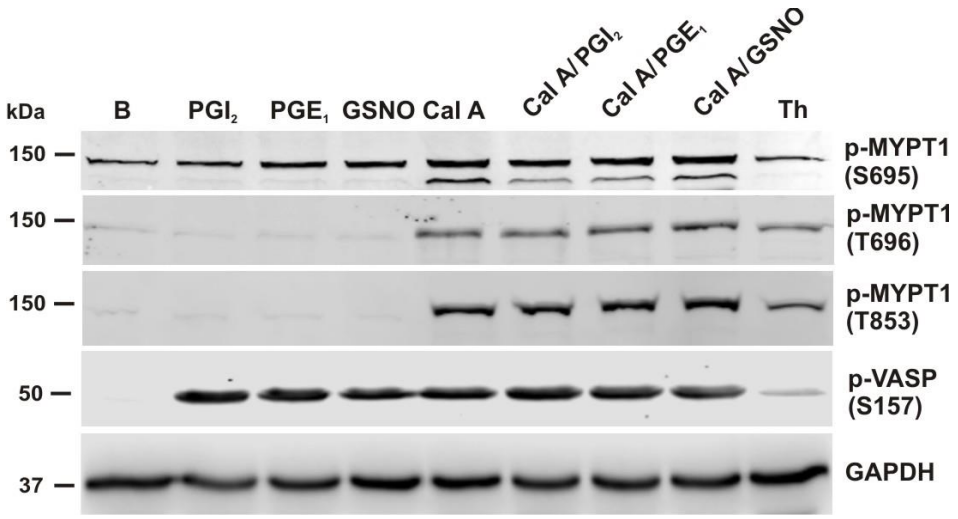

Figure 3.2: Characterisation of MYPT1 phospho-specific antibodies in platelets. Human washed platelets (1×10^9/ml) were treated with indomethacin (10 μM), apyrase (2 U/ml) and EGTA (1 mM) for 20 min at 37°C before experimentation. Platelets were stimulated with PGI_2 (100 nM), PGE_1 (100 nM), GSNO (20 μM) or thrombin (Th) (0.1 U/ml) for 60 sec in the presence or absence of calyculin A (CalA) (100 nM for 20 min prior to stimulation) and lysed in Laemmli buffer. Unstimulated basal (B) and stimulated samples were resolved by 10% SDS-PAGE and immunoblotted with anti-phospho-MYPT1-Ser695, Thr696 and Thr853 antibodies overnight at 4°C. Next day the fluorescently labelled secondary antibodies were added to visualise proteins with an Odyssey™ CLx electronic imaging system (Li-Cor). The blots were reprobed with anti-phospho-VASP-Ser157 antibody as a positive control and anti-GAPDH antibody for equal loading. The shown blot is representative of one independent experiment.

3.4. Characterisation of the phosphorylation status of MYPT1 by PGI_2 and thrombin in platelets.

Having established the specificity of commercially available phospho-specific MYPT1 antibodies we next performed a detailed characterisation of the phosphorylation sites of platelet MYPT1 in response to both PGI_2 and thrombin. Washed human platelets ($1x10^9$/ml) were prepared under same conditions as in previous section. The dose response and the time course effect of PGI_2, PGE_1 and thrombin on phosphorylation of MYPT1 at Ser695, Thr696 and Thr853 were investigated.

3.4.1. Dose response of PGI_2, PGE_1 and thrombin on MYPT1 phosphorylation

The aim of this experiment was to find the optimum concentration under which PGI_2, PGE_1 and thrombin could be used that provokes a maximum phosphorylation of Ser695, Thr696 and Thr853 of MYPT1.

Three different concentrations of PGI_2 and PGE_1 (10, 100 and 1000 nM), and four thrombin doses (0.01, 0.025, 0.05 and 0.1 U/ml) were used. At lower doses (10 and 100nM) both PGI_2 and PGE_1 induced a moderate increase (approx. 1.8 fold relative to non-stimulated platelets) in Ser695 phosphorylation, whereas at a higher dose (1000 nM) phosphorylation was slightly lower (approx. 1.6 fold) (Figure 3.3A). The effect of PGI_2 and PGE_1 is less clear to the naked eye. The electronic imaging machine (Li-Cor); however, offers clearer results. Thrombin mediated phosphorylation of MYPT1 at Thr696 also followed a similar dynamic. Higher phosphorylation (approx. 2 fold relative to non-stimulated platelets) was recorded at lower doses (0.025 U/ml) as compared to high dose (0.1 U/ml) (Figure 3.3B). However, as the figure 3.3B illustrates, the effect of thrombin is very clear with a marked increase in the phosphorylation from basal to 0.01 U/ml but there is not much difference among higher concentrations of thrombin. On the other hand, Thr853 phosphorylation mediated by thrombin was increased in a concentration

dependent manner (Figure 3.3B). This data suggests that PGI_2, PGE_1 and thrombin already exert their maximum effect at relatively low doses.

phospho-VASP-Ser157 and phospho-MLC-Ser19 were used as positive controls to validate PGI_2, PGE_1 and thrombin activities in these experiments. GAPDH was used to show that samples were loaded equally.

On the basis of dose response data we have selected 100 nM of PGI_2 and 0.1 U/ml thrombin for time course experiments, even though the maximum effect was achieved with lower doses of thrombin tested.

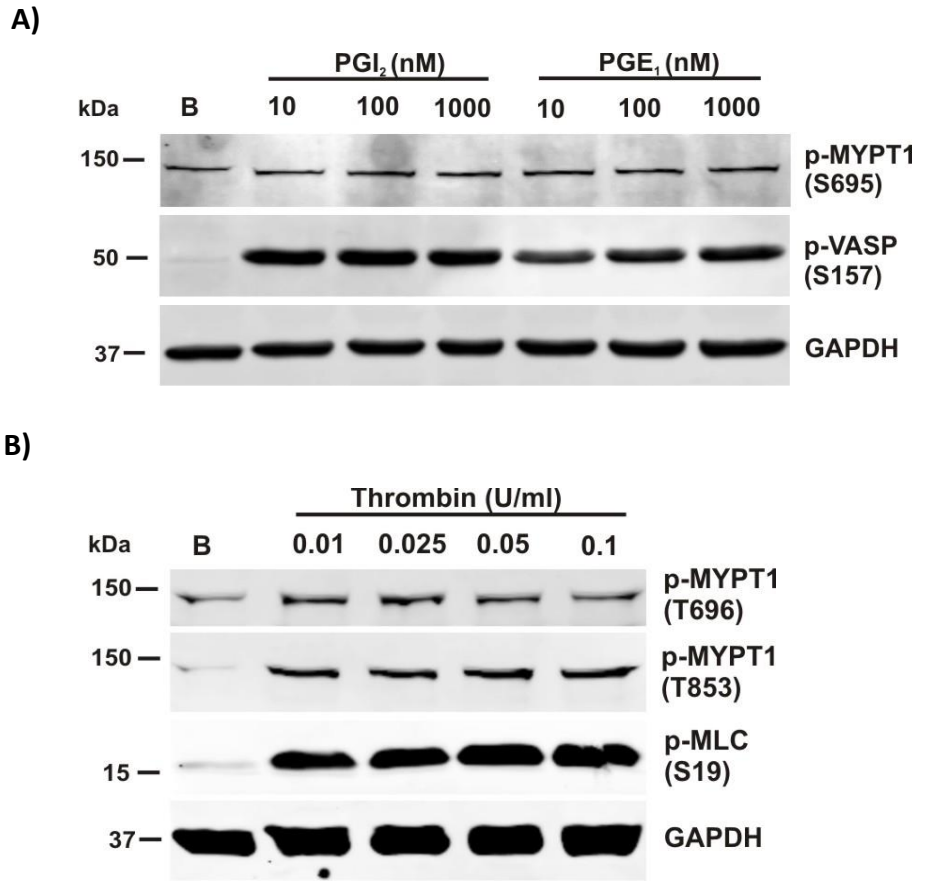

Figure 3.3: PGI_2, PGE_1 and thrombin induced phosphorylation of MYPT1. Human washed platelets (1×10^9/ml) were treated with indomethacin (10 µM), apyrase (2 U/ml) and EGTA (1 mM) for 20 min at 37°C before experimentation. Platelets were stimulated with the indicated concentrations of PGI_2 or PGE_1 **(A)** for 60 sec or thrombin **(B)** for 15 sec and lysed immediately in Laemmli buffer. Unstimulated basal (B) and stimulated samples were resolved by 10% SDS-PAGE and probed with anti-phospho-MYPT1-Ser695, Thr696 and Thr853 antibodies overnight at 4°C. Next day the fluorescently labelled secondary antibodies were used to visualise proteins with an Odyssey™ CLx electronic imaging system (Li-Cor). The blots were reprobed with anti-phospho-VASP-Ser157 and anti-phospho-MLC-Ser19 antibodies as positive controls, and anti-GAPDH antibody as loading control. The shown blot is representative of one independent experiment.

3.4.2. PGI_2 and thrombin elevate MYPT1 phosphorylation in a time dependent manner.

In this experiment we aimed to examine time dependent changes in the phosphorylation of MYPT1 in platelets stimulated by PGI_2 and thrombin. Washed human platelets ($1x10^9$/ml) were treated with PGI_2 (100 nM) or thrombin (0.1 U/ml) at indicated time points before analysing them on western blotting.

Platelets stimulated with PGI_2 showed a moderate increase in the phosphorylation of MYPT1 at Ser695, with maximum phosphorylation reached after 5 min and remaining at steady level for up to 60 min (Figure 3.4). Little phosphorylation of MYPT1 at Thr696 and no phosphorylation at Thr853 were noticed in PGI_2 treated platelets. Furthermore, some basal phosphorylation of MYPT at Ser695 was noticed in non-treated platelets, consistent with our previous experiments (Figures 3.2 and 3.3A).

On the other hand, stimulation of platelets with thrombin revealed a rapid increase in the phosphorylation of both Thr696 and Thr853 of MYPT1, with a maximum at 15 sec followed by a steady decline to basal levels at 30 min (Figure 3.5). Very low basal phosphorylation of MYPT1 at Thr696 and Thr853 suggests the presence of an active phosphatase. The phosphorylation of MYPT1 at Ser695 remained unaffected by thrombin under these conditions (Figure 3.5). These results show that PGI_2 and thrombin both increase phosphorylation of their respective serine or threonine residues in MYPT1 in a time dependent manner.

phospho-VASP-Ser157 and phospho-MLC-Ser19 were used as positive controls to confirm PGI_2 and thrombin activities. GAPDH was used as a loading control.

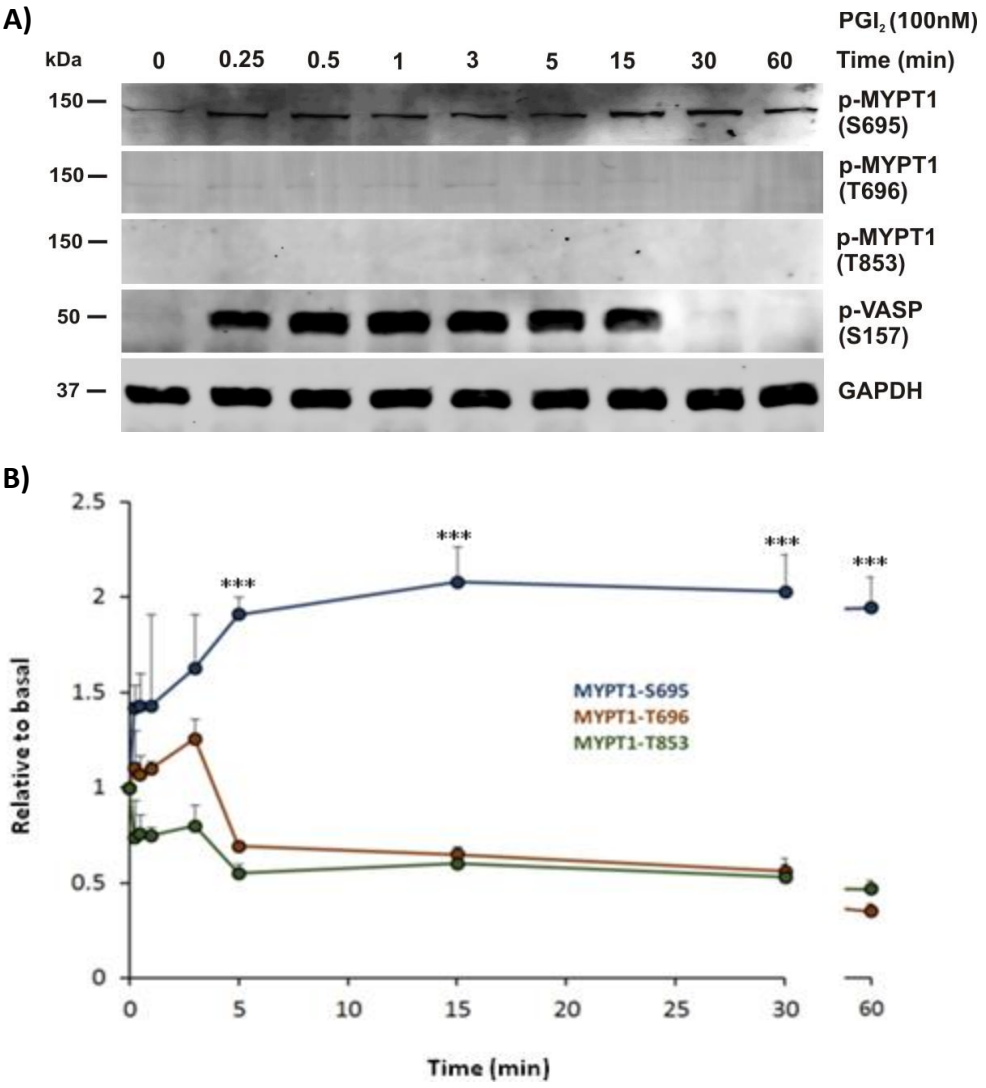

Figure 3.4: Characterisation of PGI_2 induced phosphorylation of MYPT1 in platelets. **A)** Human washed platelets (1×10^9 /ml) were treated with indomethacin (10 µM), apyrase (2 U/ml) and EGTA (1 mM) for 20 min at 37°C before experimentation. Platelets were stimulated with PGI_2 (100 nM) at indicated times points and lysed immediately in sample buffer. Proteins were resolved by 10% SDS-PAGE and immunoblotted with anti-phospho-MYPT1-Ser695, Thr696 and Thr853 antibodies overnight at 4°C. Next day the corresponding fluorescently labelled secondary antibodies were used to visualise proteins with an Odyssey™ CLx electronic imaging system (Li-Cor). The blots were reprobed with anti-phospho-VASP-Ser157 antibody as a positive control and anti-GAPDH antibody as a loading control. The shown blot is representative of three independent experiments. **B)** Phosphorylation of MYPT1 at indicated sites was quantified by densitometry, normalised to loading control (GAPDH) and calculated relative to basal (untreated) whole cell lysates. Data are presented as means ± SEM. Statistical significance calculated using one-way ANOVA (* p<0.05-0.01, ** p<0.01-0.005 and *** p<0.005).

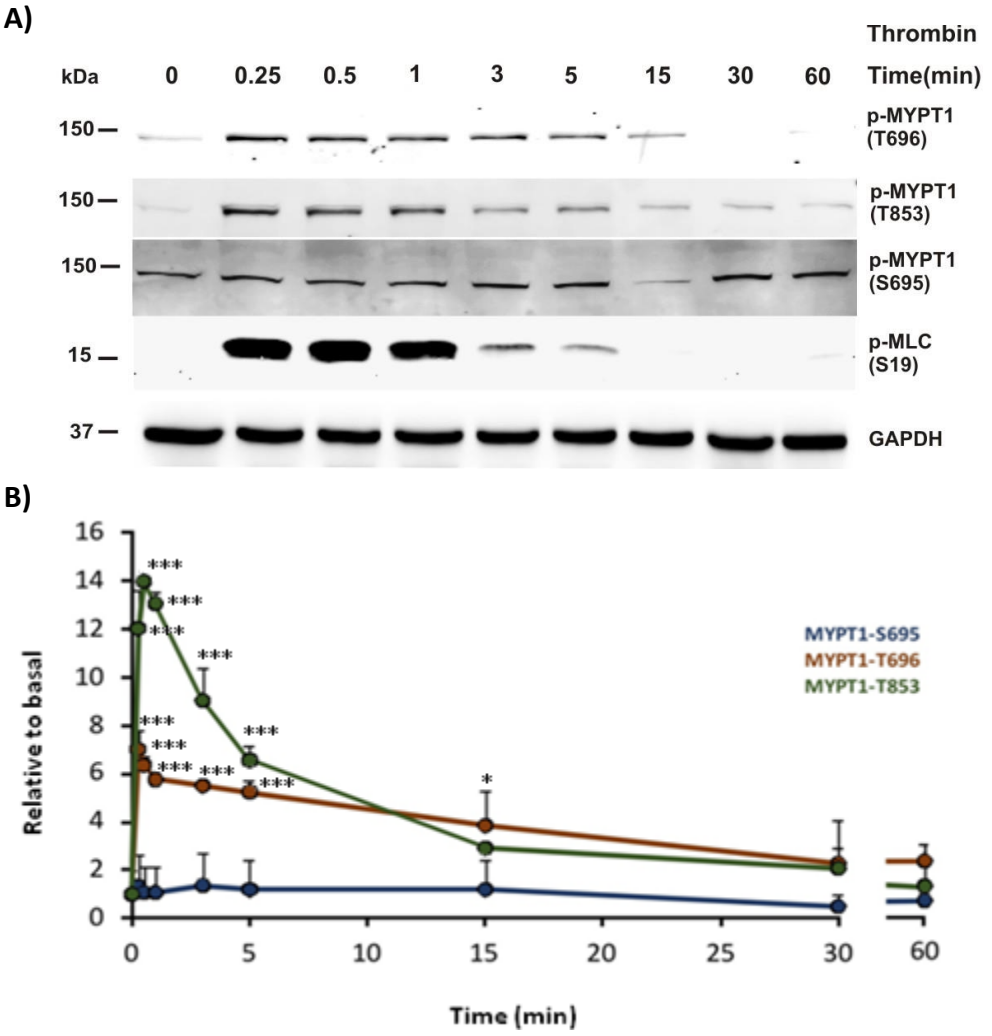

Figure 3.5: Characterisation of thrombin induced phosphorylation of MYPT1 in platelets. **A)** Human washed platelets (1×10^9/ml) were treated with indomethacin (10 µM), apyrase (2 U/ml) and EGTA (1 mM) for 20 min at 37°C. Platelets were stimulated with thrombin (0.1 U/ml) at indicated times points and lysed in Laemmli buffer. Samples were resolved by 10% SDS-PAGE and immunoblotted with anti-phospho-MYPT1-Ser695, Thr696 and Thr853 antibodies overnight at 4°C. Next day the corresponding fluorescently labelled secondary antibodies were used to visualise proteins with an Odyssey™ CLx electronic imaging system (Li-Cor). The blots were reprobed with anti-phospho-MLC-Ser19 antibody as a positive control and anti-GAPDH antibody for checking equal loading. The shown blot is representative of three independent experiments. **B)** Phosphorylation of MYPT1 at indicated sites was quantified by densitometry, normalised to loading control (GAPDH) and calculated relative to basal (untreated) whole cell lysates. Data are presented as means ± SEM. Statistical significance calculated using one-way ANOVA (* p<0.05-0.01, ** p<0.01-0.005 and *** p<0.005).

3.4.3. Characterisation of basal MYPT1 phosphorylation at Ser695

Previously (Figures 3.2, 3.3A and 3.4), we have noticed that there is always high basal phosphorylation of MYPT1 at Ser695 in human platelets. This is consistent with reports in other cell types (Grassie *et al*., 2012). We assumed this high basal phosphorylation of Ser695 is due to the presence of an active kinase involved in this process. Therefore we designed an experiment where we incubated platelets for longer period of time that subside the effect of kinase responsible for this basal phosphorylation.

Washed platelets ($1x10^9$/ml) were incubated at 37°C for up to 4 hrs before lysing in Laemmli buffer. Western blot analysis showed that there was some basal phosphorylation of MYPT1 at Ser695 even after 4 hrs of incubation illustrating that this residue is either constitutively phosphorylated basally or the presence of an active kinase (Figure 3.6). Platelets treated with PGI_2 (100 nM) at indicated times revealed a modest increase in the phosphorylation of MYPT1 at Ser695 that matches our previous experiments (Figure 3.1-3.5). Total MYPT1 antibody was used to verify the identity and amount of MYPT1.

phospho-VASP-Ser157 was used to verify the activity of PGI_2 and GAPDH was used as a control for equal loading.

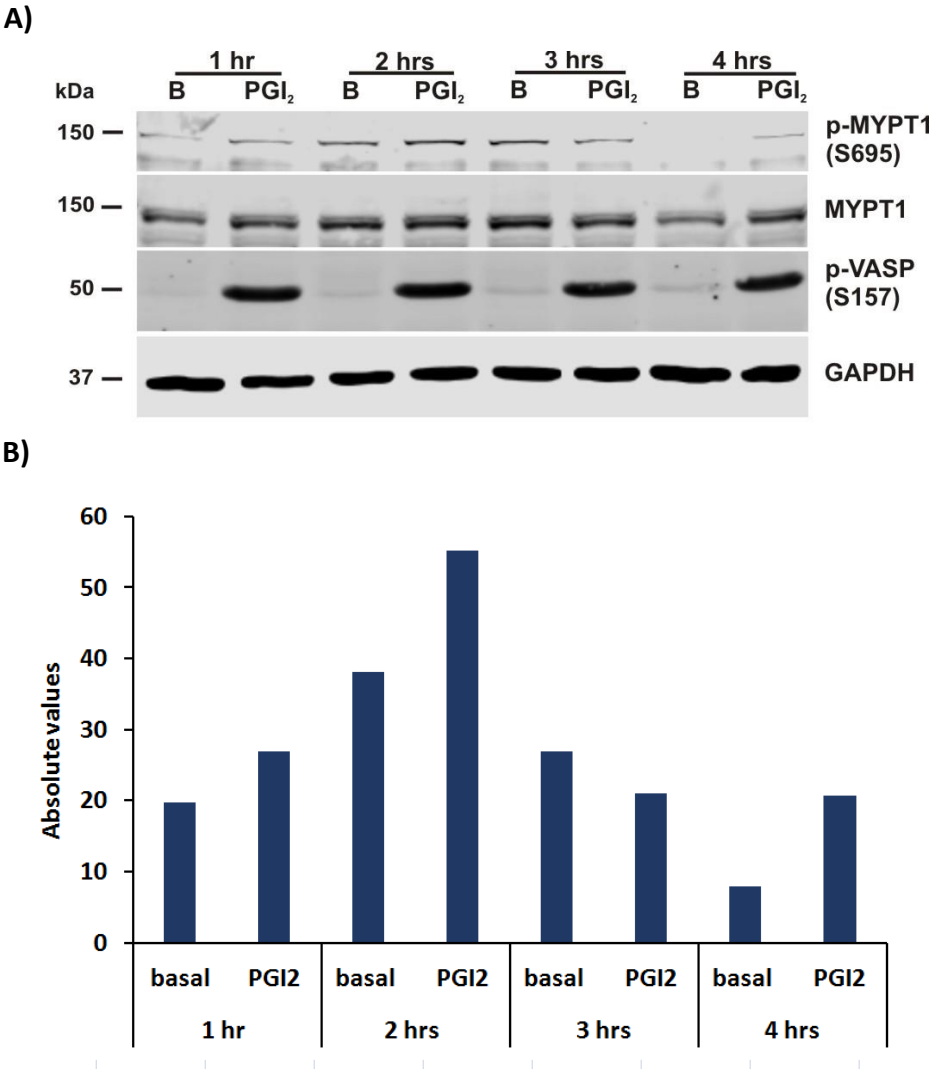

Figure 3.6: Profile of basal phosphorylation of MYPT1 at Ser695 in platelets. A) Human washed platelets (1×10^9/ml) were incubated for up to 4 hrs at 37°C before the experiment was performed. Platelets were stimulated with PGI_2 (100 nM) for 60 sec and lysed in Laemmli buffer. Unstimulated basal and stimulated samples were resolved by 10% SDS-PAGEand immunoblotted with phospho-MYPT1-Ser695 antibody overnight at 4°C. Next day the fluorescently labelled secondary antibody was used to visualise proteins with an Odyssey™ CLx electronic imaging system (Li-Cor). The blot was reprobed with anti-phospho-VASP-Ser157 antibody as a positive control. Total MYPT1 antibody was used as a control for the presence of MYPT1 proteins and anti-GAPDH antibody as a loading control. **B)** Phosphorylation of MYPT1 at indicated times was quantified by densitometry and expressed as absolute values. The shown blot is representative of one independent experiment.

3.5. MYPT1 splice variants in platelets

In the course of the work aimed at characterising the phosphorylation status of MYPT1 we noticed that the antibody we used to detect total MYPT1 consistently showed two bands at around 140 kDa, one intense band and one less intense band of a slightly higher apparent molecular weight (Figure 3.6). We suspected that our antibody was detecting alternatively spliced variants of MYPT1 in platelets. Although it is still possible that the post-translational modifications (like phosphorylation) might account for the appearance of the two bands. Recent studies have shown that alternative splicing of mRNA produces different variants of MYPT1 in smooth muscle cells (Lin & Brozovich, 2016). However, expression of MYPT1 splice variants has not been reported in platelets.

To confirm the presence of different splice variants of MYPT1, first platelets were treated with PGI_2 and thrombin for a particular amount of time, whole cell lysates were prepared, resolved by SDS-PAGE for longer time at low temperature (4°C) for better separation of protein bands and immunoblotted with both total and phospho-specific MYPT1 antibodies on the same membrane (Figure 3.7A). Our data suggests that there are two possible splice variants of MYPT1 in platelets. PGI_2 induces phosphorylation of only one splice variant of MYPT1 at the Ser695 residue (top band after matching with the corresponding MYPT1 splice variant bands), whereas thrombin induces phosphorylation of both at Thr696 and Thr853.

To confirm our immunoblotting data, the splice variants of MYPT1 were further explored in platelets by using immunoprecipitation and cAMP pull-down assay (Figure 3.7B). Immunoprecipitation was used to purify MYPT1 splice variants from platelet lysates. Since MYPT1 has been reported as a substrate of PKA (Wooldridge *et al*., 2004), cAMP pull-down assay was chosen in which cAMP agarose beads enable the pull down of PKA and its respective interactors, such as MYPT1. In this set of experiments platelet lysates were incubated with MYPT1 antibodies immobilised on protein G beads or cAMP agarose beads before being analysed on western blot. A doublet at around 140 kDa molecular weight was detected in both

immunoprecipitated and cAMP agarose beads samples, whereas no band was detected in control samples. Both splice variants appear in the immunoprecipitate in the same pattern of abundance as in whole cell lysate. Also PKA appears to interact with both splice variants because both bands are pulled down again in the same pattern of abundance as in the whole cell lysate.

In the last set of experiments we isolated washed platelets from five different donors and immunoblotted with MYPT1 antibody (Figure 3.7C) to confirm the consistency and specificity of our immunoblotting signal for MYPT1. The MYPT1 doublet was observed in the platelet lysates of all five donors.

Data from these experiments strengthen our claim that there are at least two potential splice variants of MYPT1 in platelets.

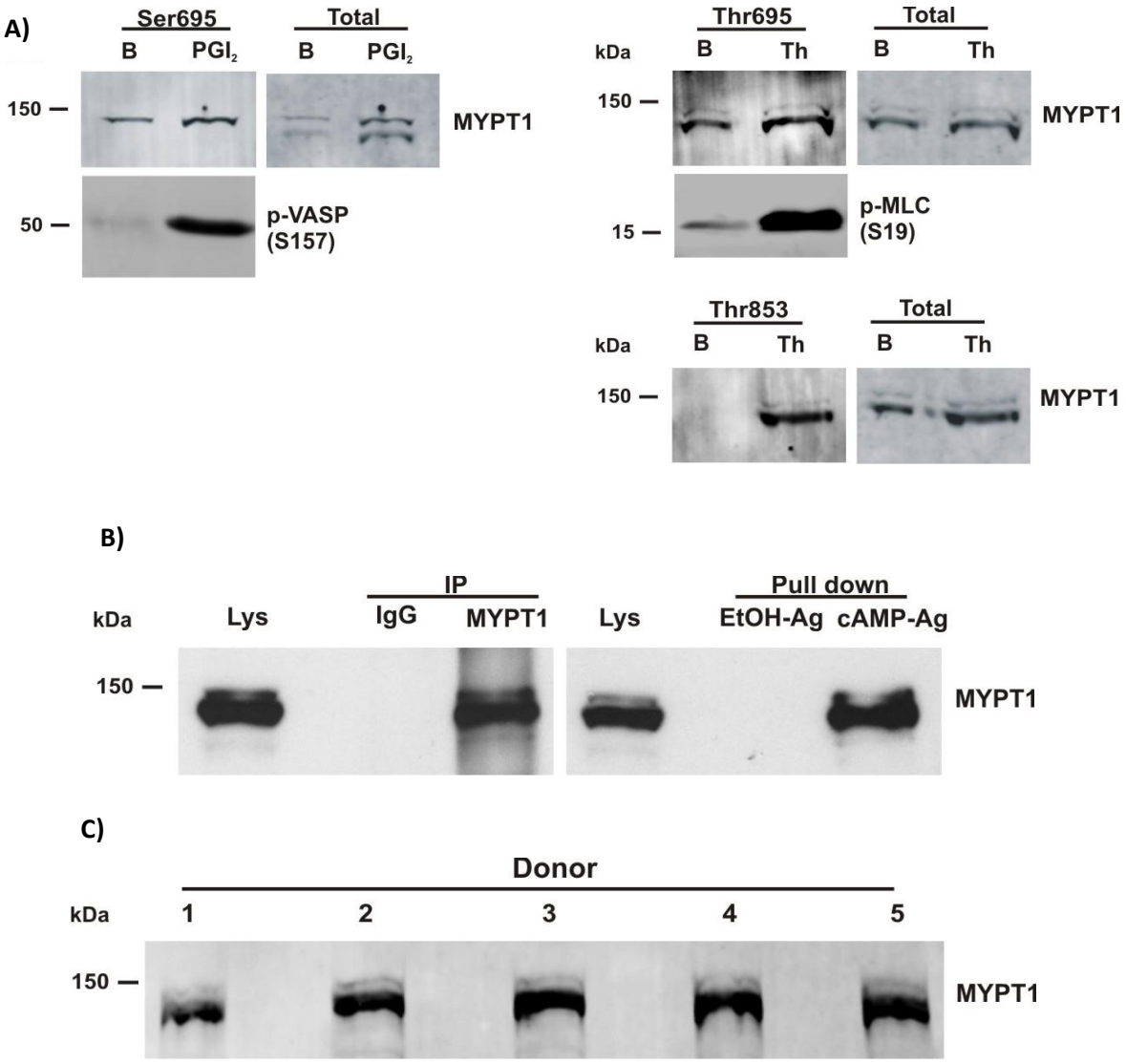

Figure 3.7: Splice variants of MYPT1 in platelets. Human washed platelets (1×10^9 /ml) were incubated with indomethacin (10 µM), apyrase (2 U/ml) and EGTA (1 mM) for 20 min at 37°C before experimentation. **A)** Platelets were stimulated with PGI_2 (100 nM) for 5 min or thrombin (0.1 U/ml) for 15 sec and lysed immediately in Laemmli buffer. Proteins were resolved by 8% SDS-PAGE and immunoblotted for phospho-MYPT1-Ser695, Thr696 and Thr853 overnight at 4°C. Next day the peroxidase conjugated secondary antibodies were added, followed by ECL detection. The blots were reprobed with anti-MYPT1 antibody as a control. Anti-phospho-VASP-Ser157 and Anti-phospho-MLC-Ser19 antibodies were used to confirm PGI_2, and thrombin activity, respectively, in this experiment. **B)** Human washed platelets (1×10^9/ml) were lysed with ice-cold immunoprecipitation lysis buffer containing protease inhibitors and incubated for 30 min on ice.

The platelet lysates (500 µg protein) were incubated either with 2 µg of MYPT1 antibodies or 25 µl of 8-AHA-cAMP agarose beads overnight at 4°C with gentle agitation. Non-reactive rabbit IgG or ethanol-agarose beads (EtOH-Ag) were used as control. Next day 25 µl of pre-equilibrated protein G sepharose beads slurry were incubated with lysate-antibody complex for 1 hr at 4°C with gentle agitation. The beads-antibody-protein complex were then pelleted by centrifugation at 1000xg for 1 min, washed 1x with lysis buffer and 2x with TBST before boiling in 2x Laemmli buffer for 5 min at 95°C. Samples were resolved by 8% SDS-PAGE and immunoblotted for MYPT1 overnight at 4°C. **A & B)** blots are representative of two independent experiments. **C)** Washed platelets (1×10^9 /ml) from five different donors were lysed in Laemmli buffer, resolved by 8% SDS-PAGE and immunoblotted for MYPT1 overnight at 4°C. Immunoblot of one experiment.

3.6. Discussion

In vascular smooth muscle cells MLCP plays an important role in the regulation of acto-myosin contractile forces in response to various endogenous stimulants. The activity of MLCP is mainly regulated via phosphorylation by two known pathways, the RhoA-ROCK pathway and the NO/PKG pathway. The RhoA-ROCK pathway phosphorylates Thr696 and Thr853 of the MLCP targeting subunit, MYPT1, and thus inhibits the activity of the myosin phosphatase and its interaction with myosin (Amano *et al*., 2010). On the other hand, the NO/PKG pathway regulates MLCP activity via two possible ways, either indirectly by inhibiting RhoA activation via phosphorylation at Ser188 (Aburima *et al*., 2017; Kitazawa *et al*., 2009) or directly by PKG mediated phosphorylation of MYPT1 at Ser695 that leads to MLCP disinhibition (Burgoyne & Eaton, 2010; Nakamura *et al*., 2007; Wooldridge *et al*., 2004).

Recent *in vitro* studies have reported that cAMP/PKA signalling in platelets also regulates MLCP activity by blocking RhoA-ROCK mediated phosphorylation of MYPT1 at Thr696 and Thr853 (Aburima *et al*., 2013; Watanabe *et al*., 2001); however, the direct effect of cAMP/PKA signalling on the phosphorylation of MYPT1 at Ser695 has not been reported yet. This chapter aimed to characterise in detail the phosphorylation of MYPT1 at Ser695, Thr696 and Thr853.

It was important to optimise first the conditions and the specificity of commercially available site-specific phospho-MYPT1 antibodies. We have noticed that phospho-MYPT1 antibodies were not very clean, picking up many additional bands, therefore it was utmost important to optimise the conditions under which these antibodies could give a clear and defined signal with the lowest number of additional bands. Our results suggest that the site-specific phospho-MYPT1-Ser695 antibody detected a clear band of the expected molecular weight (around 140 kDa) upon blocking with 5% milk powder (Figure 3.1). But blocking the membranes with milk powder also enhanced the intensity of additional bands.

The next important step was to check the specificity of commercially available phospho-MYPT1 antibodies, as it is crucial to the reliability of data interpretation. Cross-reactivity of the commercial phospho-MYPT1 antibodies have been reported before, for instance a significant signal was picked by phospho-MYPT1-Thr696 antibody in PKAc treated MYPT1 samples (Wooldridge *et al*., 2004); however, this matter was not fully investigated by Wooldridge and colleagues. Here we used platelet inhibitory (PGI_2, PGE_1, GSNO) and activatory (thrombin) agonists to confirm the specificity of our site-specific phospho-antibodies. PGI_2, PGE_1 and GSNO trigger phosphorylation of MYPT1 at Ser695 either directly by PKA/PKG signalling or indirectly by inhibiting the RhoA-ROCK pathway. On the other hand, thrombin phosphorylates MYPT1 at Thr696 and Thr853 via RhoA-ROCK pathway. Studies have shown that Thr696 and Thr853 are also phosphorylated by ILK and ZIPK (Hartshorne *et al*., 2004). Our data clearly suggest that phospho-MYPT1 antibodies are site-specific as both MYPT1-Thr696 and Thr853 antibodies picked up an expected band only in thrombin treated platelets, whereas very weak signal was detected in PGI_2, PGE_1 or GSNO treated platelets. Similarly, phospho-specific MYPT1-Ser695 antibody picked a band of expected molecular weight in the PGI_2, PGE_1 and GSNO treated platelets (Figure 3.2). The gold standard for checking the specificity of these antibodies could be using point mutagenesis in future. Consistent with other studies (Wooldridge *et al*., 2004; Grassie *et al*., 2012) we have also noticed that MYPT1 is always basally phosphorylated at Ser695 (Figure 3.3), and this basal level of phosphorylation was not affected by thrombin, suggesting that thrombin has no effect on Ser695 phosphorylation. As in smooth muscle cells, where basal phosphorylation of MYPT1 at Ser695 is involved in maintaining basal vascular tone through inhibition of calcium sensitisation (Neppl *et al*., 2009), we also assume that in platelets the basal phosphorylation of MYPT1 at Ser695 could possibly be involved in keeping MLCP in association with the acto-myosin contractile machinery (myosin IIa) where it dephosphorylates MLC thus keeping platelets in a quiescent state. Furthermore, Neppl and co-workers (2009) reported that a nitric oxide synthase inhibitor (L-NAME) completely abolished the

basal phosphorylation of Ser695 in endothelial cells, suggesting that the cGMP/PKG pathway is actively involved in this process. An explanation for this high basal Ser695 phosphorylation is the presence of basally active adenylyl cyclase 6 as reported by Pieroni *et al.* (1995) or the presence of another active kinase that is involved in this process. This basal phosphorylation at Ser695 in platelets could be further investigated by using adenylyl cyclases and PKA/PKG inhibitors.

Our calyculin A data also explain that the phosphorylation of Thr696 is not physically blocking the phosphorylation of adjacent Ser695 and vice versa, which is consistent with the study of Neppl and co-workers (2009). They showed that in cerebral arteries the phosphorylation of Thr696 is independent of the phosphorylation of Ser695. However, other researchers argue against this observation, claiming that the phosphorylation of Thr696 does physically block the phosphorylation of Ser695 and vice versa in ileal smooth muscle cells (Wooldridge *et al*., 2004). Nakamura *et al*. (2007) reported that phosphorylation of Ser695 is blocking the phosphorylation of Thr696, but the phosphorylation of Thr696 does not block the phosphorylation of Ser695, slightly different from what we have seen in our results.

Furthermore, we present for the first time a detailed characterisation of phosphorylation of MYPT1 at serine and threonine residues in platelets. Our time course data shows that the platelet inhibitory stimulant, PGI_2 triggers a modest increase in the phosphorylation of MYPT1 at Ser695 as compared to basal, and this increase in the phosphorylation remained steady for at least 60 min. PGI_2 did not provoke the phosphorylation of MYPT1 at Thr696 and Thr853. However, there is some inconsistency in the literature regarding phosphorylation of MYPT1 via cAMP/PKA signalling. Grassie and co-workers (2012) reported that cAMP/PKA signalling also triggers phosphorylation of MYPT1 at Thr696 and Thr853 in rat caudal artery smooth muscle cells, this dual role of cAMP signalling on MYPT1 phosphorylation at serine and threonine residues has not been reported in

platelets. This inconsistency in the phosphorylation of MYPT1 could be due to the differences in the cell type and experimental conditions.

On the other hand, activation of platelets with thrombin triggered a rapid increase in the phosphorylation of both Thr696 and Thr853 with maximum phosphorylation at 15 sec. However, the phosphorylation of these residues rapidly dropped within 5 min contrary to the phosphorylation of MYPT1 at Ser695 residue in PGI_2 treated platelets. This rapid decline in a time dependent manner in the phosphorylation of MYPT1 at threonine residues shows an active role of myosin phosphatase. *In vitro* studies have shown that myosin phosphatase dephosphorylates MYPT1 at Thr696 and Thr853 (Kaneko-Kawano *et al*., 2012: Khromov *et al*., 2009; Kiss *et al*., 2008). Kimura and colleagues (1996) reported that myosin phosphatase directly dephosphorylates its targeting subunit MYPT1 during RhoA-ROCK signalling. Furthermore, very low or no phosphorylation of these threonine residues was observed in our experiments at basal level, which suggests that the phosphatase activity is so intense that it removes all the phosphate groups and keep these threonine residues dephosphorylated under basal conditions. Moreover, our calyculin A data is clearly supporting this notion that an active phosphatase is involved in this process (Figure 3.2). Based on this phosphorylation data and current findings from the literature, we proposed a model to understand the effect of thrombin and PGI_2 on the phosphorylation of MYPT1 at serine and threonine residues in platelets (Figure 3.9).

Previously it has been reported that phosphorylation of MYPT1 significantly affects the MLCP activity, structure and location. In smooth muscle cells the phosphorylation of MYPT1 plays an important role in the regulation of MLCP activity, holoenzyme structure and its subcellular distribution. Shin and co-workers (2002) showed that the RhoA-ROCK induced phosphorylation of MYPT1 at Thr696 triggers the translocation of MLCP towards the cell membrane and subsequent dissociation of the holoenzyme complex, which results in reduced MLCP activity. Similarly, in platelets Aburima *et al.* (2013 & 2017) showed that the

phosphorylation of MYPT1 at Thr853 via RhoA-ROCK signalling significantly reduced MLCP activity. They propose that reduction in MLCP activity is related to the dissociation of the MLCP holoenzyme and subsequent translocation of MYPT1 towards the cell membrane where it forms a complex with RhoA-ROCK. Both PGE_1 and NO via PKA/PKG significantly reversed the inhibitory effect triggered by RhoA-ROCK signalling on myosin phosphatase activity and inhibited the dissociation of the holoenzyme complex (Neppl *et al*., 2009; Aburima *et al*., 2017 & 2013). These studies clearly suggest that phosphorylation of MYPT1 affects the MLCP activity, holoenzyme structure and location. We have also attempted to investigate the effect of phosphorylation on the distribution of MYPT1 in platelets by using a subcellular fractionation approach. However, our investigation was not successful as MYPT1 protein degraded very quickly in fractionation buffer. We have also tried to examine this effect in spread platelets by using phospho-specific MYPT1 antibodies. Again this result was also not very promising as the phospho-antibodies staining was very week.

A novel aspect of this work was to explore the expression of different splice variants of MYPT1 in platelets. Various splice variants of MYPT1 have been identified in various cell types with unique variations in the C-terminal leucine zipper (LZ) region or with the central insert (CI). All these variants are products of cassette-type alternative splicing of the gene, *PPP1R12A* at central and a 3' exons (Hartshorne *et al*., 1998) (Figure 3.8). The human *PPP1R12A* gene contains 27 exons. Alternative splicing of exon 15 (identical to exon 13 in rat) and exon 25 (exon 23 in rat) generate CI and LZ variants of MYPT1 (Butler *et al*., 2013). Only two of the splice variants of MYPT1 are well studied, MYPT1 with or without the C-terminal LZ motif (LZ^+ MYPT1 & LZ^- MYPT1) (splice variants 1 and 6 of figure 3.8); very little information and experimental confirmation of other splice variants are available.

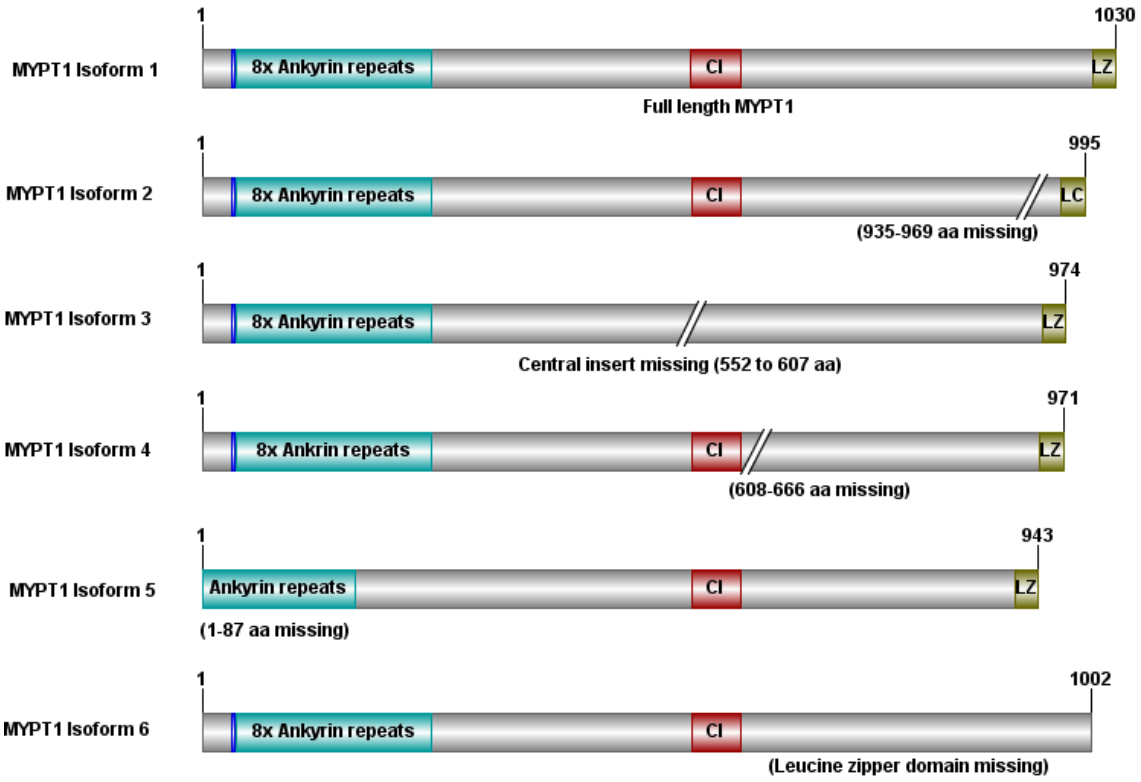

Figure 3.8: Schematic representations of MYPT1 splice variants. Shown are six known splice variants of MYPT1 in human (Uniprot number O14974). The cyan bar represents the PP1c binding domain and 8x ankyrin repeats; CI, central insert; blue bar, RhoA-ROCK binding motif; pink bar, PKA binding domain; LZ, leucine zipper domain.

Both *in vitro* and *in vivo* studies have shown that phosphorylation of only LZ^+ MYPT1 at Ser695 by PKG is associated with the relaxation of smooth muscle cells (Butler *et al*., 2013). *In vitro* studies have also shown that MYPT1-CI variants are involved in the agonist induced calcium sensitisation. Furthermore, Yuen *et al.* (2011) have reported that the rate of phosphorylation of MYPT1 was higher in the splice variant of MYPT1 with CI than without CI. Our western blot and immunoprecipitation data (Figure 3.7A & B) suggest that there are at least two potential splice variants of MYPT1 in platelets, possibly MYPT1 with LZ motif and MYPT1 without either CI or LZ motif. PGI_2 causes phosphorylation of only one isoform at Ser695, the top band, which we identified by aligning the phospho-MYPT-Ser695 band to the total MYPT1 bands. This top band is possibly a full length MYPT1 with LZ domain, whereas thrombin causes phosphorylation of both the variants at Thr696 and Thr853. The literature suggests that in smooth muscle cells

the interaction of PKG with the LZ domain of MYPT1 is responsible for the activation of MLCP (Surks *et al*., 1999). Later Huang *et al.* (2004) and Given *et al.* (2007) suggested that the LZ domain of MYPT1 is not actually responsible for the interaction with PKG but is required for PKG mediated MLCP activation and smooth muscle relaxation. We were also expecting that if this is the case PKA would interact with both the splice variants of MYPT1. Figure 3.7B showed that PKA does interact with both splice variants of MYPT1. This data confirms that the interaction of PKA with MYPT1 splice variants is independent of the phosphorylation of MYPT1 serine residue. Based on these results, we assume that there are possibly two pools of MYPT1 in platelets, which are differentially distributed and phosphorylated at Ser695 or Thr696. One pool can be in the cell periphery, where PKA phosphorylates MYPT1 at Ser695 and regulates MLC phosphorylation and acto-myosin contractile machinery. The second pool, on the other hand, can be in the cell cytosol where MYPT1 is mainly under the influence of RhoA-ROCK signalling, which is required for MLC phosphorylation. This paradigm would be consistent with the spatial compartmentalisation of cAMP signalling (Raslan *et al*., 2015a; Seino & Shibasaki, 2005). At this stage we are not aware of what role PKA is playing by interacting with the splice variant of MYPT1 that is not affected by PGI_2 or whether this interaction has any effect on the activity of MLCP. We are also not aware whether the expression of these isoforms in platelets would remain the same or it changes during disease conditions such as atherosclerosis. Currently we also do not know what the situation of these splice variants is in megakaryocytes. There are two possible ways to confirm the identity of these two splice variants of MYPT1 in platelets. By designing specific primers and verifying the presence of these variants in the extracted mRNA of platelets using PCR or by performing mass spectrometry.

Conclusion

To summarise, we have successfully characterised the optimum conditions for western blotting with commercially available phospho-specific MYPT1 antibodies.

We have demonstrated that phospho-antibodies are site-specific and the phosphorylation of MYPT1 at Ser695, Thr696 and Thr853 is at submaximal levels. In this chapter we have also investigated time dependent changes in the phosphorylation of MYPT1 at Ser695, Thr696 and Thr853. Furthermore, we have shown for the first time that there are two possible splice variants of MYPT1 in platelets; however, only one is under the influence of cAMP/PKA signalling in platelets.

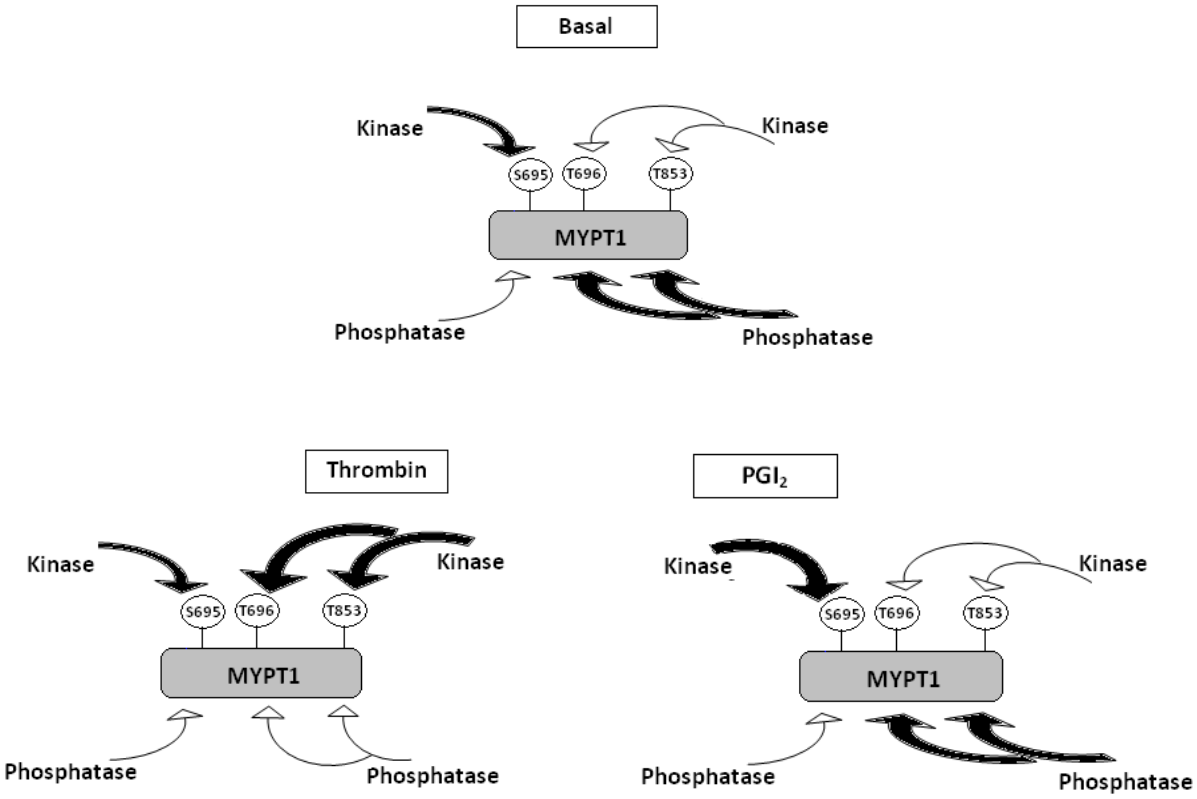

Figure 3.9: A Schematic diagram showing the effect of thrombin and PGI_2 on MYPT1. Both cyclic nucleotide-dependent protein kinases (PKA/PKG) and myosin phosphatase are active at basal level. PKA/PKG phosphorylates MYPT1 at Ser695, whereas myosin phosphatase or an unknown phosphatase dephosphorylates Thr696 and Thr853. Upon thrombin stimulation, RhoA-ROCK and possibly ILK and ZIP kinases phosphorylate MYPT1 at Thr696 and Thr853, which results in inhibition of myosin phosphatase. Phosphorylation of Ser695 is not affected by thrombin. PGI_2/NO via PKA/PKG restore myosin phosphatase activity by preventing RhoA-ROCK mediated phosphorylation of Thr696 and Thr853.

Chapter 4: Association of the MLCP targeting subunit MYPT1 with protein kinase A

4.1. Introduction

The cAMP signalling pathway is one of the key endogenous negative regulatory mechanisms in blood platelets. The foremost effector of cAMP signalling in platelets is protein kinase A (PKA), a kinase composed of two catalytic subunits and two regulatory subunits (Raslan & Naseem, 2014) (Figure 1.14).

In platelets there are two types of PKA, type I and type II, divided on the basis of their regulatory subunits (RI and RII), although their relative roles are not clearly resolved. These two types of regulatory subunits are further divided into α and β subtypes, encoded by four different genes, giving raise to four functionally distinct isoforms (RIα, RIβ, RIIα, RIIβ). In platelets all four PKA regulatory subunit isoforms have been reported (Burkhart *et al*., 2012). When two cAMP molecules interact with each regulatory subunit, the PKA undergoes conformational changes that trigger the dissociation of catalytic subunits from the cAMP-bound regulatory subunits (Taylor *et al*., 1990). The catalytic subunits then phosphorylate a number of downstream substrates on serine and threonine residues and subsequently suppress platelet activation (Raslan & Naseem, 2014). One of the known substrates of PKA is the myosin binding subunit (MYPT1) of MLCP. PKA catalytic subunit phosphorylates MYPT1 and disinhibits MLCP activity in smooth muscle cells (Wooldridge *et al*., 2004). Aburima *et al.* (2013) have demonstrated that cAMP/PKA signalling activates MLCP and maintains the holoenzyme structure by inhibiting RhoA-ROCK mediated phosphorylation of MYPT1. However, the molecular mechanism by which PKA regulates MLCP is poorly understood and requires clarification.

In many cell types including platelets cAMP-dependent PKA signalling is spatio-temporally regulated by a group of proteins called A kinase anchoring proteins (AKAPs), which allows multiple cAMP signalling events function simultaneously and

regulate distinct biological responses (Raslan *et al*., 2015; Pidoux & Taskén, 2010). AKAPs are a structurally diverse group of proteins but share one common function. They are molecular scaffolds that bind to the D/D domain of PKA regulatory subunits via their amphipathic helix and target the kinase through their unique targeting domain to its substrates at specific intracellular locations, thus defining distinct intracellular signalling compartments (Pidoux & Taskén, 2010). So far over 70 different AKAPs (including splice variants) from 43 different genes have been identified (Welch *et al*., 2010; Scholten *et al*., 2008), among which ∼15 are expressed in platelets (Raslan *et al*., 2015a). Most AKAPs bind to type II PKA (Rababa'h *et al*., 2015); however, some AKAPs have dual specificity and associate with type I PKA too (Means *et al*., 2011). Aside from binding PKA many AKAPs also function as scaffolds for several other signalling proteins that are involved in signalling transduction, such as PDEs, protein phosphatases and protein kinases, and thus coordinate multiple signalling pathways (Pidoux & Taskén, 2010).

MYPT1 strikingly fulfils several criteria used to define AKAPs. It acts as a scaffold protein that binds to the catalytic subunit (PP1cδ) at its N-terminus and localises it close to its substrate (Alessi *et al*., 1992). The N-terminus of MYPT1 is composed of 8 ankyrin repeats that are also important for regulation and targeting of MLCP. MYPT1 also provides a platform for many signalling and cytoskeleton proteins such as PKG, RhoA-ROCK, moesin and myosin, thus allowing the formation of multienzyme complexes (Butler *et al*., 2013). Furthermore, the structural analysis of MYPT1 showed the presence of a putative amphipathic helical sequence, a typical feature of an AKAP, at the end of its C-terminus (Matsumura & Hartshorne, 2008). However, the interaction of MYPT1 with PKA at molecular level has not been studied before. This chapter aims to investigate in detail the association of MYPT1 with PKA and whether this association is in AKAP fashion or not.

The aims of this chapter are:

- To characterise commercially available PKA antibodies.

- To investigate which PKA isoform is associated with MYPT1 in platelets under basal conditions.
- To map the interaction of MYPT1 and PKA.
- To investigate whether MYPT1 is an AKAP.
- And to verify that the interaction of MYPT-PKA is direct.

4.2. Characterisation of commercially available PKA regulatory and catalytic subunit antibodies.

Before attempting the study of the interaction of MYPT1 with PKA, the optimal conditions for PKA regulatory and catalytic subunit antibodies were determined. As PKA regulatory and catalytic subunits share protein sequence similarities and their respective commercial antibodies are raised against whole protein, it was particularly necessary to test the absolute specificity of these antibodies towards the detection of the respective proteins.

The specificity of PKA regulatory subunit antibodies was tested against recombinant human PKA regulatory subunit proteins. cDNA clones of PKA RIα, RIIα (generous gift from Prof Kjetil Taskén, University of Oslo), RIβ and RIIβ (purchased by Dr Zaher Raslan, University of Leeds) were used to amplify PKA regulatory subunits by PCR. The amplified products were subcloned in a vector (pGEX) for expression as GST fusions in *E.coli*. Proteins were expressed and purified as described in Section 2.7.1.3, then resolved by SDS-PAGE and immunoblotted with PKA regulatory subunit antibodies. Figure 4.1A shows that both anti-PKA RIIα and RIIβ were fairly specific, reacted intensely with their respective recombinant proteins and showed no cross-reactivity to other PKA regulatory subunits including RIα and RIβ. Anti-PKA RIα was picking signal with similar intensity in both RIα and RIβ recombinant proteins and showed no cross-reactivity to PKA RIIα or RIIβ. Whereas, anti-PKA RIβ antibody was not able to detect any signals in its respective recombinant protein, which suggests that either the commercially available antibody is not sensitive enough to pick up a signal or there is less or no RIβ protein present in platelets. However, proteomic studies do indicate that there are reasonably high copy numbers of RIβ present in platelets (Table 1.1). At this moment we cannot certainly say from this data that whether both RIα and RIβ are expressed as antibody apparently recognises both proteins and RIβ antibody did not work. However, proteomics and transcriptomic studies suggest that both are present in platelets but we cannot verify at this time. Based on these findings anti-

PKA RIβ will not be further used and anti-PKA RIα will be referred to as α/β. Coomassie staining was used to show the presence of GST-tagged recombinant proteins (Figure 4.1B).

Note that some of our fusion proteins were degraded more than others. We tried to use more protease inhibitors, used pre-chilled French press and kept lysates on ice all the time but still could not prevent the degradation. This degradation profile was recognised by commercial PKA regulatory subunit antibodies.

In order to test if the MYPT1, all PKA regulatory and catalytic subunit antibodies could identify the presence of their respective proteins in human platelets, 40 µg of whole platelets lysate was resolved on SDS-PAGE and immunoblotted for MYPT1, PKA regulatory and catalytic subunit. Figure 4.1C shows that MYPT1 and all PKA regulatory subunit antibodies detected their respective proteins at expected molecular sizes in platelets. Human umbilical vein endothelial cells (HUVECs) lysate was used as positive control. Commercially available PKA catα subunit antibody recognised two bands in platelet lysate, whereas in HUVEC lysate the antibody picked only a single band at expected molecular weight (42 kDa) (Figure 4.1D). The doublet of PKA catα was further investigated by using GST-tagged PKA catβ protein, suggesting that the antibody is potentially recognising two isoforms, PKA catα and catβ, in platelet lysates.

These results suggest that all four PKA regulatory subunits, PKA catalytic subunit and MYPT1 are present in platelets. Commercially available anti-PKA RIIα and RIIβ antibodies are fairly specific, whereas anti-PKA RIα antibody detected both RIα and RIβ isoforms in equal abundance and therefore will be considered for both isoforms. Furthermore, anti-PKA catα antibody recognises both catα and catβ isoforms in platelets.

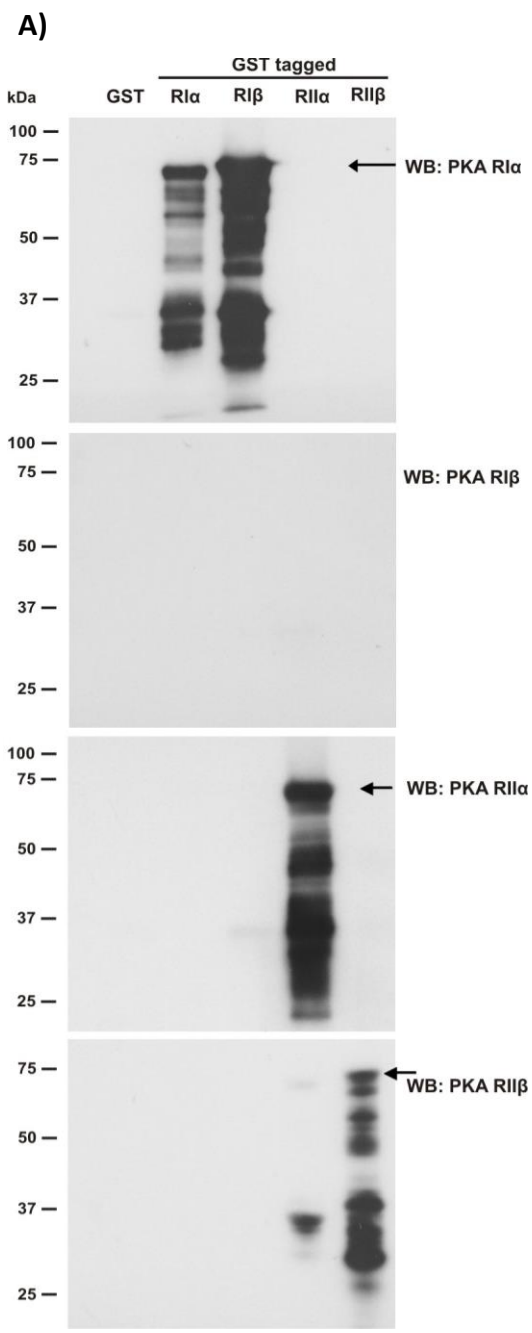
A)
GST tagged
kDa
GST
RIα
RIβ
RIIα
RIIβ
100
75
50
37
25
WB: PKA RIα
WB: PKA RIβ
WB: PKA RIIα
WB: PKA RIIβ

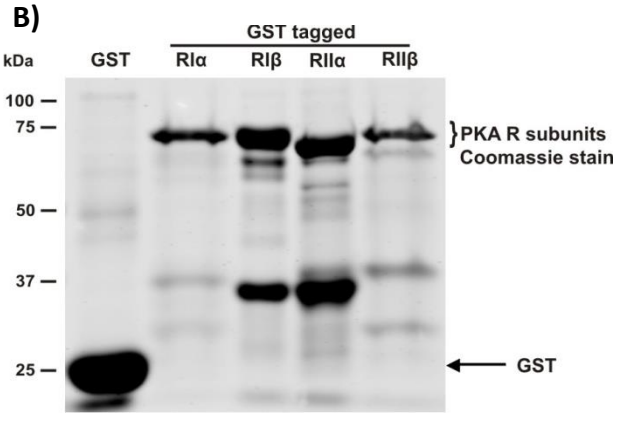
B)
GST tagged
kDa
GST
RIα
RIβ
RIIα
RIIβ
100
75
50
37
25
PKA R subunits
Coomassie stain
GST

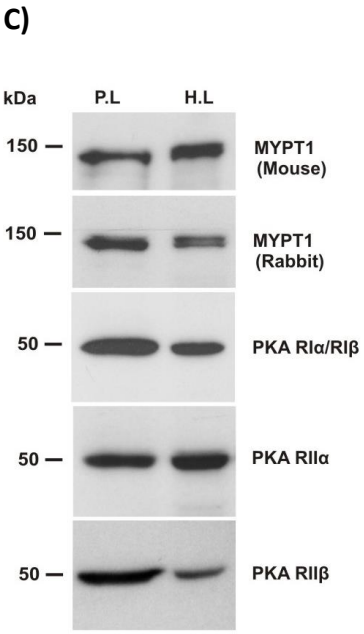
C)
kDa
P.L
H.L
150
150
50
50
50
MYPT1
(Mouse)
MYPT1
(Rabbit)
PKA RIα/RIβ
PKA RIIα
PKA RIIβ

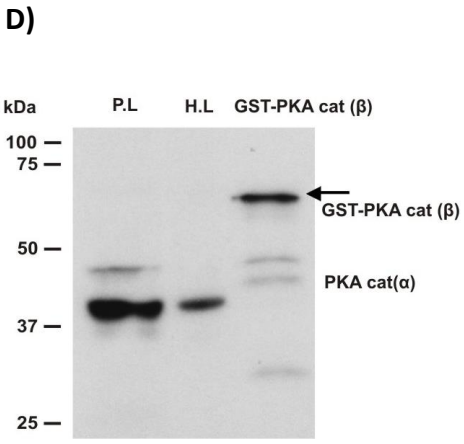
D)
kDa
P.L
H.L
GST-PKA cat (β)
100
75
50
37
25
GST-PKA cat (β)
PKA cat(α)

Figure 4.1: Characterisation of MYT1, PKA regulatory and catalytic subunit antibodies. A) PKA regulatory subunits (RIα, RIβ, RIIα and RIIβ) were expressed as a GST fusions in *E. coli* XL-1blue strain and purified by incubating the soluble fraction with 25 µl of pre-equilibrated glutathione sepharose beads slurry for 1 hr at 4°C with gentle agitation. After purification recombinant proteins were eluted in Laemmli buffer, resolved by 10% SDS-PAGE and immunoblotted with anti-PKA RIα, RIβ, RIIα and RIIβ antibodies. **B)** One gel of panel A was stained with Coomassie-Brilliant-Blue to show the presence of GST fusion proteins. **C)** Human washed platelets ($1X10^9$/ml) (P.L) and HUVECs lysates (H.L) were resolved by 10% SDS-PAGE and immunoblotted with anti-PKA RIα/β, RIIα, RIIβ and two different MYPT1 antibodies. **D)** Human washed platelets ($1X10^9$/ml) lysate, HUVECs lysate and GST-tagged PKA catβ were resolved by 10% SDS-PAGE before immunoblotted with anti-PKA catα antibody. Data from one independent experiment.

4.3. MYPT1 interacts with PKA in platelets

Having established the specificity of PKA regulatory subunit antibodies, next we wanted to investigate the interaction of MYPT1 with PKA in platelets by using three different biochemical approaches, co-immunoprecipitation, cAMP pull-down assay and GST pull-down assay.

4.3.1. Co-immunoprecipitation of MYPT1 and PKA from platelets

A conventional co-immunoprecipitation approach was carried out to identify MYPT1-PKA interactions by using target specific antibodies in platelets. This technique involves immunoprecipitation of MYPT1 from platelet lysates followed by immunoblotting with isoform specific PKA regulatory subunit antibodies. Washed platelets ($1x10^9$/ml) were prepared as in section 2.6.1 and lysed in ice cold lysis buffer before incubation with the MYPT1 antibody overnight at 4°C with gentle agitation. Next, immune complexes were immobilised on pre-equilibrated protein G sepharose beads, washed, eluted, resolved on SDS-PAGE, and analysed by western blot. Figure 4.2 shows that MYPT1 and presumably all four isoforms of PKA regulatory subunits are associated in platelets at the non-activated state, suggesting that they are part of the same complex. Rabbit IgG, used as a negative control, failed to precipitate either MYPT1 or PKA regulatory subunits. PKA catalytic subunit and PP1cδ were used as positive controls as they constitutively associate with PKA and MYPT1, respectively, under basal conditions.

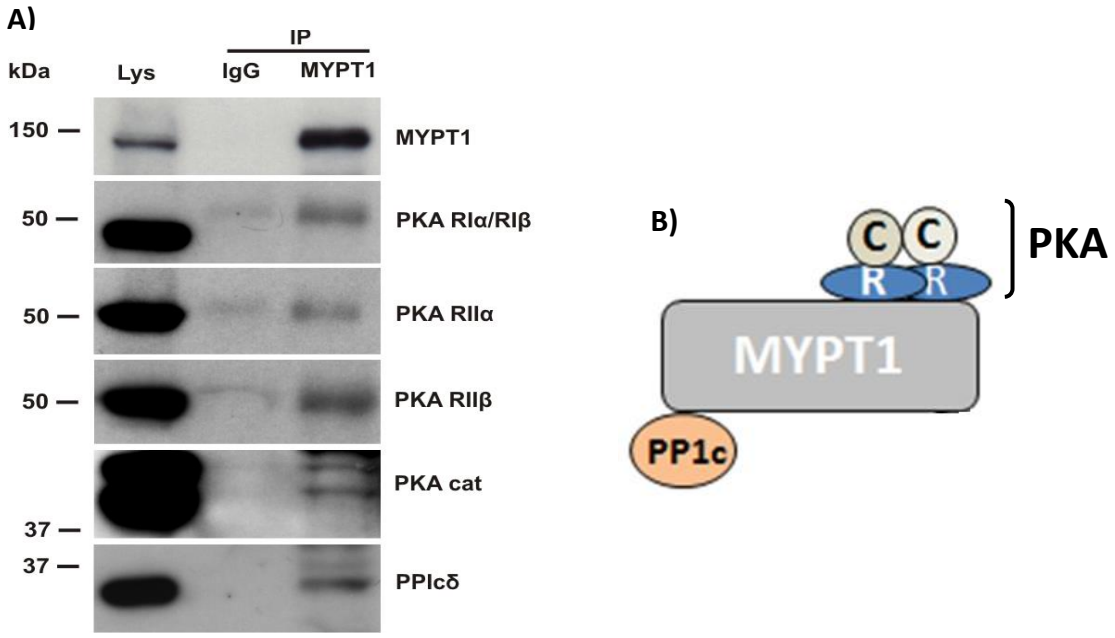

Figure 4.2: MYPT1 associates with PKA in platelets. **A)** Washed human platelets (1×10^9 /ml) were lysed with ice cold immunoprecipitation lysis buffer containing protease inhibitors and incubated for 30 min on ice. The platelet lysates (500 µg proteins) were incubated with 2 µg of MYPT1 rabbit antibodies or total rabbit IgG overnight at 4°C with gentle agitation. Next day 25 µl of pre-equilibrated protein G sepharose beads slurry were incubated with the lysate-antibody complex for 1 hr at 4°C with gentle agitation. The beads-antibody-protein complex was then pelleted by centrifugation at 1000xg for 1 min, washed 1x with lysis buffer and 2x with TBST before being boiled in Laemmli buffer for 5 min at 95°C. Immuno-complexes were resolved by 10% SDS-PAGE and immunoblotted with anti-MYPT1, anti-PKA RIα/β, RIIα and RIIβ antibodies overnight at 4°C. Next day the corresponding peroxidase conjugated secondary antibodies were used, followed by ECL detection. The blots were reprobed with anti-PKA cat subunit and anti-PP1c antibodies as positive controls. Shown blots are representative of three independent experiments. IP: immunoprecipitation, Lys: lysate. **B)** A cartoon depicting the possible interaction of the regulatory subunits of PKA and MYPT1 under non-activated (basal) state in platelets. R: regulatory subunit, C: catalytic subunit

4.3.2. cAMP pull-down of PKA and MYPT1

We further demonstrated the interaction of MYPT1 with PKA regulatory subunits using a cAMP pull-down assay in which cAMP bound agarose beads are used to enrich cAMP binding proteins including PKA and its substrates. Platelet lysates were prepared in ice cold lysis buffer and were incubated with cAMP agarose or EtOH-agarose beads overnight at 4°C with gentle rotation. Beads were washed, resolved on SDS-PAGE and immunoblotted with MYPT1 and PKA regulatory subunit antibodies. Figure 4.3 shows that all four PKA regulatory subunits were pulled-down from platelets along with MYPT1 by cAMP-agarose beads. No association was observed in EtOH-agarose beads, which were used as negative control. These control beads are blocked with ethanolamine to prevent PKA association to beads. This data validates our co-immunoprecipitation results (Section 4.3.1), which illustrates that MYPT1 and PKA are part of same complex in platelets. PKA catalytic subunit and PP1cδ constitutively bind to PKA regulatory subunits and MYPT1, respectively, and were used as positive controls.

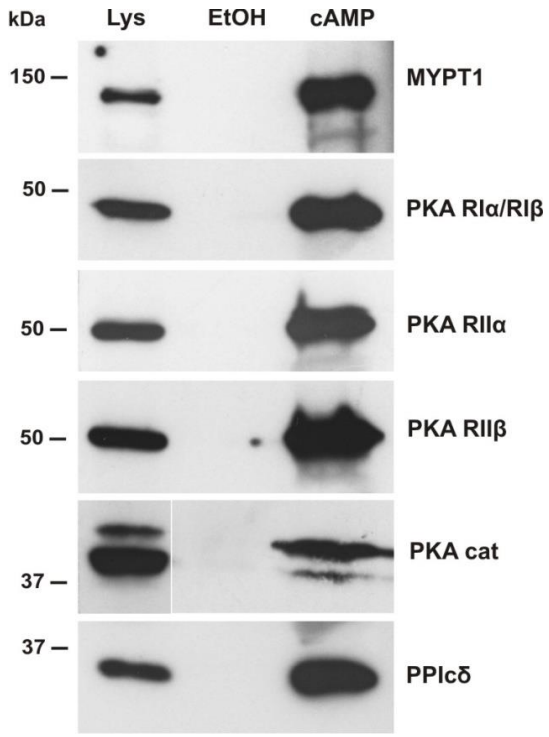

Figure 4.3: Interaction of MYPT1-PKA in platelets. Human washed platelets (1×10^9 /ml) were lysed with ice-cold lysis buffer containing protease inhibitors and incubated for 30 min on ice. The platelet lysates (500 µg of protein) were incubated with 25 µl of 8-AHA-cAMP agarose beads or the control agarose (EtOH - no cAMP) beads overnight at 4°C with gentle agitation. Next day beads-protein complex were then pelleted by centrifugation at 1000xg for 1 min, washed 1x with lysis buffer and 2x with TBST before being boiled in Laemmli buffer for 5 min at 95°C. Samples were resolved by 10% SDS-PAGE and immunoblotted with anti-PKA RIα/RIβ, RIIα, RIIβ and anti-MYPT1 antibodies overnight at 4°C. Next day the peroxidase conjugated secondary antibodies were used, followed by ECL detection. The Blots were reprobed with anti-PKA catα subunit and anti-PP1c antibodies as positive control. Shown blots are representative of two independent experiments.

4.3.3. GST pull-down of PKA with MYPT1

We next aimed to examine the interaction of MYPT1 with the exogenous PKA regulatory subunits using a complementary approach, a GST pull-down assay. Lysates from non-activated platelet were mixed with PKA regulatory subunits expressed recombinantly as GST fusion proteins and bound to glutathione sepharose beads (Figure 4.4A). All four GST-PKA regulatory subunits were able to pull-down MYPT1 from platelet lysates, whereas no association of MYPT1 with GST alone was observed (Figure. 4.4B). This data confirms that MYPT1 and PKA interact with each other in platelets. The PKA catα constitutively interacts with all PKA regulatory subunits and was used as a positive control. A gel stained with Coomassie-Brilliant-Blue was used to show the presence of GST fusion proteins.

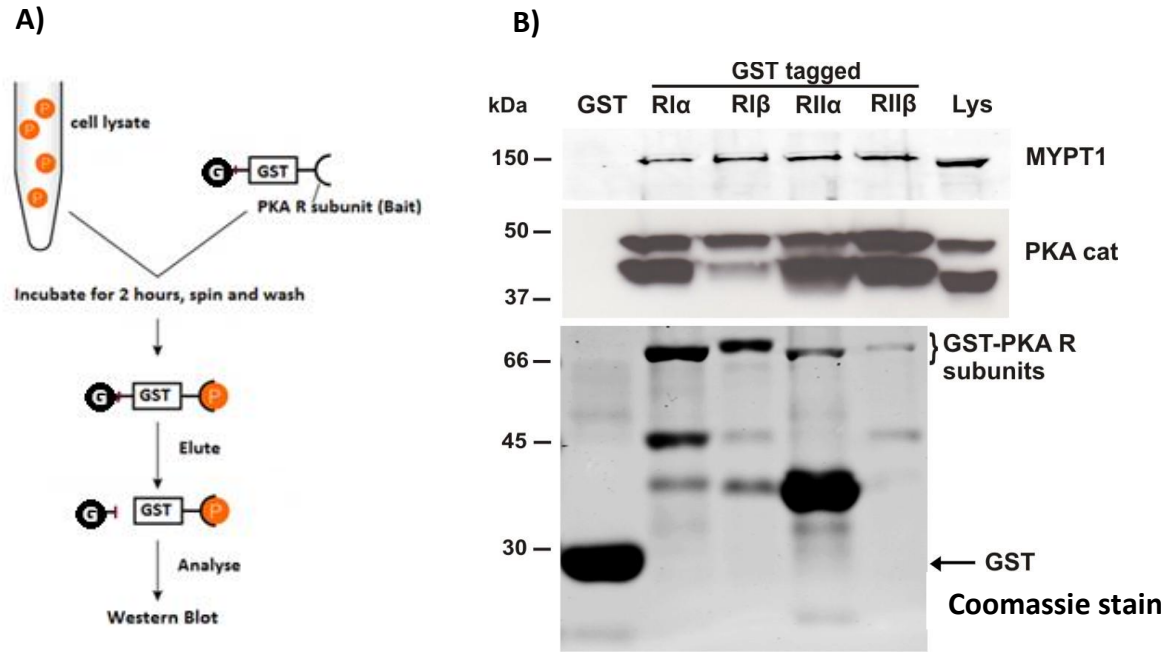

Figure 4.4: *In vitro* association ofMYPT1 with PKA regulatory subunits in resting platelets. A) A schematic diagram of the GST pull-down assay. P, protein: G, glutathione beads. **B)** Human washed platelets (1×10^9 /ml) were lysed in 1% Triton X-100 ice cold lysis buffer containing protease inhibitors and incubated for 30 min on ice. PKA regulatory subunits (RIα, RIβ, RIIα and RIIβ) were expressed as GST fusion in *E. coli* XL-1 blue strain and purified by incubating the soluble fraction with 25 µl of pre-equilibrated glutathione sepharose beads slurry for 1 hr at 4°C with gentle agitation. After purification, 500 µg of platelet lysates were added to the beads for 2 hrs at 4°C with gentle agitation. The beads-protein complex was then pelleted by centrifugation at 1000xg for 1 min, washed 1x with lysis buffer and 2x with TBST before being boiled in Laemmli buffer for 5 min at 95°C. Samples were resolved by 10% SDS-PAGE and incubated with anti-MYPT1 antibody overnight at 4°C. Next day the corresponding peroxidase conjugated secondary antibodies were added, followed by ECL detection. The blots were reprobed with anti-PKA catalytic subunit antibody as a positive control. One gel was stained with Coomassie-Brilliant-Blue as a control. Shown blots are representative of four independent experiments.

4.4. Mapping the interaction of MYPT1 with PKA regulatory subunits

Having confirmed that MYPT1 interacts with PKA in platelets, we next wanted to investigate the exact region of MYPT1 responsible for the interaction. However, platelets are anucleated and therefore not amenable to direct genetic manipulation. For this reason we had to switch to a cell line human embryonic kidney cells (293T HEK cells) where we can explore this interaction at the molecular level. To begin with, the truncated versions of MYPT1 and PKA were generated in this study as shown in figure 4.5.

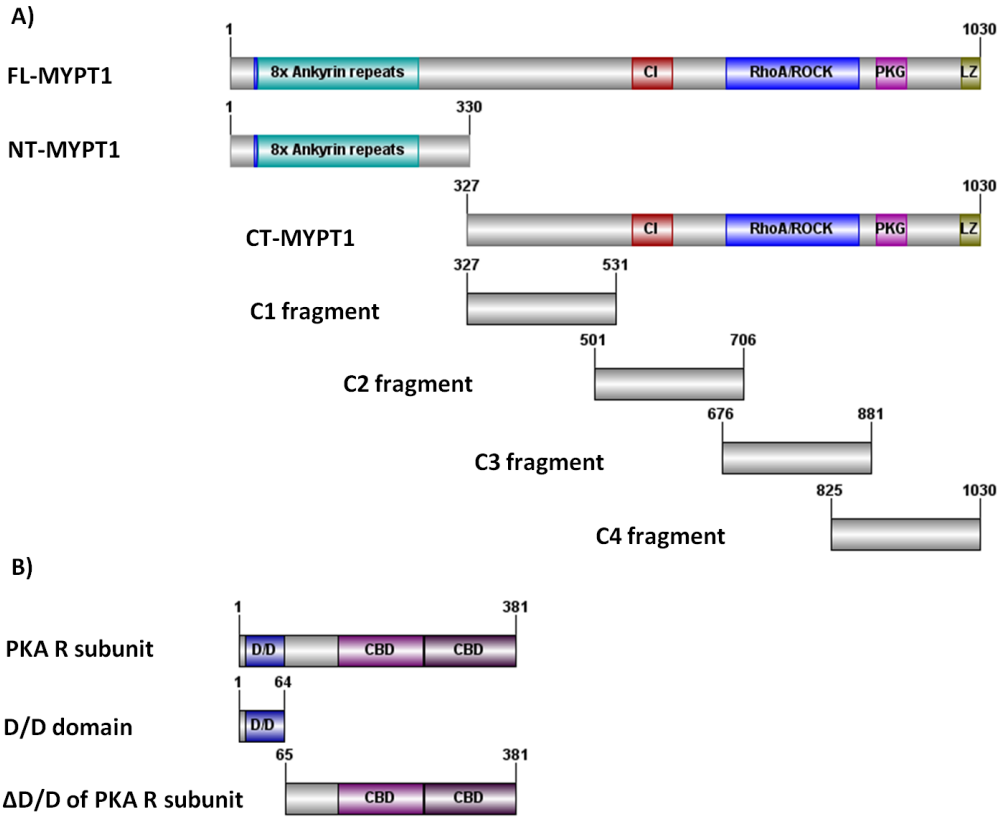

Figure 4.5: Schematic diagram of various MYPT1 and PKA constructs used in this study. Different tags (Myc, GST, His, GFP) were attached to the N-terminus as detailed in the corresponding experiments. A detailed list of all constructs can be found in sections 2.1.7-2.1.9. **A)** MYPT1 is composed of an N-terminal domain with PP1c binding site (RVXF, highlighted in blue line), followed by 8 ankyrin repeats, a highly variable central insert (CI), RhoA-Rock binding site, PKG binding region and a coiled-coil C- terminal domain with a leucine zipper motif (LZ). **B)** All PKA regulatory subunits have same domain structures, N-terminal dimerisation and docking domain D/D, followed by two cyclic nucleotide binding domains (CBD).

4.4.1. Bioinformatics analysis of MYPT1 amino acid sequence

We hypothesised that MYPT1 interacts with PKA in an AKAP manner and allows cAMP/PKA signalling to control actin dynamics through regulating the activity of PP1c and thereby the phosphorylation of MLC. If MYPT1 functions as an AKAP it would have an amphipathic helix that would mediate the interaction with the D/D domain of the regulatory subunits of PKA. We analysed the secondary structure of the MYPT1 amino acid sequence for the presence of a possible amphipathic helix using computer software called HeliQuest (Gautier *et al*., 2008). The main characteristics of amphipathic helices is that they are 14 to 18 amino acids long α-helices, where one side of the helix has hydrophobic residues and the opposite side has hydrophilic residues.

First of all we screened the whole MYPT1 protein sequence through the HeliQuest screening α-Helix tool and found five potential sequences that could possibly make amphipathic helices. Next we analysed our potential sites through the HeliQuest analysis tool. These sites were selected on the basis of their hydrophobicity, hydrophobic moment, formation of hydrophobic-hydrophilic faces and minimum numbers of hydrophobic residues. Special residues such as glycine and proline-containing hydrophobic faces were excluded as they have poor helical forming properties and disrupt the α-helix. After the analysis only two regions, aa267-285 and aa986-1004, were selected that could possibly form amphipathic helices (Figure 4.6A). Furthermore, the physicochemical properties of these two regions revealed a strong amphipathic character comparable with the known AKAP disruptor peptides (RIAD and Ht31), which were used as models during this bioinformatics analysis (Figure 4.6B). This data suggests that MYPT1 could be an AKAP with hypothetical amphipathic helices.

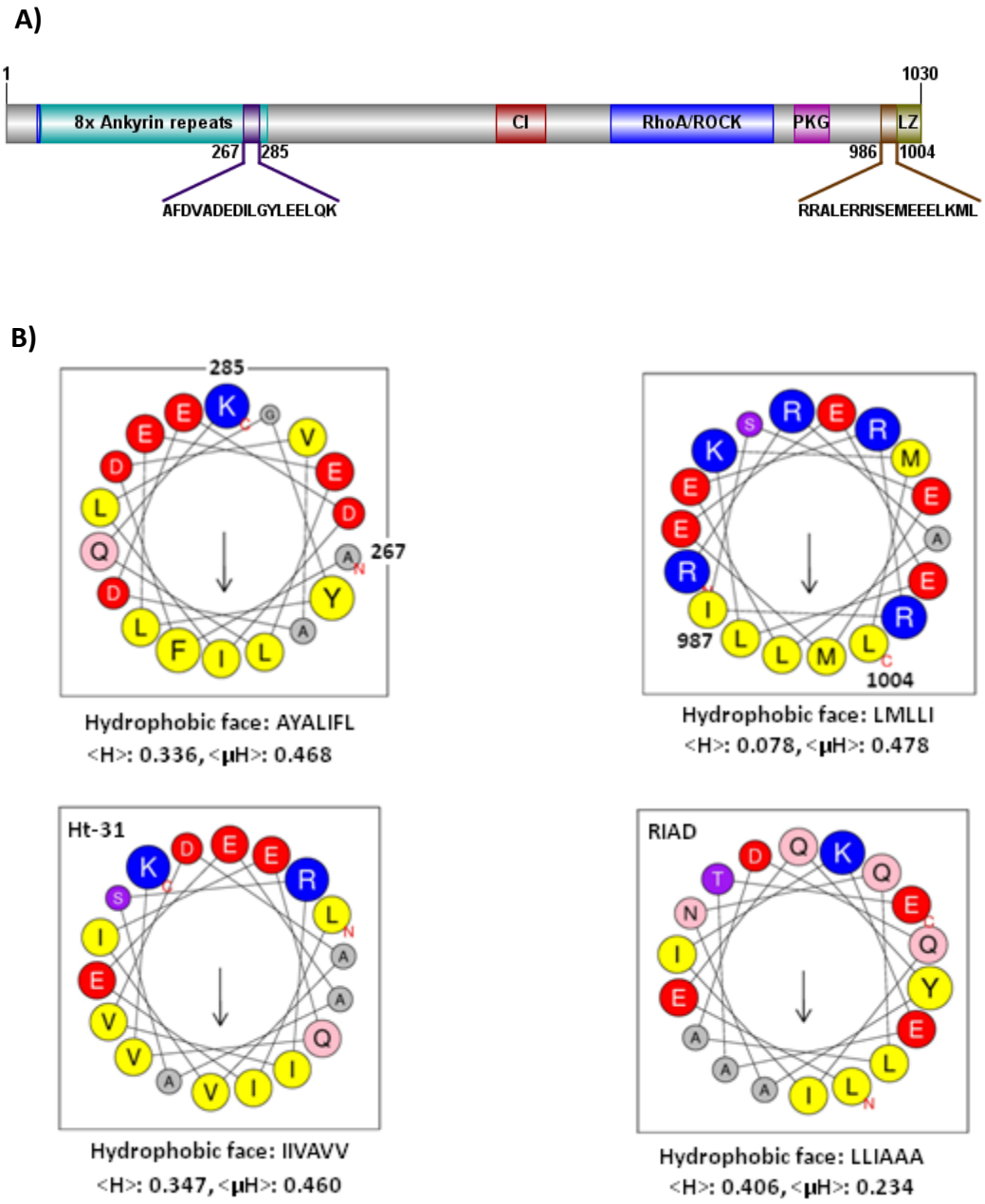

Figure 4.6: Identification of potential amphipathic helices in MYPT1. A) A schematic diagram of MYPT1 domains with putative amphipathic helical regions that are underscored and numbered. **B).** Helical wheel representations were generated from the amino acid residues aa267-285 and aa987-1004 of these potential helical regions using the HeliQuest software (Gautier *et al*., 2008). First, size of the analysis window was set to 18 amino acids, then the putative helical sequence entered and run for analysis. The physicochemical properties, hydrophobicity, hydrophobic moment and formation of hydrophobic-hydrophilic faces and numbers of hydrophobic residues of each sequence were then compared with known synthetic peptides, Ht31 and RIAD.

Yellow represent hydrophobic residues; blue, basic residues; red, acidic residues; pink, asparagine and glutamine; green, proline; purple, serine and threonine; gray, other residues. The position of first (N) and last (C) residues and hydrophobic face of the corresponding sequences are indicated. The arrow represents direction of hydrophobic moment. The number of amino acids, hydrophobic moment and mean hydrophobicity values are indicated for each helix. These values are generated in arbitrary units by the HeliQuest. Hydrophobicity, <H>; hydrophobic moment, <μH>.

4.4.2. PKA binding region within MYPT1

In order to test bioinformatics data several pull-down assays were performed with truncations of MYPT1 expressed in HEK cells (Figure 4.5).

Full length MYPT1 was divided into two major fragments: N-terminal fragment comprising amino acids 1-330 (designated as NT) and C-terminal fragment comprising amino acids 327-1030 (designated as CT) (Figure 4.7A). 293T HEK cells were transiently transfected as in section 2.5.4 with plasmids to allow expression of Myc-tagged MYPT1 (Full length, NT and CT) constructs. After 24 hrs cell lysates were prepared and subjected to pull-down experiments with GST-PKA regulatory subunits bound to glutathione sepharose beads (section 2.7.2). As shown in figure 4.7, only CT-MYPT1 interacted with GST-PKA regulatory subunits but not NT-MYPT1.

This result suggests that the N-terminus, which carries one of the two MYPT1 potential amphipathic helices, is not involved in the interaction between MYPT1 and PKA. Full length MYPT1 interacted, as expected, with all PKA regulatory subunits. GST alone was used as a negative control. Coomassie staining was used to show the presence of GST fusion proteins.

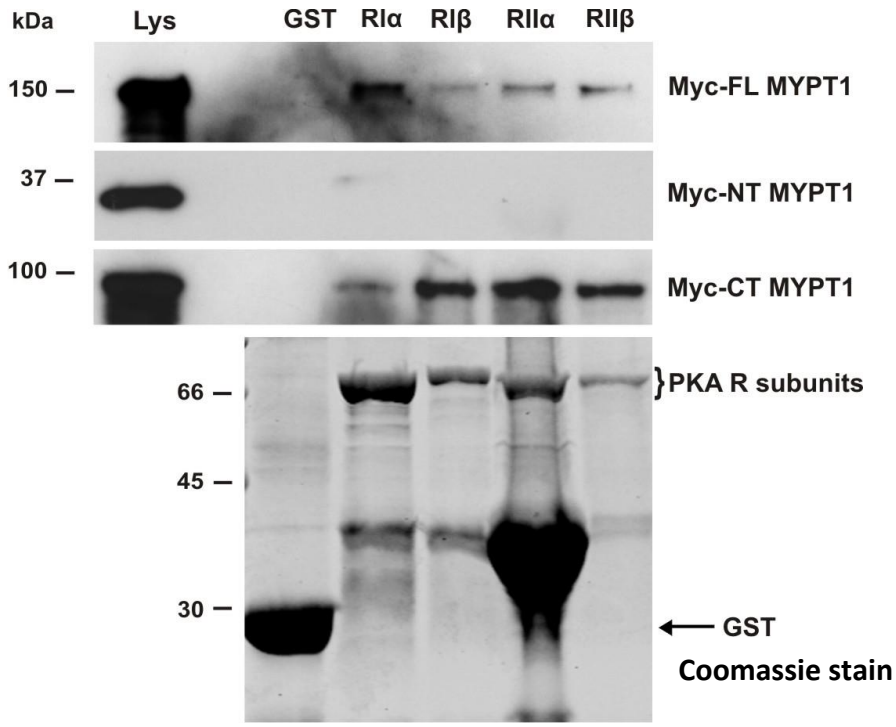

Figure 4.7: Mapping of the MYPT1-PKA interaction. 293T HEK cells were transiently transfected with constructs allowing expression of Myc-MYPT1 (full length, N-terminal and C-terminal) for 24 hrs at 37°C. Cells were lysed in 1% Triton X-100 containing protease inhibitors. PKA regulatory subunits (RIα, RIβ, RIIα and RIIβ) were expressed as a GST fusions in *E. coli* XL-1 blue strain and purified by incubating the soluble fraction with 25 µl of pre-equilibrated glutathione sepharose beads slurry for 1 hr at 4°C with gentle agitation. After purification, beads complexes were added to HEK cells lysate for 2 hrs at 4°C. Samples were resolved by 10% SDS-PAGE and immunoblotted with anti-Myc antibody overnight at 4°C. Next day the corresponding peroxidase conjugated secondary antibody was used, followed by ECL detection. One gel was stained with Coomassie-Brilliant-Blue as a control. Blots are representative of two independent experiments.

4.4.3. Mapping the PKA binding region within the C-terminus of MYPT1

In order to narrow down the binding region of MYPT1 with PKA regulatory subunits the C-terminus was subdivided into four overlapping fragments designated as C1, C2, C3 and C4. Each fragment was 200 amino acids long with 30 overlapping residues as shown in figure 4.5A: C1 (aa327-531), C2 (aa501- 706), C3 (aa676-881) and C4 (aa825-1030). 293T HEK cells were transiently transfected with plasmids to allow expression of these Myc-tagged fragments (section 2.5.4). After 24 hrs, lysates were prepared and subjected to pull-down assays with GST-PKA regulatory subunits immobilised to glutathione sepharose beads, then analysed by western blot for the presence of the indicated tagged proteins. On the basis of our bioinformatics data we were expecting that the C4 fragment would be involved in the interaction. However, figure 4.8 clearly reveals that only the C2 fragment was strongly associated with PKA regulatory subunits. Weak binding was also revealed with the C1 fragment, suggesting that the binding motif may reside somewhere in the beginning of C2 that is overlapping with the end of C1. Note that this C2 fragment contains the central insert region of MYPT1 protein. GST alone was used as negative control.

This result, combined with the pull-down using NT-MYPT1 suggests that MYPT1 is not interacting with PKA in an AKAP fashion, as the predicted amphipathic helices are not involved in the interaction. This was further explored in section 4.7.

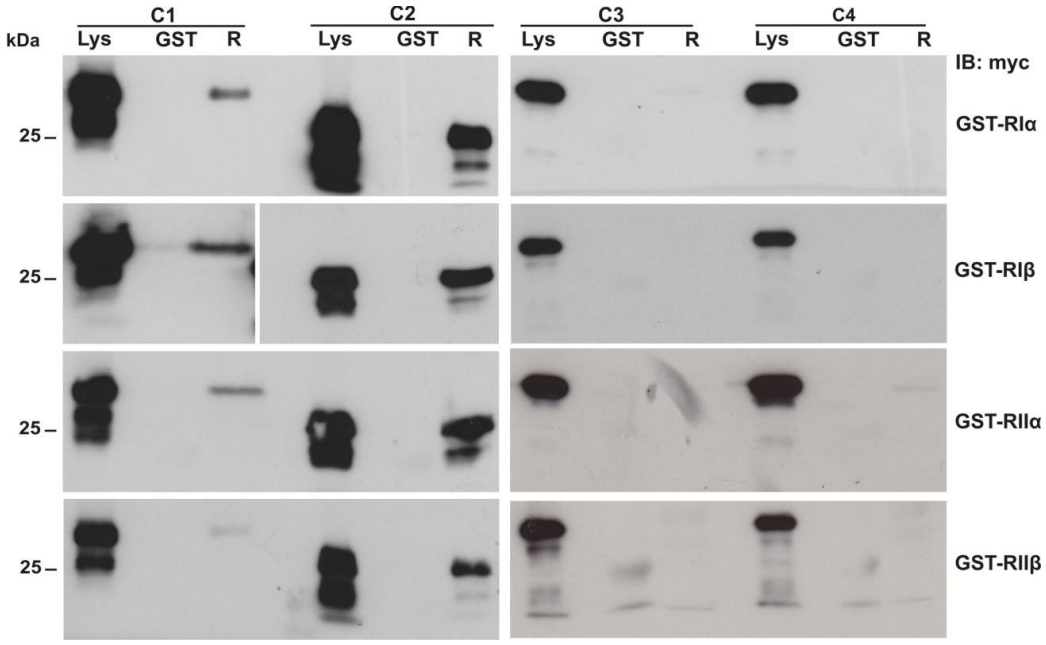

Figure 4.8: Binding motif of MYPT1 with PKA. 293T HEK cells were transfected with constructs allowing expression of Myc-tagged C-terminal fragments of MYPT1 (C1, C2, C3, C4) for 24 hrs at 37°C. After incubation cells were lysed in 1% Triton X-100 containing protease inhibitors. PKA regulatory subunits (RIα, RIβ, RIIα and RIIβ) were expressed as a GST fusions in *E. coli* XL-1 blue strain and purified by incubating the soluble fraction with 25 µl of pre-equilibrated glutathione sepharose beads slurry for 1 hr at 4°C with gentle agitation. After purification, HEK cells lysates were added to the beads for 2 hrs at 4°C under rotary shaking. Samples were resolved by 10% SDS-PAGE and immunoblotted with anti-Myc antibody overnight at 4°C. Next day the peroxidase conjugated secondary antibody was used, followed by ECL detection. Shown blots are representative of two independent experiments. IB: immunoblot, Lys: lysate, R: regulatory subunit.

4.4.4. Narrowing down the MYPT1 region interacting with PKA

To further narrow down the binding motif of PKA on MYPT1, the C2 fragment of MYPT1 was divided into five smaller fragments. Some of these fragments are with and others are the without central insert (CI) region of MYPT1. We hypothesise that the CI could either be a potential binding motif for PKA or at least potentiate the interaction of MYPT1 with PKA regulatory subunits. As shown in figure 4.9A the fragments are designated as C2N, CI, C2NCI, C2C and CIC2C according to their location. C2N contains N-terminal residues aa501-551 just before the CI region starts, the CI includes central insert residues aa552-608, C2C has C-terminal residues aa609-706 just after the CI, C2NCI contains N-terminal and CI residues aa501-608, and CIC2C comprises the CI and C-terminal residues aa552-706 respectively.

Recombinant C2 subfragments were subcloned in a GST vector (pGEX) as in section 2.3 and transformed in *E.coli* XL-1blue strain. After expression as in section 2.7.1.3 and lysis, pellet and supernatant fractions were separated by centrifugation and resolved on SDS-PAGE along with total lysates before and after induction. Coomassie staining showed bands of the expected sizes in induced samples and these bands are recovered in the supernatant samples (Figure 4.9B). Additionally, bacterial supernatants were purified by incubating with pre-equilibrated glutathione sepharose beads slurry, resolved on SDS-PAGE and analysed by Coomassie staining to check the integrity of the expressed proteins. Figure 4.9C illustrates that most of the proteins were degraded very heavily even in the presence of high concentrations of proteases and phosphatases inhibitors. Therefore, I was not able to use them for pull-down experiments to narrow down the interaction.

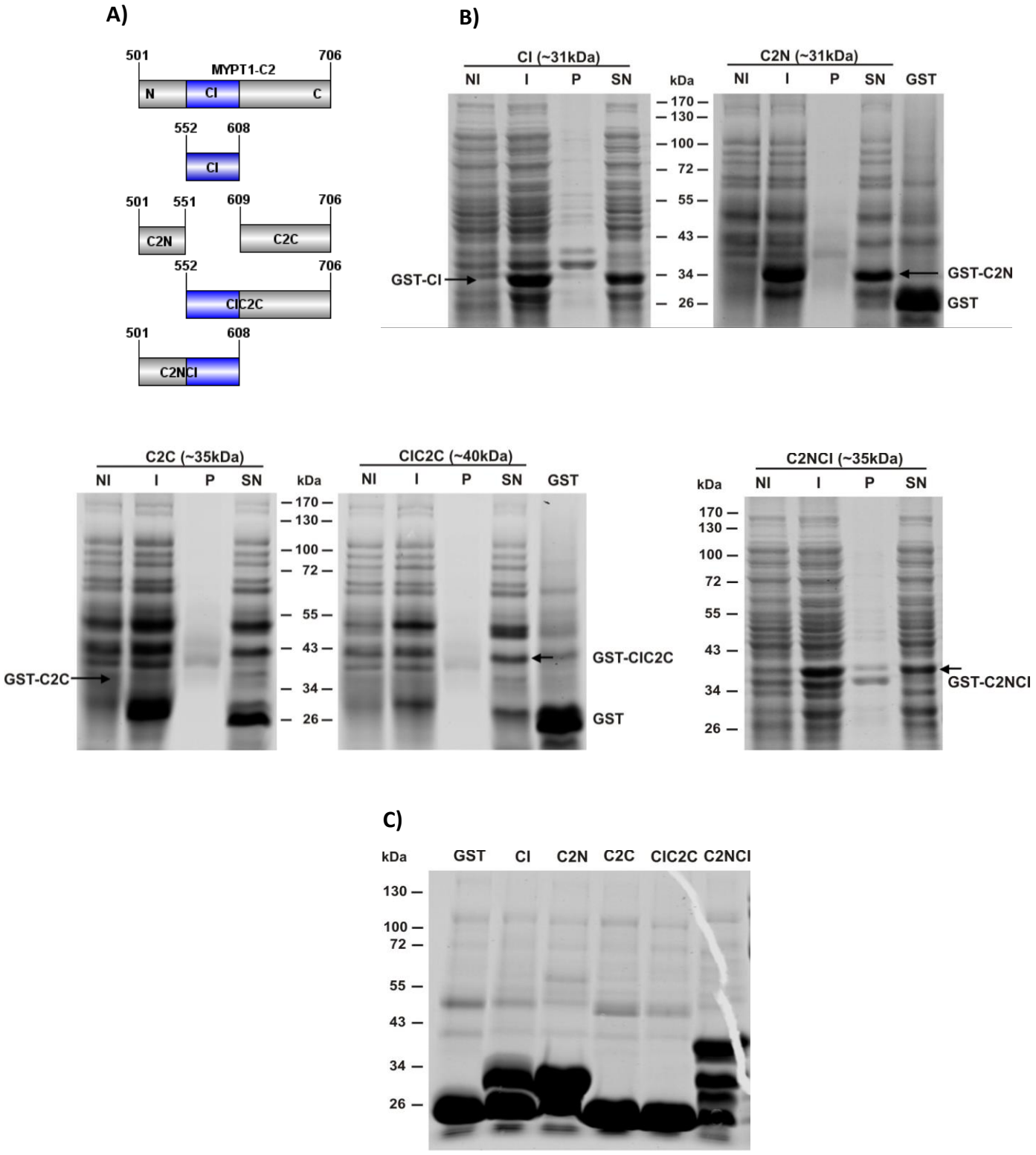
A)
501
706
MYPT1-C2
N
CI
C
552
608
CI
501
551
609
706
C2N
C2C
552
706
CIC2C
501
608
C2NCI
B)
CI (~31kDa)
NI
I
P
SN
kDa
170
130
100
72
55
43
34
26
GST-CI
C2N (~31kDa)
NI
I
P
SN
GST
GST-C2N
GST
C2C (~35kDa)
NI
I
P
SN
kDa
GST-C2C
CIC2C (~40kDa)
NI
I
P
SN
GST
GST-CIC2C
GST
C2NCI (~35kDa)
kDa
NI
I
P
SN
GST-C2NCI
C)
kDa
GST
CI
C2N
C2C
CIC2C
C2NCI
130
100
72
55
43
34
26

Figure 4.9: Constructs of C2 subfragments of MYPT1. **A)** Schematic diagram of MYPT1-C2 subfragments that were expressed as GST fusion in *E.coli* XL-1blue. B**)** Protein expression was induced with 0.5 mM IPTG for 2 hrs at 37°C in XL-1blue strain before lysed by sonication. Pellet (P) and supernatant (SN) samples as well as bacterial lysates before (NI) and after (I) induction were prepared, resolved by 10% SDS PAGE and stained with Coomassie-Brilliant-Blue. **C)** Bacterial supernatants (400 µl) were incubated with pre-equilibrated glutathione sepharose beads slurry (25 µl) for 1 hr at 4 with gentle shaking. After purification samples were washed, eluted, resolved by 10% SDS-PAGE and stained with Coomassie-Brilliant-Blue. NI: non-induced, I: induced, P: pellet, SN: supernatant. Data from one independent experiment.

4.5. Does MYPT1 interact directly with PKA?

Having established that all four PKA regulatory subunits interact with the C2 fragment of MYPT1, we next wanted to explore whether this interaction is direct or mediated by any AKAP and other interacting proteins. Our previous approaches (Co-IP, pull-down assays) cannot discriminate between direct and indirect protein-protein interaction because we used whole cell lysates where binding maybe indirect and mediated by an unknown protein. Therefore, the valid approach would be to express our respective proteins in a suitable expression system and then purify them to homogeneity. We preferred using a bacterial expression system, which is cheaper and less cumbersome than using mammalian or other systems. We expressed both MYPT1-C2 and PKA regulatory subunits in *E.coli*, purified and subjected them to binding experiments. If an interaction with purified proteins is seen, it can be concluded that the interaction is direct.

4.5.1. Expression and purification of MYPT1-C2 fragment.

Recombinant MYPT1-C2 fragment was subcloned in a His vector (pQE32), transformed in XL-1blue strain of *E.coli* and protein expression was induced for two hrs at 37°C or overnight at 20°C with 0.5 mM IPTG as in section 2.7.1.4. After lysis, pellet and supernatant fractions were separated by centrifugation and resolved by SDS-PAGE. Coomassie blue staining revealed that there was no visible protein expression in XL-1 blue strain (Figure 4.10A). Then, we tried Rosetta 2 and Rosetta-gami strains of *E.coli* and followed similar expression procedures as above. Figure 4.10B illustrates that there was visible protein expression in these two strains; however, the expression was leaky with much of the protein in pellet fractions in both strains. This leaky expression was further tested by western blot. Aliquots of non-induced, induced, pellet and supernatant samples of both Rosetta 2 and Rosetta-gami strains were resolved along with a negative control (a bacterial supernatant of PKA RIIβ) and affinity purified His-MYPT1-C2 samples on SDS-PAGE and immunoblotted with anti-His antibody. Figure 4.10C shows that anti-His antibody detected a band at the expected molecular weight in non-induced

samples, confirming that the expression was leaky. No signal was observed in GST PKA RIIβ that was used as negative control. Note that this blot also shows that considerable amount of protein is present in soluble fractions of both bacterial strains so we attempted to purify the recombinant proteins by incubating soluble fractions with nickel charged agarose beads (Ni-NTA agarose beads) as in section 2.7.1.4. Coomassie staining shows that the Ni-NTA agarose beads moderately pulled down His-MYPT1-C2 fragments; however, many additional bacterial proteins were pulled down too even after stringently washing with increased concentration of salt and imidazole (Figure 4.10C). As we were not able to efficiently purify His-MYPT1-C2 fragment, we decided to change the expression system.

We subcloned the MYPT1-C2 fragment in a GST vector (pGEX) as in section 2.3, transformed in XL-1 blue (section 2.4) and a quick protein expression test was carried out (section 2.7.1.3). Transformants were induced with IPTG for 2 hrs at 37°C followed by lysis by sonication and centrifugation to separate soluble and insoluble fractions. Then total lysates before and after induction along with the samples of soluble and insoluble fractions were resolved by SDS-PAGE. The protein expression was evaluated by Coomassie staining, which showed a band of the expected size after induction and this band is recovered in the soluble fraction confirming protein solubility (Figure 4.10D). In addition, GST tagged MYPT1-C2 fragment was purified with glutathione sepharose beads and evaluated by Coomassie staining. The SDS-PAGE showed efficient purification with minimum contaminants (Figure 4.10D). In view of these results we decided to go ahead with the GST fusion of MYPT1-C2.

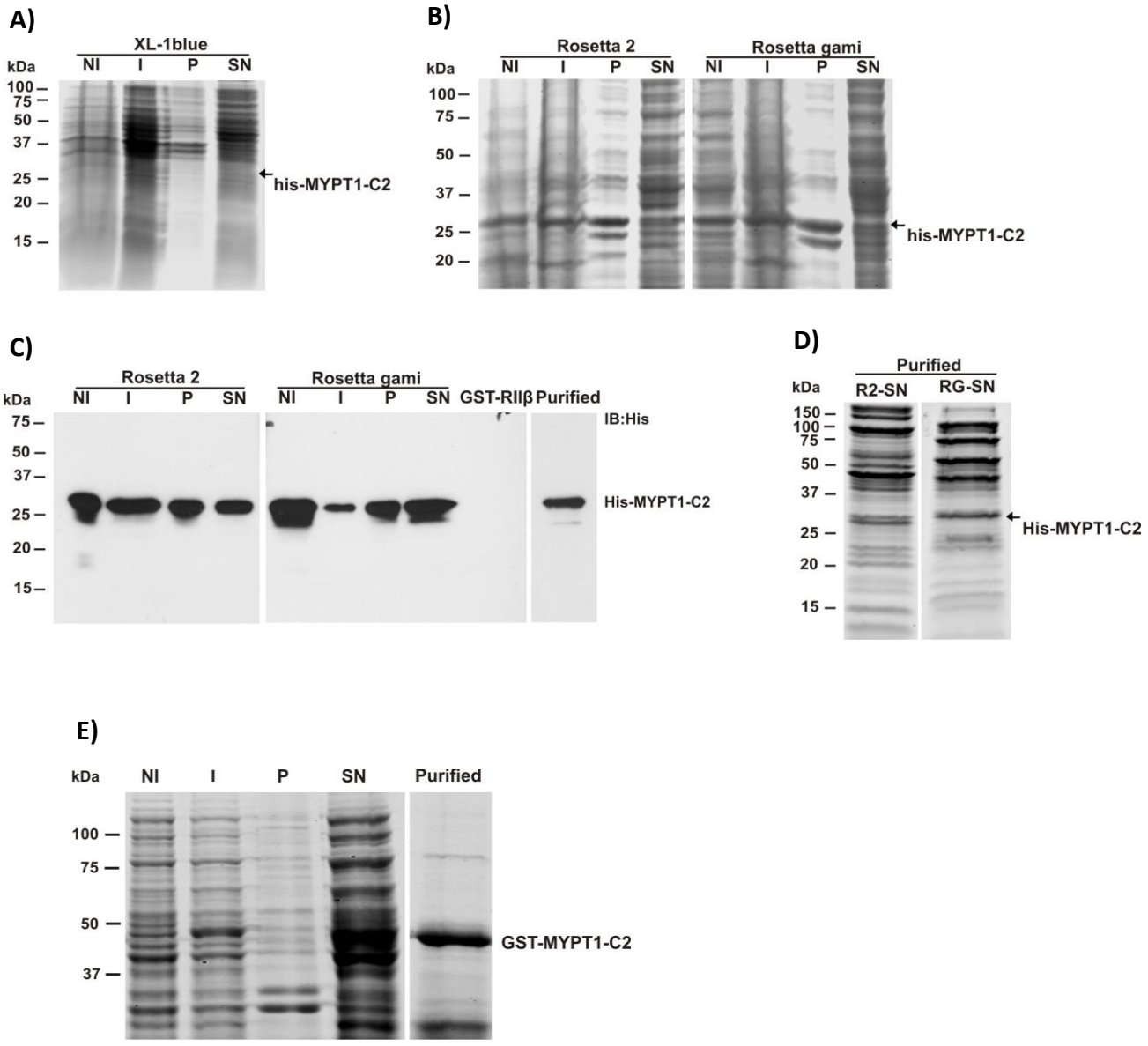

Figure 4.10: Expression and purification of MYPT1-C2 (aa501-706) fragment.

A & B) The MYPT1-C2 fragment was expressed as His fusion protein in *E.coli* XL-1blue, Rosetta 2 and Rosetta-gami strains. Bacterial cells were lysed and soluble and insoluble fractions were separated by centrifugation. Total lysates before and after induction along with samples of soluble and insoluble fractions were resolved by 10% SDS PAGE and stained with Coomassie-Brilliant-Blue. **C)** Bacterial samples of non-induced, induced, pellet and supernatant of Rosetta 2 and Rosetta-gami strains along with GST-PKA RIIβ (negative control) and purified His-MYPT1-C2 fragment were resolved by SDS-PAGE and immunoblotted with anti-His antibody. **D)** Bacterial supernatants of His-MYPT1-C2 fragment of both Rosetta 2 and Rosetta-gami were incubated with 25 µl Ni-NTA agarose

for 1hr at 4°C with gentle shaking. After purification samples were resolved by 10% SDS-PAGE and stained with Coomassie-Brilliant-Blue. **E)**. GST-MYPT1-C2 fragment was expressed in *E.coli* XL-1blue. Cells were lysed and soluble and insoluble fractions were separated. Total lysates before and after induction and aliquots of soluble and insoluble fractions along with affinity purified GST-MYPT1-C2 fragments were resolved by 10% SDS-PAGE and stained with Coomassie-Brilliant-Blue. NI: non-induced, I: induced, P: pellet, SN: supernatant. Data from one independent experiment.

4.5.2. Expression and purification of PKA regulatory subunits RIβ and RIIβ.

As all four PKA regulatory subunits interact with MYPT1, we selected one each from PKA type I and type II isoforms, more specifically PKA RIβ and RIIβ, for the direct binding experiments. PKA RIβ and RIIβ inserts were retrieved from pEGFP-C2 plasmid, subcloned in a His vector (pQE32) and a quick protein expression test (2 hrs at 37°C) was carried out in four different strains of *E.coli*, namely XL-1blue, M15 (pREP4), Rosetta 2 and Rosetta-gami as in section 2.7.1.4.

As shown in figure 4.11A only XL-1blue and M15 (pREP4) strains were able to express PKA RIβ and RIIβ, whereas no visible protein expression was observed in Rosetta 2 and Rosetta-gami strains. Next, solubility of both recombinant PKA RIβ and RIIβ was tested. We selected XL-1blue strain for solubility test as the expression of both recombinant proteins was comparable to the expression in M15 (pREP4) strain. Bacterial cells were lysed via sonication and centrifuged to separate soluble and insoluble fractions. Aliquots of total lysates before and after induction along with samples of the soluble and insoluble fractions were then resolved by SDS-PAGE and stained with Coomassie-Brilliant-Blue. Figure 4.11B reveals that most of the recombinant PKA RIβ and RIIβ are present in the soluble fraction at the expected molecular weight, whereas part of the protein, especially PKA RIIβ is also present in the insoluble fraction. Furthermore, His-PKA RIβ and RIIβ were purified by incubating with Ni-NTA agarose beads for 1 hr at 4°C with gentle agitation. After washing, protein was eluted from beads, resolved on SDS-PAGE and stained with Coomassie-Brilliant-Blue. The SDS-PAGE shows that the His-PKA RIβ was efficiently purified with least contaminants, whereas PKA RIIβ was moderately purified with some contaminants (Figure 4.11C).

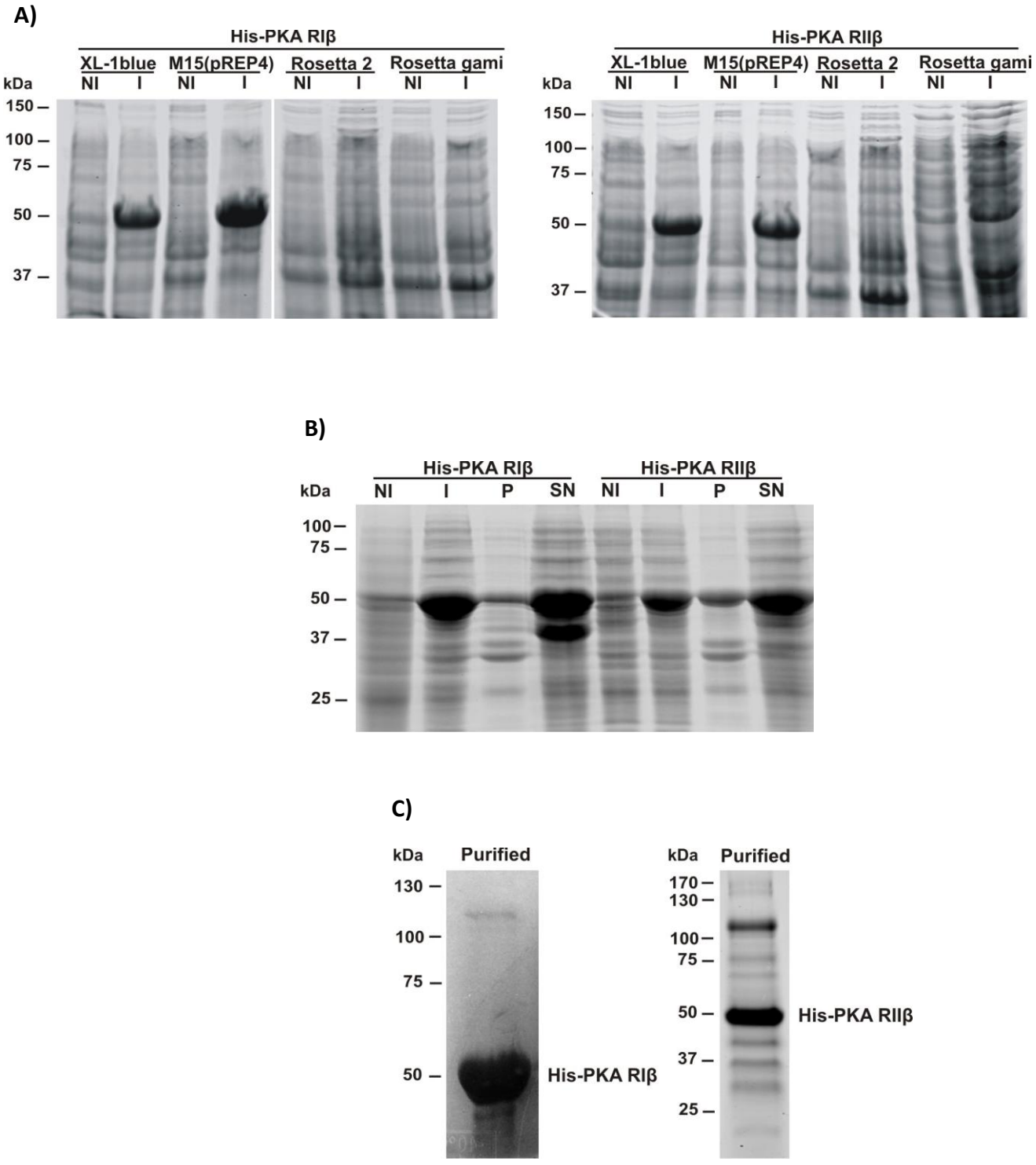

Figure 4.11: Expression and purification of PKA RIβ and RIIβ. PKA RIβ and RIIβ were expressed as His-tagged protein in *E.coli* XL-1blue, M15 (pREP4), Rosetta 2 and Rosetta-gami strains. **A)** Bacterial cells were lysed before and after induction in Laemmli buffer; samples were then resolved by 10% SDS PAGE and stained with Coomassie-Brilliant-Blue. **B)** Bacteria were lysed by sonication and then centrifuged to separate soluble and insoluble fractions. Total lysates before

and after induction along with samples of soluble and insoluble fractions were resolved by 10% SDS-PAGE and stained with Coomassie-Brilliant-Blue. **C)** Bacterial supernatants of PKA RIβ and RIIβ subunits were incubated with 25 µl Ni-NTA agarose beads for 1 hr at 4°C with gentle agitation. After purification, samples were resolved by 10% SDS-PAGE and stained with Coomassie-Brilliant-Blue. NI: non-induced, I: induced, P: pellet, SN: supernatant. Data from one experiment.

4.5.3. MYPT1-C2 (aa501-706) and PKA directly interact *in vitro* in GST pull-down assay

Having established the expression and solubility of GST-MYPT1-C2 and His-PKA RIβ and RIIβ subunits, we next wanted to examine the interaction of MYPT1-C2 with PKA regulatory subunits using a GST pull-down assay. Recombinant GST-MYPT-C2 fragment was immobilised on glutathione sepharose beads and incubated with the bacterial supernatants of His-tagged PKA regulatory subunits (PKA RIβ and RIIβ) for 1 hr at 4°C with gentle shaking. After washing, protein complexes were eluted from the beads by boiling in Laemmli buffer resolved on SDS-PAGE and analysed by western blot. Figure 4.12 shows that both PKA regulatory subunits were pulled-down by GST-MYPT1-C2 fragment, whereas no association was observed with GST only. Coomassie staining was used as a control to show the presence of the GST and the GST-MYPT1-C2 fragment. This experiment demonstrates that MYPT1 and PKA are potentially interacting directly, although there is still a possibility that a bacterial protein bridges the interaction, as we used bacterial supernatants of His-PKA RIβ and RIIβ instead of using purified proteins.

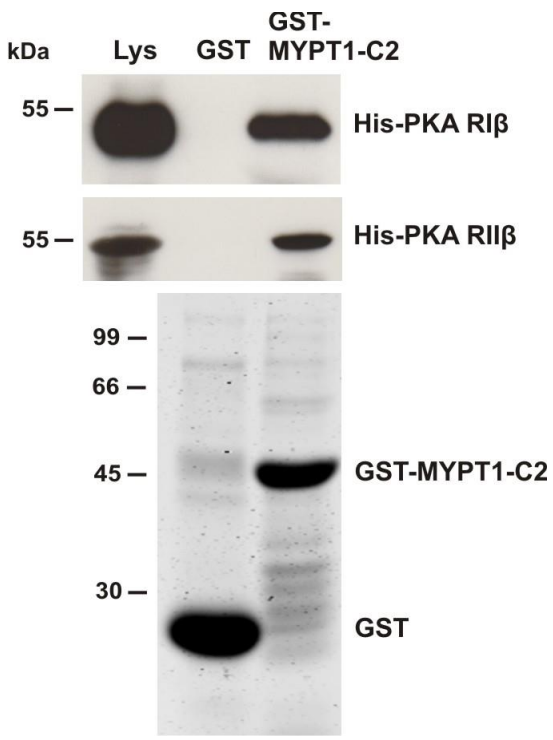

Figure 4.12: Direct interaction of MYPT1 with PKA in GST pull-down assay. GST-MYPT1-C2 was purified from 500 µl of bacterial supernatant by incubation with 25 µl of pre-equilibrated glutathione sepharose beads slurry for 1 hr at 4°C with gentle agitation. Glutathione beads were then washed and incubated with 400 µl of supernatants of PKA regulatory subunits (RIβ and RIIβ) for 1 hr at 4°C. After washing, protein complexes were eluted by boiling in Laemmli buffer, resolved by 10% SDS-PAGE and immunoblotted with anti-His antibody. One gel was stained with Coomassie-Brilliant-Blue as a control. Shown blots are representative of three independent experiments.

4.6. Is MYPT1 an AKAP?

As described in more detail in section 1.4, AKAPs are a special group of proteins that tether PKA to distinct intracellular locations (Pidoux and Taskén, 2010). These proteins directly interact with the D/D domain of PKA regulatory subunits and then spatially and temporally restrict the activity of PKA (Raslan *et al*., 2015a). Having confirmed that the C2 fragment of MYPT1 directly interacts with the PKA regulatory subunits (Figure 4.12) and not via any of the predicted amphipathic helices (Figure 4.7 & 4.8), we next sought to investigate whether this direction interaction takes place with the D/D domain of PKA regulatory subunits. To this end we adopted two different pull-down approaches, using synthetic AKAP disruptor peptide (Ht31) and deletion mutants of the D/D domain of PKA regulatory subunits.

Ht31 is a non-specific AKAP disruptor peptide, which is able to uncouple the anchoring of both PKA type I and type II to AKAPs (Stokka *et al*., 2006). The concentration of Ht31 used in this experiment was selected based on previous studies (Raslan *et al*., 2015). To begin with, the functional sensitivity of Ht31 was tested via platelet aggregometry. Washed platelets ($2.5x10^8$/ml) were subjected to a platelet aggregation assay as in section 2.6.2. Platelets treated with thrombin (0.1 U/ml) showed maximum aggregation response, which was completely reversed by pretreatment with PGI_2 (100 nM). Pre-incubating platelets with Ht31 (2 µM) resulted in a substantial reversal of PGI_2 induced inhibition of platelet aggregation, suggesting that the disruptor peptide is functionally active (Figure 4.13A).

We next tested Ht31 in GST pull-down assays by using recombinant GST-MYPT1-C2 fragment and His-PKA RIβ and RIIβ proteins. Pull-down experiments were performed as in section 4.5.3 with the only difference that His-PKA RIβ and RIIβ were pretreated with 2 µM Ht31 disruptor peptide for 30 min at room temperature. Figure 4.13B illustrates that Ht31 did not disrupt the interaction of

MYPT1-C2 with both PKA RIβ and RIIβ proteins, suggesting that MYPT1 does not interact with PKA in an AKAP manner. GST only was used as a negative control.

This was further confirmed by using truncated versions of PKA RIβ and RIIβ proteins. Two truncated proteins of PKA RIβ and RIIβ were designed, N-terminus D/D domain and D/D deletion (ΔD/D) of PKA regulatory subunits as shown in figure 4.5. N-terminus D/D domain of PKA RIβ comprised amino acid 1-70 and ΔD/D comprised amino acid 71-381. PKA RIIβ D/D domain comprised amino acids 1-50 and ΔD/D aa51-418. Both truncated proteins of PKA RIβ and RIIβ were subcloned in His-tagged pQE32 vector, expressed in *E.coli* XL-1blue strain and protein expression was tested via Coomassie staining as in section 2.7.1.4. Truncated D/D domains fragments of both PKA RIβ and RIIβ did not express visibly (not shown), whereas expression and solubility of ΔD/D were good (Figure 4.13C). Next pull-down assays were performed as in section 4.5.3 by using GST-MYPT1-C2 fragment and His tagged ΔD/D of PKA RIβ and RIIβ.

In Figure 4.13D it was observed that MYPT1-C2 is able to pull down both ΔD/D PKA RIβ and PKA RIIβ, suggesting that the DD domain of PKA regulatory subunits is not required for the interaction with MYPT1. No association was detected with GST only. All together the data presented here shows that MYPT1 does not require D/D domain of PKA regulatory subunit for interaction, clearly indicating that MYPT1 does not follow the mechanism of interaction characteristic of AKAPs.

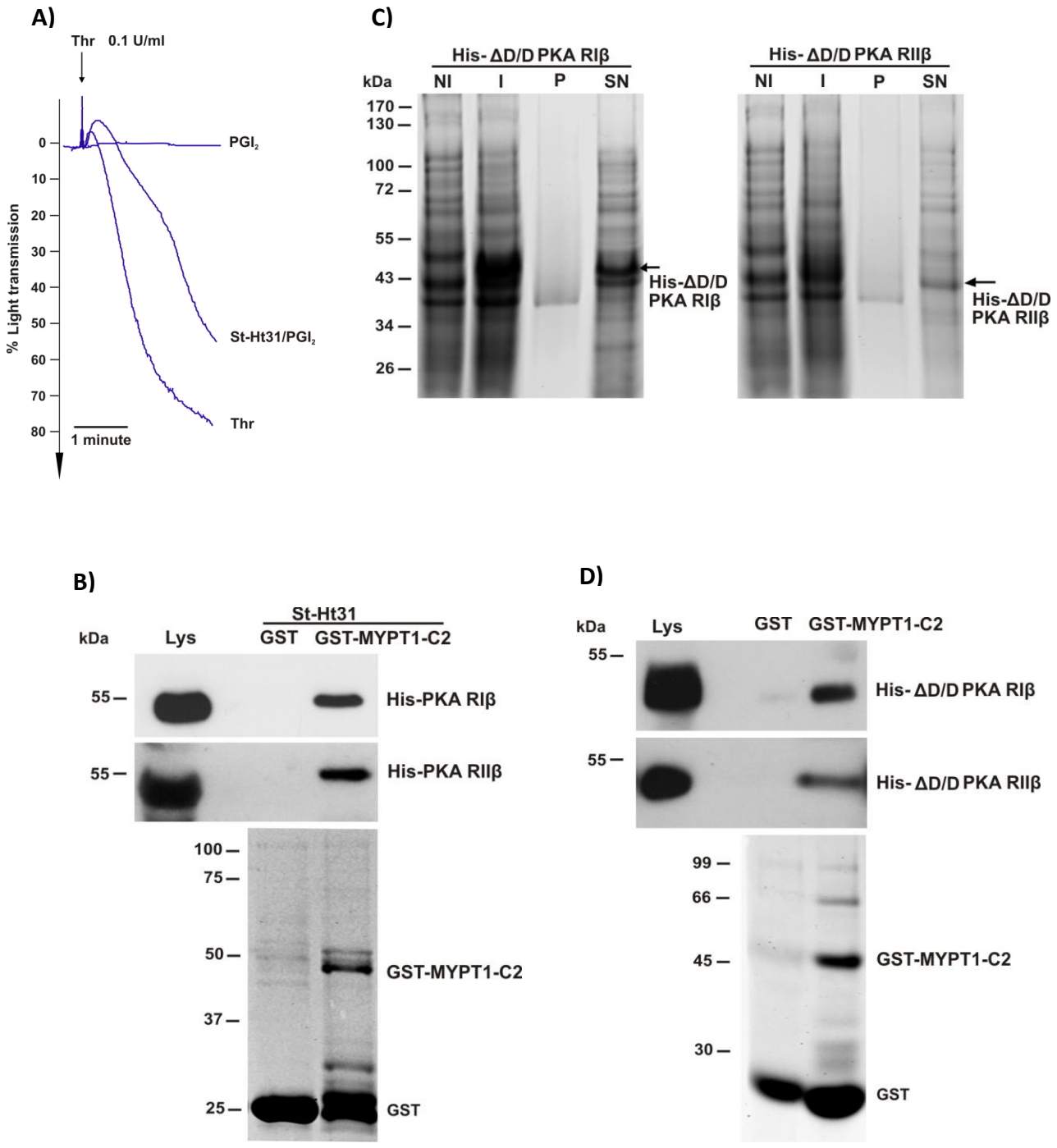

4.13: Interaction of MYPT1 with PKA regulatory subunits in GST pull-down assay.

A) Washed platelets ($2.5x10^8$/ml) were stimulated with thrombin (0.1U/ml) or preincubated with Ht31 (2µM) for 30 min at 37°C. Platelets were then treated with PGI_2 (100 nM) for 1 min before activation with thrombin (0.1U/ml). Aggregation traces were recorded for 4 min under stirring (1000 rpm) using a Chrono-log dual channel light transmission aggregometer. Traces were generated by Aggro/Link computer software. **B)** GST-MYPT1-C2 was purified from 500 µl of

bacterial supernatant by incubation with 25 µl of pre-equilibrated glutathione sepharose beads for 1 hr at 4°C with gentle agitation. Supernatants of PKA RIβ and RIIβ were preincubated with Ht31 (2 µM) for 20 min at room temperature. GST-MYPT1-C2-beads were then added and incubated for 1 hr at 4°C. Samples were resolved by 10% SDS-PAGE and immunoblotted with anti-His antibody. **C)** Bacterial cells were lysed by sonication and then centrifuged to separate soluble and insoluble fractions. Total lysates before and after induction along with samples of soluble and insoluble fractions were resolved by 10% SDS-PAGE and stained with Coomassie-Brilliant-Blue. **D)** GST-MYPT1-C2 was purified from 500 µl of bacterial supernatant by incubation with 25 µl of pre-equilibrated glutathione sepharose beads for 1 hr at 4°C with gentle agitation. Glutathione beads were then washed and incubated with 400 µl of supernatants of ΔD/DPKA RIβ and RIIβ for 1 hr at 4°C. Samples were resolved by 10% SDS-PAGE and immunoblotted with anti-His antibody. Gels stained with Coomassie-Brilliant-Blue were used as control. Shown data are representative of two independent experiments.

4.7. Discussion

cAMP-dependent PKA is a serine/threonine kinase that propagates cAMP signalling events by phosphorylating a number of downstream substrate proteins including MYPT1, RapIb, IP_3R, Gα13, PDE3A, VASP, GPIbβ, MLCK and possibly many more (Wooldridge *et al*., 2004; Smolenski, 2012; Schwarz *et al*., 2001). Upon phosphorylation these substrate proteins regulate many cellular processes such as calcium mobilisation, cytoskeleton remodelling, integrin activation, degranulation, expression of surface molecules and G-proteins inhibition (Schwarz *et al*., 2001). In platelets, the list of potential PKA substrate is continuously growing (Beck *et al*., 2014); however, only a handful of substrates have been studied in detail (Smolenski, 2012). There are two types of PKA that are differentially distributed. PKA type I is chiefly located in membrane fractions, whereas PKA type II is cytosolic (Raslan *et al*., 2015a). This distinct subcellular distribution of PKA is regulated through the interaction with anchoring proteins (AKAPs) that contribute to the specificity of PKA signalling. These anchoring proteins not only tether PKA to particular subcellular locations but also scaffold many other proteins, like phosphatases and phosphodiesterases, thus forming a local signalling node (Pidoux and Taskén, 2010). Similar to AKAPs, MYPT1, a known PKA substrate, anchors many proteins in addition to PP1c, M20 and myosin including PP2B, 14-3-3β, M-RIP, ILK, ZIP kinase and PKG. Furthermore, MYPT1 also provides a stage for protein-protein interactions. Mahavadi *et al.* (2014) showed that PKG facilitates M-RIP phosphorylation via anchoring with MYPT1. While this protein-protein interaction of MYPT1 with PKG has been well documented by many researchers (Lee *et al*., 2007; Given *et al*., 2007; Huang *et al*., 2004; Surks *et al*., 1999), the association of MYPT1 with PKA has not been investigated before.

In this chapter we present evidence how MYPT1 interacts with PKA and addressed whether this interaction is in an AKAP fashion. Towards this purpose, we first evaluated the specificity and selectivity of the commercial PKA regulatory and catalytic subunits antibodies by utilising GST fusion proteins (Figure 4.1).

As both PKA RIα and RIβ are closely related, sharing over 85% amino acid sequence similarity (Taylor *et al*., 2012), it was necessary to confirm the absolute specificity of their respective antibodies. Western blot confirmed that PKA RIα antibody is not absolutely specific as it recognised both PKA RIα and RIβ with the same intensity, whereas PKA RIb antibody was not able to pick signal in their respective lysate, suggesting that the antibody do not react with the target protein (Figure 4.1A).

Thus on the basis of this experiment we used only PKA RIα antibody throughout this study for the detection of both RIα and RIβ isoforms. On the other hand, PKA RIIα and RIIβ antibodies were quite specific, did not cross-react with each other and with other PKA isoforms. Both RIIα and RIIβ antibodies detected bands only in their respective lysates even though these two subunits also share similar amino acid sequence (Taylor *et al*., 2012) (Figure 4.1A).

The next important step before investigating the interaction of MYPT1 with PKA was to confirm the expression of all four PKA regulatory subunits, catalytic subunits and MYPT1 in platelets. Western blot shows that all PKA regulatory subunits, catalytic subunits and MYPT1 proteins are present in platelets (Figure 4.1C & D). This is in line with proteomic and transcriptomic studies carried out by many researchers in platelet biology (Burkhart *et al*., 2012; Rowley *et al*., 2011). While assessing the specificity of commercial antibodies we noticed that PKA catα antibody was always detecting a doublet in platelet lysates (Figure 4.1D). Initially we thought that the higher molecular weight band is an additional band, which is non-specifically recognised by PKA catα antibody; however, using purified GST-tagged PKA catβ protein confirmed that the antibody is indeed detecting both PKA cat α and β isoforms in platelets. As both are closely related, sharing 93% amino acid sequence similarity (Cadd & McKnight, 1989), the chance of cross-reactivity is high, which is also mentioned by the manufacturer.

More than a decade ago MYPT1 was reported as a PKA substrate in smooth muscle cells (Wooldridge *et al*., 2004); however, it has not been shown how PKA interacts

with MYPT1 and regulates acto-myosin based contractile machinery via modulating MLCP activity. In this chapter we have revealed for the first time that MYPT1 and all PKA regulatory subunits are present in a same complex in platelets (Figure 4.2). This finding was further supported by cAMP pull-down and GST pull-down assays (Figure 4.3 & 4.4). However, at this stage we did not know whether this association of MYPT1 with PKA regulatory subunits is direct or mediated for example by any AKAP protein. Also these *in vitro* findings do not tell us the functional significance of this interaction, probably keeping the contractile machinery of platelets in quiescent state.

On the basis of our biochemical data we initially hypothesised that MYPT1 could be an AKAP and interact with PKA in an AKAP manner. As the hallmark signature motif of the AKAPs is a 14-18 amino acid long amphipathic helix (Carr *et al*., 1991), we started our investigation by analysing the protein sequence of MYPT1 for the presence of potential amphipathic helices. Our computational studies revealed that there are at least two possible regions that may potentially contribute in the formation of amphipathic helices. One is at the N-terminal (aa267-285) and second at the end of C-terminal of MYPT1 (aa986-1004) (Figure 4.6). On the basis of these findings we initially generated two truncated versions of MYPT1 protein that cover these two bioinformatically predicated amphipathic helixes. Our pull-down result in HEK cells show that only the C-terminal fragment of MYPT1 is involved in the interaction with PKA possibly via C-terminal amphipathic helix (Figure 4.7).

GST pull-down experiments with a set of overlapping fragments covering the C-terminal MYPT1 fragment confirmed that the proposed C-terminal amphipathic helix of MYPT1 is not involved in the interaction with PKA. These experiments allowed to narrow-down the binding motif of MYPT1 with PKA regulatory subunits to a 200 amino acid long fragment designated as C2 (aa501-708). This C2 fragment of MYPT1 associates with all four PKA regulatory subunits (Figure 4.8). However, at this stage we couldn't rule out that MYPT1 is not an AKAP as there are some AKAPs, for example pericentrin, a centrosomal anchoring protein, that lack

amphipathic helical structure but still interact with the D/D domain of PKA (Diviani *et al*., 2000). After these pull-down experiments we moved our focus toward the C2 fragment of MYPT1. Note that this fragment harbours the central insert region of MYPT1 protein. Recent studies in smooth muscle cells have shown that the central insert region modulates PKG mediated phosphorylation of MYPT1. The rate of the phosphorylation of MYPT1 by PKG was much lower in central insert deficient splice variant as compared to the full length MYPT1 (Yuen *et al*., 2014). Furthermore, Kim *et al.* (2012) have reported that the central insert region may potentiate the binding of MYPT1 N-terminus with the protein phosphatase, as in a central insert depleted splice variant the binding of MYPT1 with the protein phosphatase was significantly reduced in endothelial cells. We hypothesise that the central insert may be involved in the interaction with PKA and may possibly affect the MLCP activity via potentiating the phosphorylation of MYPT1 at Ser695. Direct involvement of the central insert is in question as if it is directly interacting with the PKA then we would only be able to pull-down one splice variant via GST pull-down (Figure 4.3) and cAMP pull-down assays from platelets lysate (shown in chapter 3, Figure 3.5B). So to explore the role of the central insert in the interaction with PKA, we subdivided the C2 fragment into five fragments. Some of them were lacking the central insert (Figure 4.9A). However, due to instability of expressed proteins we were not able to confirm the involvement of the central insert in this binding study (Figure 4.9). A summary of our mapping studies is illustrated as in Figure 4.14.

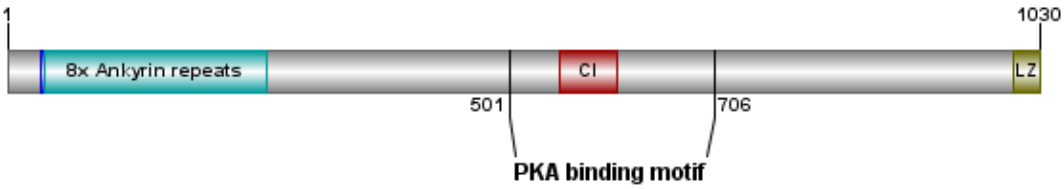

Structure	Amino acids	Association with PKA
	1-1030	***
	1-330	
	331-1030	***
	327-531	*
	501-706	***
	676-881	
	825-1030	

Figure 4.14: Summary of MYPT1 association with PKA regulatory subunits. MYPT1 is 1030 amino acids long. GST pull-down experiments have shown that the region comprising amino acids 501-706 are responsible for the interaction with all four PKA regulatory subunits. Weak interaction of PKA was shown with amino acids 327-531.

It is not ideal to study protein-protein interaction using mammalian cell lines because of the presence of other binding partners, which may possibly interfere or mediate the interaction of our proteins of interest. Thus to rule out any mammalian proteins interference, we expressed both the MYPT1-C2 fragment and PKA regulatory subunits in *E.coli* strains, purified them via affinity chromatography and subjected them to pull-down experiments (Figure 4.10 and 4.11). Figure 4.12 confirms that MYPT1 is potentially interacting directly with PKA regulatory subunits. Accumulating evidence suggests that cAMP signalling via PKA phosphorylates MYPT1 at Ser695 and results in increased endothelial barrier integrity both *in vivo* and *in vitro* (Batori *et al*., 2016, 2017; Kasa *et al*., 2015; Aslam

et al., 2010). Hyper-reactivity of platelets has also been reported in defective cAMP-dependent PKA signalling (Smolenski, 2012). Furthermore, malfunctioning of PKA-MYPT1 proteins has been linked to various disease conditions, such as acute lung injury (Kasa *et al*., 2015), coronary heart diseases (Yu *et al*., 2014), hypertension, asthma, inflammation and diabetes (Eto *et al*., 2009). We believe that the direct interaction of MYPT1 with PKA may possible play an important role in protecting platelets from hyper-reactive state, a state where they are responsible for thrombogenic disorder. Furthermore, our results also rule out the possibility of any AKAP protein involvement in the interaction of MYPT1 with PKA.

Similar to the centrosomal protein, pericentrin, while does not require an amphipathic helix for binding with the D/D domain of PKA, we also wanted to examine whether this is the case with MYPT1 interacting with the D/D domain of PKA regulatory subunit, a characteristic binding motif for AKAP proteins. This will confirm whether MYPT1 is a pericentrin-like AKAP or a substrate that interacts with PKA in an AKAP independent manner. To achieve this, we first used a well-established approach that relies on a synthetic peptide Ht31, which disrupts the interaction of PKA-AKAP by competing with AKAPs for the binding with the D/D domain of PKA (Calejo & Taskén, 2015). This peptide has been used extensively in order to determine the functional relevance of PKA-AKAP interaction in different cellular functions, such as regulation of ion channels (Fraser & Scott, 1999), arrest of sperm motility (Vijayaraghavan *et al*., 1997), hormone-mediated secretion of insulin (Lester *et al*., 1997) and the transcription factor CREB phosphorylation (Feliciello *et al*., 1997).

Figure 4.13B reveals that the Ht31 peptide did not disrupt the interaction of MYPT1-C2 fragment with PKA regulatory subunits, suggesting that MYPT1 is possibly not interacting with the D/D domain of PKA. However, it would be worth testing Ht31 inhibition experiment with the full length MYPT1 construct in case that the C2 fragment has some conformation constraints. Furthermore, this Ht31 disruptor peptide data cannot provide absolute assurance that the D/D domain is

not involved in the interaction due to absence of a positive control in our results. Hence we prepared PKA regulatory subunit constructs lacking the D/D domain as approached by Lin *et al.* (2013) (Figure 4.5). GST pull-down assays confirmed that MYPT1 still interacts with the D/D depleted PKA regulatory subunits, indicating that the D/D domain of PKA is not critically required for this interaction (Figure 4.13D). However, MYPT1 may bind to the D/D domain in addition to the rest of PKA regulatory subunit, but we were not able to rule out that the D/D domain is not involved. Together this data reveals that neither AKAP disruptor peptide Ht31 nor deletion of the D/D domain of PKA abolished the interaction of MYPT1 with PKA regulator subunits, hence validating that MYPT1 interaction with PKA is not in AKAP fashion and MYPT1 does not qualifying as a genuine AKAP.

Conclusion

In summary the data presented in this chapter demonstrate that MYPT1 and PKA are part of the same complex in platelets under non-activatory conditions. We successfully mapped the interaction of MYPT1 with all four PKA regulatory subunits to a 200 amino acids long fragment (MYPT1-C2) in the centre of the MYPT1. Our findings have also shown for the first time that MYPT1 interacts with PKA directly and this direct interaction does not require either an amphipathic helix of MYPT1 or the D/D domain of PKA regulatory subunits, confirming that MYPT1 does not interact with PKA in an AKAP manner.

Chapter 5: Subcellular distribution of PKA and MYPT1 proteins in blood platelets

5.1. Introduction

In platelets there are four genetically distinct and functionally non-redundant PKA regulatory subunit isoforms (RIα, RIβ, RIIα and RIIβ (Burkhart *et al*., 2012). These PKA isoforms interact and phosphorylate numerous target substrate proteins, including MYPT1 and thus protect platelets from a hyper-reactive state. In previous chapters, we have shown that MYPT1 is a target of cAMP/PKA signalling in human platelets. We have also shown that MYPT1 associates with all four PKA regulatory subunits in human platelets. However, the subcellular localisation and the relative contribution of each PKA isoform and MYPT1 to the regulation of distinct platelet functions are not clearly understood. Recent immunofluorescence and fractionation studies have shown that PKA type I is primarily located in the membrane fraction, whereas type II is in the cytosolic compartment (Raslan *et al*., 2015a) in resting platelets. This differential distribution of PKA supports the notion of distinct cAMP/PKA compartments, with PKA possibly regulating a distinct function in a particular compartment at a specific time. However, Raslan *et al.* (2015a) were not able to dissect the subcellular distribution of individual PKA isoforms of type I and type II in platelets. On the other hand, Burgers and co-workers (2012) have examined the subcellular distribution of individual PKA isoforms in HeLa cells. They reported that PKA RIα and RIβ strongly localised at the plasma membrane, whereas RIIα and RIIβ were mainly cytosolic. Both of these studies suggest that PKA RI isoforms are not always in the cytosol as initially proposed (Feliciello *et al*., 2000; Corbin *et al*., 1977).

In various cell types including smooth muscle cells, epithelial cells and fibroblasts MYPT1 has been reported throughout the cell including plasma membrane, cytosol and nucleus (Murata *et al.,* 1997; Inagaki *et al*., 1997). Fukata and co-workers (1998) have shown that MYPT1 is markedly concentrated at membrane

ruffling areas and cell-cell junctions in tetradecanoylphorbol-13-acetate (TPA) treated Madin-Darby Canine Kidney (MDCK) epithelial cells. In freshly isolated ferret portal vein, MYPT1 was distributed throughout the cell cytoplasm; however, upon stimulation with PGF2α, MYPT1 translocated to the plasma membrane (Shin *et al*., 2002). This agonist-dependent translocation of MYPT1 was further explored by Lontay *et al.* (2005) and Neppl *et al.* (2009) using HepG2 cells and an intact cerebral vasculature. They have shown that at resting state MYPT1 is uniformly distributed throughout the cell including the nucleus and upon treatment with okadaic acid and the TXA_2 analogue U46619 the plasma membrane localisation of MYPT1 was markedly increased. They also confirmed their immunostaining data with a cell fractionation approach, where agonist stimulation caused a profound accumulation of MYPT1 in the membrane fraction.

Very little is known about the precise subcellular localisation of MYPT1 in platelets. Muranyi and co-workers (1998) have reported for the first time that MYPT1 is predominantly found in the detergent insoluble actin cytoskeleton and membrane fractions and relatively very little in the soluble fractions of resting platelets. Later, Kiss and colleagues (2002) have shown a similar distribution pattern of MYPT1 in platelets under basal conditions. However, none of these studies have used image-based techniques to investigate the precise subcellular localisation of MYPT1 in platelets. If we aim to understand PKA and MYPT1 function in a physiological context then the rigorous characterisation of the subcellular localisation of these proteins is the step that needs to be explored. Thus the lack of information on the subcellular localisation of individual PKA regulatory subunits and MYPT1 in platelets prompted us to investigate this aspect.

The aims of this chapter are:

- Characterise the localisation of MYPT1 and PKA isoforms in resting platelets.

- Study the effect of fibrinogen matrix on the localisation of MYPT1 and PKA isoforms in platelets.
- Investigate the co-localisation of MYPT1 and PKA isoforms in resting and spread platelets.

5.2. Subcellular localisation of MYPT1 in resting platelets.

In order to examine the subcellular localisation of MYPT1 protein in resting platelets, we first prepared washed platelets in the presence or absence of indomethacin and apyrase to block the effect of secondary signalling events, fixed them in suspension with 4% PFA and spun them down onto poly-L-lysine coated glass coverslips. Platelets were then permeabilised with Triton X-100 and immunostained with anti-MYPT1 mouse monoclonal and rabbit polyclonal antibodies followed by species-specific Alexa fluor conjugated secondary antibodies. The cells were then counterstained with FITC-phalloidin to visualise F-actin. Fluorescently labelled secondary antibodies alone were used as negative control to test the non-specific binding.

It was observed that both rabbit polyclonal and mouse monoclonal antibodies effectively stain MYPT1 in resting platelets (Figure 5.1). In the presence of indomethacin and apyrase, the staining of MYPT1 by both mouse monoclonal and rabbit polyclonal antibodies was very clear and followed a similar labelling pattern, punctate staining in the cell cytoplasm with some co-localisation with F-actin in the cell cortex (Figure 5.1A).

On the other hand, in the absence of indomethacin and apyrase treatment, MYPT1 staining with anti-MYPT1 mouse monoclonal antibody is preferentially in the cell periphery, co-localised with cortical F-actin, whereas with anti-MYPT1 rabbit polyclonal antibody the staining was throughout the cell cytoplasm including cell periphery, suggesting that either the rabbit polyclonal antibody sensitivity is high or it is detecting non-specifically additional proteins (Figure 5.1B).

Both *in-vitro* binding and immunofluorescence data suggest that MYPT1 strongly associates with myosin IIa (Hartshorne *et al*., 1998; Johnson *et al*., 1997; Hirano *et al*., 1997; Inagaki *et al*., 1997). These studies are consistent with our immunostaining data, which confirms that MYPT1 strongly co-localises with

myosin IIa in resting platelets (Figure 5.1C). In platelets pretreated with indomethacin and apyrase, the labelling of myosin IIa was distributed throughout the cell including some cortical localisation with F-actin (Figure 5.1C, lower panel).

A)

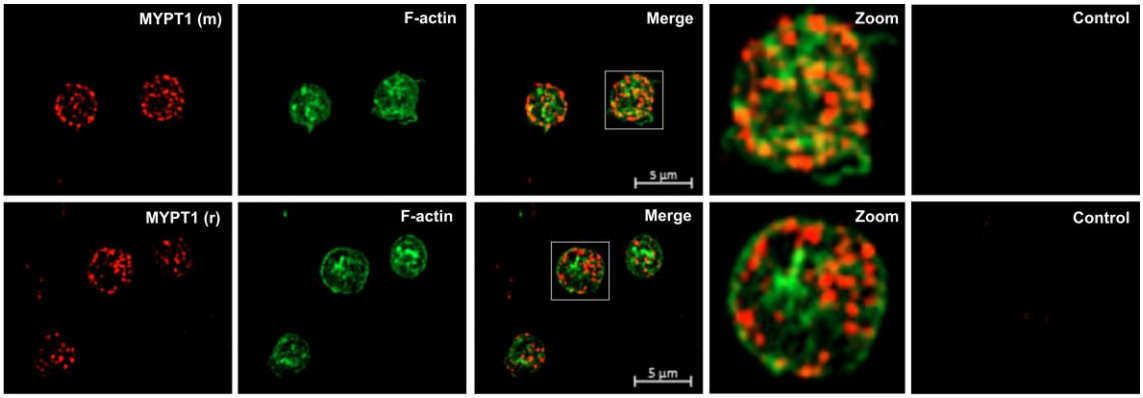
MYPT1 (m)
F-actin
Merge
Zoom
Control
5 µm
MYPT1 (r)
F-actin
Merge
Zoom
Control
5 µm

B)

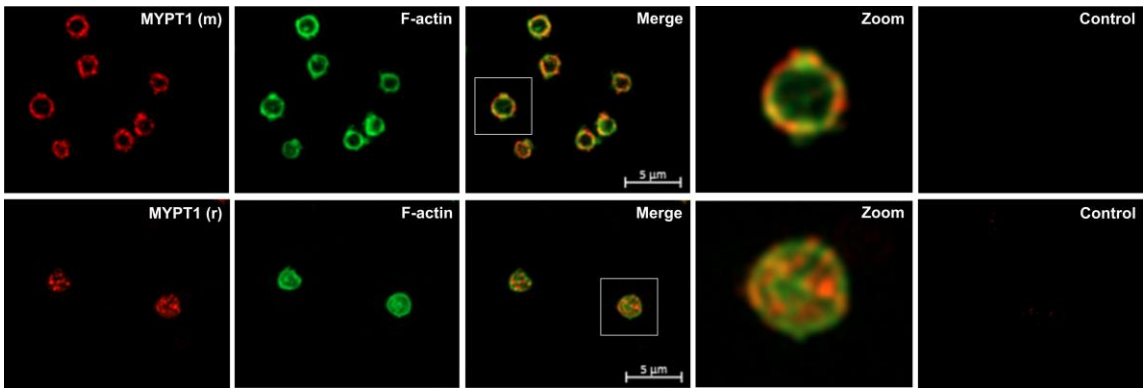
MYPT1 (m)
F-actin
Merge
Zoom
Control
5 µm
MYPT1 (r)
F-actin
Merge
Zoom
Control
5 µm

C)

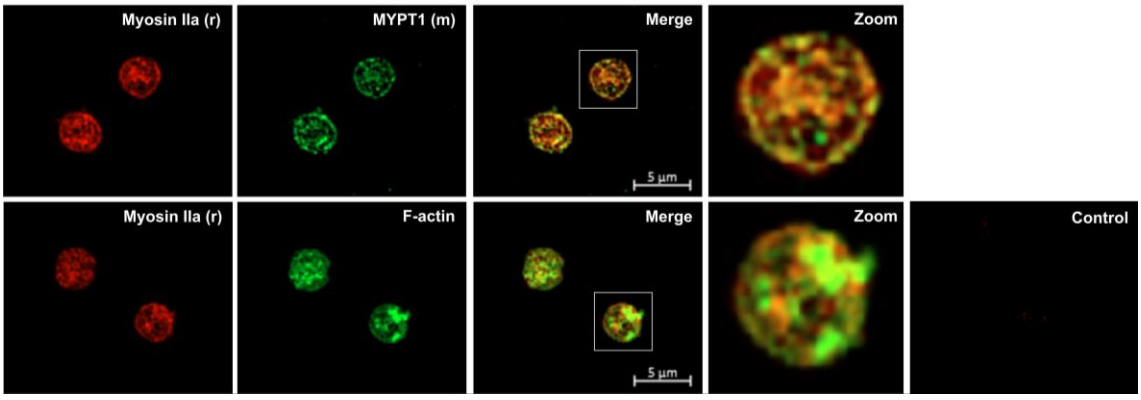
Myosin IIa (r)
MYPT1 (m)
Merge
Zoom
5 µm
Myosin IIa (r)
F-actin
Merge
Zoom
Control
5 µm

Figure 5.1: Subcellular distribution of MYPT1 protein in resting platelets. Human washed platelets ($5x10^6$/ml) were prepared in the presence **(A & C)** or absence **(B)** of indomethacin (10 µM) and apyrase (2 U/ml) and fixed in suspension with 4% PFA before being spun down for 10 min at 250xg on poly-L-lysine coated glass coverslips. Platelets were then washed, permeabilised with 0.3% Triton X-100 for 5 min and incubated with anti-MYPT1 mouse monoclonal, rabbit polyclonal or anti-myosin IIa rabbit polyclonal antibodies for 1 hr at room temperature. This was followed by species-specific fluorescently labelled Alexa fluor568 (red) conjugated secondary antibody for 1 hr and counterstained with FITC-Phalloidin (1 µg/ml) (green) for 20 min at room temperature. The coverslips were then mounted on glass slides using gelvatol and images were taken via Zeiss ApoTome.2 fluorescence microscope equipped with a 100x oil immersion objective. Secondary antibody alone was used as a negative control. Representative images are central Z-slices from Z stacks. Z-slices were taken at 0.15 µm intervals through the platelet. All images were deconvolved and underwent contrast enhancement to remove background fluorescence. Shown images are representative of at least three independent experiments. The white inset in the merge image has been zoomed in the adjacent panel. Scale bars are indicated.

5.3. Subcellular localisation of PKA regulatory subunits in resting platelets.

The functional diversity of PKA has been well documented in many cell types including platelets; however, neither the precise subcellular distribution of PKA regulatory subunit isoforms nor their physiological role within the distinct compartments, particularly in platelets, has been well explained. Thus we set out to characterise in detail the localisation of all four PKA regulatory subunit isoforms in relation to that of F-actin in human platelets under basal level using immunofluorescence techniques.

Human washed platelets were prepared in the presence or absence of indomethacin and apyrase, fixed and adhered to poly-L-lysine coated coverslips as mentioned in section 5.2. After permeabilisation platelets were immunostained with mouse monoclonal anti-PKA regulatory subunit antibodies, RI (m), RIIα (m), RIIβ (m) and counterstained with FITC-phalloidin for F-actin. In indomethacin and apyrase treated platelets, PKA RI (m) antibody, which stains both RIα and RIβ isoforms, was sporadically distributed throughout the cell, with strong accumulation at the cell periphery, consistent with the study conducted by Raslan and co-workers (2015a) (Figure 5.2A). On the other hand, PKA RIIα and RIIβ immunostaining patterns were very similar: punctate staining mainly in the cell cytoplasm; however, RIIβ staining was stronger and slightly diffused (Fig. 5.2A).

In the absence of indomethacin and apyrase, the immunostaining pattern of the PKA regulatory subunits was similar to that observed in the presence of those drugs (Figure 5.2B). This data clearly suggests that PKA RI accumulates mainly at the cell periphery, whereas PKA RIIα and RIIβ are more diffusely localised in the cytoplasm in human platelets.

A)

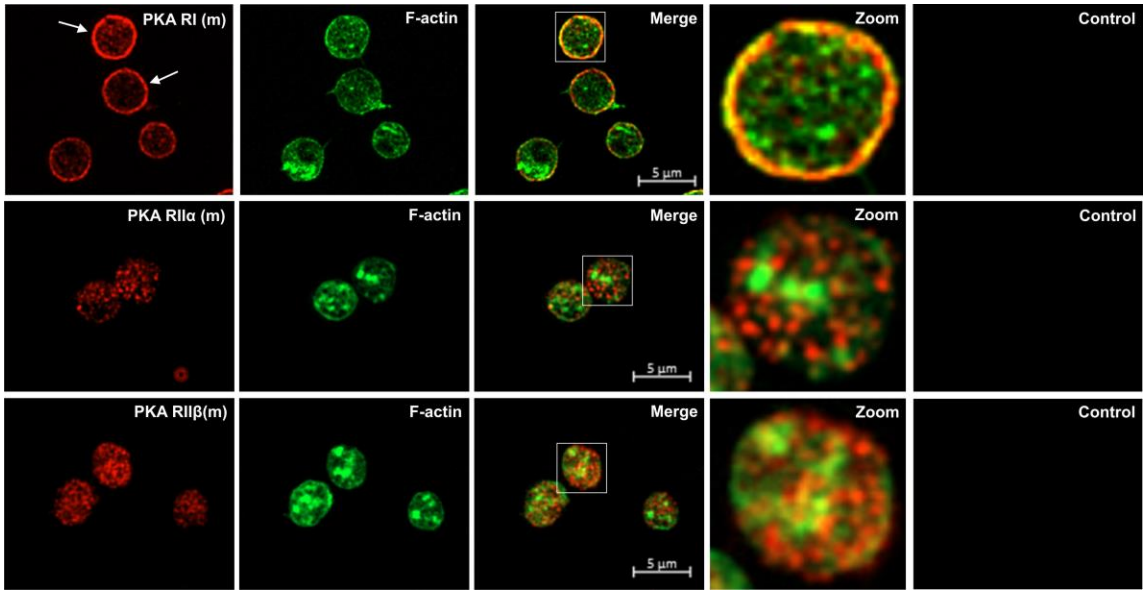
PKA RI (m)
F-actin
Merge
Zoom
Control
5 µm
PKA RIIα (m)
F-actin
Merge
Zoom
Control
5 µm
PKA RIIβ(m)
F-actin
Merge
Zoom
Control
5 µm

B)

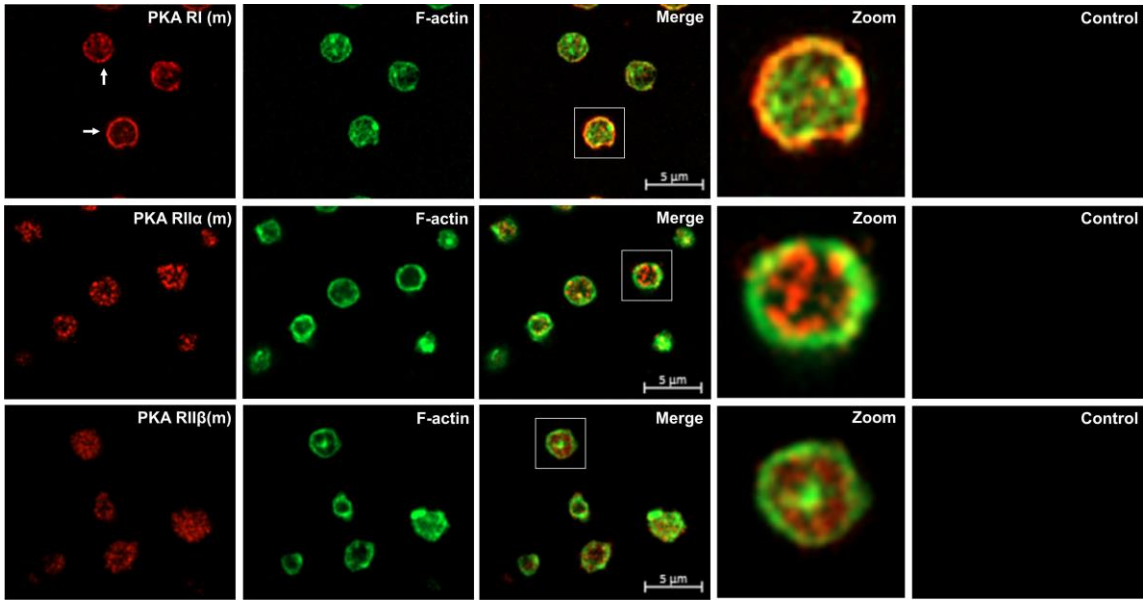
PKA RI (m)
F-actin
Merge
Zoom
Control
5 µm
PKA RIIα (m)
F-actin
Merge
Zoom
Control
5 µm
PKA RIIβ(m)
F-actin
Merge
Zoom
Control
5 µm

Figure 5.2: Subcellular distribution of PKA regulatory subunits in resting platelets. Human washed platelets ($5x10^6$/ml) were prepared in the presence **(A)** or absence **(B)** of indomethacin (10 μM) and apyrase (2 U/ml) as described in Figure 5.1. After permeabilisation with 0.3% Triton X-100 for 5 min, platelets were incubated with anti-PKA RI (m), RIIα (m) and RIIβ (m) antibodies for 1 hr at room temperature. This was followed by species-specific fluorescently labelled Alexa fluor568 (red) conjugated secondary antibody for 1 hr and counterstained with FITC-phalloidin (1 μg/ml) (green) for 20 min at room temperature. The coverslips were then mounted on glass slides using gelvatol and images were taken via Zeiss ApoTome.2 fluorescence microscope equipped with a 100x oil immersion objective. Secondary antibody alone was used as a negative control. Representative images are central Z-slices from Z stacks. Z-slices were taken at 0.15 μm intervals through the platelet. All images were deconvolved and underwent contrast enhancement to remove background fluorescence. Shown images are representative of at least three independent experiments. The white inset in the merge image has been zoomed in the adjacent panel. White arrows indicate circular accumulation of PKA RI at the cell periphery. Scale bars are indicated.

5.4. Co-localisation of MYPT1 and PKA regulatory subunits in resting platelets.

Having previously shown in chapter 4, section 4.3 that MYPT1 associates with all four PKA regulatory subunits in basal platelets; here we aimed to assess immunofluorescence-based association of MYPT1 with PKA regulatory subunits in resting platelets. In these set of experiments I was only able to use rabbit polyclonal MYPT1 antibody, as all the available PKA regulatory subunit antibodies in the laboratory were mouse monoclonal. This rabbit polyclonal MYPT1 antibody gives more punctate staining than the mouse monoclonal one.

Human washed platelets were prepared in the presence or absence of indomethacin and apyrase, fixed and adhered to poly-L-lysine coated coverslips as mentioned in section 5.2. After permeabilisation platelets were double immunostained with MYPT1 and PKA regulatory subunit antibodies before images were acquired with a fluorescence microscope. Both in the presence (A) or absence (B) of indomethacin and apyrase, MYPT1 did not entirely co-localise with the PKA regulatory subunits (Figure 5.3). Co-localisation of MYPT1 with PKA RI is mainly observed at the cell periphery, whereas with RIIα and RIIβ the association was mostly at the cytoplasm. A significant fraction of unbound MYPT1 and PKA is still present throughout the cytoplasm, suggesting that these proteins are not interacting only with each other but have a number of other binding partners.

A)

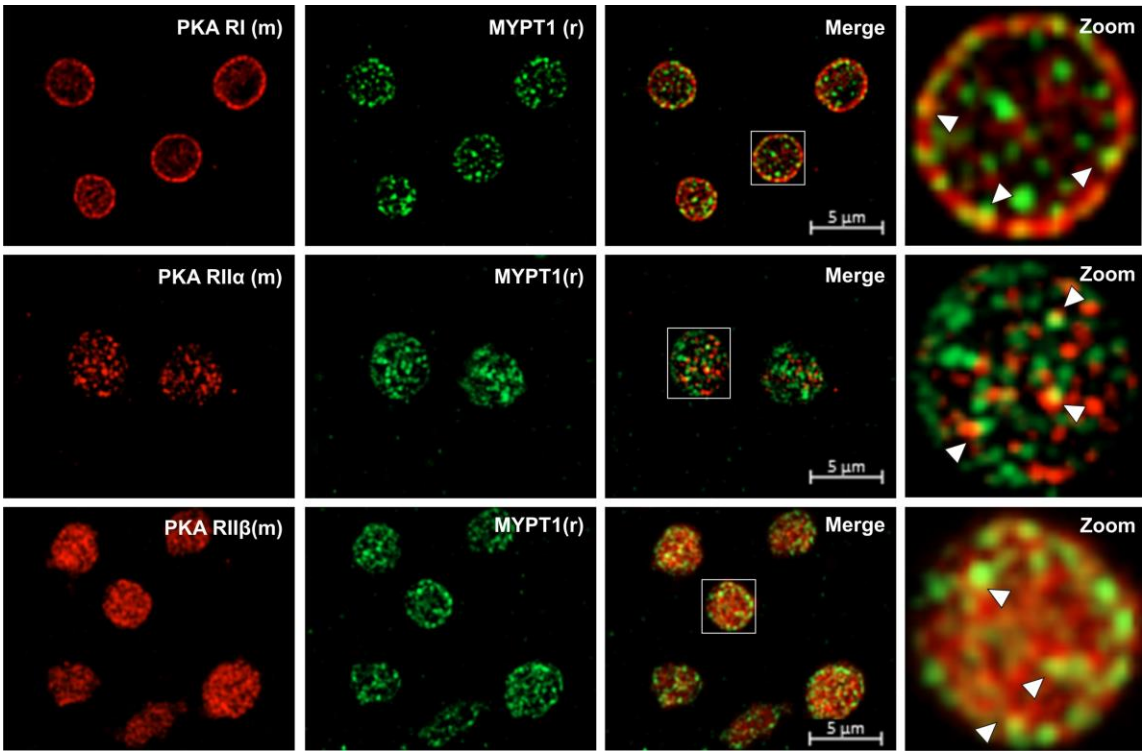
PKA RI (m)
MYPT1 (r)
Merge
Zoom
5 µm
PKA RIIα (m)
MYPT1(r)
Merge
Zoom
5 µm
PKA RIIβ(m)
MYPT1(r)
Merge
Zoom
5 µm

B)

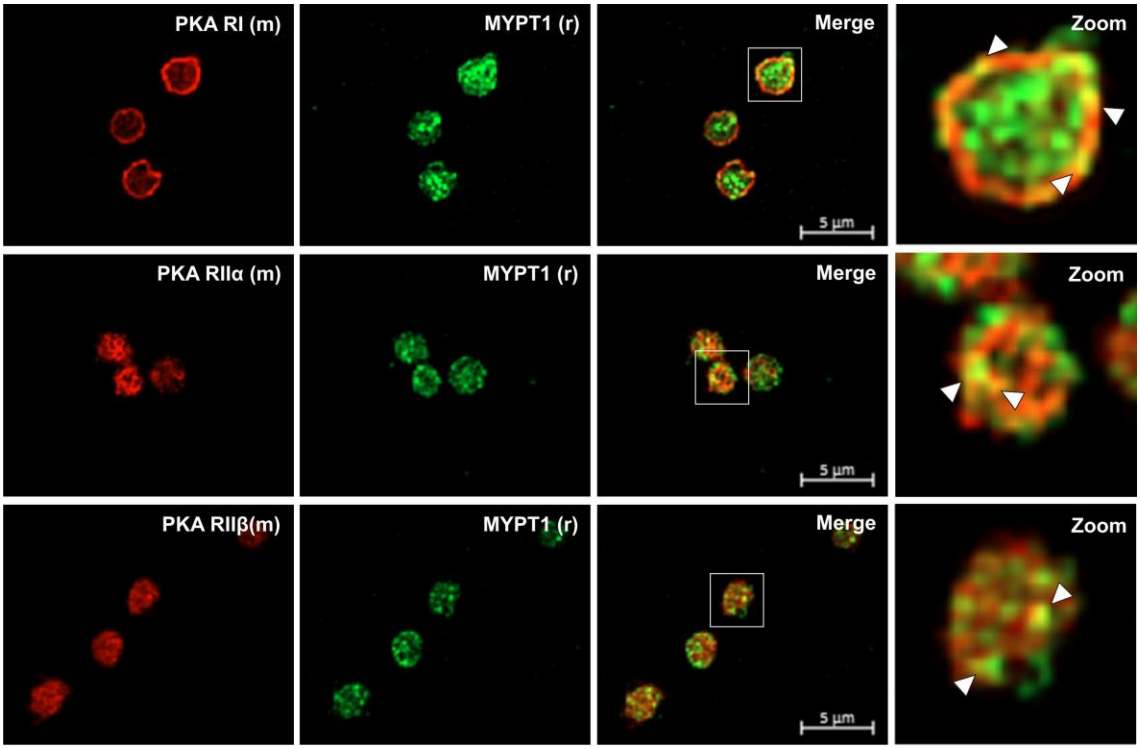
PKA RI (m)
MYPT1 (r)
Merge
Zoom
5 µm
PKA RIIα (m)
MYPT1 (r)
Merge
Zoom
5 µm
PKA RIIβ(m)
MYPT1 (r)
Merge
Zoom
5 µm

Figure 5.3: Co-localisation of MYPT1 with PKA regulatory subunits in resting platelets. Human washed platelets ($5x10^6$/ml) were prepared in the presence **(A)** or absence **(B)** of indomethacin (10 μM) and apyrase (2 U/ml) as described in Figure 5.1. After permeabilisation with 0.3% Triton X-100 for 5 min, platelets were doubled stained with anti-MYPT1 (r) and anti-PKA RI (m), RIIα (m) and RIIβ (m) antibodies for 1 hr at room temperature. This was followed by species-specific fluorescently labelled Alexa fluor568 (red) and Alexa fluor488 (green) conjugated secondary antibodies for 1 hr at room temperature. The coverslips were then mounted on glass slides using gelvatol and images were taken via Zeiss ApoTome.2 fluorescence microscope equipped with a 100x oil immersion objective. Representative images are central Z-slices from Z stack. Z-slices were taken at 0.15 μm intervals through the platelet. All images were deconvolved and underwent contrast enhancement to remove background fluorescence. Shown images are representative of at least three independent experiments. The white inset in the merge image has been zoomed in the adjacent panel. White arrow-heads indicate co-localisation of two proteins. Scale bars are indicated.

5.5. Subcellular localisation of MYPT1 in spread platelets.

Having explored the distribution of MYPT1 in resting platelets, we next wanted to investigate whether the localisation of MYPT1 remains the same or changes in activated platelets spread on a fibrinogen matrix.

In order to visualise MYPT1 distribution, human washed platelets were spread on fibrinogen-coated coverslips for 45 min at 37°C, fixed with 4% PFA and permeabilised with 0.3% Triton X-100. After permeabilisation platelets were immunostained with anti-MYPT1 mouse monoclonal or rabbit polyclonal antibodies followed by fluorescently labelled secondary antibodies. Cells were then counterstained with FITC-phalloidin to visualise F-actin. Fluorescently labelled secondary antibodies alone were used as negative controls. Immunofluorescence microscopy revealed that both antibodies efficiently stained MYPT1 in spread platelets. As compared to resting platelets, MYPT1 staining in spread platelets is more pronounced and concentrated in the cell centre at around the granulomere area. Some co-localisation with actin is also observed at stress fibres due possibly to the association of MYPT1 with myosin (Murata *et al*., 1997) and some with peripheral cortical actin (Figure 5.4). In spread platelets myosin IIa strongly co-localises with stress fibres. However, its association with MYPT1 was less conspicuous (Figure 5.4, last two lower panels).

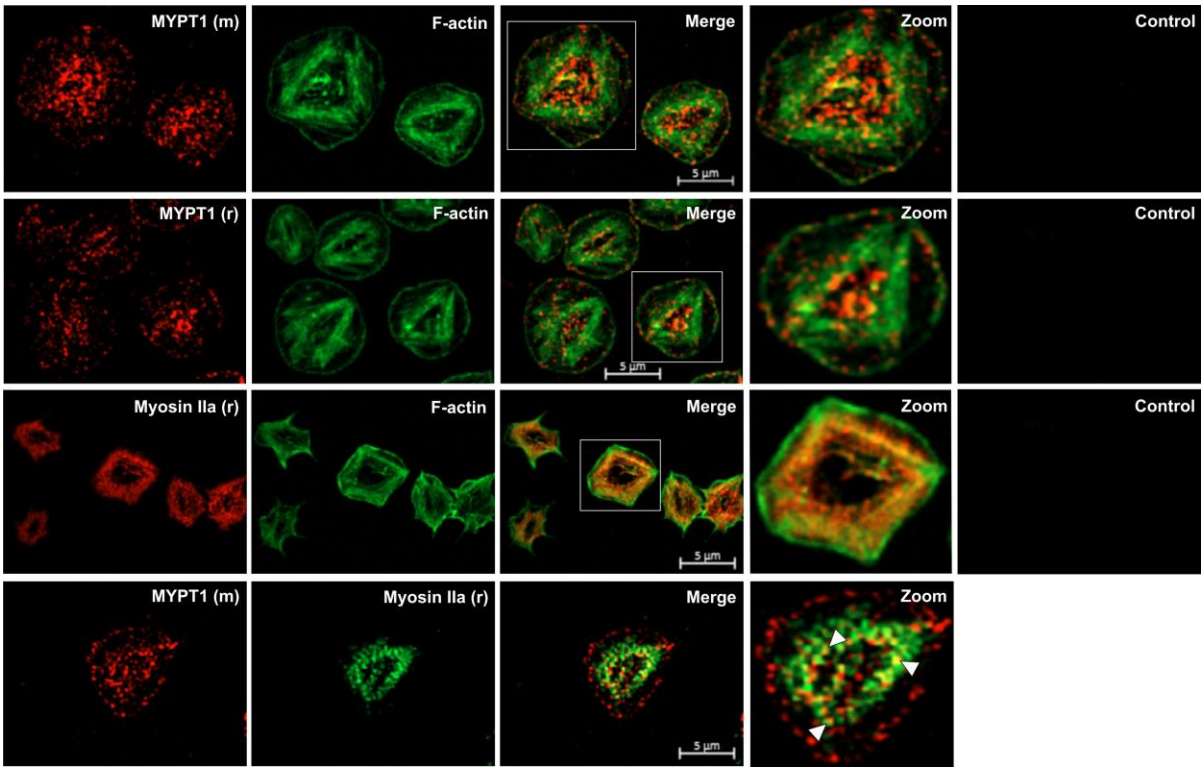

Figure 5.4: Subcellular distribution of MYPT1 protein in platelets spread on fibrinogen. Human washed platelets ($1x10^7$/ml) were incubated on fibrinogen (100 µg/ml) coated cover slips for 45 min at 37°C, fixed with 4 % PFA and permeabilised with 0.3% Triton X-100. Platelets were then stained with anti-MYPT1 mouse monoclonal, rabbit polyclonal and anti-myosin IIa rabbit polyclonal antibodies for 1 hr at room temperature. This was followed by species-specific fluorescently labelled Alexa fluor568 (Red) conjugated secondary antibody for 1 hr at room temperature and counterstained with FITC-phalloidin (1 µg/ml) for 20 min to visualise F-actin. The cover slips were then mounted on glass slides using gelvatol and images were taken via Zeiss ApoTome.2 fluorescence microscope equipped with a 100x oil immersion objective. Fluorescently labelled secondary antibody alone was used as a negative control. Representative images are central Z-slices from Z stack. Z-slices were taken at 0.15 µm intervals through the platelet. All images were deconvolved and underwent contrast enhancement to remove background fluorescence. Shown images are representative of at least three independent experiments. The white inset in the merge image has been zoomed in the adjacent panel. White arrow-heads indicate co-localisation of two proteins. Scale bars are indicated.

5.6. Subcellular localisation of PKA regulatory subunits in spread platelets.

The aim of this experiment was to study the localisation of PKA regulatory subunit isoforms in activated platelets.

To begin with, human washed platelets were spread on fibrinogen coated cover slips for 45 min, fixed with 4% PFA and permeabilised with 0.3% Triton X-100 for 5 min at room temperature. Cells were then stained with anti-PKA regulatory subunit antibodies RI (m), RIIα (m), RIIβ (m) followed by counterstaining with FITC-phalloidin to visualise F-actin. It was observed that PKA RI (m), which stains both RIα and RIβ isoforms, was very distinct, diffuse throughout the cell with strong circular shaped labelling at the cell centre at around the granulomere area (Figure 5.5).

On the other hand, PKA RIIα staining is punctate and diffuse throughout the cell cytoplasm with some peripheral co-localisation with cortical actin, whereas PKA RIIβ staining is also detected throughout the cell cytoplasm as of PKA RIIα but was very strong in certain locations, such as the cell centre and the cell cortex. This result shows that each of PKA regulatory subunits followed a unique localisation pattern in spread platelets.

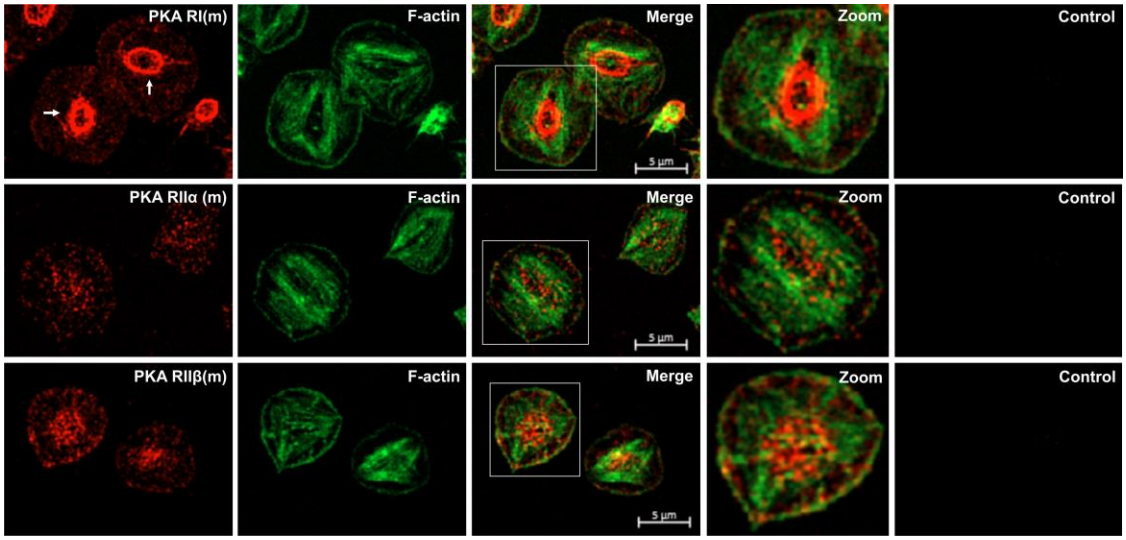

Figure 5.5: Subcellular distribution of PKA regulatory subunits in platelets spread on fibrinogen. Human washed platelets ($1x10^7$/ml) were incubated on fibrinogen (100 µg/ml) coated cover slips for 45 min at 37°C, fixed with 4 % PFA and permeabilised with 0.3% Triton X-100. Platelets were then stained with anti-PKA RI (m), RIIα (m) and RIIβ (m) antibodies for 1 hr at room temperature. This was followed by species-specific fluorescently labelled Alexa fluor568 (Red) conjugated secondary antibody for 1 hr at room temperature and counterstained with FITC-phalloidin (1 µg/ml) for 20 min to visualise F-actin. The coverslips were then mounted on glass slides using gelvatol and images were taken via Zeiss ApoTome.2 fluorescence microscope equipped with a 100x oil immersion objective. Fluorescently labelled Secondary antibody alone was used as a negative control. Representative images are central Z-slices from Z stack. Z-slices were taken at 0.15µm intervals through the platelet. All images were deconvolved and underwent contrast enhancement to remove background fluorescence. Shown images are representative of at least three independent experiments. The white inset in the merge image has been zoomed in the adjacent panel. White arrows indicate circular accumulation of PKA RI at the cell centre. Scale bars are indicated.

5.7. Co-localisation of MYPT1 and PKA regulatory subunits in spread platelets

As we have shown previously (chapter 4, section 4.5.3) that MYPT1 directly interacts with PKA regulatory subunits by using biochemical approaches, here we set out to examine the association of MYPT1 with PKA regulatory subunits using immunofluorescence techniques on spread platelets.

Human washed platelets were spread, fixed and permeabilised as mentioned in section 5.5. After permeabilisation platelets were double stained with MYPT1 and PKA regulatory subunit antibodies followed by Alexa fluor conjugated secondary antibodies. Fluorescence microscopy showed that PKA RI (m) strongly co-localised with MYPT1 in the cell centre. Weak co-localisation with MYPT1 is also observed in the cell cortex. In contrast, PKA RIIα and RIIβ less conspicuously co-localised with MYPT1 both in the cortex and centre of the cell (Figure 5.6). This data suggests that in activated platelets the distribution of both MYPT1 and PKA regulatory subunits markedly changed as compared to resting platelets and co-localisation was evident in particular regions. However, a note of caution is due here since the fluorescence microscope resolution limit is 200 nm.

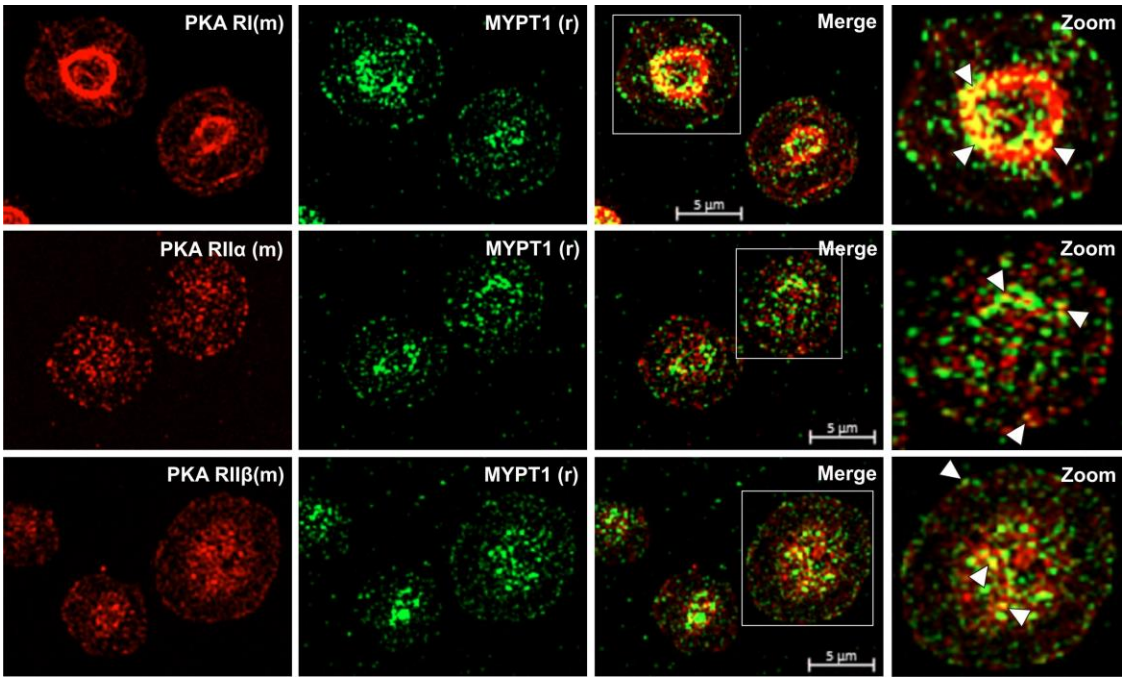

Figure 5.6: Co-localisation of MYPT1 with PKA regulatory subunits in platelets spread on fibrinogen. Human washed platelets ($1x10^7$/ml) were incubated on fibrinogen (100 µg/ml) coated cover slips for 45 min at 37°C, fixed with 4% PFA and permeabilised with 0.3% Triton X-100. Platelets were then double-stained with anti-MYPT1 (r) and anti-PKA RI (m), RIIα (m) and RIIβ (m) antibodies for 1 hr at room temperature. This was followed by species-specific fluorescently labelled Alexa fluor568 (Red) and Alexa fluor488 (green) conjugated secondary antibodies for 1 hr at room temperature. The coverslips were then mounted on glass slides using gelvatol and images were taken via Zeiss ApoTome.2 fluorescence microscope equipped with a 100x oil immersion objective. Representative images are central Z-slices from Z stack. Z-slices were taken at 0.15 µm intervals through the platelet. All images were deconvolved and underwent contrast enhancement to remove background fluorescence. Shown images are representative of at least three independent experiments. The white inset in the merge image has been zoomed in the adjacent panel. White arrow-heads indicate co-localisation of two proteins. Scale bars are indicated.

5.8. Discussion

In platelets PKA is a key negative regulatory enzyme that upon activation by cAMP regulates numerous key cellular activities via phosphorylating serine and threonine residues of downstream substrate proteins (Smolenski, 2012). Gene cloning and biochemical studies indicate that there are four isoforms of PKA regulatory subunits (RIα, RIβ, RIIα, RIIβ) (McKnight *et al*., 1988). Each isoform is considerably heterogeneous in its roles even within single cell types (Taylor *et al*., 2012; Skalhegg & Taskén, 2000; Taylor *et al*., 1990). These isoforms are believed to be arranged in close proximity with various signalling molecules in particular compartments, which is increasingly recognised as a crucial aspect for the specificity of cAMP/PKA signalling in blood platelets (Raslan *et al.*, 2015a). In this chapter, we establish in detail the localisation of PKA regulatory subunit isoforms and their known substrate MYPT1 in platelets. We have shown that the PKA regulatory subunits reside in distinct compartments with MYPT1 both in resting and activated platelets using fluorescence microscopy.

The general understanding of the subcellular distribution of PKA regulatory subunit isoforms is that PKA type I is mainly in the cytoplasm, whereas PKA type II resides in the cell periphery. Several biochemical studies on cell lysates showed that PKA type I is largely found in the supernatant fraction, whereas PKA type II is associated to particulate materials (Kovanich *et al*., 2010; Montoliu *et al*., 2007; Feliciello *et al*., 2000; Deviller *et al*., 1984; Brunton *et al*., 1981; Corbin *et al*., 1977). However, this general consideration of PKA distribution in the cell has more recently been questioned (Raslan *et al*., 2015a; Burgers *et al*., 2012). These researchers have reported that PKA type I is mainly found in the cell periphery, whereas PKA type II in the cytoplasm by using immunofluorescence microscopy and cell fractionation approaches.

Our findings on the PKA isoforms distribution, especially in resting platelets, are consistent with these recent investigators (Raslan *et al*., 2015a; Burgers *et al*., 2012) (Figure 5.3). Furthermore, we have noticed a strong circular labelling of

PKA RI at the cell periphery, which may possibly indicates its co-localisation with the microtubule ring in resting platelets as reported by Huang *et al.* (2013) and Ozer & Halpain (2000) in other cell types. Other studies have also shown that a specific GPCR agonist selectively triggers a particular pool of PKA regulatory subunit isoforms that phosphorylate a specific set of substrate proteins (Di Benedetto *et al*., 2008). For example, in cardiomyocytes β-adrenergic stimulation triggers membrane bound PKA regulatory subunit activity, whereas PGE_1 stimulation results in the activation of the cytosolic pool of PKA (Hayes *et al*., 1980). This selective activation of PKA regulatory subunit isoforms may lead to the phosphorylation of specific sets of downstream substrate proteins and thus keep signalling events localised to that particular compartment. It would be worth seeing the effect of various agonists at least on the cellular distribution of a particular PKA isoform in platelets too by using fluorescence microscopy.

In the case of activated platelets spread on fibrinogen matrix the PKA regulatory subunits markedly re-arranged their cellular distribution, PKA RI mostly translocated from the cell periphery to the cell centre where it is arranged in a circular pattern. Again this circular labelling of PKA RI may possibly suggest its association with the microtubule ring that reassembles at the granulomere area in spread platelets (White &Sauk, 1984). Haung and co-workers (2013) have reported that PKA associates with microtubules and regulates the elongation of neurites. We speculate that in blood platelets PKA may also associate with microtubules and regulate various microtubule related activities, such as platelet aggregation (Menche *et al*., 1980), secretion, thrombus formation (Meyer *et al*., 2012) and clot retraction (Shepro *et al*., 1969). However, the association of PKA with the microtubule ring in blood platelets should be confirmed with immunofluorescence microscopy and affinity binding assays. On the other hand, PKA RIIα and RIIβ concentrated in two distinct compartments, in the cell centre and in the cell periphery and this peripheral localisation is more pronounced in the case of PKA RIIβ (Figure 5.5). This distinct localisation pattern of each PKA

regulatory subunit in platelets strengthens the claim of their individual role in distinctive cellular functions in a particular cell (Taylor *et al*., 2012).

Research studies have shown that the distribution of PKA regulatory subunits in a particular locus or compartment where they target specific substrate proteins that regulate particular cellular activities is majorly due to the interaction with anchoring and scaffold proteins (Taylor *et al*., 2012; Pidoux & Taskén, 2010). The role of anchoring proteins in the specificity of PKA signalling has been well investigated in other cell types and more recently reported in blood platelets where PKA type I is localised in lipid rafts and phosphorylates GPIbβ glycoprotein via interaction with a novel anchoring protein, moesin (Raslan *et al*., 2015a). However, the participation of scaffold proteins such as MYPT1 has not been investigated to date.

MYPT1 is a targeting subunit of MLCP that directs myosin phosphatase towards its substrate proteins. It scaffolds PP1c at the N-terminus and M20 at the C-terminus. It also binds to certain signalling proteins, such as PKG, PKA and Rho kinases and regulates, via PP1c, the phosphorylation of myosin IIa that controls acto-myosin responses both in smooth muscle and non-muscle cells (Butler *et al*., 2013). In resting platelets MYPT1 is distributed throughout the cells with some peripheral cellular distribution (Figure 5.1). This is in line with previously published work conducted by Shin *et al.* (2002) in ferret portal vein smooth muscle cells. Shin and co-workers (2002) and later Lontay *et al.* (2005) and Neppl *et al.* (2009) have also reported that MYPT1 translocates to the plasma membrane upon agonist stimulation. In activated platelets spread on fibrinogen MYPT1 is distributed in a specific pattern, strong granular staining at the cell centre and some peripheral localisation with cortical actin (Figure 5.4A). This labelling pattern of MYPT1 in spread platelets was not disturbed even after treatment with a high dose of PIG_2 (100 nM) (data not shown). However, the ideal state would be to test the effect of PIG_2 on the distribution of MYPT1 in suspended platelets. This subcellular distribution of MYPT1 in spread platelets

was further investigated in association with two pivotal proteins of activatory and inhibitory signalling pathways, myosin IIa and PKA.

Cell fractionation, fluorescence microscopy and affinity chromatography studies have shown that myosin IIa strongly interacts with MYPT1 (Johnson *et al*., 1997; Ichikawa *et al*., 1996). Our immunostaining data in resting platelets also revealed strong co-localisation of MYPT1 with myosin IIa throughout the cell (Figure 5.1C). However, in platelets spread on fibrinogen MYPT1 is not entirely associated with the myosin filaments and a significant fraction of MYPT1 is present throughout the cytoplasm and in the cell periphery where its interaction with myosin is not evident (Figure 5.4). This may indicate that MYPT1 interacts with other substrates in addition to myosin. Furthermore, this suggest that platelet activation potentially triggers the dissociation of MYPT1-PP1c from myosin IIa, which may be a prerequisite for the sustained phosphorylation of myosin light chain as proposed by Khasnis *et al.* (2014); Neppl *et al.* (2009) and Velasco *et al.* (2002). However, the concept of MYPT1 translocation to the cell membrane after activation as suggested by Aburima *et al.* (2013) is not very obvious in our immunofluorescence images. Inagaki *et al.* (1997) and Murata *et al.* (1997) have also detected a similar intracellular distribution pattern of MYPT1 with myosin IIa as in our spread platelets. These reports together with our immunostaining data suggest that MYPT1 may have many other binding partners other than myosin IIa.

In chapter 4 our biochemical data strongly suggests that MYPT1 associates with all four PKA regulatory subunits in human platelets. This *in-vitro* binding was further investigated in both resting and spread platelets using fluorescence microscopy. In resting platelets MYPT1 is mainly co-localised with the PKA RI in the cell periphery, whereas with the PKA RIIα and RIIβ the association was fairly cytoplasmic (Figure 5.3). This suggests that there are possibly two pools of MYPT1 and PKA regulatory subunits, which are differentially distributed, in human platelets. The concept of PKA compartmentalisation is very new in

platelet biology and requires further elucidation. On the other hand, in spread platelets MYPT1 strongly co-localised with PKA RI in the granulomere area and partial association was detected with PKA RIIα and RIIβ in the cell centre and in the cell periphery (Figure 5.6). It is also worth noting that although isolated MYPT1 strongly associates with PKA, the majority of both MYPT1 and PKA regulatory subunits are present in an unbound arrangement throughout the cytoplasm, suggesting that these proteins have various other binding partners (Matsumura & Hartshorne, 2008; Beck *et al.*, 2014). Furthermore, MYPT1 staining both in resting and spread platelets is very granular and it would be worth investigating the association of MYPT1 with different platelets granules, such as alpha granules and dense granules by using antibodies that recognise specific components of these granules (anti-thrombospondin or anti-fibrinogen for alpha granule and anti-CD63 or anti-Lamp2 for dense granules). MYPT1 strongly co-localises with PKA RI, particularly in the cell periphery in resting platelets and in the granulomere area in spread platelets, where the microtubule ring resides (White & Sauk, 1984). Further work needs to be performed, such as triple immunostaining of MYPT1, PKA RI and microtubule using antibodies. If confirmed, the co-localisation of MYPT1 and PKA RI at microtubules may possibly be involved in stabilising the microtubule ring in resting platelets and reassembling in spread platelets.

Conclusion

Collectively, the data presented in this chapter provide insights into the concept of compartmentalisation of PKA and its association with MYPT1 in blood platelets. In blood platelets PKA RI isoforms are mainly localised in the cell periphery, whereas PKA RII isoforms are distributed throughout the cytoplasm. MYPT1 associates with PKA RI in the cell periphery and with PKA RII in the cytosol, suggesting that there are two distinct pools of MYPT1 and PKA isoforms exist that are differentially localised in blood platelets.

Chapter 6: General discussion

The phosphorylation of MYPT1 plays an important role in the regulation of the acto-myosin contractile machinery that is required for platelet shape change during activation. Previously it has been demonstrated that PKA regulates MYPT1 phosphorylation via inhibiting the RhoA-ROCK pathway in thrombin-stimulated platelets. This is required for the activation (disinhibition) of MLCP (Aburima *et al*., 2013). Similarly, in SMCs, both PKA and PKG reverse the inhibitory phosphorylation of MYPT1 at Thr696 and Thr853 and depression of MLCP activity via inhibiting the RhoA-ROCK pathway (Nakamura *et al*., 2007; Azam *et al*., 2007). In this study we aimed at identifying new mechanisms that regulate PKA-mediated phosphorylation of MYPT1 function on MLCP activity in blood platelets. Here, we first characterized the role of the cAMP-elevating agent PGI_2 and the platelet agonist thrombin on the phosphorylation of MYPT1. We also explored the presence of different splice variants of MYPT1 that might be differentially regulated by cAMP/PKA signalling. Furthermore, we examined in detail the interaction of MYPT1 with PKA and explored whether MYPT1 is an AKAP and therefore interacts with PKA in an AKAP manner. Finally, we investigated the cellular distribution of both MYPT1 and PKA in the context of distinct subcellular compartments both in resting and spread platelets by immunohistochemistry.

6.1. Phosphorylation of MYPT1 in blood platelets

In many cell types, including platelets, the acto-myosin contractile machinery is chiefly under the influence of MLCK and MLCP, which determines the extent of MLC phosphorylation and acto-myosin ATPase activity. Although MLCK activation depends on cytosolic calcium concentration, MLCP activity is also subject to modulation by a number of signalling proteins (Somlyo & Somlyo, 2003). Platelet agonists, such as thrombin and TXA_2, activate the small GTPase RhoA, which in turn activates its downstream effector ROCK. This results in phosphorylation of MYPT1 at Thr696 and Thr853, increased inhibition of the phosphatase activity

and MLC phosphorylation, independently of changes in calcium concentration (Aburima & Naseem, 2014). Conversely, in SMCs activated PKA and PKG phosphorylate MYPT1 at Ser695 and increase MLC dephosphorylation through activation (disinhibition) of MLCP activity leading to calcium desensitization (Nakamura *et al*., 1999; Lee & Kitazawa, 1997). However, in platelets, cyclic nucleotides-mediated phosphorylation of MYPT1 at Ser695 has not been investigated before. In this thesis we show for the first time that cAMP elevating agents moderately increase the phosphorylation level of MYPT1 at Ser695 in a concentration and time-dependent fashion (Figure 3.3A & 3.4). This moderate increase in the phosphorylation level is potentially directly related to increased MLCP activity in platelets as previously shown by Aburima and Naseem (2014). However, in SMCs, which express similar isoforms of MLCP, the phosphorylation of MYPT1 at Ser695 has not been reported to increase the activity of MLCP, but rather disinhibits MLCP activity by relieving phosphorylation of inhibitory residues (Nakamura *et al*., 2007; Wooldridge *et al*., 2004). These researchers have shown that the phosphorylation of MYPT1 at Ser695 physically blocks the phosphorylation of the adjacent inhibitory residue, Thr696, and vice versa, thus inhibiting or disinhibiting (activating) the activity of MLCP. However, in platelets, our calyculin A data suggests that the phosphorylation of MYPT1 at Thr696 is not physically blocking the phosphorylation of the adjacent Ser695 and vice versa (Figure 3.2). This is in line with the work conducted by Neppl and co-workers (2009), who have reported that in intact cerebral arteries the phosphorylation of Thr696 is independent of the phosphorylation of Ser695. In addition, the phosphorylation of MYPT1 at Thr696 in thrombin-treated platelets has no effect on the phosphorylation of adjacent Ser695 in our time course experiments (Figure 3.5), further strengthening our observation that Thr696 is not physically blocking or reducing the phosphorylation of Ser695 as suggested by Nakamura *et al.* (2007) and Wooldridge *et al.* (2004). Because of the above inconsistencies, the precise contribution of the phosphorylation of MYPT1 at Ser695 to the activity of MLCP requires further investigation.

On the contrary, the inhibition of MLCP activity via phosphorylation of MYPT1 at Thr696 and Thr853 has been well documented in the literature (Hartshorne *et al*., 2004). Koga and Ikebe (2008) showed that the RhoA-ROCK mediated phosphorylation of MYPT1 increases its affinity towards 14-3-3, which triggers MLCP dissociation from myosin IIa and attenuates MLCP activity. Later, Khromov *et al.* (2009) suggested that RhoA-ROCK mediated phosphorylation of MYPT1 at Thr696 and Thr853 inhibits MLCP activity possibly via docking of these phospho-residues to the active cleft of PP1c and causing autoinhibition of MLCP activity. Recently, in blood platelets, Aburima *et al.* (2013; 2017) revealed that the thrombin-mediated RhoA-ROCK activation significantly decreases MLCP activity via inhibitory phosphorylation of MYPT1 at Thr853. Together these studies clearly suggest that RhoA-ROCK mediated phosphorylation of MYPT1 inhibits MLCP activity. Although a number of other kinases, such as ILK and ZIP kinases have also been reported to increase the inhibitory phosphorylation of MYPT1 at Thr696 and Thr853, the physiological importance of these events are less clear (Hartshorne *et al*., 2004). Moreover, studies have shown that the phosphorylation of MYPT1 is responsible for the structure and subcellular distribution of the MLCP holoenzyme. In SMCs, phosphorylation at Thr696 and Thr853 activates the dissociation of the MLCP holoenzyme from myosin IIa, which is required for increased MLC phosphorylation (Velasco *et al*., 2002). Similarly, Shin *et al.* (2002) revealed that in SMCs RhoA-ROCK mediated phosphorylation of MYPT1 at Thr696 triggers the translocation of the MYPT1-PP1c complex from the cytosol to the plasma membrane, which is followed by the dissociation of PP1c from MYPT1 and subsequently PP1c returns to the cytosol, where it has reduced phosphatase activity towards phosphorylated myosin IIa. In platelets, phosphorylation of MYPT1 at Thr853 in thrombin-stimulation also triggers the dissociation of PP1c from MYPT1 (Aburima *et al*., 2013) and once free, PP1c showed low catalytic activity towards myosin IIa (Terrak *et al*., 2004). Interestingly, cyclic nucleotides via PKA and PKG significantly inhibited the translocation and dissociation of the MLCP holoenzyme, which is

required for increase phosphatase activity (Neppl *et al*., 2009). We have also attempted to examine the role of cAMP elevating agents on the subcellular distribution of MYPT1 in human platelets using subcellular fractionation and immunofluorescence techniques. However, our attempts were not successful as the MYPT1 protein degraded very rapidly in fractionation buffer and the signal of phospho-specific MYPT1 antibodies was very weak and inconclusive.

Similar to SMCs, in platelets phosphorylation of MYPT1 at Ser695 is basally high, suggesting that there is an active adenylyl cyclase or a constitutively active PKA or an unknown kinase or a reduced phosphatase level involved in this process (Figure 3.1-3.7). Another possible explanation would be the presence of platelet-derived NO (Freedman *et al*., 1997), which could possibly be responsible for high basal phosphorylation of Ser695. In endothelial cells a NOS inhibitor (L-NAME) completely abolished the basal phosphorylation of Ser695, indicating that the cGMP-PKG pathway is involved in this process (Neppl *et al*., 2009). However, this aspect needs to be investigated in platelets by using PKA/PKG inhibitors. Additionally, in SMCs, high basal phosphorylation of Ser695 is responsible for preserving basal vascular tone (Grassie *et al*., 2012; Neppl *et al*., 2009; Wooldridge *et al*., 2004). We speculate that in platelets high basal Ser695 phosphorylation may be involved in keeping the inhibitory threshold levels high for platelet activation. Furthermore, this high basal phosphorylation potentially preserves the MLCP holoenzyme in complex with myosin IIa, which is required for maintaining MLC dephosphorylation and thus keeping platelets in a non-adherent state.

In SMCs and endothelial cells the RhoA-ROCK pathway increases the phosphorylation of MYPT1 at Thr696 and Thr853, with no baseline phosphorylation of these residues (Yuen *et al*., 2014; Kitazawa *et al*., 2003). We found that in platelets thrombin rapidly increases phosphorylation of MYPT1 at Thr696 and Thr853 in a dose and time-dependent manner, with minimal baseline phosphorylation of these residues (Figure 3.3B & 3.5). These basal levels are

possibly due to the presence of an active regulatory phosphatase. Previous *in vitro* studies have shown that the MLCP directly dephosphorylates MYPT1 inhibitory residues, Thr696 and Thr853, during RhoA-ROCK signalling, indicating the involvement of this phosphatase in the regulation of MYPT1 phosphorylation (Kaneko-Kawano *et al*., 2012; Khromov *et al*., 2009; Kiss *et al*., 2008; Kimura *et al*., 1996). Furthermore, our results suggest that PGI_2 does not provoke the phosphorylation of inhibitory residues, indicating that these residues are exclusively phosphorylated by platelet activatory signals, which is in line with the work carried out in 293T HEK cells by Yuen *et al.* (2014) (Figure 3.4).

6.2. Splice variants of MYPT1 in blood platelets

A novel aspect of this work was to investigate the expression of different splice variants of MYPT1 in platelets. Research studies have revealed several splice variants of MYPT1 in various cell types in human, birds and insects. These splice variants are generated by cassette-type alternative splicing of a single gene, *PPP1R12A*, at central exon and 3' exon sections and involve the presence or absence of central insert (CI) and C-terminal leucine zipper (LZ) domains (Ito *et al*., 2004). Of these splice variants, the C-terminal leucine zipper variants are well characterised in the literature. Huang *et al.* (2004) have shown that in cultured SMCs the over-expression of the MYPT1 splice variant containing the LZ motif (LZ^+ MYPT1) but not the splice variant lacking this motif (LZ^- MYPT) increases MLC dephosphorylation in response to cGMP elevating agents (8Br-cGMP). They have also reported that the cGMP-activated PKG interacts with both splice variants; however, only the LZ^+ MYPT1 variant was able to induce smooth muscle relaxation, suggesting that the LZ motif is essential for PKG-mediated smooth muscle relaxation. Similarly, 8Br-cGMP only increases MLCP activity in 293T HEK cells expressing the LZ^+ MYPT1, but not the LZ^- MYPT1 splice variant, indicating that the relative expression of MYPT1 splice variants determines the magnitude of MLCP activity (Yuan *et al*., 2014). In SMCs, the LZ^- MYPT1 variant has low intrinsic MLCP activity and higher Thr696 and Thr853 phosphorylation as

compared to the LZ^+ MYPT1 variant. Furthermore, relative expression of these splice variants is tissue specific, developmentally regulated as well as modulated in a number of diseases (Singh *et al*., 2011; Payne *et al*., 2006; Karim *et al*., 2004; Khatri *et al*., 2001). Recent studies have suggested that the changes in the expression of MYPT1 splice variants markedly contribute to changes in the sensitivity to cGMP-mediated smooth muscle vasodilation that are associated with several pathological conditions including heart failure, pulmonary hypertension, portal hypertension and pregnancy-induced hypertension (Yuen *et al*., 2014).

Our data clearly suggests that there are at least two splice variants of MYPT1 in platelets, which are differentially phosphorylated by cAMP elevating agents (Figure 3.7). PKA interacts with both splice variants; however, only one is phosphorylated at Ser695, whereas in thrombin-stimulated platelets both variants are phosphorylated at Thr696 and Thr853. The basis of this differential phosphorylation by PKA is not known yet as there are no splice variant-specific antibodies available that could be used to dissect the role of each splice variant on platelet function. At this moment of time, we are also not aware of the identity and relative contributions of these splice variants on the activity of MLCP holoenzyme. We also do not know what the situation of these splice variants is in megakaryocytes and whether the expression of these variants changes in platelets especially during disease conditions, such as atherosclerosis. Nevertheless, on the basis of this study we assume that there are potentially two splice variants of MYPT1, which are possibly distributed into two different pools. One pool is exclusively under the influence of RhoA-ROCK, while the second pool is under both PKA and RhoA-ROCK. This assumption would be consistent with the spatial compartmentalisation of cAMP signalling (Raslan *et al*., 2015a; Seino & Shibasaki, 2005).

6.3. Interaction of MYPT1 with PKA regulatory subunits

The data we present in this thesis and the work of others clearly suggest that all four PKA regulatory subunit isoforms are present in platelets. They are generally classified into two types, type I and type II (Figure 4.1). These regulatory subunits are differentially distributed and control a number of cellular activities in various cell types (Taylor *et al*., 2012; 2008; Pidoux & Taskén, 2010). In platelets, the cellular distribution and activity of these isoforms have not been characterised until very recently (Raslan *et al*., 2015a). Raslan *et al.* (2015a) showed that type I subunits are distributed in the cell periphery where they are involved in the down-regulation via phosphorylation of the surface glycoprotein (GPIbβ), a subunit of the GPIb-V-IX complex required for vWF-platelet interaction. However, the precise role of these isoforms in the regulation of the platelet contractile apparatus is fairly unknown. Here we show for the first time that all four PKA regulatory subunits interact with MYPT1 (Figures 4.2-4.4). Our experiments clearly show that MYPT1 and PKA regulatory subunits along with their catalytic partners are in a complex in platelets. Unfortunately, due to unavailability of MYPT1 and PKA regulatory subunit-specific inhibitors and their murine KO models, we were not able to explore the physiological significance of this MYPT1-PKA interaction in platelet function. Platelets are inherently difficult cells to manipulate and their lack of nucleus precludes direct genetic manipulation, which further limited our investigations. Nevertheless, we selected a mammalian cell line (293T HEK), successfully mapped the interaction and confirmed that only the central region of MYPT1 (aa501-706) is directly involved in the interaction with all four PKA regulatory subunits (Figure 4.12). At this moment, we were not able to explore whether the direct interaction of MYPT1 with the PKA regulatory subunits has any effect on MYPT1 phosphorylation and the activity of MLCP.

Initially we hypothesized that MYPT1 is an AKAP as it displays striking similarities with known AKAPs, such as acting as a scaffold for PP1c to localise it close to its substrates as well as binding of PKG, RhoA, myosin and PKA, to allow the

formation of multienzyme complexes (Butler *et al*., 2013). Indeed, structural analysis of MYPT1 shows the presence of amphipathic helices, one at the N-terminus (aa267-285) and second at the end of C-terminus (aa986-1004), typically found in AKAPs, which may act to localise PKA to a particular subcellular regions via interacting with the D/D domain of the regulatory subunits (Figure 4.6). Our biochemical findings suggest that MYPT1 does not interact with PKA in an AKAP fashion, as neither the amphipathic helices of MYPT1 are involved nor the D/D domain of PKA is required for interaction (Figure 4.7, 4.8 & 4.13). Although MYPT1 directly interacts with PKA in a non-AKAP fashion, it cannot be ruled out that an AKAP tethers PKA towards MYPT1 and is responsible for PKA-mediated MLCP activation. Recently AKAP2 has been reported to regulate PKA-mediated MLCP activity via directly associating with MYPT1. Deletion of AKAP2 abolished PKA-mediated activation of MLCP, which is required for MLC dephosphorylation and increased endothelial cells contraction and preservation (Batori *et al*., 2017). In platelets the identification of an AKAP that is tethering PKA towards MYPT1 could easily be investigated by utilizing standard approaches, such as PKA-R overlay assays and mass spectrometry-based chemical proteomics experiments. The later approach has proven their value in capturing, identifying and characterising novel AKAPs (Scholten *et al*., 2008).

On the basis of our results, we suggest the following model of MYPT1 and PKA interaction in blood platelets (Figure 6.1). At basal level PKA has been reported to phosphorylate numerous downstream substrate proteins (El-Daher *et al*., 1996). In this study, we have noticed that MYPT1 is basally phosphorylated at Ser695 (Chapter 3, section 3.4.3) possibly via direct association with basally active PKA, which results in active MLCP that reduce phosphorylation of MLC and thus keep platelets in non-adherent state (Figure 6.1A). This basal PKA activity is either due to the presence of a constitutively active adenylyl cyclase that maintain intracellular cAMP level or the presence of cAMP-independent pathway required for keeping platelets in dormant state. Stimulation of platelets with PGI_2 causes

activation of PKA that moderately enhances the phosphorylation of MYPT1 at Ser695 and the activity of the MLCP, which are responsible for inhibition or reversal of platelets activation (Figure 6.1B). On the other hand, thrombin stimulation leads to the activation of RhoA-ROCK signalling, which phosphorylates MYPT1 at Thr696 and Thr853, resulting in MLCP inhibition and subsequent phosphorylation of MLC, which leads to reversal platelets activation (6.1C).

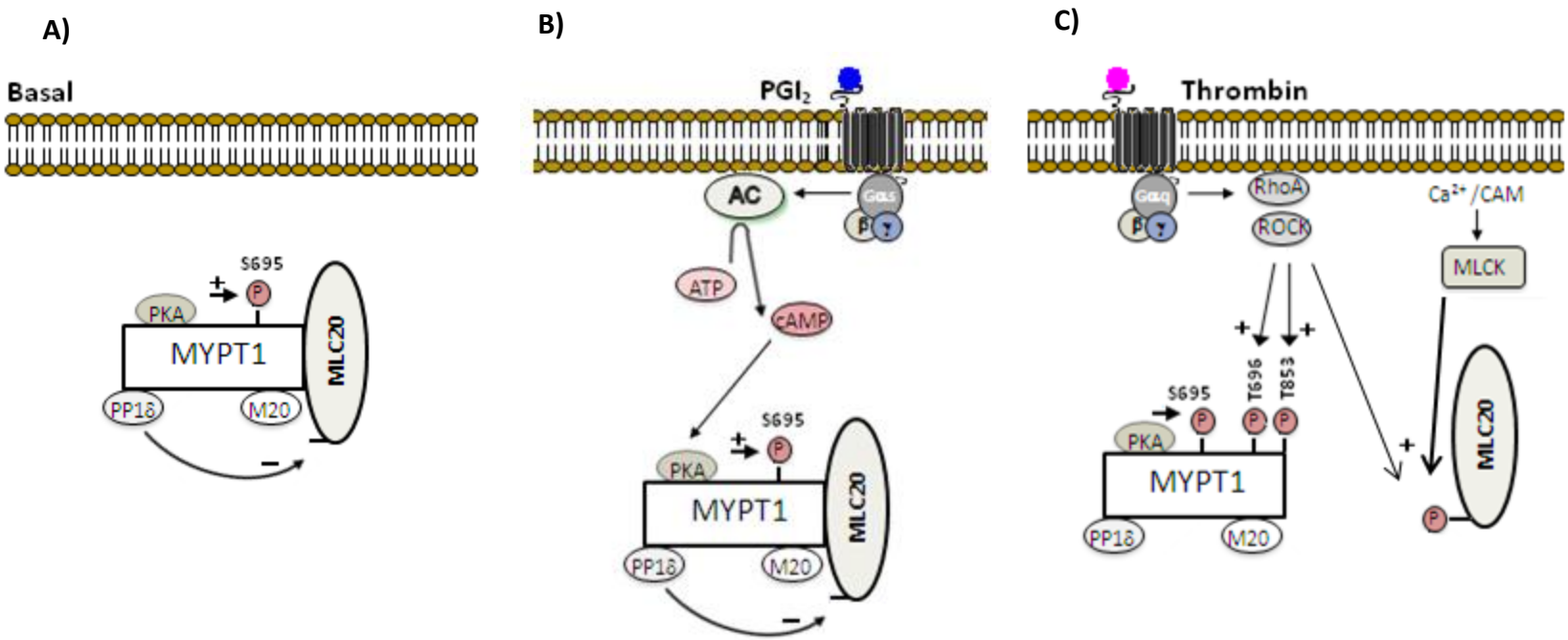

Figure 6.1: A proposed model of MYPT1-PKA interaction in platelets. A) In resting platelets PKA regulatory subunits directly interact with the MYPT1 in a way that the PKA catalytic subunit docks on the Ser695 of MYPT1 and induces its phosphorylation. The phosphorylated MYPT1 then targets MLCP to myosin and thus keeps the contractile machinery in an inactive state by continually dephosphorylating MLC. These events contribute to keeping platelets in a quiescent state. **B)** Platelets stimulated with PGI_2 cause PKA activation via increased intracellular cAMP level. PKA in the presence of cAMP moderately increases the phosphorylation of MYPT1 at Ser695 and MLCP activity. MLCP via MYPT1 remains associated with myosin (Johnson *et al.*, 1997) dephosphorylates MLC and results in platelet inhibition. **C)** Platelets stimulated with thrombin trigger activation of RhoA, which then activates ROCK kinase that phosphorylates MYPT1 at Thr696 and Thr853, inhibits MLCP activity and probably dissociates MLCP holoenzyme from myosin (Aburima *et al.*, 2013; Khasnis *et al.*, 2014; Neppl *et al.*, 2009; Velasco *et al.*, 2002), thus decreasing the dephosphorylating activity of MLCP towards MLC. Concurrently thrombin also triggers increased intracellular calcium release that leads to the calmodulin (CAM) dependent activation of MLCK. Both RhoA-ROCK (Amano *et al.*, 1996) and MLCK (Somlyo & Somlyo, 1994) phosphorylate MLC and potentiate myosin IIa-based motor activities that lead to platelet activation. Note that thrombin has no effect on the phosphorylation of Ser695 as it remains equivalent to basal level.

6.4. Cellular distribution of MYPT1 and PKA in blood platelets

The idea of compartmentalised cAMP-PKA signalling has long been proposed (Buxton & Brunton, 1983); however, in platelets it has only recently been demonstrated (Raslan *et al*., 2015a). As our binding studies suggest that MYPT1 directly interacts with PKA regulatory subunits and if PKA regulatory subunits are organised in different compartments as proposed by Raslan *et al.* (2015a), MYPT1 may also be differentially arranged in these compartments along with PKA. To explore this hypothesis, we used double-labelling immunofluorescence and fluorescence microscopy to investigate the subcellular localization of MYPT1 and PKA regulatory subunits. In resting platelets adhered to poly-L-lysine, MYPT1 and PKA RI are mainly co-localised in the cell periphery where MYPT1 may possibly be responsible for positioning PKA RI nearby membrane protein substrates, such as GPCRs and GPIbβ, which have been shown to be regulated via phosphorylation by PKA (Raslan *et al*., 2015a; Smolenski, 2012). Furthermore, this peripheral PKA RI may phosphorylate MYPT1 at Ser695, which is responsible for MLCP disinhibition and subsequent inhibition of HDAC6. This enzyme is required for microtubule deacetylation and disintegration in activated platelets (Joo & Yamada, 2014; Aslan *et al*., 2013). On the other hand, co-localisation of MYPT1 with PKA RIIα and RIIβ is predominantly seen in the cell cytoplasm, which suggests that PKA RIIα and RIIβ are targeted in the cell cytoplasm where they may catalyze the phosphorylation of MYPT1 and other proteins that are important to the regulation of the contractile apparatus (Figure 5.3). This differential distribution of PKA regulatory subunits along with MYPT1 in resting platelets suggest the presence of different compartments of cAMP signalling where MYPT1 may target PKA towards its particular substrate proteins, which is responsible for distinct cellular activities. In return, PKA phosphorylates MYPT1 in these compartments, which is responsible for MLCP activation and subsequent inhibition of the platelet contractile machinery. Due to this differential distribution of PKA regulatory subunits along with MYPT1, one may also assume that MYPT1-PKA RI may play a role in regulating the marginal band of

microtubules and MYPT1-PKA RIIα and RIIβ in the acto-myosin contractile machinery.

Once platelets become activated as they spread on fibrinogen, the cellular distribution of MYPT1 and PKA regulatory subunits entirely changed. MYPT1 strongly co-localised with PKA RI in the cell centre where PKA RI concentrated in a circular pattern. It can be inferred from this result that MYPT1 and PKA RI possibly associate with the microtubule ring in the cell centre where these two proteins may be involved in the reassembly and stability of microtubules in spread platelets, which is potentially needed to accumulate organelles in the cell centre for secretory reaction (Sadoul, 2015). By contrast with PKA RIIα and RIIβ the co-localisation of MYPT1 was consistently to two regions, cell centre and some fair peripheral localization especially with PKA RIIβ, indicating two distinct compartments of PKA responsible for localized cAMP signalling (Figure 5.6). To the best of our knowledge the differential distribution of MYPT1 and PKA regulatory subunits is also a novel observation as this has not been reported previously, particularly in spread platelets.

To summarise, the work presented in this thesis clearly identifies MYPT1 as a novel PKA substrate protein in blood platelets. Our data shows that human platelets express two MYPT1 splice variants, which are differentially regulated by cAMP signalling. Furthermore, our data shows that MYPT1 directly interacts with PKA regulatory subunits and possibly influences cellular functions. We believe that advancing our understanding of how MYPT1-PKA interaction influences cellular activities will reveal new pathways that regulate platelet activation and present target for novel antithrombotic therapeutics.

6.5. Future work

The key findings of this study, such as splice variants of MYPT1 and interaction of MYPT1 with PKA have opened up a number of avenues that need to be considered in future investigation.

- The identity of MYPT1 splice variants in platelets can be confirmed in mRNA of platelets using RT-PCR with specific primers. Once the identity of these variants has been confirmed we can either over-express them as tagged fusion proteins in mammalian cells or could possibly generate antibodies against specific variants and confirm their subcellular distribution even in platelets via immunohistochemistry or cell fractionation techniques. This will help us to dissect their specific roles in the cell function.

  Our biochemical data suggests that PKA interacts with both splice variants of MYPT1; however, only the one with slightly higher molecular weight is phosphorylated through PGI_2 signalling. Confirming the identity of these splice variants will help us to investigate the role of the missing motif on the phosphorylation of Ser695 and MLCP activity. For example, in SMCs, MYPT1 splice variants carrying the LZ motif serve to target PKG and affect MLCP activity; however, it is not known whether the LZ motif plays any role in the phosphorylation of MYPT1 on Ser695.

  In SMCs and platelets, the relationship between the activity of MLCP and the phosphorylation of MYPT1 has been well documented (Aburima & Naseem, 2014; Hartshorne *et al*., 2004). However, very little is known about the relative expression of different splice variants of MYPT1 in disease conditions. Karim *et al.* (2004) have reported that in congestive heart failure (CHF) the expression of the LZ^+ MYPT1 splice variant was markedly reduced in the smooth muscle cells of aorta and iliac artery as compared to control animals, indicating that CHF is associated with a decrease in the relative expression of the LZ^+ MYPT1 splice variants. However, in platelets, we are not aware whether MYPT1 splice

variants are also differentially expressed in disease conditions, such as atherosclerosis, metabolic disorders or infection that could be investigated in patients or animal models. If that is the case then the modulation of MYPT1 splice variants expression may open a new and possibly more effective avenue for treating patients with atherosclerosis.

- There are no specific inhibitors or knock-out models of MYPT1 and PKA regulatory subunits available that could be used to explore the functional relevance of MYPT1-PKA interaction in blood platelets. Furthermore, the inability to genetically modify platelets further restricted our hands to study the role of this interaction on platelet function. To overcome these limitations one could explore this protein-protein interaction in suitable mammalian cell lines that are easily manipulated by genetic engineering. For example, HUVEC cells as they have cyclic nucleotide and thrombin signalling pathways similar to platelets and could be used to investigate the effect of MYPT1-PKA interaction on functions, such as membrane permeability. Therefore, to begin with, the contents of endogenous MYPT1 or PKA could be lowered by siRNA-mediated knock-down and the effects of PGI_2 and thrombin on the cell permeability assessed by measuring transendothelial electrical resistance.

- It would be of interest to determine the role of individual isoforms of PKA on MYPT1 phosphorylation. This could easily be achieved by using an expression system e.g. human MEG-01 cell line as they express IP receptors, PKA RIα, RIβ, RIIβ and PKA-catalytic, synthesise cAMP and phosphorylate VASP in response to PGI_2. siRNA-mediated selective silencing of PKA isoforms would be introduced in the MEG-01 cell line to isolate isoform specific effects on MYPT1 phosphorylation and signalling. This strategy has been successfully used to isolate PKA-RII specific events in endothelial cells.

- It may also be of benefit to examine the effects of MYPT1 phosphorylation on MLCP activity, structure of the holoenzyme and subcellular localisation. This could be explored via point mutation of Ser695, Thr696 and Thr853, followed by expression in HUVEC cells and assessed the consequences of these mutations on MLCP holoenzyme structure using co-immunoprecipitation. The effects of mutations on subcellular localisation could be examined using immunohistochemistry and cell fractionation approaches. The effects of mutations on MLCP activity could be determined using SensoLyte protein phosphatase assay kit with immunoprecipitated PP1c.

- One could also examine the effects of MYPT1-PKA interaction on the activity of MLCP and MYPT1 phosphorylation. The easy approach to follow this would be to either delete or mutate the binding motif of MYPT1 involved in the association with PKA, followed by expression in mammalian cells, immunoprecipitation of mutated MYPT1 or PKA from cell lysates pretreated with or without PGI_2, analyze phosphorylation of MYPT1 via western blotting and measure PP1c activity using SensoLyte protein phosphatase assay kit.

References:

Aburima, A. and Naseem, K.M., 2014. Platelet myosin light chain phosphatase: keeping it together. *Biochemical Society Transactions*, *42*(2), pp.279-283.

Aburima, A., Walladbegi, K., Wake, J.D. and Naseem, K.M., 2017. cGMP signalling inhibits platelet shape change through regulation of the RhoA-Rho Kinase-MLC phosphatase signalling pathway. *Journal of Thrombosis and Haemostasis*,*15*(8), pp.1668-1678.

Aburima, A., Wraith, K.S., Raslan, Z., Law, R., Magwenzi, S. and Naseem, K.M., 2013. cAMP signaling regulates platelet myosin light chain (MLC) phosphorylation and shape change through targeting the RhoA-Rho kinase-MLC phosphatase signaling pathway. *Blood*, *122*(20), pp.3533-3545.

Ahmad, F., Boulaftali, Y., Greene, T.K., Ouellette, T.D., Poncz, M., Feske, S. and Bergmeier, W., 2011. Relative contributions of stromal interaction molecule 1 and CalDAG-GEFI to calcium-dependent platelet activation and thrombosis. *Journal of Thrombosis and Haemostasis*, *9*(10), pp.2077-2086.

Alessi, D., Macdougall, L.K., Sola, M.M., Ikebe, M. and Cohen, P., 1992. The control of protein phosphatase-1 by targetting subunits. *The FEBS Journal*, *210*(3), pp.1023-1035.

Alto, N.M., Soderling, S.H., Hoshi, N., Langeberg, L.K., Fayos, R., Jennings, P.A. and Scott, J.D., 2003. Bioinformatic design of A-kinase anchoring protein-in silico: a potent and selective peptide antagonist of type II protein kinase A anchoring. *Proceedings of the National Academy of Sciences*, *100*(8), pp.4445-4450.

Amano, M., Nakayama, M. and Kaibuchi, K., 2010. Rho-kinase/ROCK: a key regulator of the cytoskeleton and cell polarity. *Cytoskeleton*, *67*(9), pp.545-554.

André, P., Prasad, K.S., Denis, C.V., He, M., Papalia, J.M., Hynes, R.O., Phillips, D.R. and Wagner, D.D., 2002. CD40L stabilizes arterial thrombi by a β3 integrin–dependent mechanism. *Nature Medicine*, *8*(3), pp.247-252.

Antl, M., von Brühl, M.L., Eiglsperger, C., Werner, M., Konrad, I., Kocher, T., Wilm, M., Hofmann, F., Massberg, S. and Schlossmann, J., 2007. IRAG mediates NO/cGMP-dependent inhibition of platelet aggregation and thrombus formation. *Blood*, *109*(2), pp.552-559.

Arehart, E., Stitham, J., Asselbergs, F.W., Douville, K., MacKenzie, T., Fetalvero, K.M., Gleim, S., Kasza, Z., Rao, Y., Martel, L. and Segel, S., 2008. Acceleration of cardiovascular disease by a dysfunctional prostacyclin receptor mutation. *Circulation Research*, *102*(8), pp.986-993.

Arimura, T., Suematsu, N., Zhou, Y.B., Nishimura, J., Satoh, S., Takeshita, A., Kanaide, H. and Kimura, A., 2001. Identification, characterization, and functional analysis of heart-specific myosin light chain phosphatase small subunit. *Journal of Biological Chemistry*, *276*(9), pp.6073-6082.

Armstrong, R.A., 1996. Platelet prostanoid receptors. *Pharmacology and Therapeutics*, *72*(3), pp.171-191.

Aslam, M., Härtel, F.V., Arshad, M., Gündüz, D., Abdallah, Y., Sauer, H., Piper, H.M. and Noll, T., 2010. cAMP/PKA antagonizes thrombin-induced inactivation of endothelial myosin light chain phosphatase: role of CPI-17. *Cardiovascular Research*, *87*(2), pp.375-384.

Aslan, J.E., Phillips, K.G., Healy, L.D., Itakura, A., Pang, J. and McCarty, O.J., 2013. Histone deacetylase 6-mediated deacetylation of α-tubulin coordinates cytoskeletal and signaling events during platelet activation. *American Journal of Physiology-Cell Physiology*, *305*(12), pp.C1230-C1239.

Aszódi, A., Pfeifer, A., Ahmad, M., Glauner, M., Zhou, X.H., Ny, L., Andersson, K.E., Kehrel, B., Offermanns, S. and Fässler, R., 1999. The vasodilator- stimulated phosphoprotein (VASP) is involved in cGMP-and cAMP-mediated inhibition of agonist-induced platelet aggregation, but is dispensable for smooth muscle function. *The EMBO Journal*, *18*(1), pp.37-48.

Azam, M.A., Yoshioka, K., Ohkura, S., Takuwa, N., Sugimoto, N., Sato, K. and Takuwa, Y., 2007. Ca^{2+}-independent, inhibitory effects of cyclic adenosine 5'-monophosphate on Ca^{2+} regulation of phosphoinositide 3-kinase C2α, Rho, and myosin phosphatase in vascular smooth muscle. *Journal of Pharmacology and Experimental Therapeutics*, *320*(2), pp.907-916.

Aye, T.T., Mohammed, S., van den Toorn, H.W., Van Veen, T.A., van der Heyden, M.A., Scholten, A. and Heck, A.J., 2009. Selectivity in enrichment of cAMP-dependent protein kinase regulatory subunits type I and type II and their interactors using modified cAMP affinity resins. *Molecular and Cellular Proteomics*, *8*(5), pp.1016-1028.

Bátori, R., Kumar, S., Bordán, Z., Cherian-Shaw, M., Kovács-Kása, A., MacDonald, J.A., Fulton, D.J., Erdődi, F. and Verin, A.D., 2017. Differential mechanisms of adenosine-and ATPγS-induced microvascular endothelial barrier strengthening. *Journal of cellular physiology*, 10.1002/jcp.26419

Batori, R.K., Kumar, S., Kasa, A. and Verin, A.D., 2016. Differential role of PKA/MLCP axis in ATP-and adenosine-induced microvascular endothelial barrier enhancement. *The FASEB Journal*, *30* (1 Supplement), pp.727-737.

Bauer, M., Retzer, M., Wilde, J.I., Maschberger, P., Essler, M., Aepfelbacher, M., Watson, S.P. and Siess, W., 1999. Dichotomous regulation of myosin phosphorylation and shape change by Rho-kinase and calcium in intact human platelets. *Blood*, *94*(5), pp.1665-1672.

Beazely, M.A., Alan, J.K. and Watts, V.J., 2005. Protein kinase C and epidermal growth factor stimulation of Raf1 potentiates adenylyl cyclase type 6 activation in intact cells. *Molecular Pharmacology*, *67*(1), pp.250-259.

Beck, F., Geiger, J., Gambaryan, S., Veit, J., Vaudel, M., Nollau, P., Kohlbacher, O., Martens, L., Walter, U., Sickmann, A. and Zahedi, R.P., 2014. Time-resolved characterization of cAMP/PKA-dependent signaling reveals that platelet inhibition is a concerted process involving multiple signaling pathways. *Blood*, *123*(5), pp.e1-e10.

Bellucci, S. and Caen, J., 2002. Molecular basis of Glanzmann's thrombasthenia and current strategies in treatment. *BloodReviews*, *16*(3), pp.193-202.

Bender, A.T. and Beavo, J.A., 2006. Cyclic nucleotide phosphodiesterases: molecular regulation to clinical use. *Pharmacological Reviews*, *58*(3), pp.488-520.

Bender, M., Thon, J.N., Ehrlicher, A.J., Wu, S., Mazutis, L., Deschmann, E., Sola-Visner, M., Italiano, J.E. and Hartwig, J.H., 2015. Microtubule sliding drives proplatelet elongation and is dependent on cytoplasmic dynein. Blood, 125(5), pp.860-868.

Bernardi, B., Guidetti, G.F., Campus, F., Crittenden, J.R., Graybiel, A.M., Balduini, C. and Torti, M., 2006. The small GTPase Rap1b regulates the cross-talk between platelet integrin α2β1 and integrin αIIbβ3. *Blood*, *107*(7), pp.2728-2735.

Billington, N., Wang, A., Mao, J., Adelstein, R.S. and Sellers, J.R., 2013. Characterization of three full-length human nonmuscle myosin II paralogs. *Journal of Biological Chemistry*, *288*(46), pp.33398-33410.

Bilodeau, M.L. and Hamm, H.E., 2007. Regulation of protease-activated receptor (PAR) 1 and PAR4 signaling in human platelets by compartmentalized cyclic nucleotide actions. *Journal of Pharmacology and Experimental Therapeutics*,*322*(2), pp.778-788.

Bizzozero, J., 1882. On a new blood particle and its role in thrombosis and blood coagulation. *Virchows Archiv Fur Pathologisch AnatomieUnd Physiologie Und Klinische Medizin*,*90*, pp.261-332.

Blackmore, P.F., 2011. Biphasic effects of nitric oxide on calcium influx in human platelets. *Thrombosis Research*, *127*(1), pp.e8-e14.

Blair, P. and Flaumenhaft, R., 2009. Platelet α-granules: basic biology and clinical correlates. *Blood Reviews*, *23*(4), pp.177-189.

Blockmans, D., Deckmyn, H. and Vermylen, J., 1995. Platelet activation. *Blood Reviews*, *9*(3), pp.143-156.

Bodnar, R.J., Xi, X., Li, Z., Berndt, M.C. and Du, X., 2002. Regulation of glycoprotein Ib-IX-von Willebrand factor interaction by cAMP-dependent protein kinase-mediated phosphorylation at Ser166 of glycoprotein Ibβ. *Journal of Biological Chemistry*, *277*(49), pp.47080-47087.

Boilard, E., Nigrovic, PA., Larabee, K., Watts, G.F., Coblyn, J.S., Weinblatt, M.E., Massarotti, E.M., Remold-O'Donnell, E., Farndale, R.W., Ware, J., Lee, D.M., 2010. Platelets amplify inflammation in arthritis via collagen dependent micro particle production. *Science,* 327, pp.580-583.

Bolz, S.S., Vogel, L., Sollinger, D., Derwand, R., de Wit, C., Loirand, G. and Pohl, U., 2003. Nitric oxide-induced decrease in calcium sensitivity of resistance arteries is attributable to activation of the myosin light chain phosphatase and antagonized by the RhoA-Rho kinase pathway. *Circulation*, *107*(24), pp.3081-3087.

Born, G. V. R., 1962. Aggregation of blood platelets by adenosine diphosphate and its reversal. *Nature, 194*, pp.927–929.

Brass, L.F., Jiang, H., Wu, J., Stalker, T.J. and Zhu, L., 2006. Contact-dependent signaling events that promote thrombus formation. *Blood Cells, Molecules, and Diseases*, *36*(2), pp.157-161.

Brass, L.F., Zhu, L.I. and Stalker, T.J., 2005. Minding the gaps to promote thrombus growth and stability. *The Journal of Clinical Investigation*, *115*(12), pp.3385-3392.

Brass, L.F., Manning, D.R., Cichowski, K. and Abrams, C.S., 1997. Signaling through G proteins in platelets: to the integrins and beyond. *Thrombosis and Haemostasis*, *78*(1), pp.581-589.

Brill, A., Fuchs, T.A., Chauhan, A.K., Yang, J.J., De Meyer, S.F., Köllnberger, M., Wakefield, T.W., Lämmle, B., Massberg, S. and Wagner, D.D., 2011. von Willebrand factor–mediated platelet adhesion is critical for deep vein thrombosis in mouse models. *Blood*, *117*(4), pp.1400-1407.

Broos, K., Feys, H.B., De Meyer, S.F., Vanhoorelbeke, K. and Deckmyn, H., 2011. Platelets at work in primary hemostasis. *Blood Reviews*, *25*(4), pp.155-167.

Brunton, L.L., Hayes, J.S. and Mayer, S.E., 1981. Functional compartmentation of cyclic AMP and protein kinase in heart. *Advances in Cyclic Nucleotide Research*, *14*, pp.391-397.

Burgers, P.P., Ma, Y., Margarucci, L., Mackey, M., van der Heyden, M.A., Ellisman, M., Scholten, A., Taylor, S.S. and Heck, A.J., 2012. A small novel A-kinase anchoring protein (AKAP) that localizes specifically protein kinase A-regulatory subunit I (PKA-RI) to the plasma membrane. *Journal of Biological Chemistry*, *287*(52), pp.43789-43797.

Burgoyne, J.R. and Eaton, P., 2010. Oxidant sensing by protein kinases A and G enables integration of cell redox state with phosphoregulation. *Sensors*, *10*(4), pp.2731-2751.

Burkhart, J.M., Vaudel, M., Gambaryan, S., Radau, S., Walter, U., Martens, L., Geiger, J., Sickmann, A. and Zahedi, R.P., 2012. The first comprehensive and quantitative analysis of human platelet protein composition allows the comparative analysis of structural and functional pathways. *Blood*, *120*, pp.73-82.

Butler, T., Paul, J., Europe-Finner, N., Smith, R. and Chan, E.C., 2013. Role of serine-threonine phosphoprotein phosphatases in smooth muscle contractility. *American Journal of Physiology-Cell Physiology*, *304*(6), pp.C485-C504.

Butt, E., Abel, K., Krieger, M., Palm, D., Hoppe, V., Hoppe, J. and Walter, U., 1994. cAMP-and cGMP-dependent protein kinase phosphorylation sites of the focal adhesion vasodilator-stimulated phosphoprotein (VASP) in vitro and in intact human platelets. *Journal of Biological Chemistry*, *269*(20), pp.14509-14517.

Butt, E., Immler, D., Meyer, H.E., Kotlyarov, A., Laaß, K. and Gaestel, M., 2001. Heat Shock Protein 27 Is a Substrate of cGMP-dependent Protein Kinase in Intact Human Platelets phosphorylation-induced actin polymerization caused by HSP27 mutants. *Journal of Biological Chemistry*, *276*(10), pp.7108-7113.

Butt, E., Gambaryan, S., Göttfert, N., Galler, A., Marcus, K. and Meyer, H.E., 2003. Actin binding of human LIM and SH3 protein is regulated by cGMP-and cAMP-dependent protein kinase phosphorylation on serine 146. *Journal of Biological Chemistry*, *278*(18), pp.15601-15607.

Buxton, I.L. and Brunton, L.L., 1983. Compartments of cyclic AMP and protein kinase in mammalian cardiomyocytes. *Journal of Biological Chemistry*, *258*(17), pp.10233-10239.

Bye, A.P., Unsworth, A.J. and Gibbins, J.M., 2016. Platelet signaling: a complex interplay between inhibitory and activatory networks. *Journal of Thrombosis and Haemostasis*, *14*(5), pp.918-930.

Cadd, G. and McKnight, G.S., 1989. Distinct patterns of cAMP-dependent protein kinase gene expression in mouse brain. *Neuron*, *3*(1), pp.71-79.

Calejo, A.I.C. and Taskén, K., 2015. Targeting protein–protein interactions in complexes organized by A kinase anchoring proteins. *Frontiers in pharmacology*, *6*, p.192.

Cao, W., Mattagajasingh, S.N., Xu, H., Kim, K., Fierlbeck, W., Deng, J., Lowenstein, C.J. and Ballermann, B.J., 2002. TIMAP, a novel CAAX box protein regulated by TGF-β1 and expressed in endothelial cells. *American Journal of Physiology-Cell Physiology*, *283*(1), pp.C327-C337.

Carr, D.W., Stofko-Hahn, R.E., Fraser, I.D., Bishop, S.M., Acott, T.S., Brennan, R.G. and Scott, J.D., 1991. Interaction of the regulatory subunit (RII) of cAMP-dependent protein kinase with RII-anchoring proteins occurs through an amphipathic helix binding motif. *Journal of Biological Chemistry*, *266*(22), pp.14188-14192.

Carr, D.W., Stofko-Hahn, R.E., Fraser, I.D., Cone, R.D. and Scott, J.D., 1992. Localization of the cAMP-dependent protein kinase to the postsynaptic densities by A-kinase anchoring proteins. Characterization of AKAP 79. *Journal of Biological Chemistry*, *267*(24), pp.16816-16823.

Chaterjee, M., Huang, Z. and Zhang, W., 2011. Distinct platelet packaging, release and surface expression of proangiogenic and antiangiogenic factors upon different platelet stimuli. *Blood*, *117*, pp.3907-11.

Chauhan, A.K., Motto, D.G., Lamb, C.B., Bergmeier, W., Dockal, M., Plaimauer, B., Scheiflinger, F., Ginsburg, D. and Wagner, D.D., 2006. Systemic antithrombotic effects of ADAMTS13. *Journal of Experimental Medicine*, *203*(3), pp.767-776.

Chen, Y., Harry, A., Li, J., Smit, M.J., Bai, X., Magnusson, R., Pieroni, J.P., Weng, G. and Iyengar, R., 1997. Adenylyl cyclase 6 is selectively regulated by protein kinase A phosphorylation in a region involved in Gαs stimulation. *Proceedings of the National Academy of Sciences*, *94*(25), pp.14100-14104.

Chen, M. and Stracher, A., 1989. In situ phosphorylation of platelet actin-binding protein by cAMP-dependent protein kinase stabilizes it against proteolysis by calpain. *Journal of Biological Chemistry*, *264*(24), pp.14282-14289.

Chirkov, Y.Y. and Horowitz, J.D., 2007. Impaired tissue responsiveness to organic nitrates and nitric oxide: a new therapeutic frontier?. *Pharmacology andTherapeutics*, *116*(2), pp.287-305.

Chrzanowska-Wodnicka, M., Smyth, S.S., Schoenwaelder, S.M., Fischer, T.H. and White, G.C., 2005. Rap1b is required for normal platelet function and hemostasis in mice. *Journal of Clinical Investigation*, *115*(3), pp.680-687.

Cicmil, M., Thomas, J.M., Leduc, M., Bon, C. and Gibbins, J.M., 2002. Platelet endothelial cell adhesion molecule-1 signaling inhibits the activation of human platelets. *Blood*, 99(1), pp.137-144.

Clark, K., Langeslag, M., Figdor, C.G. and van Leeuwen, F.N., 2007. Myosin II and mechanotransduction: a balancing act. *Trends in Cell Biology*, *17*(4), pp.178-186.

Clemetson, K.J., 2012. Platelets and primary haemostasis. *Thrombosis Research*, *129*(3), pp.220-224.

Coghlan, V.M., Perrino, B.A., Howard, M., Langeberg, L.K., Hicks, J.B., Gallatin, W.M. and Scott, J.D., 1995. Association of protein kinase A and protein phosphatase 2B with a common anchoring protein. *Science*, *267*(5194), pp.108-111.

Cohen, P.T., 2002. Protein phosphatase 1–targeted in many directions. *Journal of Cell Science*, *115*(2), pp.241-256.

Corbin, J.D., Keely, S.L. and Park, C.R., 1975. The distribution and dissociation of cyclic adenosine 3': 5'-monophosphate-dependent protein kinases in adipose, cardiac, and other tissues. *Journal of Biological Chemistry*, *250*(1), pp.218-225.

Corbin, J.D., Soderling, T.R. and Park, C.R., 1973. Regulation of adenosine 3', 5'-monophosphate-dependent protein kinase I. Preliminary characterization of the adipose tissue enzyme in crude extracts. *Journal of Biological Chemistry*, *248*(5), pp.1813-1821.

Corbin, J.D., Sugden, P.H., Lincoln, T.M. and Keely, S.L., 1977. Compartmentalization of adenosine 3': 5'-monophosphate and adenosine 3': 5'-monophosphate-dependent protein kinase in heart tissue. *Journal of Biological Chemistry*, *252*(11), pp.3854-3861.

Corbin, J.D., Turko, I.V., Beasley, A. and Francis, S.H., 2000. Phosphorylation of phosphodiesterase-5 by cyclic nucleotide-dependent protein kinase alters its catalytic and allosteric cGMP-binding activities. *The FEBS Journal*, *267*(9), pp.2760-2767.

Coxon, C.H., Geer, M.J. and Senis, Y.A., 2017. ITIM receptors: more than just inhibitors of platelet activation. *Blood, 129*(26), pp.3407-3418.

Crittenden, J.R., Bergmeier, W., Zhang, Y., Piffath, C.L., Liang, Y., Wagner, D.D., Housman, D.E. and Graybiel, A.M., 2004. CalDAG-GEFI integrates signaling for platelet aggregation and thrombus formation. *Nature Medicine*, *10*(9), pp.982-986.

Dangel, O., Mergia, E., Karlisch, K., Groneberg, D., Koesling, D. and Friebe, A., 2010. Nitric oxide-sensitive guanylyl cyclase is the only nitric oxide receptor mediating platelet inhibition. *Journal of Thrombosis and Haemostasis*, *8*(6), pp.1343-1352.

Daniel, J.L., Molish, I.R., Rigmaiden, M. and Stewart, G., 1984. Evidence for a role of myosin phosphorylation in the initiation of the platelet shape change response. *Journal of Biological Chemistry*, *259*(15), pp.9826-9831.

Danielewski, O., Schultess, J. and Smolenski, A., 2005. The NO/cGMP pathway inhibits Rap1 activation in human platelets via cGMP-dependent protein kinase I. *Thrombosis and Haemostasis*, *94*(02), pp.319-325.

Davi, G., Patrono, C., 2007. Platelet activation and atherothrombosis. *The New England Journal of Medicine*, *357*(24), pp.2482-2494.

De Meyer, S.F., Deckmyn, H. and Vanhoorelbeke, K., 2009. von Willebrand factor to the rescue. *Blood*, *113*(21), pp.5049-5057.

Dessauer, C.W., Chen-Goodspeed, M. and Chen, J., 2002. Mechanism of Gαi-mediated inhibition of type V adenylyl cyclase. *Journal of Biological Chemistry*, *277*(32), pp.28823-28829.

Deviller, P., Valuer, P., Bata, J. and Saez, J.M., 1984. Distribution and characterization of cAMP-dependent protein kinase isoenzymes in bovine adrenal cells. *Molecular and Cellular Endocrinology*, *38*(1), pp.21-30.

Di Benedetto, G., Zoccarato, A., Lissandron, V., Terrin, A., Li, X., Houslay, M.D., Baillie, G.S. and Zaccolo, M., 2008. Protein kinase A type I and type II define distinct intracellular signaling compartments. *Circulation Research*, *103*(8), pp.836-844.

Diagouraga, B., Grichine, A., Fertin, A., Wang, J., Khochbin, S. and Sadoul, K., 2014. Motor-driven marginal band coiling promotes cell shape change during platelet activation. J Cell Biol, 204(2), pp.177-185.

Dirksen, W.P., Vladic, F. and Fisher, S.A., 2000. A myosin phosphatase targeting subunit isoform transition defines a smooth muscle developmental phenotypic switch. *American Journal of Physiology-Cell Physiology*, *278*(3), pp.C589-C600.

Dippold, R.P. and Fisher, S.A., 2014. Myosin phosphatase isoforms as determinants of smooth muscle contractile function and calcium sensitivity of force production. *Microcirculation*, *21*(3), pp.239-248.

Diviani, D., Langeberg, L.K., Doxsey, S.J. and Scott, J.D., 2000. Pericentrin anchors protein kinase A at the centrosome through a newly identified RII-binding domain. *Current Biology*, *10*(7), pp.417-420.

Donnellan, P.D. and Kinsella, B.T., 2009. Immature and mature species of the human Prostacyclin Receptor are ubiquitinated and targeted to the 26S proteasomal or lysosomal degradation pathways, respectively. *Journal of Molecular Signaling*, *4*(1), p.7.

Dopheide, S.M., Maxwell, M.J. and Jackson, S.P., 2002. Shear-dependent tether formation during platelet translocation on von Willebrand factor. *Blood*, *99*(1), pp.159-167.

Dutta-Roy, A.K. and Sinha, A.K., 1987. Purification and properties of prostaglandin E1/prostacyclin receptor of human blood platelets. *Journal of Biological Chemistry*, *262*(26), pp.12685-12691.

Eigenthaler, M., Nolte, C., Halbrugge, M. and Walter, U., 1992. Concentration and regulation of cyclic nucleotides, cyclic-nucleotide-dependent protein kinases and one of their major substrates in human platelets. *The FEBS Journal*, *205*(2), pp.471-481.

El-Daher, S.S., Eigenthaler, M., Walter, U., Furuichi, T., Miyawaki, A., Mikoshiba, K., Kakkar, V.V. and Authi, K.S., 1996. Distribution and activation of cAMP-and cGMP-dependent protein kinases in highly purified human platelet plasma and intracellular membranes. *Thrombosis and Haemostasis*, *76*(6), pp.1063-1071.

El-Daher, S.S., Patel, Y., Siddiqua, A., Hassock, S., Edmunds, S., Maddison, B., Patel, G., Goulding, D., Lupu, F., Wojcikiewicz, R.J. and Authi, K.S., 2000. Distinct localization and function of 1, 4, 5 IP3 receptor subtypes and the 1, 3, 4, 5 IP4 receptor GAP1 IP4BP in highly purified human platelet membranes. *Blood*, *95*(11), pp.3412-3422.

Eto, M., 2009. Regulation of cellular protein phosphatase-1 (PP1) by phosphorylation of the CPI-17 family, C-kinase-activated PP1 inhibitors. *Journal of Biological Chemistry*, *284*(51), pp.35273-35277.

Farndale, R.W., Sixma, J.J., Barnes, M.J. and De Groot, P.G., 2004. The role of collagen in thrombosis and hemostasis. *Journal of Thrombosis and Haemostasis*, *2*(4), pp.561-573.

Feil, R., Lohmann, S.M., de Jonge, H., Walter, U. and Hofmann, F., 2003. Cyclic GMP-dependent protein kinases and the cardiovascular system. *Circulation Research*, *93*(10), pp.907-916.

Feliciello, A., Gallo, A., Mele, E., Porcellini, A., Troncone, G., Garbi, C., Gottesman, M.E. and Avvedimento, E.V., 2000. The localization and activity of cAMP-dependent protein kinase affect cell cycle progression in thyroid cells. *Journal of Biological Chemistry*, *275*(1), pp.303-311.

Feliciello, A., Li, Y., Avvedimento, E.V., Gottesman, M.E. and Rubin, C.S., 1997. A-kinase anchor protein 75 increases the rate and magnitude of cAMP signaling to the nucleus. *Current Biology*, *7*(12), pp.1011-1014.

Fisher, S.A., 2010. Vascular smooth muscle phenotypic diversity and function. *Physiological Genomics*, *42*(3), pp.169-187.

Flaumenhaft, R., 2003. Molecular basis of platelet granule secretion. *Arteriosclerosis, Thrombosis, and Vascular Biology*, *23*(7), pp.1152-1160.

Flaumenhaft, R. and Koseoglu, S., 2016. Platelet contents. *In*: Schulz, H. And Italiano, J. (ed.) *Molecular and Cellular Biology of Platelet Formation* (pp. 133-152). Springer International Publishing.

Foster, C.J., Prosser, D.M., Agans, J.M., Zhai, Y., Smith, M.D., Lachowicz, J.E., Zhang, F.L., Gustafson, E., Monsma Jr, F.J., Wiekowski, M.T. and Abbondanzo, S.J., 2001. Molecular identification and characterization of the platelet ADP receptor targeted by thienopyridine antithrombotic drugs. *Journal of Clinical Investigation*, *107*(12), pp.1591-1598.

Fox, J.E. and Berndt, M.C., 1989. Cyclic AMP-dependent phosphorylation of glycoprotein Ib inhibits collagen-induced polymerization of actin in platelets. *Journal of Biological Chemistry*, *264*(16), pp.9520-9526.

Fox, J.E., and Phillips, D.R., 1983. Polymerization and organization of actin filaments within platelets. *Seminars in Hematology*, *20*(4), pp.243–260.

Francis, S.H., Blount, M.A. and Corbin, J.D., 2011. Mammalian cyclic nucleotide phosphodiesterases: molecular mechanisms and physiological functions. *Physiological Reviews*, *91*(2), pp.651-690.

Francis, S.H., Busch, J.L. and Corbin, J.D., 2010. cGMP-dependent protein kinases and cGMP phosphodiesterases in nitric oxide and cGMP action. *Pharmacological Reviews*, *62*(3), pp.525-563.

Francis, S.H. and Corbin, J.D., 1994. Structure and function of cyclic nucleotide-dependent protein kinases. *Annual Review of Physiology*, *56*(1), pp.237-272.

Frangos, J.A., Eskin, S.G., McIntire, L.V. and Ives, C.L., 1985. Flow effects on prostacyclin production by cultured human endothelial cells. *Science*, *227*(4693), pp.1477-1480.

Franke, B., Akkerman, J.W.N. and Bos, J.L., 1997. Rapid Ca^{2+}-mediated activation of Rap1 in human platelets. *The EMBO Journal*, *16*(2), pp.252-259.

Fraser, I.D. and Scott, J.D., 1999. Modulation of ion channels: a “current” view of AKAPs. *Neuron*, *23*(3), pp.423-426.

Freedman, J.E., Loscalzo, J., Barnard, M.R., Alpert, C., Keaney, J.F. and Michelson, A.D., 1997. Nitric oxide released from activated platelets inhibits platelet recruitment. *Journal of Clinical Investigation*, *100*(2), pp.350-356.

Friebe, A. and Koesling, D., 2003. Regulation of nitric oxide-sensitive guanylyl cyclase. *Circulation Research*, *93*(2), pp.96-105.

Fu, K., Mende, Y., Bhetwal, B.P., Baker, S., Perrino, B.A., Wirth, B. and Fisher, S.A., 2012. Tra2β protein is required for tissue-specific splicing of a smooth muscle myosin phosphatase targeting subunit alternative exon. *Journal of Biological Chemistry*, *287*(20), pp.16575-16585.

Fujioka, M., Takahashi, N., Odai, H., Araki, S., Ichikawa, K., Feng, J., Nakamura, M., Kaibuchi, K., Hartshorne, D.J., Nakano, T. and Ito, M., 1998. A new isoform of human myosin phosphatase targeting/regulatory subunit (MYPT2): cDNA cloning, tissue expression, and chromosomal mapping. *Genomics*, *49*(1), pp.59-68.

Fukami, M. H., Holmsen, H., Kowalska, M. A., Niewiarowski, S., 2001. Platelet secretion. In R. W. Colman, J. Hirsch, V. J. Marder, A. W. Clowes, & J. N. George (Eds.), *Hemostasis and Thrombosis: Basic Principles and Clinical Practice* (4th.ed., pp. 516–573). Philadelphia: Lippincott Williams &Wilkins.

Fukata, Y., Kimura, K., Oshiro, N., Saya, H., Matsuura, Y. and Kaibuchi, K., 1998. Association of the myosin-binding subunit of myosin phosphatase and moesin: dual regulation of moesin phosphorylation by Rho-associated kinase and myosin phosphatase. *The Journal of Cell Biology*, *141*(2), pp.409-418.

Fox, J.E., 2001. Cytoskeletal proteins and platelet signaling. *Thrombosis and Haemostasis*, *86*(1), pp.198-213.

Fox, J.E., 1993. The platelet cytoskeleton. *Thrombosis and Haemostasis*, *70*(6), pp.884-893.

Gailly, P., Wu, X., Haystead, T.A., Somlyo, A.P., Cohen, P.T., Cohen, P. and Somlyo, A.V., 1996. Regions of the 110-kDa Regulatory Subunit M110 Required for Regulation of Myosin-Light-Chain-Phosphatase Activity in Smooth Muscle. *The FEBS Journal*, *239*(2), pp.326-332.

Galler, A.B., Arguinzonis, M.I.G., Baumgartner, W., Kuhn, M., Smolenski, A., Simm, A. and Reinhard, M., 2006. VASP-dependent regulation of actin

cytoskeleton rigidity, cell adhesion, and detachment. *Histochemistry and Cell Biology*, *125*(5), pp.457-474.

Gambaryan, S., Friebe, A. and Walter, U., 2012. Does the NO/sGC/cGMP/PKG pathway play a stimulatory role in platelets?. *Blood*, *119*(22), pp.5335-5336. author reply 5336–5337.

Gambaryan, S., Geiger, J., Schwarz, U.R., Butt, E., Begonja, A., Obergfell, A. and Walter, U., 2004. Potent inhibition of human platelets by cGMP analogs independent of cGMP-dependent protein kinase. *Blood*, *103*(7), pp.2593-2600.

Gambaryan, S., Kobsar, A., Hartmann, S., Birschmann, I., Kuhlencordt, P.J., Müller-Esterl, W., Lohmann, S.M. and Walter, U., 2008. NO-synthase-/NO-independent regulation of human and murine platelet soluble guanylyl cyclase activity. *Journal of Thrombosis and Haemostasis*, *6*(8), pp.1376-1384.

Gambaryan, S., Kobsar, A., Rukoyatkina, N., Herterich, S., Geiger, J., Smolenski, A., Lohmann, S.M. and Walter, U., 2010. Thrombin and collagen induce a feedback inhibitory signaling pathway in platelets involving dissociation of the catalytic subunit of protein kinase a from an NFκB-IκB complex. *Journal of Biological Chemistry*, *285*(24), pp.18352-18363.

Gao, T., Yatani, A., Dell'Acqua, M.L., Sako, H., Green, S.A., Dascal, N., Scott, J.D. and Hosey, M.M., 1997. cAMP-dependent regulation of cardiac L-type Ca 2+ channels requires membrane targeting of PKA and phosphorylation of channel subunits. *Neuron*, *19*(1), pp.185-196.

Garcia, A., Kim, S., Bhavaraju, K., Schoenwaelder, S.M. and Kunapuli, S.P., 2010. Role of phosphoinositide 3-kinase β in platelet aggregation and thromboxane A2 generation mediated by Gi signalling pathways. *Biochemical Journal*, *429*(2), pp.369-377.

Gautier, R., Douguet, D., Antonny, B. and Drin, G., 2008. HELIQUEST: a web server to screen sequences with specific α-helical properties. *Bioinformatics*, *24*(18), pp.2101-2102.

Geer, M.J., van Geffen, J.P., Gopalasingam, P., Vögtle, T., Smith, C.W., Heising, S., Kuijpers, M.J., Tullemans, B.M., Jarvis, G.E., Eble, J.A. and Jeeves, M., 2018. Uncoupling ITIM receptor G6b-B from tyrosine phosphatases Shp1 and Shp2 disrupts murine platelet homeostasis. *blood, 132*(13), pp.1413-1425.

Getz, T.M., Dangelmaier, C.A., Jin, J., Daniel, J.L. and Kunapuli, S.P., 2010. Differential phosphorylation of myosin light chain (Thr) 18 and (Ser) 19 and functional implications in platelets. *Journal of Thrombosis and Haemostasis*, *8*(10), pp.2283-2293.

Giguère, V., Gallant, M.A., de Brum-Fernandes, A.J. and Parent, J.L., 2004. Role of extracellular cysteine residues in dimerization/oligomerization of the human prostacyclin receptor. *European Journal of Pharmacology*, *494*(1), pp.11-22.

Given, A.M., Ogut, O. and Brozovich, F.V., 2007. MYPT1 mutants demonstrate the importance of aa888–928 for the interaction with PKGIα. *American Journal of Physiology-Cell Physiology*, *292*(1), pp.C432-C439.

Gkaliagkousi, E., Ritter, J. and Ferro, A., 2007. Platelet-derived nitric oxide signaling and regulation. *Circulation Research*, *101*(7), pp.654-662.

Gogstad, G. O., Hagen, I., Krutnes, M. B., Solum, N. O., 1982. Dissociation of the Glycoprotein IIB-IIIA complex in isolated human platelet membranes - Dependence of pH and divalent cations. *Biochimica et Biophysica Acta, 689*(1), pp.21-30.

Golebiewska, E.M. and Poole, A.W., 2015. Platelet secretion: From haemostasis to wound healing and beyond. *Blood Reviews*. *29*(3), pp.153–162.

Gong, H., Shen, B., Flevaris, P., Chow, C., Lam, S.C.T., Voyno-Yasenetskaya, T.A., Kozasa, T. and Du, X., 2010. G protein subunit Gα13 binds to integrin αIIbβ3 and mediates integrin "outside-in" signaling. *Science*, *327*(5963), pp.340-343.

Gopalakrishna, R., Chen, Z.H. and Gundimeda, U., 1993. Nitric oxide and nitric oxide-generating agents induce a reversible inactivation of protein kinase C activity and phorbol ester binding. *Journal of Biological Chemistry*, *268*(36), pp.27180-27185.

Goto, S., Ikeda, Y., Saldívar, E. and Ruggeri, Z.M., 1998. Distinct mechanisms of platelet aggregation as a consequence of different shearing flow conditions. *Journal of Clinical Investigation*, *101*(2), pp.479-486.

Goto, S., Salomon, D.R., Ikeda, Y. and Ruggeri, Z.M., 1995. Characterization of the unique mechanism mediating the shear-dependent binding of soluble von Willebrand factor to platelets. *Journal of Biological Chemistry*, *270*(40), pp.23352-23361.

Grant, P.G., Mannarino, A.F. and Colman, R.W., 1988. cAMP-mediated phosphorylation of the low-Km cAMP phosphodiesterase markedly stimulates its catalytic activity. *Proceedings of the National Academy of Sciences*, *85*(23), pp.9071-9075.

Grassie, M.E., Moffat, L.D., Walsh, M.P. and MacDonald, J.A., 2011. The myosin phosphatase targeting protein (MYPT) family: a regulated mechanism for achieving substrate specificity of the catalytic subunit of protein phosphatase type 1δ. *Archives of Biochemistry and Biophysics*, *510*(2), pp.147-159.

Grassie, M.E., Sutherland, C., Ulke-Lemée, A., Chappellaz, M., Kiss, E., Walsh, M.P. and MacDonald, J.A., 2012. Cross-talk between Rho-associated kinase and cyclic nucleotide-dependent kinase signaling pathways in the regulation of smooth muscle myosin light chain phosphatase. *Journal of Biological Chemistry*, *287*(43), pp.36356-36369.

Gresele, P., Momi, S. and Falcinelli, E., 2011. Anti-platelet therapy: phosphodiesterase inhibitors. *British Journal of Clinical Pharmacology*, *72*(4), pp.634-646.

Gurbel, P.A., Kuliopulos, A. and Tantry, U.S., 2015. G-protein–coupled receptors signaling pathways in new antiplatelet drug development. *Arteriosclerosis, Thrombosis, and Vascular Biology*, *35*(3), pp.500-512.

Haas, S., Hansson, J., Klimmeck, D., Loeffler, D., Velten, L., Uckelmann, H., Wurzer, S., Prendergast, Á.M., Schnell, A., Hexel, K. and Santarella-Mellwig, R., 2015. Inflammation-induced emergency megakaryopoiesis driven by hematopoietic stem cell-like megakaryocyte progenitors. Cell stem cell, 17(4), pp.422-434.

Halbrügge, M., Friedrich, C., Eigenthaler, M., Schanzenbächer, P. and Walter, U., 1990. Stoichiometric and reversible phosphorylation of a 46-kDa protein in human platelets in response to cGMP-and cAMP-elevating vasodilators. *Journal of Biological Chemistry*, *265*(6), pp.3088-3093.

Halbrügge, M. and Walter, U., 1989. Purification of a vasodilator-regulated phosphoprotein from human platelets. *The FEBS Journal*, *185*(1), pp.41-50.

Harbeck, B., Hüttelmaier, S., Schlüter, K., Jockusch, B.M. and Illenberger, S., 2000. Phosphorylation of the vasodilator-stimulated phosphoprotein regulates its interaction with actin. *Journal of Biological Chemistry*, *275*(40), pp.30817-30825.

Hartshorne, D.J., Ito, M. and Erdödi, F., 2004. Role of protein phosphatase type 1 in contractile functions: myosin phosphatase. *Journal of Biological Chemistry*, *279*(36), pp.37211-37214.

Hartshorne, D.J., Ito, M. and Erdo, F., 1998. Myosin light chain phosphatase: subunit composition, interactions and regulation. *Journal of Muscle Research and Cell Motility*, *19*(4), pp.325-341.

Hartwig, J. H., 2013. In *Platelets* (Michelson, A. D., ed.) 3rd Ed., pp. 145–168, Academic Press, London.

Haslam, R.J., Dickinson, N.T. and Jang, E.K., 1999. Cyclic nucleotides and phosphodiesterases in platelets. *Thrombosis and Haemostasis*, *82*(2), pp.412-423.

Hathaway, D.R., Eaton, C.R. and Adelstein, R.S., 1981. Regulation of human platelet myosin light chain kinase by the catalytic subunit of cyclic AMP-dependent protein kinase. *Nature*, *291*(5812), pp.252-254.

Hauser, W., Knobeloch, K.P., Eigenthaler, M., Gambaryan, S., Krenn, V., Geiger, J., Glazova, M., Rohde, E., Horak, I., Walter, U. and Zimmer, M., 1999. Megakaryocyte hyperplasia and enhanced agonist-induced platelet activation in vasodilator-stimulated phosphoprotein knockout mice. *Proceedings of the National Academy of Sciences*, *96*(14), pp.8120-8125.

Hata, Y., Kaibuchi, K., Kawamura, S., Hiroyoshi, M., Shirataki, H. and Takai, Y., 1991. Enhancement of the actions of smg p21 GDP/GTP exchange protein by the protein kinase A-catalyzed phosphorylation of smg p21. *Journal of Biological Chemistry*, *266*(10), pp.6571-6577.

Hayes, J.S., Brunton, L.L. and Mayer, S.E., 1980. Selective activation of particulate cAMP-dependent protein kinase by isoproterenol and prostaglandin E1. *Journal of Biological Chemistry*, *255*(11), pp.5113-5119.

Hayes, J.S., Lawler, O.A., Walsh, M.T. and Kinsella, B.T., 1999. The Prostacyclin Receptor Is Isoprenylated isoprenylation is required for efficient receptor-effector coupling. *Journal of Biological Chemistry*, *274*(34), pp.23707-23718.

Hettasch, J.M. and Sellers, J.R., 1991. Caldesmon phosphorylation in intact human platelets by cAMP-dependent protein kinase and protein kinase C. *Journal of Biological Chemistry*, *266*(18), pp.11876-11881.

Hidaka, H. and Asano, T., 1976. Human blood platelet 3′: 5′-cyclic nucleotide phosphodiesterase: isolation of low-Km and high-Km

phosphodiesterase. *Biochimica et Biophysica Acta (BBA)-Enzymology*, *429*(2), pp.485-497.

Hirano, K., Derkach, D.N., Hirano, M., Nishimura, J. and Kanaide, H., 2003. Protein kinase network in the regulation of phosphorylation and dephosphorylation of smooth muscle myosin light chain. *Molecular and Cellular Biochemistry*, *248*(1-2), pp.105-114.

Hirano, K., Phan, B.C. and Hartshorne, D.J., 1997. Interactions of the subunits of smooth muscle myosin phosphatase. *Journal of Biological Chemistry*, *272*(6), pp.3683-3688.

Hirano, M., Niiro, N., Hirano, K., Nishimura, J., Hartshorne, D.J. and Kanaide, H., 1999. Expression, subcellular localization, and cloning of the 130-kDa regulatory subunit of myosin phosphatase in porcine aortic endothelial cells. *Biochemical and Biophysical Research Communications*, *254*(2), pp.490-496.

Hoffmeister, M., Riha, P., Neumüller, O., Danielewski, O., Schultess, J. and Smolenski, A.P., 2008. Cyclic nucleotide-dependent protein kinases inhibit binding of 14-3-3 to the GTPase-activating protein Rap1GAP2 in platelets. *Journal of Biological Chemistry*, *283*(4), pp.2297-2306.

Hofmann, F., Bernhard, D., Lukowski, R. and Weinmeister, P., 2009. cGMP regulated protein kinases (cGK). In *cGMP: Generators, Effectors and Therapeutic Implications* (pp. 137-162). Springer Berlin Heidelberg.

Horstrup, K., Jablonka, B., Hönig-Liedl, P., Just, M., Kochsiek, K. and Walter, U., 1994. Phosphorylation of Focal Adhesion Vasodilator-Stimulated Phosphoprotein at Ser157 in Intact Human Platelets Correlates with Fibrinogen Receptor Inhibition. *The FEBS Journal*, *225*(1), pp.21-27.

Hou, Y., Carrim, N., Wang, Y., Gallant, R.C., Marshall, A. and Ni, H., 2015. Platelets in hemostasis and thrombosis: novel mechanisms of fibrinogen-independent platelet aggregation and fibronectin-mediated protein wave of hemostasis. *Journal of Biomedical Research*, *29*(6), pp.437-444.

Hoylaerts, M.F., Yamamoto, H., Nuyts, K., Vreys, I., Deckmyn, H., Vermylen, J., 1997. von Willebrand factor binds to native collagen VI primarily via its A1 domain. *Biochemical Journal,324*(Pt1), pp.185–191.

Huang, Q.Q., Fisher, S.A. and Brozovich, F.V., 2004. Unzipping the role of myosin light chain phosphatase in smooth muscle cell relaxation. *Journal of Biological Chemistry*, *279*(1), pp.597-603.

Huang, Y.A., Kao, J.W., Tseng, D.T.H., Chen, W.S., Chiang, M.H. and Hwang, E., 2013. Microtubule-associated type II protein kinase A is important for neurite elongation. *PLoS One*, *8*(8), p.e73890.

Hunter, R.W., MacKintosh, C. and Hers, I., 2009. Protein kinase C-mediated phosphorylation and activation of PDE3A regulate cAMP levels in human platelets. *Journal of Biological Chemistry*, *284*(18), pp.12339-12348.

Hurley, J.H., 1999. Structure, mechanism, and regulation of mammalian adenylyl cyclase. *Journal of Biological Chemistry*, *274*(12), pp.7599-7602.

Ichikawa, K., Hirano, K., Ito, M., Tanaka, J., Nakano, T. and Hartshorne, D.J., 1996. Interactions and properties of smooth muscle myosin phosphatase. *Biochemistry*, *35*(20), pp.6313-6320.

Inagaki, N., Nishizawa, M., Ito, M., Fujioka, M., Nakano, T., Tsujino, S., Matsuzawa, K., Kimura, K., Kaibuchi, K. and Inagaki, M., 1997. Myosin binding subunit of smooth muscle myosin phosphatase at the cell-cell adhesion sites in MDCK cells. *Biochemical and Biophysical Research Communications*, *230*(3), pp.552-556.

Italiano, J.E., Richardson, J.L., Patel-Hett, S., Battinelli, E., Zaslavsky, A., Short, S., Ryeom, S., Folkman, J. and Klement, G.L., 2008. Angiogenesis is regulated by a novel mechanism: pro-and antiangiogenic proteins are organized into separate platelet α granules and differentially released. *Blood, 111*(3), pp.1227-1233.

Ito, M., Feng, J., Tsujino, S., Inagaki, N., Inagaki, M., Tanaka, J., Ichikawa, K., Hartshorne, D.J. and Nakano, T., 1997. Interaction of smooth muscle myosin phosphatase with phospholipids. *Biochemistry*, *36*(24), pp.7607-7614.

Ito, M., Nishikawa, M., Fujioka, M., Miyahara, M., Isaka, N., Shiku, H. & Nakano, T., 1996. Characterization of the isoenzymes of cyclic nucleotide phosphodiesterase in human platelets and the effects of E4021. *Cell Signal, 8*(8), pp.575-581.

Ito, M., Nakano. T., Erdodi, F., Hartshorne, D.J., 2004. Myosin phosphatase: structure, regulation and function. *Molecular and Cellular Biochemistry,* 259(1–2), pp.197–209.

Jackson, S.P., 2007. The growing complexity of platelet aggregation. *Blood*, *109*(12), pp.5087-5095.

Jaffe, A.B. and Hall, A., 2005. Rho GTPases: biochemistry and biology. *Annual Review of Cell and Developmental Biology*, *21*, pp.247-269.

Jarnæss, E., Ruppelt, A., Stokka, A.J., Lygren, B., Scott, J.D. and Taskén, K., 2008. Dual specificity A-kinase anchoring proteins (AKAPs) contain an additional binding region that enhances targeting of protein kinase A type I. *Journal of Biological Chemistry*, *283*(48), pp.33708-33718.

Jay, D., García, E.J. and de la Luz Ibarra, M., 2004. In situ determination of a PKA phosphorylation site in the C-terminal region of filamin. *Molecular and Cellular Biochemistry*, *260*(1), pp.49-53.

Johnson, D., Cohen, P., Chen, M.X., Chen, Y.H. and Cohen, P.T., 1997. Identification of the regions on the M110 subunit of protein phosphatase 1M that interact with the M21 subunit and with myosin. *The FEBS Journal*, *244*(3), pp.931-939.

Johnson, D.A., Akamine, P., Radzio-Andzelm, E., Madhusudan, and Taylor, S.S., 2001. Dynamics of cAMP-dependent protein kinase. *Chemical Reviews*, *101*(8), pp.2243-2270.

Johnson, G.J., Leis, L.A., Krumwiede, M.D. and White, J.G., 2007. The critical role of myosin IIA in platelet internal contraction. *Journal of Thrombosis and Haemostasis*, *5*(7), pp.1516-1529.

Joo, E.E. and Yamada, K.M., 2014. MYPT1 regulates contractility and microtubule acetylation to modulate integrin adhesions and matrix assembly. *Nature Communications*, *5*, p.3510.

Jung, S.M., Moroi, M., Soejima, K., Nakagaki, T., Miura, Y., Berndt, M.C., Gardiner, E.E., Howes, J.M., Pugh, N., Bihan, D. and Watson, S.P., 2012. Constitutive dimerization of glycoprotein VI (GPVI) in resting platelets is essential for binding to collagen and activation in flowing blood. *Journal of Biological Chemistry*, 287, pp.30000-30013.

Kahn, N.N., Mueller, H.S. and Sinha, A.K., 1990. Impaired prostaglandin E1/I2 receptor activity of human blood platelets in acute ischemic heart disease. *Circulation Research*, *66*(4), pp.932-940.

Kahner, B.N., Shankar, H., Murugappan, S., Prasad, G.L. and Kunapuli, S.P., 2006. Nucleotide receptor signaling in platelets. *Journal of Thrombosis and Haemostasis*, *4*(11), pp.2317-2326.

Kaneko-Kawano, T., Takasu, F., Naoki, H., Sakumura, Y., Ishii, S., Ueba, T., Eiyama, A., Okada, A., Kawano, Y. and Suzuki, K., 2012. Dynamic regulation of myosin light chain phosphorylation by Rho-kinase. *PLoS One*, *7*(6), pp.e39269-e39269.

Kapiloff, M.S., Rigatti, M. and Dodge-Kafka, K.L., 2014. Architectural and functional roles of A kinase–anchoring proteins in cAMP microdomains. *The Journal of General Physiology*, *143*(1), pp.9-15.

Karim, S.M., Rhee, A.Y., Given, A.M., Faulx, M.D., Hoit, B.D. and Brozovich, F.V., 2004. Vascular Reactivity in Heart Failure. *Circulation Research*, *95*(6), pp.612-618.

Kasa, A., Gorshkov, B., Kumar, S., Dimitropoulou, C., Catravas, J., Black, S. and Verin, A., 2015. The role of myosin phosphatase in pulmonary vascular endothelial barrier preservation in vivo. *The FASEB Journal*, *29*(1 Supplement), pp.797-799.

Kaushansky, K., 2006. Lineage-specific hematopoietic growth factors. *New England Journal of Medicine*, *354*(19), pp.2034-2045.

Khasnis, M., Nakatomi, A., Gumpper, K. and Eto, M., 2014. Reconstituted human myosin light chain phosphatase reveals distinct roles of two inhibitory phosphorylation sites of the regulatory subunit, MYPT1. *Biochemistry*, *53*(16), pp.2701-2709.

Khatri, J.J., Joyce, K.M., Brozovich, F.V. and Fisher, S.A., 2001. Role of myosin phosphatase isoforms in cGMP-mediated smooth muscle relaxation. *Journal of Biological Chemistry*, *276*(40), pp.37250-37257.

Khromov, A., Choudhury, N., Stevenson, A.S., Somlyo, A.V. and Eto, M., 2009. Phosphorylation-dependent autoinhibition of myosin light chain phosphatase accounts for Ca2+ sensitization force of smooth muscle contraction. *Journal of Biological Chemistry*, *284*(32), pp.21569-21579.

Kim, K.M., Csortos, C., Czikora, I., Fulton, D., Umapathy, N.S., Olah, G. and Verin, A.D., 2012. Molecular characterization of myosin phosphatase in endothelium. *Journal of Cellular Physiology*, *227*(4), pp.1701-1708.

Kimura, K., Ito, M., Amano, M., Chihara, K., Fukata, Y., Nakafuku, M., Yamamori, B., Feng, J., Nakano, T., Okawa, K. and Iwamatsu, A., 1996. Regulation of myosin phosphatase by Rho and Rho-associated kinase (Rho-kinase). *Science*, *273*(5272), pp.245-248.

Kirchmaier, C.M. and Pillitteri, D., 2010. Diagnosis and management of inherited platelet disorders. *Transfusion Medicine and Hemotherapy*, *37*(5), pp.237-246.

Kiss, A., Lontay, B., Bécsi, B., Márkász, L., Oláh, É., Gergely, P. and Erdődi, F., 2008. Myosin phosphatase interacts with and dephosphorylates the retinoblastoma protein in THP-1 leukemic cells: its inhibition is involved in the attenuation of daunorubicin-induced cell death by calyculin-A. *Cellular Signalling*, *20*(11), pp.2059-2070.

Kitazawa, T., Eto, M., Woodsome, T.P. and Khalequzzaman, M.D., 2003. Phosphorylation of the myosin phosphatase targeting subunit and CPI-17 during calcium sensitization in rabbit smooth muscle. *The Journal of Physiology*, *546*(3), pp.879-889.

Kitazawa, T., Semba, S., Huh, Y.H., Kitazawa, K. and Eto, M., 2009. Nitric oxide-induced biphasic mechanism of vascular relaxation via dephosphorylation of CPI-17 and MYPT1. *The Journal of Physiology*, *587*(14), pp.3587-3603.

Klages, B., Brandt, U., Simon, M.I., Schultz, G. and Offermanns, S., 1999. Activation of G12/G13 results in shape change and Rho/Rho-kinase–mediated myosin light chain phosphorylation in mouse platelets. *The Journal of Cell Biology*, *144*(4), pp.745-754.

Knighton, D.R. and Zheng, J., 1991. Crystal Structure of the Catalytic Subunit of Cyclic Adenosine Monophosphate--Dependent Protein Kinase. *Science*, *253*(5018), pp.407-414.

Kodigepalli, K.M., Bowers, K., Sharp, A. and Nanjundan, M. 2015. Roles and regulation of phospholipid scramblases. *FEBS letters*,*589*(1),pp.3–14.

Koga, Y. and Ikebe, M., 2008. A novel regulatory mechanism of myosin light chain phosphorylation via binding of 14-3-3 to myosin phosphatase. *Molecular Biology of The Cell*, *19*(3), pp.1062-1071.

Kovanich, D., van der Heyden, M.A., Aye, T.T., van Veen, T.A., Heck, A.J. and Scholten, A., 2010. Sphingosine Kinase Interacting Protein is an A-Kinase

Anchoring Protein Specific for Type I cAMP-Dependent Protein Kinase. *Chembiochem*, *11*(7), pp.963-971.

Kulkarni, S., Dopheide, S.M., Yap, C.L., Ravanat, C., Freund, M., Mangin, P., Heel, K.A., Street, A., Harper, I.S., Lanza, F. and Jackson, S.P., 2000. A revised model of platelet aggregation. *The Journal of Clinical Investigation*, *105*(6), pp.783-791.

Iafrati, M.D., Vitseva, O., Tanriverdi, K., Blair, P., Rex, S., Chakrabarti, S., Varghese, S. and Freedman, J.E., 2005. Compensatory mechanisms influence hemostasis in setting of eNOS deficiency. *American Journal of Physiology-Heart and Circulatory Physiology*, *288*(4), pp.H1627-H1632.

Lai, H.L., Lin, T.H., Kao, Y.Y., Lin, W.J., Hwang, M.J. and Chern, Y., 1999. The N terminus domain of type VI adenylyl cyclase mediates its inhibition by protein kinase C. *Molecular Pharmacology*, *56*(3), pp.644-650.

Lai, H.L., Yang, T.H., Messing, R.O., Ching, Y.H., Lin, S.C. and Chern, Y., 1997. Protein kinase C inhibits adenylyl cyclase type VI activity during desensitization of the A2a-adenosine receptor-mediated cAMP response. *Journal of Biological Chemistry*, *272*(8), pp.4970-4977.

Lankhof, H., Schiphorst, M.E., Bracke, M., Wu, Y.P., Ijsseldijk, M.J., Vink, T. and Sixma, J.J., 1996. A3 domain is essential for interaction of von Willebrand factor with collagen type III. *Thrombosis and Haemostasis*, *75*(6), pp.950-958.

Lee, E., Hayes, D.B., Langsetmo, K., Sundberg, E.J. and Tao, T.C., 2007. Interactions between the leucine-zipper motif of cGMP-dependent protein kinase and the C-terminal region of the targeting subunit of myosin light chain phosphatase. *Journal of Molecular Biology*, *373*(5), pp.1198-1212.

Lee, M.R., Li, L. and Kitazawa, T., 1997. Cyclic GMP causes Ca2+ desensitization in vascular smooth muscle by activating the myosin light chain phosphatase. *Journal of Biological Chemistry*, *272*(8), pp.5063-5068.

Léon, C., Eckly, A., Hechler, B., Aleil, B., Freund, M., Ravanat, C., Jourdain, M., Nonne, C., Weber, J., Tiedt, R. and Gratacap, M.P., 2007. Megakaryocyte-restricted MYH9 inactivation dramatically affects hemostasis while preserving platelet aggregation and secretion. *Blood, 110*(9), pp.3183-3191.

Leslie M. (2010). Cell biology: beyond clotting: the powers of platelets. S*cience*, *328*(5978), pp.562-564.

Lester, L.B., Langeberg, L.K. and Scott, J.D., 1997. Anchoring of protein kinase A facilitates hormone-mediated insulin secretion. *Proceedings of the National Academy of Sciences*, *94*(26), pp.14942-14947.

Li, Z., Delaney, M.K., O'brien, K.A. and Du, X., 2010. Signaling during platelet adhesion and activation. *Arteriosclerosis, Thrombosis, and Vascular Biology*, *30*(12), pp.2341-2349.

Li, Z., Xi, X. and Du, X., 2001. A mitogen-activated protein kinase-dependent signaling pathway in the activation of platelet integrin αIIbβ3. *Journal of Biological Chemistry*, *276*(45), pp.42226-42232.

Lin, C., Guo, X., Lange, S., Liu, J., Ouyang, K., Yin, X., Jiang, L., Cai, Y., Mu, Y., Sheikh, F. and Ye, S., 2013. Cypher/ZASP is a novel A-kinase anchoring protein. *Journal of Biological Chemistry*, *288*(41), pp.29403-29413.

Lin, S. and Brozovich, F.V., 2016. MYPT1 isoforms expressed in HEK293T cells are differentially phosphorylated after GTPγS treatment. *Journal of Smooth Muscle Research*, *52*(0), pp.66-77.

Lin, T.H., Lai, H.L., Kao, Y.Y., Sun, C.N., Hwang, M.J. and Chern, Y., 2002. Protein kinase C inhibits type VI adenylyl cyclase by phosphorylating the regulatory N domain and two catalytic C1 and C2 domains. *Journal of Biological Chemistry*, *277*(18), pp.15721-15728.

Lontay, B., Kiss, A., Gergely, P., Hartshorne, D.J. and Erdődi, F., 2005. Okadaic acid induces phosphorylation and translocation of myosin phosphatase target subunit 1 influencing myosin phosphorylation, stress fiber assembly and cell migration in HepG2 cells. *Cellular Signalling*, *17*(10), pp.1265-1275.

López, J.A. and Dong, J.F., 1997. Structure and function of the glycoprotein Ib-IX-V complex. *Current Opinion in Hematology*, *4*(5), pp.323-329.

Loscalzo J, Schafer A (2002). *Thrombosis and Hemorrhage,* edn. Lippincott Williams &Wilkins.

Lowry, O. H., Rosebrough, N. J., Farr, A. L., Randall, R. J. (1951). Protein measurement with the Folin phenol reagent. *Journal of Biological Chemistry,193*(1), pp.265-275.

Lucas, K.A., Pitari, G.M., Kazerounian, S., Ruiz-Stewart, I., Park, J., Schulz, S., Chepenik, K.P. and Waldman, S.A., 2000. Guanylyl cyclases and signaling by cyclic GMP. *Pharmacological Reviews*, *52*(3), pp.375-414.

Ma, Y.Q., Qin, J. and Plow, E.F., 2007. Platelet integrin αIIbβ3: activation mechanisms. *Journal of Thrombosis and Haemostasis*, *5*(7), pp.1345-1352.

Mabuchi, K., Gong, B.J., Langsetmo, K., Ito, M., Nakano, T. and Tao, T., 1999. Isoforms of the small non-catalytic subunit of smooth muscle myosin light chain phosphatase. *Biochimica et Biophysica Acta (BBA)-Protein Structure and Molecular Enzymology*, *1434*(2), pp.296-303.

Machlus, K.R. and Italiano, J.E., 2013. The incredible journey: From megakaryocyte development to platelet formation. *Journal of Cell Biology*, *201*(6), pp.785-796.

Macphee, C.H., Reifsnyder, D.H., Moore, T.A., Lerea, K.M. and Beavo, J.A., 1988. Phosphorylation results in activation of a cAMP phosphodiesterase in human platelets. *Journal of Biological Chemistry*, *263*(21), pp.10353-10358.

Mahavadi, S., Nalli, A., Al-Shboul, O. and Murthy, K.S., 2014. Inhibition of MLC20 phosphorylation downstream of Ca2+ and RhoA: a novel mechanism involving phosphorylation of myosin phosphatase interacting protein (M-RIP) by PKG and stimulation of MLC phosphatase activity. *Cell Biochemistry and Biophysics*, *68*(1), pp.1-8.

Malinin, N.L., Zhang, L., Choi, J., Ciocea, A., Razorenova, O., Ma, Y.Q., Podrez, E.A., Tosi, M., Lennon, D.P., Caplan, A.I. and Shurin, S.B., 2009. A point mutation in KINDLIN3 ablates activation of three integrin subfamilies in humans. *Nature Medicine*, *15*(3), pp.313-318.

Malinski, T., Radomski, M.W., Taha, Z. and Moncada, S., 1993. Direct electrochemical measurement of nitric oxide released from human platelets. *Biochemical and Biophysical Research Communications*, *194*(2), pp.960-965.

Manganello, J.M., Huang, J.S., Kozasa, T., Voyno-Yasenetskaya, T.A. and Le Breton, G.C., 2003. Protein kinase A-mediated phosphorylation of the Gα13 switch I region alters the Gαβγ13-G protein-coupled receptor complex and inhibits Rho activation. *Journal of Biological Chemistry*, *278*(1), pp.124-130.

Manns, J.M., Brennan, K.J., Colman, R.W. and Sheth, S.B., 2002. Differential regulation of human platelet responses by cGMP inhibited and stimulated cAMP phosphodiesterases. *Thrombosis and Haemostasis*, *87*(05), pp.873-879.

Marcus, A.J., Broekman, M.J., Drosopoulos, J.H.F., Islam, N., Alyonycheva, T.N., Safier, L.B., Hajjar, K.A., Posnett, D.N., Schoenborn, M.A., Schooley, K.A., Gayle, R.B., Maliszewski, C.R., 1997. The endothelial cell ecto-ADPaseresposible for inhibition of platelet function is CD39. *Journal of Clinical Investigation, 99*(6), pp.1351-1360.

Margarucci, L., Roest, M., Preisinger, C., Bleijerveld, O.B., van Holten, T.C., Heck, A.J. and Scholten, A., 2011. Collagen stimulation of platelets induces a rapid spatial response of cAMP and cGMP signaling scaffolds. *Molecular BioSystems*, *7*(7), pp.2311-2319.

Marshall, S.J., Senis, Y.A., Auger, J.M., Feil, R., Hofmann, F., Salmon, G., Peterson, J.T., Burslem, F. and Watson, S.P., 2004. GPIb-dependent platelet activation is dependent on Src kinases but not MAP kinase or cGMP-dependent kinase. *Blood*, *103*(7), pp.2601-2609.

Martin, C., Morales, L.D. and Cruz, M.A., 2007. Purified A2 domain of von Willebrand factor binds to the active conformation of von Willebrand factor and blocks the interaction with platelet glycoprotein Ibα. *Journal of Thrombosis and Haemostasis*, *5*(7), pp.1363-1370.

Massberg, S., Sausbier, M., Klatt, P., Bauer, M., Pfeifer, A., Siess, W., Fässler, R., Ruth, P., Krombach, F. and Hofmann, F., 1999. Increased adhesion and aggregation of platelets lacking cyclic guanosine 3', 5'-monophosphate kinase I. *Journal of Experimental Medicine*, *189*(8), pp.1255-1264.

Matsumura, F. and Hartshorne, D.J., 2008. Myosin phosphatase target subunit: Many roles in cell function. *Biochemical and Biophysical Research Communications*, *369*(1), pp.149-156.

Maurice, D.H. and Haslam, R.J., 1990. Molecular basis of the synergistic inhibition of platelet function by nitrovasodilators and activators of adenylate cyclase: inhibition of cyclic AMP breakdown by cyclic GMP. *Molecular Pharmacology*, *37*(5), pp.671-681.

Mazharian, A., Wang, Y.J., Mori, J., Bem, D., Finney, B., Heising, S., Gissen, P., White, J.G., Berndt, M.C., Gardiner, E.E. and Nieswandt, B., 2012. Mice lacking the ITIM-containing receptor G6b-B exhibit macrothrombocytopenia and aberrant platelet function. *Sci. Signal, 5*(248), pp.ra78-ra78.

McCarty, O.J., Larson, M.K., Auger, J.M., Kalia, N., Atkinson, B.T., Pearce, A.C., Ruf, S., Henderson, R.B., Tybulewicz, V.L., Machesky, L.M. and Watson, S.P., 2005.

Rac1 is essential for platelet lamellipodia formation and aggregate stability under flow. *Journal of Biological Chemistry*, *280*(47), pp.39474-39484.

McConnell, B.K., Popovic, Z., Mal, N., Lee, K., Bautista, J., Forudi, F., Schwartzman, R., Jin, J.P., Penn, M. and Bond, M., 2009. Disruption of protein kinase A interaction with A-kinase-anchoring proteins in the heart in vivo effects on cardiac contractility, protein kinase A phosphorylation and troponin I proteolysis. *Journal of Biological Chemistry*, *284*(3), pp.1583-1592.

McKnight, G.S., Cadd, G.G., Clegg, C.H., Otten, A.D. and Correll, L.A., 1988. Expression of wild-type and mutant subunits of the cAMP-dependent protein kinase. In *Cold Spring Harbor Symposia on Quantitative Biology*, *53*, pp.111-119. Cold Spring Harbor Laboratory Press.

McNicol, A. and Israels, S.J., 1999. Platelet dense granules: structure, function and implications for haemostasis. *Thrombosis Research*, *95*(1), pp.1-18.

Means, C.K., Lygren, B., Langeberg, L.K., Jain, A., Dixon, R.E., Vega, A.L., Gold, M.G., Petrosyan, S., Taylor, S.S., Murphy, A.N. and Ha, T., 2011. An entirely specific type I A-kinase anchoring protein that can sequester two molecules of protein kinase A at mitochondria. *Proceedings of the National Academy of Sciences*, *108*(48), pp.E1227-E1235.

Menche, D., Israel, A. and Karpatkin, S., 1980. Platelets and microtubules: effect of colchicine and D2O on platelet aggregation and release induced by calcium ionophore A23187. *Journal of Clinical Investigation*, *66*(2), pp.284-291.

Meyer, I., Kunert, S., Schwiebert, S., Hagedorn, I., Italiano, J.E., Dütting, S., Nieswandt, B., Bachmann, S. and Schulze, H., 2012. Altered microtubule equilibrium and impaired thrombus stability in mice lacking RanBP10. *Blood*, *120*(17), pp.3594-3602.

Michael, S.K., Surks, H.K., Wang, Y., Zhu, Y., Blanton, R., Jamnongjit, M., Aronovitz, M., Baur, W., Ohtani, K., Wilkerson, M.K. and Bonev, A.D., 2008. High blood pressure arising from a defect in vascular function. *Proceedings of the National Academy of Sciences*, *105*(18), pp.6702-6707.

Miggin, S.M. and Kinsella, B.T., 2002. Investigation of the mechanisms of G protein: effector coupling by the human and mouse prostacyclin receptors Identification of critical species-dependent differences. *Journal of Biological Chemistry*, *277*(30), pp.27053-27064.

Miggin, S.M., Lawler, O.A. and Kinsella, B.T., 2003. Palmitoylation of the human prostacyclin receptor Functional implications of palmitoylation and isoprenylation. *Journal of Biological Chemistry*, *278*(9), pp.6947-6958.

Mitchell, J.A. and Warner, T.D., 2006. COX isoforms in the cardiovascular system: understanding the activities of non-steroidal anti-inflammatory drugs. *Nature Reviews Drug Discovery*, *5*(1), pp.75-86.

Mitchell, J.A. and Warner, T.D., 1999. Cyclo-oxygenase-2: pharmacology, physiology, biochemistry and relevance to NSAID therapy. *British Journal of Pharmacology*, *128*(6), pp.1121-1132.

Mongillo, M., McSorley, T., Evellin, S., Sood, A., Lissandron, V., Terrin, A., Huston, E., Hannawacker, A., Lohse, M.J., Pozzan, T. and Houslay, M.D., 2004. Fluorescence resonance energy transfer–based analysis of cAMP dynamics in live neonatal rat cardiac myocytes reveals distinct functions of compartmentalized phosphodiesterases. *Circulation Research*, *95*(1), pp.67-75.

Montoliu, C., Piedrafita, B., Serra, M.A., Del Olmo, J.A., Rodrigo, J.M. and Felipo, V., 2007. A single transient episode of hyperammonemia induces long-lasting alterations in protein kinase A. *American Journal of Physiology-Gastrointestinal and Liver Physiology*, *292*(1), pp.G305-G314.

Moorhead, G., Johnson, D., Morrice, N. and Cohen, P., 1998. The major myosin phosphatase in skeletal muscle is a complex between the β-isoform of protein phosphatase 1 and the MYPT2 gene product. *FEBS Letters*, *438*(3), pp.141-144.

Moorthy, B.S., Gao, Y. and Anand, G.S., 2011. Phosphodiesterases catalyze hydrolysis of cAMP-bound to regulatory subunit of protein kinase A and mediate signal termination. *Molecular and Cellular Proteomics*, *10*(2), pp.M110-002295.

Moroi, M. and Jung, S.M., 2004. Platelet glycoprotein VI: its structure and function. *Thrombosis Research*, *114*(4), pp.221-233.

Moser, M., Nieswandt, B., Ussar, S., Pozgajova, M. and Fässler, R., 2008. Kindlin-3 is essential for integrin activation and platelet aggregation. *Nature Medicine*, *14*(3), pp.325-330.

Mullershausen, F., Friebe, A., Feil, R., Thompson, W.J., Hofmann, F. and Koesling, D., 2003. Direct activation of PDE5 by cGMP. *The Journal of Cell Biology*, *160*(5), pp.719-727.

Muranyi, A., Erdodi, F., Ito, M., Gergely, P. and Hartshorne, D., 1998. Identification and localization of myosin phosphatase in human platelets. *Biochemical Journal*, *330*(Pt1), pp.225-231.

Murata, K., Hirano, K., Villa-Moruzzi, E., Hartshorne, D.J. and Brautigan, D.L., 1997. Differential localization of myosin and myosin phosphatase subunits in smooth muscle cells and migrating fibroblasts. *Molecular Biology of the Cell*, *8*(4), pp.663-673.

Murata, T., Ushikubi, F., Matsuoka, T., Hirata, M., Yamasaki, A., Sugimoto, Y., Ichikawa, A., Aze, Y., Tanaka, T., Yoshida, N. and Ueno, A., 1997. Altered pain perception and inflammatory response in mice lacking prostacyclin receptor. *Nature*, *388*(6643), pp.678-682.

Murray, A.J., 2008. Pharmacological PKA inhibition: all may not be what it seems. *Science Signaling*, *1*(22), pp.re4-re4.

Murugappa, S. and Kunapuli, S.P., 2006. The role of ADP receptors in platelet function. *Frontiers in Bioscience: aJournal and Virtual Library*, *11*, pp.1977-1986.

Mustard, J. F., Perry, D. W., Ardlie, N. G., Packham, M. A. (1972). Preparation of suspensions of washed platelets from humans. *British Journal of Haematology 22*(2),pp.193-204.

Nagalla, S., Shaw, C., Kong, X., Kondkar, A.A., Edelstein, L.C., Ma, L., Chen, J., McKnight, G.S., López, J.A., Yang, L. and Jin, Y., 2011. Platelet microRNA-mRNA coexpression profiles correlate with platelet reactivity. *Blood*, *117*(19), pp.5189-5197.

Naik, M.U., Stalker, T.J., Brass, L.F., Naik, U.P., 2012. JAM-A protects from thrombosis by suppressing integrin αIIbβ3-depedent outside-in signaling in platelets. *Blood*, *119*(14), pp.3352-3360.

Nakai, K., Suzuki, Y., Kihira, H., Wada, H., Fujioka, M., Ito, M., Nakano, T., Kaibuchi, K., Shiku, H. and Nishikawa, M., 1997. Regulation of myosin phosphatase through phosphorylation of the myosin-binding subunit in platelet activation. *Blood*, *90*(10), pp.3936-3942.

Nakamura, K., Kimura, M. and Aviv, A., 1995. Role of cyclic nucleotides in store-mediated external Ca2+ entry in human platelets. *Biochemical Journal*, *310*(1), pp.263-269.

Nakamura, K., Koga, Y., Sakai, H., Homma, K. and Ikebe, M., 2007. cGMP-dependent relaxation of smooth muscle is coupled with the change in the phosphorylation of myosin phosphatase. *Circulation Research*, *101*(7), pp.712-722.

Nakamura, M., Ichikawa, K., Ito, M., Yamamori, B., Okinaka, T., Isaka, N., Yoshida, Y., Fujita, S. and Nakano, T., 1999. Effects of the phosphorylation of myosin phosphatase by cyclic GMP-dependent protein kinase. *Cellular Signalling*, *11*(9), pp.671-676.

Narumiya, S., Sugimoto, Y. and Ushikubi, F., 1999. Prostanoid receptors: structures, properties, and functions. *Physiological Reviews*, *79*(4), pp.1193-1226.

Naseem, K.M. and Riba, R., 2008. Unresolved roles of platelet nitric oxide synthase. *Journal of Thrombosis and Haemostasis*, *6*(1), pp.10-19.

Needleman, P., Moncada, S., Bunting, S., Vane, J.R., Hamberg, M. and Samuelsson, B., 1976. Identification of an enzyme in platelet microsomes which generates thromboxane A2 from prostaglandin endoperoxides. *Nature*, *261*(5561), pp.558-560.

Neppl, R.L., Lubomirov, L.T., Momotani, K., Pfitzer, G., Eto, M. and Somlyo, A.V., 2009. Thromboxane A2-induced bi-directional regulation of cerebral arterial tone. *Journal of Biological Chemistry*, *284*(10), pp.6348-6360.

Nieswandt, B. and Watson, S.P., 2003. Platelet-collagen interaction: is GPVI the central receptor?. *Blood*, *102*(2), pp.449-461.

Nishikawa, M., De Lanerolle, P., Lincoln, T.M. and Adelstein, R.S., 1984. Phosphorylation of mammalian myosin light chain kinases by the catalytic subunit of cyclic AMP-dependent protein kinase and by cyclic GMP-dependent protein kinase. *Journal of Biological Chemistry*, *259*(13), pp.8429-8436.

Offermanns, S., 2006. Activation of platelet functions through G protein–coupled receptors. *Circulation Research*, *99*(12), pp.1293-1304.

Ogawa, M., 1993. Differentiation and proliferation of hematopoietic stem cells. *Blood*, *81*(11), pp.2844-2853.

Okamoto, R., Kato, T., Mizoguchi, A., Takahashi, N., Nakakuki, T., Mizutani, H., Isaka, N., Imanaka-Yoshida, K., Kaibuchi, K., Lu, Z. and Mabuchi, K., 2006. Characterization and function of MYPT2, a target subunit of myosin phosphatase in heart. *Cellular Signalling*, *18*(9), pp.1408-1416.

Oliveria, S.F., Dell'Acqua, M.L. and Sather, W.A., 2007. AKAP79/150 anchoring of calcineurin controls neuronal L-type Ca 2+ channel activity and nuclear signaling. *Neuron*, *55*(2), pp.261-275.

Omori, K. and Kotera, J., 2007. Overview of PDEs and their regulation. *Circulation Research*, *100*(3), pp.309-327.

Onselaer, M.B., Hardy, A.T., Wilson, C., Sanchez, X., Babar, A.K., Miller, J.L., Watson, C.N., Watson, S.K., Bonna, A., Philippou, H. and Herr, A.B., 2017. Fibrin and D-dimer bind to monomeric GPVI. *Blood advances, 1*(19), pp.1495-1504.

Ozaki, Y., Asazuma, N., Suzuki-Inoue, K. and Berndt, M.C., 2005. Platelet GPIb-IX-V-dependent signaling. *Journal of Thrombosis and Haemostasis*, *3*(8), pp.1745-1751.

Ozer, R.S. and Halpain, S., 2000. Phosphorylation-dependent localization of microtubule-associated protein MAP2c to the actin cytoskeleton. *Molecular Biology of The Cell*, *11*(10), pp.3573-3587.

Özüyaman, B., Gödecke, A., Küsters, S., Kirchhoff, E., Scharf, R.E. and Schrader, J., 2005. Endothelial nitric oxide synthase plays a minor role in inhibition of arterial thrombus formation. *Thrombosis and Haemostasis*, *94*(06), pp.1161-1167.

Palmer, R.M., Ashton, D.S. and Moncada, S., 1988. Vascular endothelial cells synthesize nitric oxide from L-arginine. *Nature*, *333*(6174), pp.664-666.

Palmer, R.M., Ferrige, A.G. and Moncada, S., 1987. Nitric oxide release accounts for the biological activity of endothelium-derived relaxing factor. *Nature, 327*(6122),pp.524-526.

Patel, S.R., Hartwig, J.H. and Italiano Jr, J.E., 2005. The biogenesis of platelets from megakaryocyte proplatelets. *Journal of Clinical Investigation*, *115*(12), pp.3348-3354.

Patel, S.R., Richardson, J.L., Schulze, H., Kahle, E., Galjart, N., Drabek, K., Shivdasani, R.A., Hartwig, J.H. and Italiano, J.E., 2005. Differential roles of microtubule assembly and sliding in proplatelet formation by megakaryocytes. *Blood, 106*(13), pp.4076-4085.

Patil, S.B. and Bitar, K.N., 2006. RhoA-and PKC-α-mediated phosphorylation of MYPT and its association with HSP27 in colonic smooth muscle cells. *American Journal of Physiology-Gastrointestinal and Liver Physiology*, *290*(1), pp.G83-G95.

Paul, B.Z., Daniel, J.L. and Kunapuli, S.P., 1999. Platelet shape change is mediated by both calcium-dependent and-independent signaling pathways Role of p160 Rho-associated coiled-coil-containing protein kinase in platelet shape change. *Journal of Biological Chemistry*, *274*(40), pp.28293-28300.

Payne, M.C., Zhang, H.Y., Prosdocimo, T., Joyce, K.M., Koga, Y., Ikebe, M. and Fisher, S.A., 2006. Myosin phosphatase isoform switching in vascular smooth muscle development. *Journal of Molecular and Cellular Cardiology*,*40*(2), pp.274-282.

Payne, M.C., Zhang, H.Y., Shirasawa, Y., Koga, Y., Ikebe, M., Benoit, J.N. and Fisher, S.A., 2004. Dynamic changes in expression of myosin phosphatase in a model of portal hypertension. *American Journal of Physiology-Heart and Circulatory Physiology*, *286*(5), pp.H1801-H1810.

Pidoux, G. and Taskén, K., 2010. Specificity and spatial dynamics of protein kinase A signaling organized by A-kinase-anchoring proteins. *Journal of Molecular Endocrinology*, *44*(5), pp.271-284.

Pieroni, J.P., Harry, A., Chen, J., Jacobowitz, O., Magnusson, R.P. and Iyengar, R., 1995. Distinct characteristics of the basal activities of adenylyl cyclases 2 and 6. *Journal of Biological Chemistry*, *270*(36), pp.21368-21373.

Pierre, S., Eschenhagen, T., Geisslinger, G. and Scholich, K., 2009. Capturing adenylyl cyclases as potential drug targets. *Nature Reviews Drug Discovery*, *8*(4), pp.321-335.

Pigazzi, A., Heydrick, S., Folli, F., Benoit, S., Michelson, A. and Loscalzo, J., 1999. Nitric oxide inhibits thrombin receptor-activating peptide-induced phosphoinositide 3-kinase activity in human platelets. *Journal of Biological Chemistry*, *274*(20), pp.14368-14375.

Polanowska-Grabowska, R. and Gear, A.R., 1994. Role of cyclic nucleotides in rapid platelet adhesion to collagen. *Blood*, *83*(9), pp.2508-2515.

Potter, R.L. and Taylor, S.S., 1979. Relationships between structural domains and function in the regulatory subunit of cAMP-dependent protein kinases I and II from porcine skeletal muscle. *Journal of Biological Chemistry*, *254*(7), pp.2413-2418.

Prevost, N., Woulfe, D., Tanaka, T. and Brass, L.F., 2002. Interactions between Eph kinases and ephrins provide a mechanism to support platelet aggregation

once cell-to-cell contact has occurred. *Proceedings of the National Academy of Sciences*, *99*(14), pp.9219-9224.

Pugh, N., Simpson, A.M., Smethurst, P.A., de Groot, P.G., Raynal, N. and Farndale, R.W., 2010. Synergism between platelet collagen receptors defined using receptor-specific collagen-mimetic peptide substrata in flowing blood. *Blood*, *115*(24), pp.5069-5079.

Pula, G. and Poole, A.W., 2008. Critical roles for the actin cytoskeleton and cdc42 in regulating platelet integrin α2β1. *Platelets*, *19*(3), pp.199-210.

Qureshi, A.H., Chaoji, V., Maiguel, D., Faridi, M.H., Barth, C.J., Salem, S.M., Singhal, M., Stoub, D., Krastins, B., Ogihara, M. and Zaki, M.J., 2009. Proteomic and phospho-proteomic profile of human platelets in basal, resting state: insights into integrin signaling. *PloS one, 4*(10), p.e7627.

Rababa'h, A., Singh, S., Suryavanshi, S.V., Altarabsheh, S.E., Deo, S.V. and McConnell, B.K., 2014. Compartmentalization role of A-kinase anchoring proteins (AKAPs) in mediating protein kinase A (PKA) signaling and cardiomyocyte hypertrophy. *International Journal of Molecular Sciences*, *16*(1), pp.218-229.

Raslan, Z., Aburima, A. and Naseem, K.M., 2015. The Spatiotemporal Regulation of cAMP Signaling in Blood Platelets—Old Friends and New Players. *Frontiers in Pharmacology*, *6*(), p.266.

Raslan, Z., Magwenzi, S., Aburima, A., Taskén, K. and Naseem, K.M., 2015. Targeting of type I protein kinase A to lipid rafts is required for platelet inhibition by the 3', 5'-cyclic adenosine monophosphate-signaling pathway. *Journal of Thrombosis and Haemostasis*, *13*(9), pp.1721-1734.

Raslan. Z., Naseem. K.M., 2014. The control of blood platelets by cAMP signalling. *Biochemical Society Transactions*, *42*(2), pp.289–294.

Rathore, V., Stapleton, M.A., Hillery, C.A., Montgomery, R.R., Nichols, T.C., Merricks, E.P., Newman, D.K. and Newman, P.J., 2003. PECAM-1 negatively regulates GPIb/IX/V signaling in murine platelets. *Blood*, *102*(10), pp.3658-64.

Reid, H.M. and Kinsella, B.T., 2003. The α, but Not the β, Isoform of the human Thromboxane A2 receptor is a target for nitric oxide-mediated desensitization independent modulation of TPα signalling by nitric oxide and prostacyclin. *Journal of Biological Chemistry*, *278*(51), pp.51190-51202.

Reid, H.M., Mulvaney, E.P., Turner, E.C. and Kinsella, B.T., 2010. Interaction of the human prostacyclin receptor with Rab11 characterisation of a novel Rab11 binding domain within α-helix 8 that is regulated by palmitoylation. *Journal of Biological Chemistry*, *285*(24), pp.18709-18726.

Reininger A.J., 2008. Function of von Willebrand factor in haemostasis and thrombosis. *Haemophilia*, 14(Suppl 5), pp.11–26.

Ren, Q., Ye, S. and Whiteheart, S.W., 2008. The platelet release reaction: just when you thought platelet secretion was simple. *Current Opinion in Hematology*, 15(5), pp.537-541.

Rindlisbacher, B., Sidler, M.A., Galatioto, L.E. and Zahler, P., 1990. Arachidonic acid liberated by diacylglycerol lipase is essential for the release mechanism in chromaffin cells from bovine adrenal medulla. *Journal of Neurochemistry*, *54*(4), pp.1247-1252.

Rowley, J.W., Oler, A.J., Tolley, N.D., Hunter, B.N., Low, E.N., Nix, D. a., Yost, C.C., Zimmerman, G. a., Weyrich, A.S., 2011. Genome-wide RNA-seq analysis of human and mouse platelet transcriptomes. *Blood*, *118*(14), pp.101–111.

Ruggeri, Z.M., 2007. The role of von Willebrand factor in thrombus formation. *Thrombosis Research*, *120*(Supp 1), pp.S5-S9.

Ruggeri, Z.M. and Mendolicchio, G.L., 2007. Adhesion mechanisms in platelet function. *Circulation Research*, *100*(12), pp.1673-1685.

Rukoyatkina, N., Walter, U., Friebe, A. and Gambaryan, S., 2011. Differentiation of cGMP-dependent and-independent nitric oxide effects on platelet apoptosis and reactive oxygen species production using platelets lacking soluble guanylyl cyclase. *Thrombosis and Haemostasis*, *105*(05), pp.922-933.

Rybalkin, S.D., Rybalkina, I.G., Feil, R., Hofmann, F. and Beavo, J.A., 2002. Regulation of cGMP-specific phosphodiesterase (PDE5) phosphorylation in smooth muscle cells. *Journal of Biological Chemistry*, 277(5), pp.3310-3317.

Ryningen, A., Jensen, B.O. and Holmsen, H., 1998. Elevation of cyclic AMP decreases phosphoinositide turnover and inhibits thrombin-induced secretion in human platelets. *Biochimica et Biophysica Acta (BBA)-Lipids and Lipid Metabolism*, *1394*(2), pp.235-248.

Sachs, U.J. and Nieswandt, B., 2007. In vivo thrombus formation in murine models. *Circulation Research*, *100*(7), pp.979-991.

Sadoul, K., 2015. New explanations for old observations: marginal band coiling during platelet activation. *Journal of Thrombosis and Haemostasis*, *13*(3), pp.333-346.

Salles, I.I., Feys, H.B., Iserbyt, B.F., De Meyer, S.F., Vanhoorelbeke, K. and Deckmyn, H., 2008. Inherited traits affecting platelet function. *Blood Reviews*, *22*(3), pp.155-172.

Savage, B., Almus-Jacobs, F. and Ruggeri, Z.M., 1998. Specific synergy of multiple substrate–receptor interactions in platelet thrombus formation under flow. *Cell*, *94*(5), pp.657-666.

Schinner, E., Salb, K. and Schlossmann, J., 2011. Signaling via IRAG is essential for NO/cGMP-dependent inhibition of platelet activation. *Platelets*, *22*(3), pp.217-227.

Schmidt, H.H., Lohmann, S.M. and Walter, U., 1993. The nitric oxide and cGMP signal transduction system: regulation and mechanism of action. *Biochimica et Biophysica Acta (BBA)-Molecular Cell Research*, *1178*(2), pp.153-175.

Schmitt, A., Guichard, J., Massé, J.M., Debili, N. and Cramer, E.M., 2001. Of mice and men: comparison of the ultrastructure of megakaryocytes and platelets. *Experimental Hematology*, *29*(11), pp.1295-1302.

Scholten, A., Aye, T.T. and Heck, A.J., 2008. A multi-angular mass spectrometric view at cyclic nucleotide dependent protein kinases: In vivo characterization and structure/function relationships. *Mass Spectrometry Reviews*, *27*(4), pp.331-353.

Schultess, J., Danielewski, O. and Smolenski, A.P., 2005. Rap1GAP2 is a new GTPase-activating protein of Rap1 expressed in human platelets. *Blood*, *105*(8), pp.3185-3192.

Schwarz, U.R., Walter, U. and Eigenthaler, M., 2001. Taming platelets with cyclic nucleotides1. *Biochemical Pharmacology*, *62*(9), pp.1153-1161.

Scott, J. D., 1991. Cyclic nucleotide-dependent protein kinases. *Pharmacology andTherapeutics, 50*(1), pp.123-145.

Sedgwick, S.G. and Smerdon, S.J., 1999. The ankyrin repeat: a diversity of interactions on a common structural framework. *Trends in Biochemical Sciences*, *24*(8), pp.311-316.

Sehgal, S. and Storrie, B., 2007. Evidence that differential packaging of the major platelet granule proteins von Willebrand factor and fibrinogen can support their differential release. *Journal of Thrombosis and Haemostasis, 5*(10), pp.2009-2016.

Seino, S. and Shibasaki, T., 2005. PKA-dependent and PKA-independent pathways for cAMP-regulated exocytosis. *Physiological Reviews*, *85*(4), pp.1303-1342.

Senis, Y.A., Mazharian, A. and Mori, J., 2014. Src family kinases: at the forefront of platelet activation. *Blood*, *124*(13), pp.2013-2024.

Serneri, G.N., Fortini, A., Lombardi, A., Modesti, P., Abbate, R. and Gensini, G., 1984. Reduction in prostacyclin platelet receptors in active spontaneous angina. *The Lancet*, *324*(8407), pp.838-841.

Shattil, S.J., Kim, C. and Ginsberg, M.H., 2010. The final steps of integrin activation: the end game. *Nature Reviews Molecular Cell Biology*, *11*(4), pp.288-300.

Shepro, D., Belamarich, F.A. and Chao, F.C., 1969. Retardation of clot retraction after incubation of platelets with colchicine and heavy water. *Nature*, *221*(5180), pp.563-565.

Shi, Y., 2009. Serine/threonine phosphatases: mechanism through structure. *Cell*, *139*(3), pp.468-484.

Shin, H.M., Je, H.D., Gallant, C., Tao, T.C., Hartshorne, D.J., Ito, M. and Morgan, K.G., 2002. Differential association and localization of myosin phosphatase subunits during agonist-induced signal transduction in smooth muscle. *Circulation Research*, *90*(5), pp.546-553.

Siess, W. and Lapetina, E., 1989. Prostacyclin inhibits platelet aggregation induced by phorbol ester or Ca2+ ionophore at steps distal to activation of protein kinase C and Ca2+-dependent protein kinases. *Biochemical Journal, 258*(1), pp.57-65.

Sim, D. S., Merrill-Skoloff, G., Furie, B. C., Furie, B. & Flaumenhaft, R. 2004. Initial accumulation of platelets during arterial thrombus formation in vivo is inhibited by elevation of basal cAMP levels. *Blood, 103*(6), pp.2127-2134.

Singh, D.K., Sarkar, J., Raghavan, A., Reddy, S.P. and Raj, J.U., 2011. Hypoxia modulates the expression of leucine zipper-positive MYPT1 and its interaction

with protein kinase G and Rho kinases in pulmonary arterial smooth muscle cells. *Pulmonary Circulation*, *1*(4), pp.487-498.

Skalhegg, B.S. and Taskén, K., 2000. Specificity in the cAMP/PKA signaling pathway. Differential expression, regulation, and subcellular localization of subunits of PKA. *Frontier in Biosciences*, *5*(5), pp.D678-D693.

Skinner, J.A. and Saltiel, A.R., 2001. Cloning and identification of MYPT3: a prenylatable myosin targetting subunit of protein phosphatase 1. *Biochemical Journal*, *356*(1), pp.257-267.

Smith, J.B. and Willis, A.L., 1971. Aspirin selectively inhibits prostaglandin production in human platelets. *Nature*, *231*(25), pp.235-237.

Smolenski, A., 2012. Novel roles of cAMP/cGMP-dependent signaling in platelets. *Journal of Thrombosis and Haemostasis*, *10*(2), pp.167-176.

Smolenski, A., Bachmann, C., Reinhard, K., Hönig-Liedl, P., Jarchau, T., Hoschuetzky, H. and Walter, U., 1998. Analysis and regulation of vasodilator-stimulated phosphoprotein serine 239 phosphorylation in vitro and in intact cells using a phosphospecific monoclonal antibody. *Journal of Biological Chemistry*, *273*(32), pp.20029-20035.

Smolenski, A., Poller, W., Walter, U. and Lohmann, S.M., 2000. Regulation of human endothelial cell focal adhesion sites and migration by cGMP-dependent protein kinase I. *Journal of Biological Chemistry*, *275*(33), pp.25723-25732.

Somlyo, A.P. and Somlyo, A.V., 2003. Ca2+ sensitivity of smooth muscle and nonmuscle myosin II: modulated by G proteins, kinases, and myosin phosphatase. *Physiological Reviews*, *83*(4), pp.1325-1358.

Somlyo, A.P. and Somlyo, A.V., 1994. Signal transduction and regulation in smooth muscle. *Nature*, *372*(6503), pp.231-236.

Stalker, T.J., Traxler, E.A., Wu.J., Wannemacher. K.M., Cermignano. S.L., Voronov. R., Diamond. S.L., Brass. L.F., 2013. Hierarchical organization in the hemostatic response and its relationship to the platelet-signaling network. *Blood*, *121*(10). pp.1875-1885.

Steegborn, C., 2014. Structure, mechanism, and regulation of soluble adenylyl cyclases—similarities and differences to transmembrane adenylyl cyclases. *Biochimica et Biophysica Acta (BBA)-Molecular Basis of Disease*, *1842*(12), pp.2535-2547.

Stitham, J., Gleim, S.R., Douville, K., Arehart, E. and Hwa, J., 2006. Versatility and differential roles of cysteine residues in human prostacyclin receptor structure and function. *Journal of Biological Chemistry*, *281*(48), pp.37227-37236.

Stojanovic, A., Marjanovic, J.A., Brovkovych, V.M., Peng, X., Hay, N., Skidgel, R.A. and Du, X., 2006. A phosphoinositide 3-kinase-AKT-nitric oxide-cGMP signaling pathway in stimulating platelet secretion and aggregation. *Journal of Biological Chemistry*, *281*(24), pp.16333-16339.

Stokka, A.J., Gesellchen, F., Carlson, C.R., Scott, J.D., Herberg, F.W. and Taskén, K., 2006. Characterization of A-kinase-anchoring disruptors using a solution-based assay. *Biochemical Journal*, *400*(3), pp.493-499.

Subramanian, H., Zahedi, R.P., Sickmann, A., Walter, U. and Gambaryan, S., 2013. Phosphorylation of CalDAG-GEFI by protein kinase A prevents Rap1b activation. *Journal of Thrombosis and Haemostasis*, *11*(8), pp.1574-1582.

Surks, H.K., Mochizuki, N., Kasai, Y., Georgescu, S.P., Tang, K.M., Ito, M., Lincoln, T.M. and Mendelsohn, M.E., 1999. Regulation of myosin phosphatase by a specific interaction with cGMP-dependent protein kinase Iα. *Science*, *286*(5444), pp.1583-1587.

Sutherland, C., MacDonald, J.A. and Walsh, M.P., 2016. Analysis of phosphorylation of the myosin-targeting subunit of myosin light chain phosphatase by Phos-tag SDS-PAGE. *American Journal of Physiology-Cell Physiology*, *310*(8), pp.C681-C691.

Suzuki, Y., Yamamoto, M., Wada, H., Ito, M., Nakano, T., Sasaki, Y., Narumiya, S., Shiku, H. and Nishikawa, M., 1999. Agonist-induced regulation of myosin phosphatase activity in human platelets through activation of Rho-kinase. *Blood*, *93*(10), pp.3408-3417.

Takizawa, N., Schmidt, D.J., Mabuchi, K., Villa-Moruzzi, E., Tuft, R.A. and Ikebe, M., 2003. M20, the small subunit of PP1M, binds to microtubules. *American Journal of Physiology-Cell Physiology*, *284*(2), pp.C250-C262.

Tan, I., Ng, C.H., Lim, L. and Leung, T., 2001. Phosphorylation of a novel myosin binding subunit of protein phosphatase 1 reveals a conserved mechanism in the regulation of actin cytoskeleton. *Journal of Biological Chemistry*, *276*(24), pp.21209-21216.

Tang, M., Wang, G., Lu, P., Karas, R.H., Aronovitz, M., Heximer, S.P., Kaltenbronn, K.M., Blumer, K.J., Siderovski, D.P., Zhu, Y. and Mendelsohn, M.E., 2003. Regulator of G-protein signaling-2 mediates vascular smooth muscle relaxation and blood pressure. *Nature Medicine*, *9*(12), pp.1506-1512.

Taylor, S.S., Buechler, J.A. and Yonemoto, W., 1990. cAMP-dependent protein kinase: framework for a diverse family of regulatory enzymes. *Annual Review of Biochemistry*, *59*(1), pp.971-1005.

Taylor, S.S., Ilouz, R., Zhang, P. and Kornev, A.P., 2012. Assembly of allosteric macromolecular switches: lessons from PKA. *Nature Reviews Molecular Cell Biology*, *13*(10), pp.646-658.

Taylor, S.S., Kim, C., Cheng, C.Y., Brown, S.H., Wu, J. and Kannan, N., 2008. Signaling through cAMP and cAMP-dependent protein kinase: diverse strategies for drug design. *Biochimica et Biophysica Acta (BBA)-Proteins and Proteomics*, *1784*(1), pp.16-26.

Terrak, M., Kerff, F., Langsetmo, K., Tao, T. and Dominguez, R., 2004. Structural basis of protein phosphatase 1 regulation. *Nature*, 429(6993), pp.780-784.

Tertyshnikova, S., Yan, X. and Fein, A., 1998. cGMP inhibits IP3-induced Ca2+ release in intact rat megakaryocytes via cGMP-and cAMP-dependent protein kinases. *The Journal of Physiology*, *512*(1), pp.89-96.

Towbin, H., Staehelin, T. and Gordon, J., 1979. Electrophoretic transfer of proteins from polyacrylamide gels to nitrocellulose sheets: procedure and some applications. *Proceedings of the National Academy of Sciences*, *76*(9), pp.4350-4354.

Truglia, J.A. and Stracher, A., 1981. Purification and characterization of a calcium dependent sulfhydryl protease from human platelets. *Biochemical and Biophysical Research Communications*, *100*(2), pp.814-822.

Vaiyapuri, S., Moraes, L.A., Sage, T., Ali, M.S., Lewis, K.R., Mahaut-Smith, M.P., Oviedo-Orta, E., Simon, A.M. and Gibbins, J.M., 2013. Connexin40 regulates platelet function. *Nature communications*, *4*, p.2564.

Vaiyapuri, S., Jones, C.I., Sasikumar, P., Moraes, L.A., Munger, S.J., Wright, J.R., Ali, M.S., Sage, T., Kaiser, W.J., Tucker, K.L., Stain, C.J., Bye, A.P., Jones, S., Oviedo-Orta, E., Simon, A.M., Mahaut-Smith, M.P. and Gibbins, J.M., 2012. Gap junctions

and connexin hemichannels underpin haemostasis and thrombosis. *Circulation*, *125*(20), pp.2479-2491.

Van Geet, C., Izzi, B., Labarque, V. and Freson, K., 2009. Human platelet pathology related to defects in the G-protein signaling cascade. *Journal of Thrombosis and Haemostasis*, *7*(s1), pp.282-286.

Varga-Szabo, D., Pleines, I. and Nieswandt, B., 2008. Cell adhesion mechanisms in platelets. *Arteriosclerosis, Thrombosis, and Vascular Biology*, *28*(3), pp.403-412.

Velasco, G., Armstrong, C., Morrice, N., Frame, S. and Cohen, P., 2002. Phosphorylation of the regulatory subunit of smooth muscle protein phosphatase 1M at Thr850 induces its dissociation from myosin. *FEBS Letters*, *527*(1-3), pp.101-104.

Vicente-Manzanares, M., Ma, X., Adelstein, R.S. and Horwitz, A.R., 2009. Non-muscle myosin II takes centre stage in cell adhesion and migration. *Nature Reviews Molecular Cell Biology*, *10*(11), pp.778-790.

Vijayaraghavan, S., Goueli, S.A., Davey, M.P. and Carr, D.W., 1997. Protein kinase A-anchoring inhibitor peptides arrest mammalian sperm motility. *Journal of Biological Chemistry*, *272*(8), pp.4747-4752.

Vinogradova, O., Velyvis, A., Velyviene, A., Hu, B., Haas, T.A., Plow, E.F. and Qin, J., 2002. A structural mechanism of integrin αIIbβ3 “inside-out” activation as regulated by its cytoplasmic face. *Cell*, *110*(5), pp.587-597.

Wall, M.E., Francis, S.H., Corbin, J.D., Grimes, K., Richie-Jannetta, R., Kotera, J., Macdonald, B.A., Gibson, R.R. and Trewhella, J., 2003. Mechanisms associated with cGMP binding and activation of cGMP-dependent protein kinase. *Proceedings of the National Academy of Sciences*, *100*(5), pp.2380-2385.

Walsh, D.A., Perkins, J.P. and Krebs, E.G., 1968. An adenosine 3', 5'-monophosphate-dependant protein kinase from rabbit skeletal muscle. *Journal of Biological Chemistry*, *243*(13), pp.3763-3765.

Walsh, M.T., Foley, J.F. and Kinsella, B.T., 2000. The α, but not the β, isoform of the human thromboxane A2 receptor is a target for prostacyclin-mediated desensitization. *Journal of Biological Chemistry*, *275*(27), pp.20412-20423.

Wang, K., Ash, J.F. and Singer, S.J., 1975. Filamin, a new high-molecular-weight protein found in smooth muscle and non-muscle cells. *Proceedings of the National Academy of Sciences*, *72*(11), pp.4483-4486.

Wardell, M.R., Reynolds, C.C., Berndt, M.C., Wallace, R.W. and Fox, J.E., 1989. Platelet glycoprotein Ib beta is phosphorylated on serine 166 by cyclic AMP-dependent protein kinase. *Journal of Biological Chemistry*, *264*(26), pp.15656-15661.

Watanabe, Y., Ito, M., Kataoka, Y., Wada, H., Koyama, M., Feng, J., Shiku, H. and Nishikawa, M., 2001. Protein kinase C–catalyzed phosphorylation of an inhibitory phosphoprotein of myosin phosphatase is involved in human platelet secretion. *Blood*, *97*(12), pp.3798-3805.

Watson, S.P., Herbert, J.M.J. and Pollitt, A.Y., 2010. GPVI and CLEC-2 in hemostasis and vascular integrity. *Journal of Thrombosis and Haemostasis*, *8*(7), pp.1456-1467.

Wee, J.L., and Jackson, D.E., 2005. The Ig-ITIM superfamily member PECAM-1 regulates the "outside-in" signaling properties of integrin alpha(IIb)beta3 in platelets. *Blood*, *106*(12): 3816-3823.

Weksler, B.B., Marcus, A.J. and Jaffe, E.A., 1977. Synthesis of prostaglandin I2 (prostacyclin) by cultured human and bovine endothelial cells. *Proceedings of the National Academy of Sciences*, *74*(9), pp.3922-3926.

Welch, E.J., Jones, B.W. and Scott, J.D., 2010. Networking with AKAPs: context-dependent regulation of anchored enzymes. *Molecular interventions*, *10*(2), po.86-97.

Welsh, J.D., Stalker, T.J., Voronov, R., Muthard, R.W., Tomaiuolo, M., Diamond, S.L., Brass, L.F., 2014. A systems approach to hemostasis: 1. The interdependence of thrombus architechture and agonist movements in the gaps between platelets. *Blood*, *124*(11), pp.1808-1815.

Wentworth, J.K., Pula, G. and Poole, A.W., 2006. Vasodilator-stimulated phosphoprotein (VASP) is phosphorylated on Ser157 by protein kinase C-dependent and-independent mechanisms in thrombin-stimulated human platelets. *Biochemical Journal*, *393*(2), pp.555-564.

White, J. G. 2007. Platelet Structure. *In:* Michelson, A. D. (ed.) *Platelets.* 2nd ed. San Diego, CA: Academic Press.

White, J.G. and Sauk, J.J., 1984. Microtubule coils in spread blood platelets. *Blood*, *64*(2), pp.470-478.

White, J.G. and Gerrard, J.M., 1976. Ultrastructural features of abnormal blood platelets. A review. *The American Journal of Pathology*, *83*(3), pp.589-632.

Willoughby, D. and Cooper, D.M., 2007. Organization and Ca2+ regulation of adenylyl cyclases in cAMP microdomains. *Physiological Reviews*, *87*(3), pp.965-1010.

Wilson, L.S., Elbatarny, H.S., Crawley, S.W., Bennett, B.M. and Maurice, D.H., 2008. Compartmentation and compartment-specific regulation of PDE5 by protein kinase G allows selective cGMP-mediated regulation of platelet functions. *Proceedings of the National Academy of Sciences*, *105*(36), pp.13650-13655.

Wong, W. and Scott, J.D., 2004. AKAP signalling complexes: focal points in space and time. *Nature Reviews Molecular Cell Biology 5*(12), pp.959-970.

Wooldridge, A.A., MacDonald, J.A., Erdodi, F., Ma, C., Borman, M.A., Hartshorne, D.J. and Haystead, T.A., 2004. Smooth muscle phosphatase is regulated in vivo by exclusion of phosphorylation of threonine 696 of MYPT1 by phosphorylation of Serine 695 in response to cyclic nucleotides. *Journal of Biological Chemistry*, *279*(33), pp.34496-34504.

Wu, G.C., Lai, H.L., Lin, Y.W., Chu, Y.T. and Chern, Y., 2001. N-glycosylation and residues Asn805 and Asn890 are involved in the functional properties of type VI adenylyl cyclase. *Journal of Biological Chemistry*, *276*(38), pp.35450-35457.

Wu, Y., Murányi, A., Erdődi, F. and Hartshorne, D.J., 2005. Localization of myosin phosphatase target subunit and its mutants. *Journal of Muscle Research and Cell Motility*, *26*(2), pp.123-134.

Xia, D., Stull, J.T. and Kamm, K.E., 2005. Myosin phosphatase targeting subunit 1 affects cell migration by regulating myosin phosphorylation and actin assembly. *Experimental Cell Research*, *304*(2), pp.506-517.

Xiao, C.Y., Hara, A., Yuhki, K.I., Fujino, T., Ma, H., Okada, Y., Takahata, O., Yamada, T., Murata, T., Narumiya, S. and Ushikubi, F., 2001. Roles of prostaglandin I2 and thromboxane A2 in cardiac ischemia-reperfusion injury. *Circulation*, *104*(18), pp.2210-2215.

Yu, X., Li, F., Klussmann, E., Stallone, J.N. and Han, G., 2014. G protein-coupled estrogen receptor 1 mediates relaxation of coronary arteries via cAMP/PKA-

dependent activation of MLCP. *American Journal of Physiology-Endocrinology and Metabolism*, *307*(4), pp.E398-E407.

Yuen, S.L., Ogut, O. and Brozovich, F.V., 2014. Differential phosphorylation of LZ+/LZ− MYPT1 isoforms regulates MLC phosphatase activity. *Archives of Biochemistry and Biophysics*, *562*, pp.37-42.

Yuen, S.L, Ogut, O. and Brozovich, F.V., 2011. MYPT1 protein isoforms are differentially phosphorylated by protein kinase G. *Journal of Biological Chemistry*, *286*(43), pp.37274-37279.

Yusuf, M.Z., Raslan, Z., Atkinson, L., Aburima, A., Thomas, S.G., Naseem, K.M. and Calaminus, S.D.J., 2017. Prostacyclin reverses platelet stress fibre formation causing platelet aggregate instability. *Scientific Reports*, *7*(1), p.5582.

Zabel, U., Weeger, M., Mylinh, L.A. and Schmidt, H.H., 1998. Human soluble guanylate cyclase: functional expression and revised isoenzyme family. *Biochemical Journal*, *335*(1), pp.51-57.

Zeiler, M., Moser, M. and Mann, M., 2014. Copy number analysis of the murine platelet proteome spanning the complete abundance range. Molecular & Cellular Proteomics, pp.mcp-M114.

Zha, J.M., Li, H.S., Wang, Y.T., Lin, Q., Tao, M. and He, W.Q., 2016. Characterization of isoform expression and subcellular distribution of MYPT1 in intestinal epithelial cells. *Gene*, *588*(1), pp.1-6.

Zhang, G., Liu, Y., Ruoho, A.E. and Hurley, J.H., 1997. Structure of the adenylyl cyclase catalytic core. *Nature*, *386*(6622), p.247-253.

Zhang, H. and Fisher, S.A., 2007. Conditioning effect of blood flow on resistance artery smooth muscle myosin phosphatase. *Circulation Research*, *100*(5), pp.730-737.

Zhang, W. and Colman, R.W., 2007. Thrombin regulates intracellular cyclic AMP concentration in human platelets through phosphorylation/activation of phosphodiesterase 3A. *Blood*, *110*(5), pp.1475-1482.

Zhang, Z., Austin, S.C. and Smyth, E.M., 2001. Glycosylation of the human prostacyclin receptor: role in ligand binding and signal transduction. *Molecular Pharmacology*, *60*(3), pp.480-487.

Zhao, L., Liu, J., He, C., Yan, R., Zhou, K., Cui, Q., Meng, X., Li, X., Zhang, Y., Nie, Y. and Hu, R., 2017. Protein kinase A determines platelet life span and survival by regulating apoptosis. *The Journal of Clinical Investigation*, *127*(12), pp.4338-4351.

Zwaal, R.F., Comfurius, P. and Bevers, E.M., 1998. Lipid–protein interactions in blood coagulation. *Biochimica et Biophysica Acta (BBA)-Reviews on Biomembranes*, *1376*(3), pp.433-453.